AD 746284

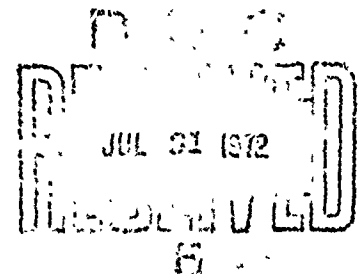# HIGH TEMPERATURE OXIDATION
OF CARBON MONOXIDE AND METHANE
IN A TURBULENT FLOW REACTOR

by
FREDERICK L. DRYER

PRINCETON UNIVERSITY
DEPARTMENT OF
AEROSPACE AND MECHANICAL SCIENCES

March 1972

JUL 31 1972

AFOSR Grant 69-1649

319

Qualified requestors may obtain
additional copies from the Defense
Documentation Center. All others
should apply to the National Tech-
nical Information Service.

Reproduction, translation, publi-
cation, use and disposal in whole
or in part by or for the United
States Government is permitted.

DOCUMENT CONTROL DATA - R&D

(Security classification of title body of abstract and indexing annotation must be entered when the overall report is classified)

1. ORIGINATING ACTIVITY (Corporate author)	2a. REPORT SECURITY CLASSIFICATION
PRINCETON UNIVERSITY DEPARTMENT OF AEROSPACE AND MECHANICAL SCIENCES PRINCETON, NEW JERSEY 08540	UNCLASSIFIED
	2b GROUP

3. REPORT TITLE

HIGH TEMPERATURE OXIDATION OF CARBON MONOXIDE AND METHANE IN A TURBULENT FLOW REACTOR

4. DESCRIPTIVE NOTES *(Type of report and inclusive dates)*

Scientific   Interim

5. AUTHOR(S) *(Last name, first name, initial)*

FREDERICK L. DRYER

6. REPORT DATE	7a. TOTAL NO. OF PAGES	7b. NO. OF REFS
March 1972	298	178

8a. CONTRACT OR GRANT NO. AFOSR-69-1649	9a. ORIGINATOR'S REPORT NUMBER(S)
b PROJECT NO. 9711-01	T-1034
c. 61102F	9b. OTHER REPORT NO(S) (Any other numbers that may be assigned this report)
d. 681308	AFOSR-TR-72-1109

10. AVAILABILITY/LIMITATION NOTICES

Approved for public release; distribution unlimited.

11. SUPPLEMENTARY NOTES	12. SPONSORING MILITARY ACTIVITY
TECH, OTHER	AF Office of Scientific Research (NAE) 1400 Wilson Boulevard Arlington, Virginia 22209

13. ABSTRACT

The high temperature oxidation reactions of carbon monoxide and methane in oxygen-rich atmospheres have been studied in a turbulent flow reactor. Spatial chemical sampling and gas chromatographic analysis techniques were developed for these studies, and the experimental methods are directly extendable to investigations of higher hydrocarbon oxidations. Overall expressions were developed for the carbon monoxide and methane disappearance rates and for the appearance rate of carbon dioxide in the methane-oxygen reaction. These and other data were used to deduce the relative importance of several elementary reactions in the oxidation mechanisms. It was concluded that other reactions in addition to hydroxyl attack on methane are important in governing the methane disappearance rate in oxygen-rich, high temperature systems. It was suggested that the reaction of oxygen atoms with methane and methyl radicals with hydrogen contribute significantly to the observed disappearance rate of methane. Thus, high temperature evaluations of the rate constant for hydroxyl attack on methane, which have neglected these latter contributions, are in error. Furthermore, a transition state description of the temperature dependence of the reaction of carbon monoxide with hydroxyl radicals suggests that this rate constant has been underestimated at high temperatures.

DD FORM 1473 1 JAN 64

14. KEY WORDS	LINK A		LINK B		LINK C	
	ROLE	WT	ROLE	WT	ROLE	WT
CHEMICAL KINETICS						
TURBULENT FLOW REACTOR						
HYDROCARBON FUELS						
METHANE-OXYGEN KINETICS						
CARBON MONOXIDE OXYGEN KINETICS						
CHEMICAL SAMPLING						

INSTRUCTIONS

HIGH TEMPERATURE OXIDATION
OF CARBON MONOXIDE AND METHANE
IN A TURBULENT FLOW REACTOR

by

FREDERICK L. DRYER

AMS Report T-1034

AFOSR Grant 69-1649

March 1972

Details of ... ...
this document ... ...
... studied on microfiche

Approved by: _Irvin Glassman_

Irvin Glassman
Professor of Aerospace Sciences
Principal Investigator

Guggenheim Laboratories for the Aerospace Propulsion Sciences
Department of Aerospace and Mechanical Sciences
Princeton University
Princeton , New Jersey

ABSTRACT

This research was directed toward the development of analytical techniques to study the chemical kinetics of hydrocarbon oxidations in a high temperature, adiabatic, turbulent flow reactor. Spatial chemical sampling and gas chromatographic analysis techniques were developed for this purpose, and the experimental methods were successfully demonstrated through kinetic studies of the oxidations of carbon monoxide and methane over the temperature range 1100 - 1400K.

The carbon monoxide-oxygen reaction in the presence of water was studied at atmospheric pressure over the temperature range 1030 - 1230K, the equivalence ratio 0.04 - 0.5, and over water concentrations of 0.1% - 3.0%. The disappearance rate of carbon monoxide was experimentally found to correlate as

$$-\frac{d[CO]}{dt} = 10^{14.6\pm0.25}\ e^{\left(\frac{-40000\pm1250}{RT}\right)}[CO]^{1.0}\ [H_2O]^{0.5}\ [O_2]^{0.25}$$

$$\text{mole cm}^{-3}\ \text{sec}^{-1}$$

Furthermore, it was experimentally shown that the rate of heat release in the carbon monoxide oxidation is proportional to the disappearance rate of carbon monoxide or appearance rate of carbon dioxide.

The reaction of methane and oxygen was studied at atmospheric pressure over the temperature range 1100 - 1400K, and the equivalence ratio range .05 - .5. Final oxidation products were carbon dioxide and water, and carbon monoxide

was observed to be a major intermediate specie of increasing importance at lower reaction temperatures. Ethane, ethylene, hydrogen, and formaldehyde were found to be present as minor intermediate species. Due to experimental difficulties, hydrogen and formaldehyde concentrations were not described spatially. However, formaldehyde, ethane, and ethylene concentrations were shown to be all of the same order. Hydrogen peroxide, methanol, acetylene and propane were shown to be present as trace intermediary species.

The methane disappearance rates in the induction phase and post-induction phase were shown to exhibit contrasting kinetic properties. In the induction phase of the reaction, the methane disappearance rate was qualitatively observed to be inhibited by the presence of methane and accelerated by the presence of oxygen. Methane disappearance rates in the post-induction phase of the reaction were quantitatively studied and were observed to be described by

$$\frac{-d[CH_4]}{dt} = 10^{13.2 \pm 0.20} \, e^{\left(\frac{-48400 \pm 1200}{RT}\right)} [CH_4]^{0.7} \, [O_2]^{0.8}$$

$$\text{mole cm}^{-3} \text{ sec}^{-1}$$

The rate of methane disappearance was found to be relatively independent of surface/volume ratio and water concentration.

The rate of appearance of carbon dioxide in the methane oxidation studies was evaluated to be

$$\frac{d[CO_2]}{dt} = 10^{14.75 \pm 0.40} \, e^{\left(\frac{-43000 \pm 2200}{RT}\right)} [CO]^{1.0} \, [H_2O]^{0.5} \, [O_2]^{0.25}$$

$$\text{mole cm}^{-3} \text{ sec}^{-1}$$

This correlation represents rates of carbon dioxide formation 3.5 times slower than those occurring in the independent study of the moist carbon monoxide oxidation. A methane-sensitized study of the moist carbon-monoxide oxidation showed that, while the carbon dioxide rate of formation was suppressed by small amounts of methane, the disappearance of methane itself was accelerated.

Associated theoretical work in conjunction with these and other experimental data showed that absolute reaction rate theory can account for the observed variation in the temperature dependence of the specific rate constants for the reaction

$$CO + OH \longrightarrow CO_2 + H$$
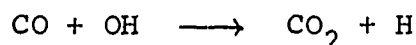
and that much of the supportive evidence for the competing reaction

$$CO + HO_2 \longrightarrow CO_2 + OH$$
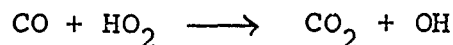
is a result of incorrect interpretation of experimental measurements. Furthermore, it was deduced that

$$CH_4 + OH \longrightarrow CH_3 + H_2O$$
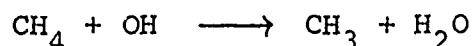
is not the primary reaction through which methane disappears in high temperature, lean-methane-oxygen reactions. Conclusive evidence suggested the reaction

$$CH_4 + O \longrightarrow CH_3 + OH$$

is important in both lean and rich methane flames, and experimental measurements suggested these two reactions as well as

$$CH_3 + H_2 \longrightarrow CH_4 + H$$

are important in the lean methane-oxygen reaction in the present study.

ACKNOWLEDGMENTS

The author takes this opportunity to acknowledge
the great debt of gratitude owed to his advisor, Professor
Irvin Glassman. His enthusiasm, advice and continued encour-
agement throughout this endeavor were greatly appreciated.
Special thanks are also extended to Dr. David W. Naegeli for
the many helpful discussions of the chemical kinetic aspects
of this research and for his suggestion of the HONO molecule
as a model for the transition complex of the carbon monoxide-
hydroxyl radical reaction.

The experimental work of this research could not
have been accomplished without the able assistance of Mr.
Joseph Sivo. His technical assistance in the design, fabri-
cation and operation of the experimental equipment is grate-
fully acknowledged. Thanks are also extended to Messrs.
C. Tamasi and D. Peoples for their assistance in the experi-
ments. The author would also like to make special mention
of the many important contributions to the experimental pro-
gram made by the late Mr. Anthony Bowzowski. His technical
talent and personal acquaintance were of great benefit to
all who knew him.

The valuable assistance of Mr. Tony Poli and his
staff in the design of various components of the apparatus
and preparation of this report is greatly appreciated.

Numerous discussions with fellow graduate students,
including Dr. Donald Hardesty, Mr. Daniel Carl, and Mr.
Richard Cohen, proved helpful.

TABLE OF CONTENTS

x

List of Figures

List of Figures

List of Figures

xiii

List of Figures

List of Figures

List of Tables

NOMENCLATURE

A   power of ten for the pre-exponent of an overall specific rate constant (dimensions depend on the reaction)

$\underline{A}$ crossectional area (cm^2)

a   overall reaction order with respect to a reactant or product

b   overall reaction order with respect to a reactant or product

c   overall reaction order with respect to a reactant or product

[C]   concentration of specie C $(mole\ cm^{-3})$

C_p specific heat at constant pressure

C_{ij} pre-exponential constant for elementary reaction i in direction j (f or r) (dimensions depend on the reaction)

d   diameter (cm)

d Q/dt   rate of energy release per unit time per unit volume

D/Dt   total derivative with respect to time

E   overall activation energy $(kcal\ mole^{-1})$

E_{ij} apparent activation energy, for elementary reaction i in the direction j (f or r) $(kcal\ mole^{-1})$

Eo_{ij} true activation energy for elementary reaction i in the direction j (f or r) (kcal mole^{-1})

k_{ov} $(10^A e^{-E/RT})$ overall specific rate constant (dimensions depend on the reaction)

k_{ij} specific rate constant for elementary reaction i in the direction j (f or r) (dimensions depend on the reaction)

m   overall reaction order

$\dot{m}$ mass flow rate (gm sec^{-1})

MW   molecular weight

n_i overall reaction order with respect to specie i

Pr   Prandtl number

ppm   parts per million

Q_{ij} pre-exponential temperature dependence for reaction i in direction j (f or r) (dimensions depend on the reaction)

r   radius (cm)

Re   Reynolds number

t   time (sec)

T   temperature (K)

v   velocity (cm sec^{-1})

x   distance (cm)

X_i^o initial mole fraction of specie i

E eddy diffusivity (cal cm^{-1} sec^{-1} k^{-1})

                                     emissivity

λ thermal conductivity (cal cm^{-1} sec^{-1} K^{-1})

ν kinematic viscosity (cm^{-1} sec^{-1})

ρ density (gm cm^{-3})

σ Stefan-Boltzman Constant (erg cm^{-1} K^{-4} sec^{-1})

σA standard deviation of the quantity A

T_{ind} characteristic time of an induction phenomena

T_{ox} characteristic time of an oxidation phenomena

T_q characteristic time for chemical quenching

T_r characteristic time of a chemical reaction

ϕ equivalence ratio

Subscripts

ad   adiabatic

eq   equilibrium

meas   measured

CHAPTER 1 - INTRODUCTION

1.1   Introduction

Air breathing propulsion and hydrocarbon fuels will maintain their great importance in transportation applications for several decades to come. Considerable research has been devoted to improving combustion performance through experimental development of better hardware and fuels, yet little more than a very general understanding of the high temperature reaction kinetics of hydrocarbon oxidations has been evolved. With increasing costs of experimental development, greater importance must be given to analytical guidance for improving performance and minimizing pollutant emissions in existing and new systems. Modeling of the necessary combustion chemistry in detail is presently an unrealizable achievement, both from lack of understanding of complete kinetic mechanisms and inaccurate or unknown elementary rate constants for many of the elementary reactions which must be included.

Thus, for engineering purposes, it is necessary to formulate global or partial global models for the complete oxidation mechanisms, and presently, only very limited kinetic data on the oxidations of the higher paraffin hydrocarbons (which comprise major percentages of conventional transportation fuels) exist. Thus, the general long range purpose of the present turbulent flow reactor study is to further the experimental knowledge necessary for guidance in the construction of such models. The turbulent flow reactor provides a

unique opportunity to study these oxidation reactions in an environment not totally unrelated to that occurring in propulsion applications, yet under controlled conditions where contribution from the complicating effects of diffusion and multidimensional convection can be minimized.

Chemical flow reactor techniques maintain great importance in the study of gaseous chemical reactions. For most gaseous reactions, large variation of reaction rate with temperature is observed, and a range of experimental conditions exist in which the chemical rate cannot be measured by static or intermittent (shock tube) techniques (i.e., the reactions are so rapid that isotropic conditions cannot be attained in static systems and are still so slow that non-ideal flow conditions result in shock tubes before measurable reaction can occur).

Fundamentally, all flow techniques employ quasi-steady flow conditions through a cylindrical tube. A chemical reaction is stabilized in some way in the flow, and the real time variable (and the reaction) is effectively "stretched" over a longitudinal distance by the flow. The "reaction zone" can then be studied by some sampling technique. Though laminar flames can be similarly "stretched" by lowering the ambient pressure, their kinetic interpretation is complicated by large gradients in concentration, temperature and velocity, and the associated problems of mass and energy transfer in the vicinity of the flame. Although the resulting interdependence of

variables can be partially circumvented by cooled flame
holders or reactant pre-heating, the range over which various
flame parameters can be changed independently is strictly
limited. Further, though flame studies have shown themselves
adequate for study of elementary chemical kinetics (e.g.,
[1-5])[*], Levy and Weinberg [6] have demonstrated that any
possibility of establishing universal global reaction mecha-
nisms (which might be applicable to highly stirred flows) is
vitiated by the strong dependence of the flame geometry on
the burner system and the surrounding environment.

It should not be construed that flow methods do not
have characteristic experimental problems of their own. Though
the experimental variables are no longer as strongly coupled
as in flames, one must be cognizant of any effects of surface,
since the diffusion time to the reactor walls is generally of
the same order as the flow time. In many cases this problem
can be alleviated (as in static systems) by proper treatment
or choice of surface materials. More tacit problems which are
often ignored are those of defining the relation between reac-
tion time and flow time, and determining to what extent mixing
effects the experimental measurements.

Most often, flow techniques have employed laminar
flow conditions in isothermal environments. Where exothermicity
of the reaction was high, the surface/volume ratio of the tube
was increased to establish the isothermal condition. Though
in some experiments Rayleigh and Fanno effects have been

---

[*]Numbers in brackets indicate references, listed beginning page
242.

considered, the assumption of one dimensional steady flow has nearly always been used to calculate the residence time of a fluid particle passing through the reactor tube.

It has long been recognized by fluid dynamicists that fully develo;_d laminar tube flow is better approximated by parabolic velocity and temperature profiles, (Hagen-Poiseuille flow), and it is not unexpected [7] that energy addition within the fluid field (as one would realize from an occurring exothermic reaction) and energy losses at the wall (to establish the necessary isothermal condition) can further distort radial velocity and temperature profiles. Batten [·] has studied the effects of laminar flow in an isothermal flow reactor, and he concluded that laminar velocity profiles can cause considerable error in calculation of contact times based on one dimensional flow.

It is clear that laminar flow must also result in inhomogeneous radial distribution of the reacting chemical species. Batten further noted that insignificant lateral mixing of adjacent streamlines occurred during observation times in his isothermal flow reactor. Coupled with the varying extent of reaction at different radial locations, radial gradients and diffusion of chemical species should result. Thus, a proper solution of the isothermal laminar flow reactor problem requires determinat_on of fluid dynamic and chemical parameters over the entire flow field.

Thus, introduction of uniform turbulence and relaxation of the imposed isothermal condition offer significant

advantages. With the transport properties of the fluid enhanced by turbulence and a near adiabatic condition established at the tube wall, time-averaged fluid mechanical and chemical properties closely approximating one dimensional quantities can be realized. Through a simple phenomenological development, Glassman and Eberstein [9,10] have shown that steady state kinetics and the time-averaged chemical kinetics of turbulent pipe flows are nearly the same for chemical reactions governed by radical species which achieve concentration levels through rapid elementary reactions. It was with these principles in mind that the original Princeton _turbulent_ flow reactor was developed by Crocco, Glassman and Smith [11].

Let us now discuss some of the background relevant to the present application of the turbulent flow reactor technique to the study of the paraffin hydrocarbon oxidations.

1.2 Background

References [12] and [13] propose methane, the simplest of the paraffin hydrocarbons, as a viable alternative to the conventional kerosene type fuels used in present commercial air transportation. Liquid methane appears to be economically competitive with conventional fuels on a cost per unit energy basis, and its additional heating value will allow payload increases of as much as 20%. Because of its very high resistance to pyrolysis, further increase in engine efficiency can be realized through use of the heat sink properties of the liquid fuel for turbine cooling.

Thus, both for the structural (and implied kinetic) simplicity of methane and its plausible future applicability as a fuel, the aforementioned hydrocarbon program was initiated with a study of the high temperature reaction of methane and oxygen. Expectations were that the experimental technique developed by Crocco, Glassman and Smith [14] and extended by Eberstein [15] and Sawyer [16] (Appendix A) successfully could be applied to this and the higher paraffin oxidation studies. The important merits of the technique, (1) of following the most important parameter in kinetic functions (temperature), while providing reasonably accurate estimates for rate, and reactant concentrations, and (2) of easily providing the volume of measurements necessary for statistical treatment of reaction rate data, have been amply demonstrated in [15] and [16]. That the method in general must be abandoned in the studies of paraffin hydrocarbon oxidations is by no means intuitively clear and warrants some discussion.

Application of the technique is restricted to the class of chemical reactions which meet two assumptions necessary for determination of an analytical expression relating the reactant concentrations and concentration gradients to the release of energy during the chemical reaction. These assumptions are:

(1) A "final" temperature plateau must exist somewhere in the reaction zone and can be associated with the completion of a chemical reaction sequence.

(2) An "overall" stoichiometric relation between
fuel and oxidizer consumed and energy released
exists and is invariant throughout the sequence;
i.e., energy release is a linear function of
reactants consumed.

Sawyer [15] noted that the existence of a "final
temperature plateau must be associated with total reaction
of one of the initial reactants, but not necessarily to its
completely oxidized or reduced state. The elementary reac-
tions of a chemical mechanism generally occur simultaneously
over the same time scale, and the effect of each upon the
overall energy release is indistinguishable. However, where
inhibition by reactants, products or reaction intermediates
is present and the chemical reaction proceeds through several
oxidized or reduced states, some of the elementary reactions
leading to the next oxidized or reduced state can be selec-
tively inhibited. Thus, certain regions of the energy
release profile of the total oxidation or reduction can be
related to the occurrence of partial oxidation/reduction
steps (although the contribution of each of the elementary
steps to the heat release will still be indistinguishable).
An example of this class of reactions is the reaction of
hydrazine and nitrogen dioxide. Above $800^{\circ}K$, Sawyer found
that the stoichiometric reaction,

$$N_2H_4 + NO_2 \longrightarrow 2H_2O + \frac{3}{2} N_2$$
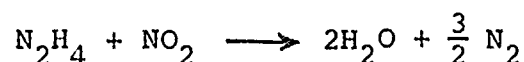
produces an energy release profile characterized by two steps (see Figure 1.1). This phenomenon can be accounted for if the reduction of NO_2 to N_2 proceeds sequentially through two steps:

i) complete reduction of NO_2 to NO by

$$NO_2 + N_2H_4 \longrightarrow \tfrac{1}{2}N_2H_4 + H_2O + NO + \tfrac{1}{2}N_2$$
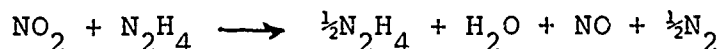
ii) secondary reduction of NO to N_2 by

$$NO + \tfrac{1}{2}N_2H_4 \longrightarrow H_2O + N_2$$

If the second reduction step is considered to be slower than the first and is very effectively inhibited by a product or intermediary[*] in the partial oxidation of N_2H_4, the energy release profile of Figure 1.1 will result. It is not necessary that the presence of a sequential multi-step reaction be as evident in the heat release profile as it is in this example. If the existence can be definitively established by other experimental evidence (e.g., sudden change in the heat release gradient or chemical analysis), the value of the temperature (T_i) separating the regions can be analytically calculated. Application of the previously developed techniques to this class of reactions is then tractable using the proper stoichiometric relation and Equation (A-9) and Equation (A-10) (Appendix A).

That the oxidations of paraffin hydrocarbons at high temperatures might be members of this class of reactions was first suggested by Friedman and Burke [17]. Comparison of

[*]Sawyer [15] suggests the inhibitor is water.
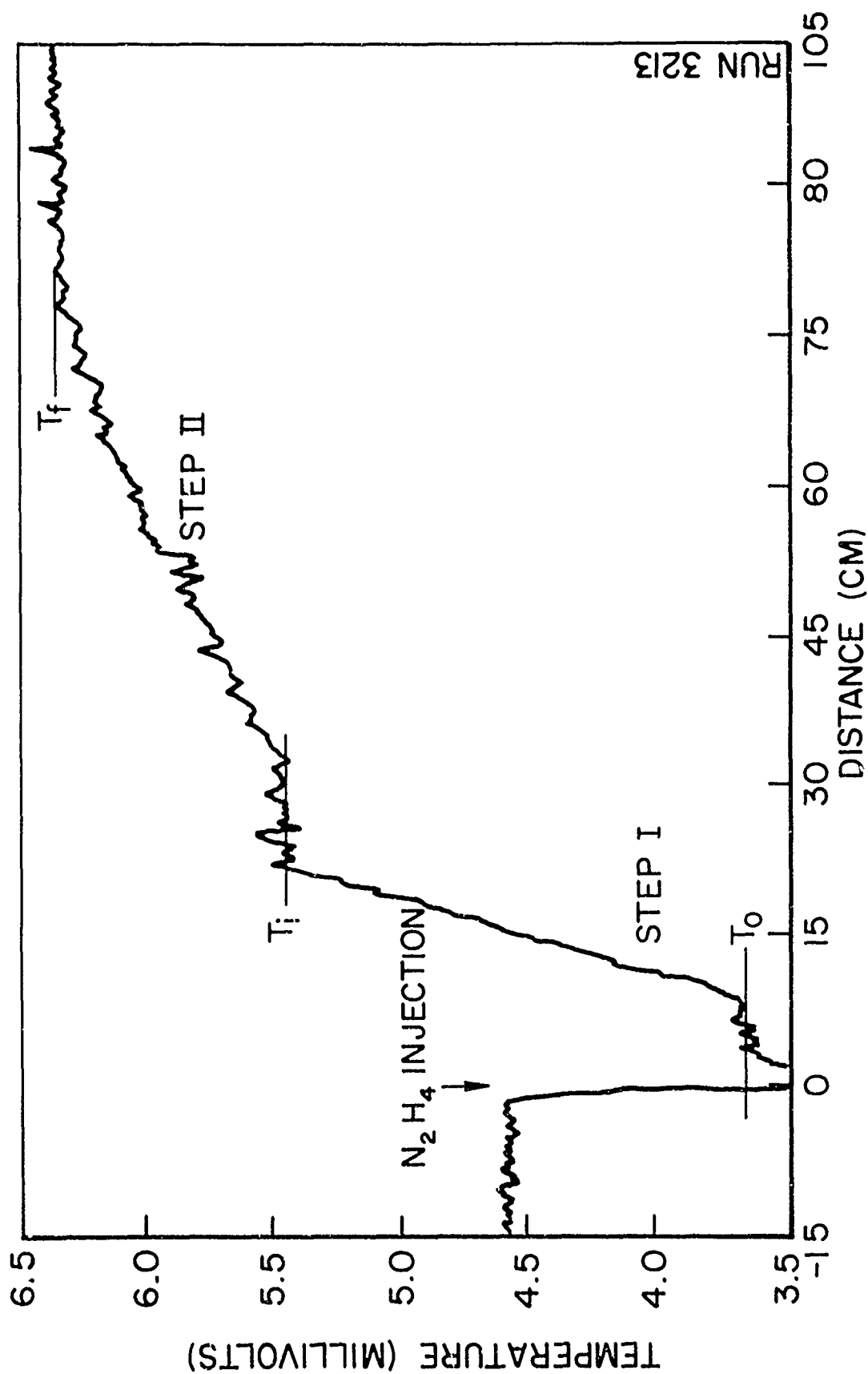
FLOW REACTOR
TEMPERATURE PROFILE, HYDRAZINE / NITROGEN DIOXIDE
REACTION

FIGURE I.I

JP13 - 4058-65

thermocouple measurements with a region of intense luminosity
in a low pressure propane flame led them to suggest that the
flame might consist of a two stage reaction zone:

i) a region of intense luminosity associated
with the oxidation of the hydrocarbon fuel
to CO and H_2O

$$C_3H_8 + \frac{7}{2} O_2 \longrightarrow 3CO + 4H_2O$$

ii) a second region in which the produced CO
is converted to CO_2

$$3CO + \frac{3}{2} O_2 \longrightarrow 3CO_2$$
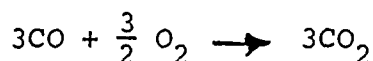
Early chemical sampling of low pressure propane
flames [18], C_2 hydrocarbon flames [19] and methane flames [20]
quantitatively established the general hydrocarbon oxidation
mechanism suggested above. However, these experiments also
demonstrated that the two stage oxidation process is not com-
pletely sequential. That is, the inhibition mechanism of the
secondary oxidation of CO does not prevent significant forma-
tion of CO_2 before the hydrocarbons disappear. Comparison of
the results of [20] with lower temperature laminar flow reactor
studies of the methane oxidation [21,22] suggested that the
inhibition was generally much more effective at temperatures
and conditions similar to those in the Princeton turbulent
flow reactor. Results of the capillary isothermal flow reactor
study of Burgoyne and Hirsch [21] are illustrated in Figure 1.2
where the products resulting in a fixed residence time (30 msec)
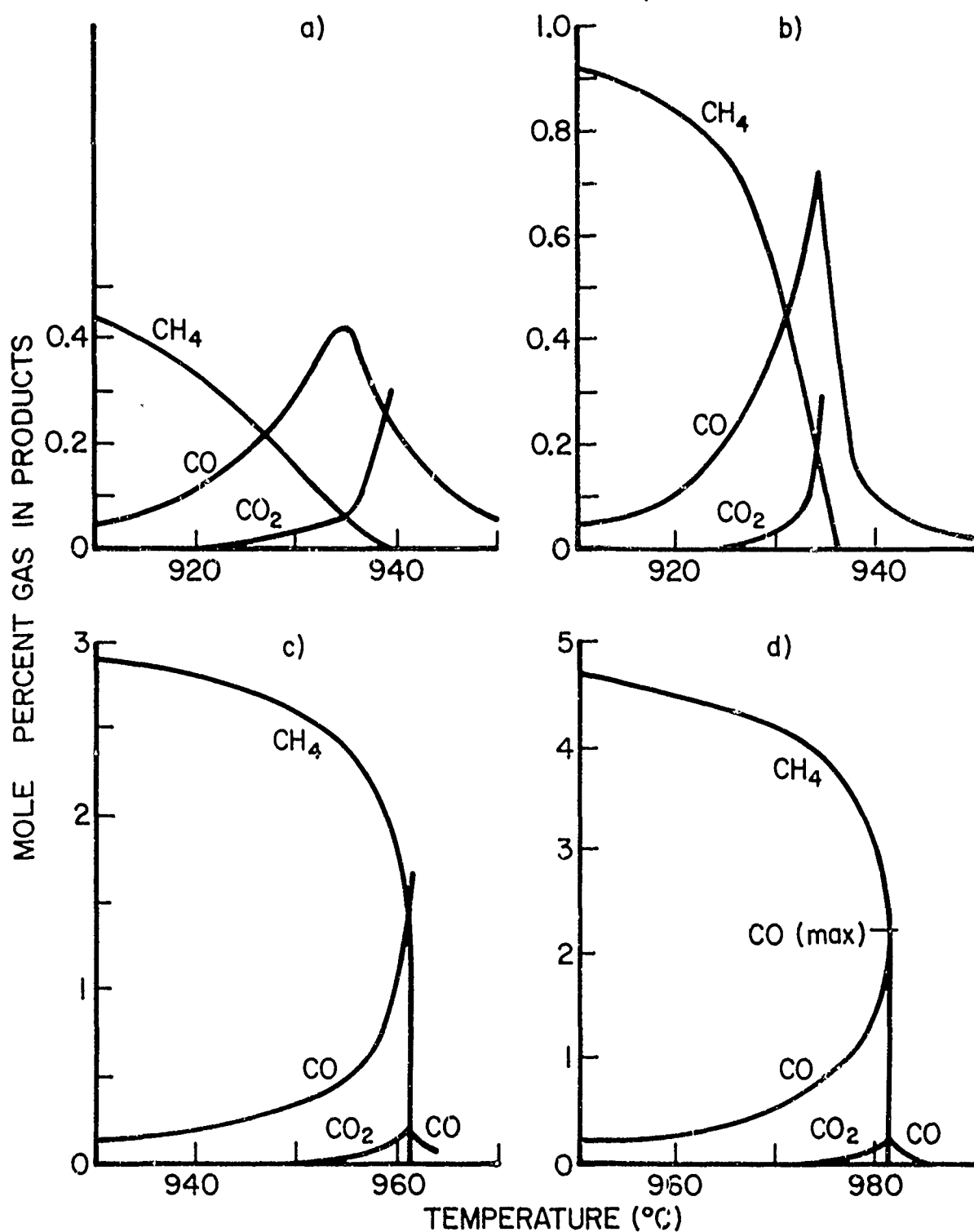
ISOTHERMAL CAPILLARY FLOW REACTOR STUDY, REF. [21]

COMBUSTION OF METHANE/AIR MIXTURE CONTAINING a) 0.5, b) 1.0, c) 3.0, and d) 5.0 % OF METHANE. AVERAGE RESIDENCE TIME ABOUT 30 msec

REPRODUCTION IN PART FROM REF. [21]

FIGURE I.2

are plotted versus the isothermal temperature of their capillary reactor. Their conclusions were restricted to qualitative interpretation of experimental results, and those important to the present argument were that:

i) Most of the resulting carbon from the methane oxidized appears in products as carbon monoxide until consumption of the methane is virtually complete.

ii) Only insignificant quantities of the total carbon of the initial methane ever appear as formaldehyde or species (unspecified) other than CO, CO_2, or CH_4.

These same conclusions were more clearly evident in the ensuing methane oxidation study of Pratt [22] in a 2.5 cm diameter laminar flow reactor. An example of some of his data is presented in Figure 1.3.

1.3   Preliminary Experimental Measurements

Having discussed background to the immediate work, let us look at some experimental evidence which drastically effected its development. An example of cursory turbulent flow reactor measurements of the heat release profile for the reaction of methane in air is shown in Figure 1.4. Comparison of the experimental heat release per mole of initial methane (assuming adiabatic conditions),
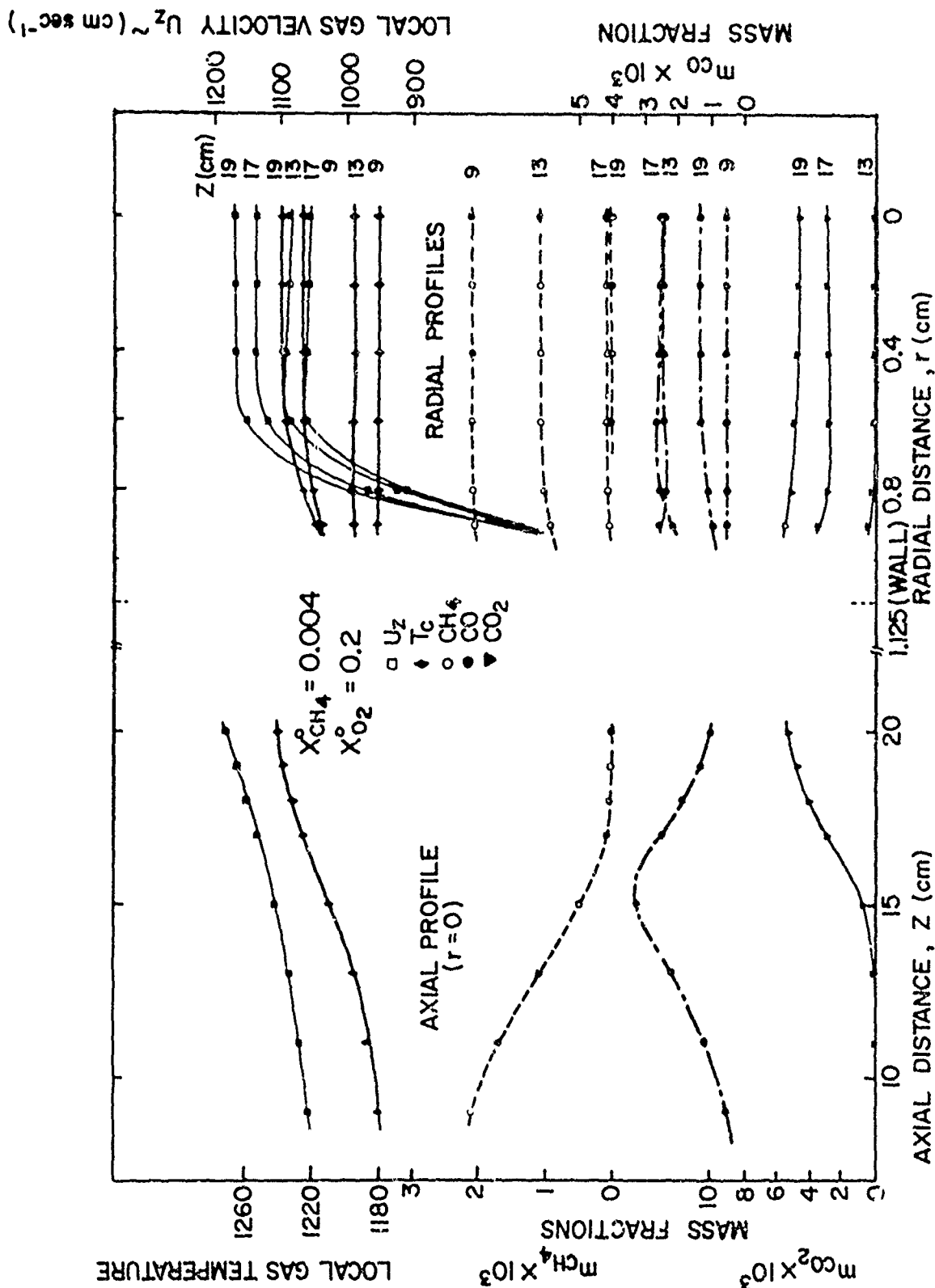
REACTION OF 0.4% CH_4 IN AIR
PROFILES OF VELOCITY, TEMPERATURE AND COMPOSITION
2.5 cm LAMINAR FLOW REACTOR, REF. [22]

REPRODUCED IN PART FROM REF. [22]

FIGURE 1.3

FIGURE 1.4

FLOW REACTOR
TEMPERATURE PROFILE, METHANE/AIR
REACTION

RUN 181
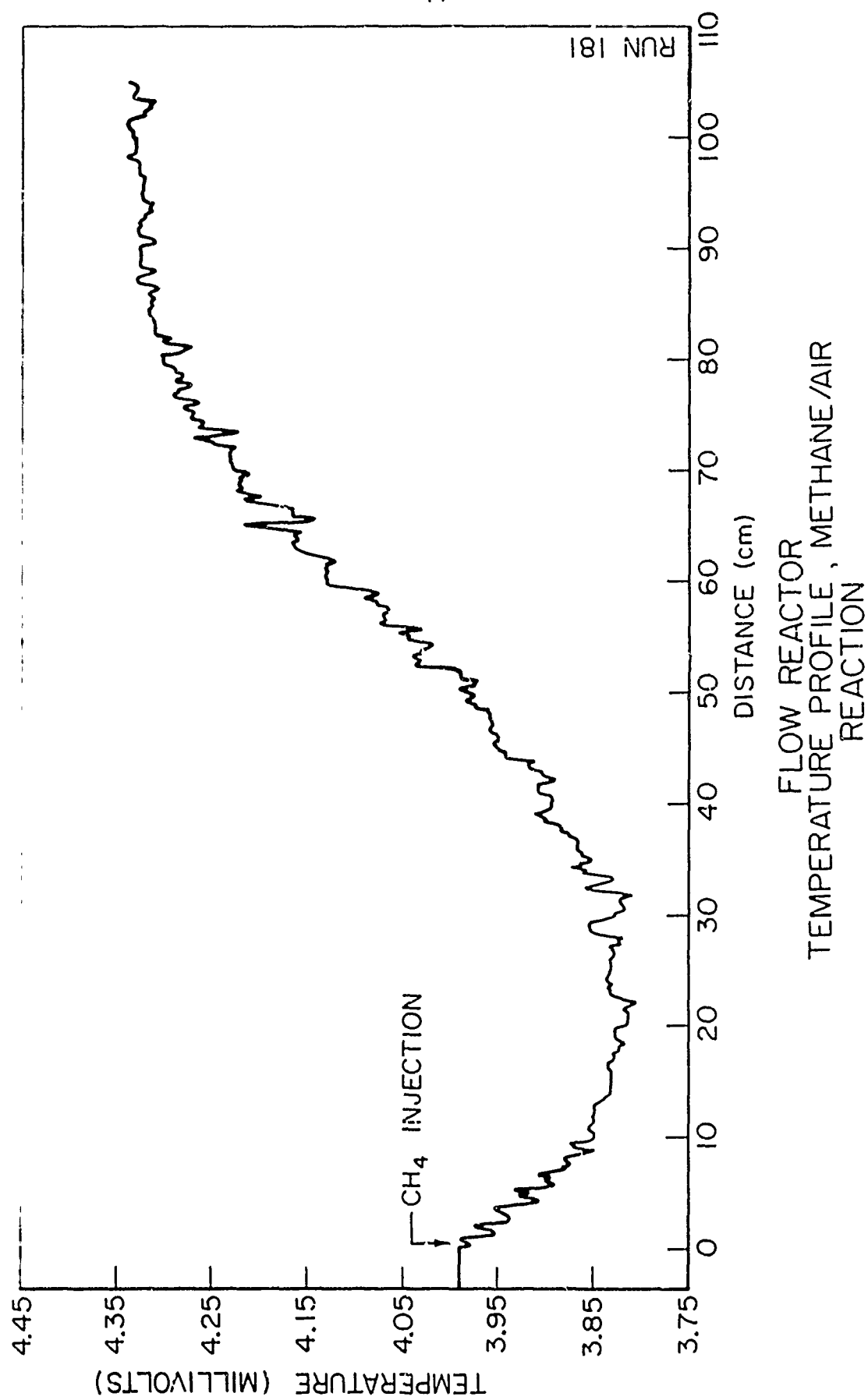
$$\Delta H_{exp_{CH_4}} \doteq \frac{C_p(N_2)}{X^o_{CH_4}} (T_f - T_o)$$

$$\doteq 185 \frac{kcal}{mole\ CH_4}$$

to the theoretical value for

$$CH_4 + 2\ O_2 \longrightarrow CO_2 + 2\ H_2O, \quad \Delta H_{298_{CH_4}} = 192 \frac{kcal}{mole\ CH_4}$$
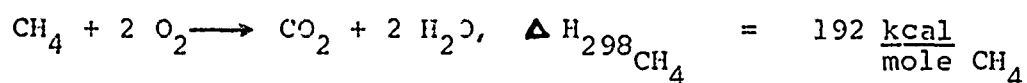
confirmed that complete oxidation of methane occurs during the time scale of observation; however, thermal measurements offered no evidence of a sequential two step reaction. This fact was not surprising; the results of Kozlov [23] indicated that, for equal concentrations of CH_4 and CO, the overall rate of oxidation of CO is approximately 50 times that for the oxidation of CH_4 to CO and H_2O. However, he also demonstrated that while the rate of oxidation of CO increases with the concentration of CO, the oxidation of methane was retarded by increasing methane concentrations. Thus, as the ratio $[CH_4]/[CO]$ decreases near the proposed transition in the sequential mechanism, the rates (and heat release rates) could become comparable. At the transition, the heat release profile could remain smooth.

Axial chemical sampling of the reaction zone was proposed as a conclusive test of the sequential model. Gas samples were removed from a methane air reaction using a water

cooled sampling probe and the samples were analyzed for CO, CO_2 and CH_4 using a Beckman G.C. 1 gas chromatograph. The results were used only in a qualitative manner. Let it be stated without further detail that the accuracy of the measurements was not adequate for quantitative interpretation. Results of one of the more complete tests are illustrated in Figure 1.5. It is clearly evident that observations differ significantly from those of Burgoyne and Hirsch [21] and Pratt [22] (Figures 1.2 and 1.3 respectively). Inhibition of the carbon monoxide reaction is not as complete as in the laminar reactor studies, and better than 50% of the initial methane has reacted in 30 msecs at temperatures lower than that ($900^{\circ}C$) at which Burgoyne and Hirsch observed no reaction at all.

Comparison of the carbon content of CO, CO_2 and CH_4 to that of the initial reactant indicated the presence of some intermediary reactant species, possibly HCHO, though the chemical character of the species was not experimentally verified. However, it was unlikely that the carbon discrepancy could be attributed solely to experimental error. Further qualitative sampling experiments established that the degree of production of carbon dioxide during the oxidation of methane to carbon monoxide is a function of both temperature and initial reactant concentrations. Cursory investigation of the propane/air reaction proved that the heat release per mole of initial propane consumed was also variable with extent of reaction, reactant temperature, and initial reactant stoichiometry,

FLOW REACTOR CHEMICAL ANALYSIS PROFILES
METHANE/AIR REACTION

FIGURE 1.5

JP13 R4142-70
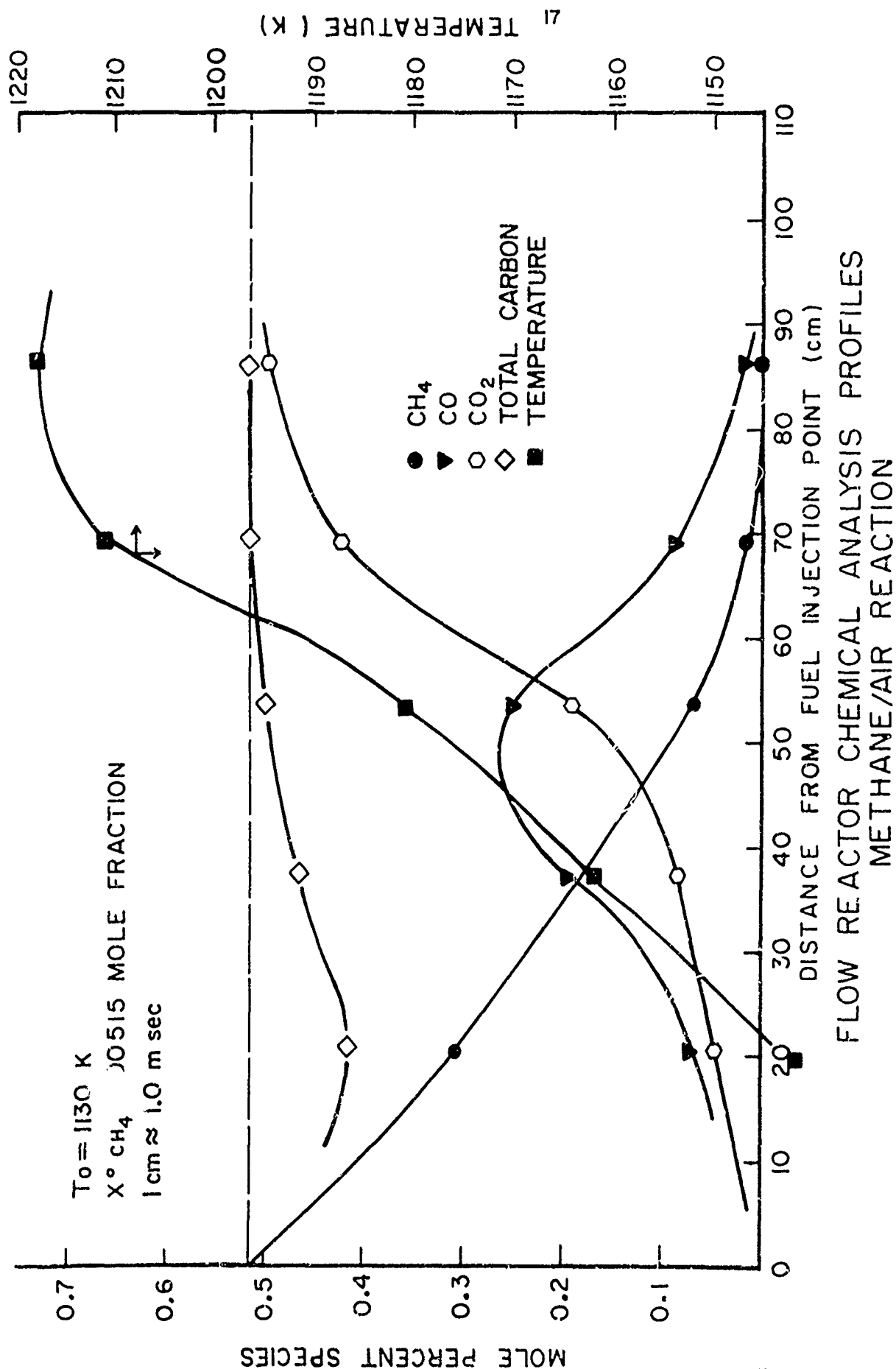
and similar chemical analysis established the presence of at least two (unidentified) intermediate chemical species (other than carbon monoxide) occurring during its complete oxidation. Thus, it was conclusively established that in the environment of the turbulent flow reactor, the oxidations of propane and methane are not closely approximated by the previously posed two step sequential mechanism. Indeed, without these experimental results in the turbulent flow reactor, previous evidence would have led to an erroneous conclusion. This fact provides further proof that comparison of chemical kinetic data resulting from different experimental techniques or even from different systems using the same techniques often can be misleading.

Summarizing the results of the previous discussion, chemical analysis of the oxidation reactions of propane and methane near $1000^{\circ}C$ confirms significant departure from theories which predict a linear relationship of energy release and reactants consumed; and thus, at these temperatures, the simple thermal analysis technique (described in Appendix A) used so effectively in previous work in this laboratory appears to be inapplicable to the study of the oxidations of these hydrocarbons. The departure arises from coincident occurence of the oxidation of the initial fuel to CO and the oxidation of CO to CO_2, and further complications from formation of intermediates (such as formaldehyde) are possible. Since the oxidations of higher paraffins most likely proceed through

degradation to and subsequent oxidation of hydrocarbons of
lower carbon number, a similar conclusion is inferred for the
higher paraffins as well. These facts force spatial chemical
analysis to be requisite for understanding of the chemical
reactions occurring in the turbulent flow reactor.

The significance of developing a versatile chemical
analysis system for use with the turbulent flow reactor cannot
be over-emphasized. Generation of a more complete chemical
and thermal characterization of a reaction must necessarily
increase the complexity of the experiment; however, such
characterization, in addition to providing data necessary for
engineering design (global or semi-global modeling), should
greatly enhance the possibility of unraveling the true kinetic
mechanism of the overall reaction and will in some cases per-
mit evaluation of elementary rate constants.

The most powerful chemical analysis technique for
stable chemical species presently appears to be gas chromato-
graphy (GC). In contrast to mass spectrometric (MS) and non-
dispersive infrared (NDIR) techniques, GC generally requires
quenching and storage of discrete samples, although in some
instances use of Gollay type columns [24] permits chromato-
graphy to be rapid enough to be used with on-line sampling
techniques. The complications of sample storage (e.g., surface
absorption, polymerization or other low temperature reactions)
are balanced by the universal sensitivity and fundamental
simplicity of the GC method. In comparison, NDIR techniques

exhibit both selective sensitivity and inseparable inter-
ference for chemical species of interest in higher hydro-
carbon oxidation studies. Further, if the number of unknown
species is large (as will be the case in the higher hydro-
carbon oxidation analyses), resulting MS spectrums become
so complex that, though sufficient theory exists for their
separation into the respective components, desired accuracy
of analyses cannot be realized [25]. Though the application
of the extensive GC techniques developed to study the oxida-
tion reaction of methane and carbon monoxide may not appear
necessary, the versatility and power of the techniques will
be necessary for analysis of the higher hydrocarbon oxida-
tions, and it is the proposed purpose of the present work to
construct techniques extendable to these studies.

1.4   Summary of Objectives

        Thus, the objectives of the present work are:

(1)   development of a general gas sampling and
       analysis technique employing gas chromato-
       graphy as the analysis tool and

(2)   application of this technique to the study
       of the oxidation of methane and carbon
       monoxide in the turbulent flow reactor.

        Further, while fulfilling these objectives, the
long-range objective of extension of the techniques to study
of the higher-paraffin oxidations must be kept in mind.

1.5 Presentation Outline

Chapter 2 will discuss the pertinent background and instrumentation of the turbulent flow reactor system, while Chapter 3 will be devoted to description of apparatus developed for kinetic measurements in the reactor. Chapter 4 will present a summary of experimental methods, while Chapters 5 and 6 will be devoted to presentation and discussion of the experimental measurements on the carbon monoxide and methane oxidations. A summary of conclusions and their relevance to future work are presented in the concluding chapter.

CHAPTER 2 - INSTRUMENTATION--THE FLOW REACTOR

Construction of a turbulent flow reactor system for studies of the paraffin hydrocarbon oxidations was guided by the previous studies of Crocco, Glassman, and Smith [11,14], Swigart [26], Eberstein [15,27] and Sawyer [16,28,29]. All studies including the present one attempt to experimentally model several theoretical considerations which facilitate interpretation of the experimental measurements, and these considerations will be reviewed in the following paragraphs.

2.1 Theory

Fundamentally, the turbulent flow reactor is a cylindrical tube through which a hot inert carrier gas flows at velocities high enough to attain uniform turbulent flow conditions (see Figure 2.1). The reactor tube is constructed so that the wall temperature rapidly equilibrates to the local temperature of the flowing gas (adiabatic wall). Small amounts of fuel and oxidizer are added to the inert carrier, and the turbulent mixing rapidly produces a homogeneous flowing gas mixture. Proper adjustment of initial carrier temperature and reactant and carrier flow rates result in a steady one-dimensional "reaction zone" spread over a considerable length of the reactor tube. For low initial concentrations of reactants, this "spreading" produces longitudinal gradients of reacting species and energy so small that diffusion effects in this direction are negligible (relative to convection). Since the tube is large and energy addition and Mach numbers
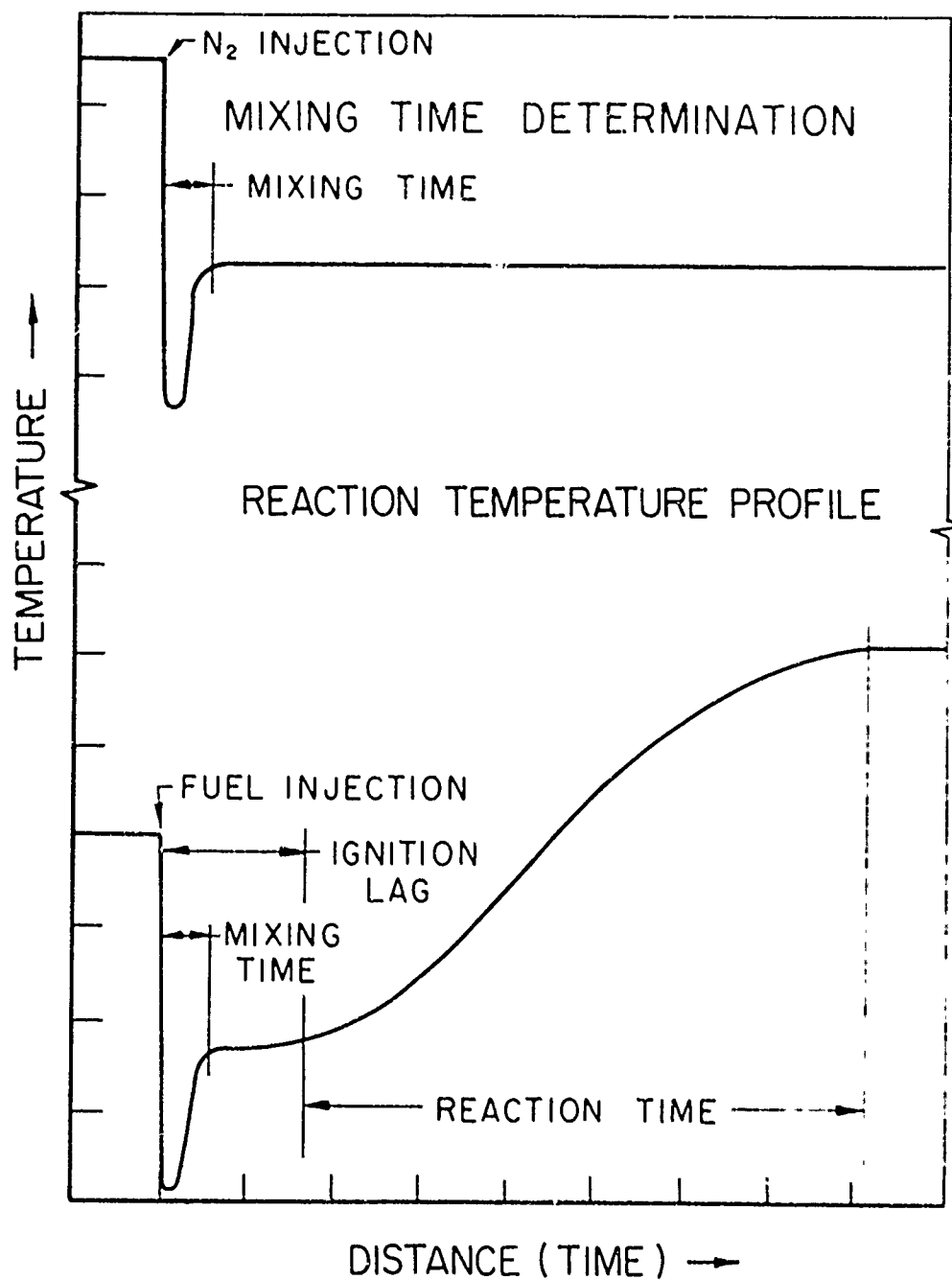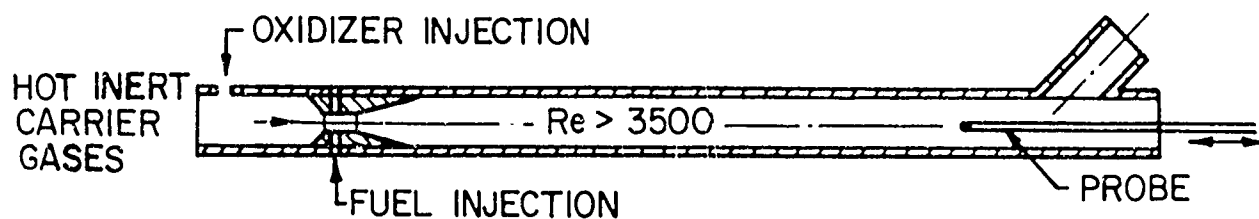
THE TURBULENT FLOW REACTOR
(THEORY)

FIGURE 2.1

are small, Rayleigh and Fanno effects are negligible, and
the static pressure throughout the flow field is constant.
Since the bulk of the flowing gas is inert carrier, the state
parameters are related by the ideal gas law, and the physical
properties of the fluid can be considered to be those of the
carrier.

The discussions of Chapter 1 and Appendix A show
that while some chemical reactions are satisfactorily charac-
terized by temperature measurements alone, others require
measurement of the longitudinal reactant and product species
profiles as well. These data can be obtained by extending
chemical sampling and/or temperature probes longitudinally
through the zone from the exit of the reactor tube. Since
the flow is steady, the longitudinal gradients of all param-
eters with distance are related to "real" time derivatives
by the convective part of the substantial derivative,

$$\frac{D}{Dt} = \cancel{\frac{\partial}{\partial t}}^{0} + v\frac{d}{dx}$$

As noted previously, v can be calculated on one-dimensional
principles, assuming fluid properties to be those of the
carrier. However, the relation of a specific axial coordinate
to real time is not well defined since the initial time
coordinate (where reaction begins) occurs at some unknown
position within the mixing region. One might suspect that
this fact could alter the reaction phenomena occurring fur-
ther downstream; however, the existence of the very fast

elementary kinetics which initiate chemical reaction before mixing is complete, permit rapid adjustment of the chemistry as the flowing gas approaches radial uniformity. Further, it is important that the turbulence necessary for rapid mixing and production of these one-dimensional characteristics does not effect the chemical kinetics. Provided the time necessary for a perturbed radical concentration to return to a level governed by static chemical kinetics is very short relative to the turbulent "eddy" lifetime, each eddy will spend most of its lifetime reacting under static conditions. Glassman and Eberstein [9,10] characterize this chemical time by the chemical relaxation time, i.e., the time necessary for a "steady state" concentration of reactive centers to be approached. As they have shown for the hydrazine decomposition, this time is generally very small in comparison to the eddy lifetime, but there is no guarantee that this condition will prevail in other reactions. Without a complete kinetic mechanism, it is difficult to argue analytically that such a condition exists; however, experimentally one can establish that the above is true if the chemical rate measurements are independent of the level of turbulence (the eddy lifetime) and therefore the carrier velocity. Summarizing the theoretical properties that the experiment, equipment, and procedure are to model:

      (1) steady reaction zone

      (2) adiabatic reactor wall

(3) one-dimensional (that is, radial
distribution of energy and species
are constant)

(4) no longitudinal diffusion of mass
or energy

(5) constant pressure reaction zone

(6) ideal gas

(7) no effect of turbulence on the
chemical kinetics

2.2   Experimental Apparatus

Modification and re-construction of much of the
previous experimental apparatus were made necessary by the
stringent experimental control requirements imposed by the
chemical sampling and analysis technique and by the very
high temperatures necessary for study of the methane oxida-
tion. The experimental equipment is comprised of: the
reactor assembly consisting of the reactor tube and support
equipment necessary for minimization of energy losses to
the reactor wall, a probe traverse mechanism for control
and position measurement of the instrumentation probes used
to characterize the "reaction zone, and carrier and reac-
tant (fuel and oxygen) flow systems which supply the reactor.
The equipment will be briefly discussed in the following
pages and the section will conclude with a summary of the
experimental procedure and control and range of the experi-
mental variables. A schematic and photographs of the
assembled equipment are presented in Figures 2.2 - 2.5.

FIGURE 2.2

CHEMICAL KINETIC FLOW REACTOR

FLOW REACTOR INSTRUMENTATION

FIGURE 2.3

REACTANT CONTROLS

REACTANT MONITORING
EQUIPMENT

CARRIER FLOW CONTROLS
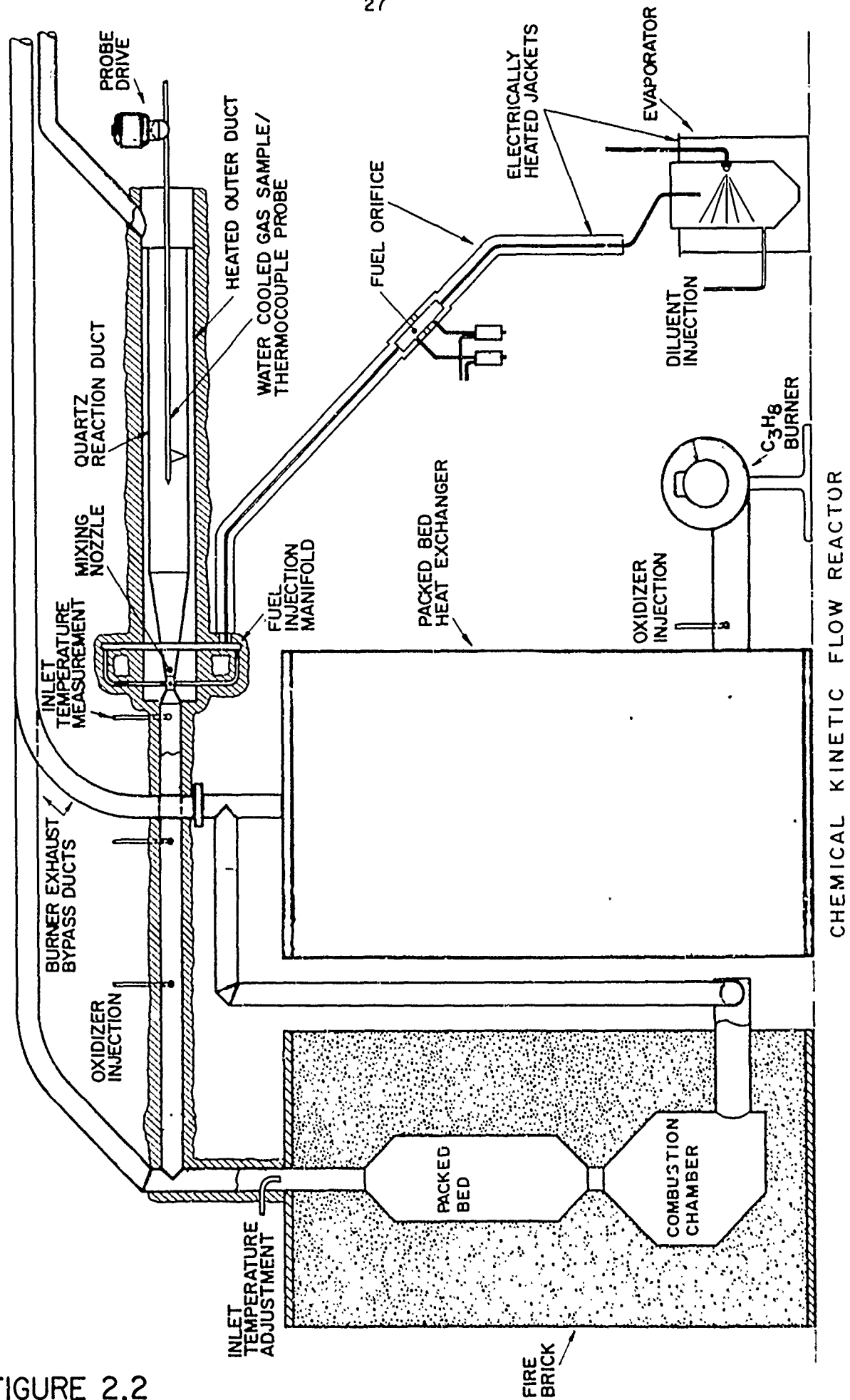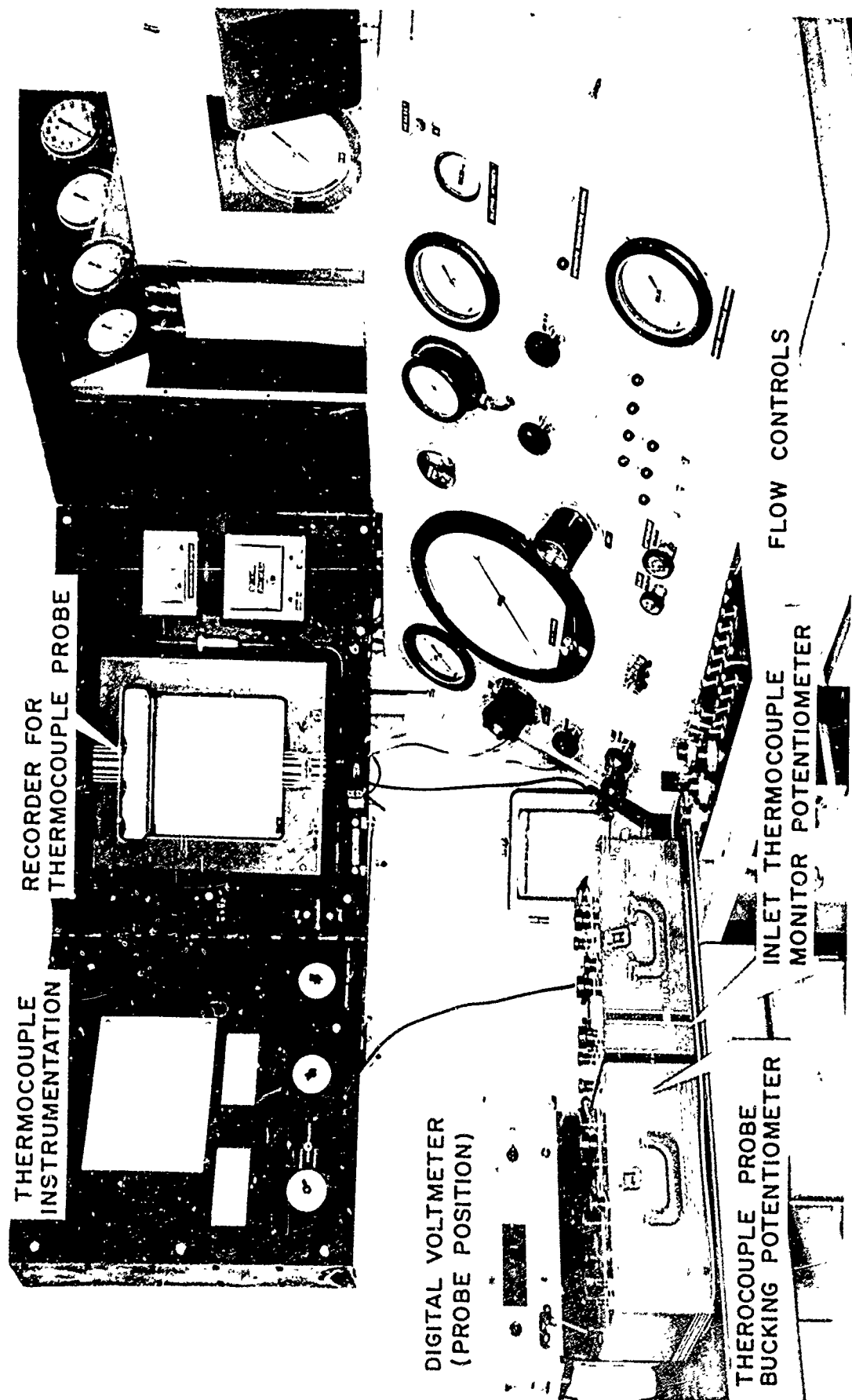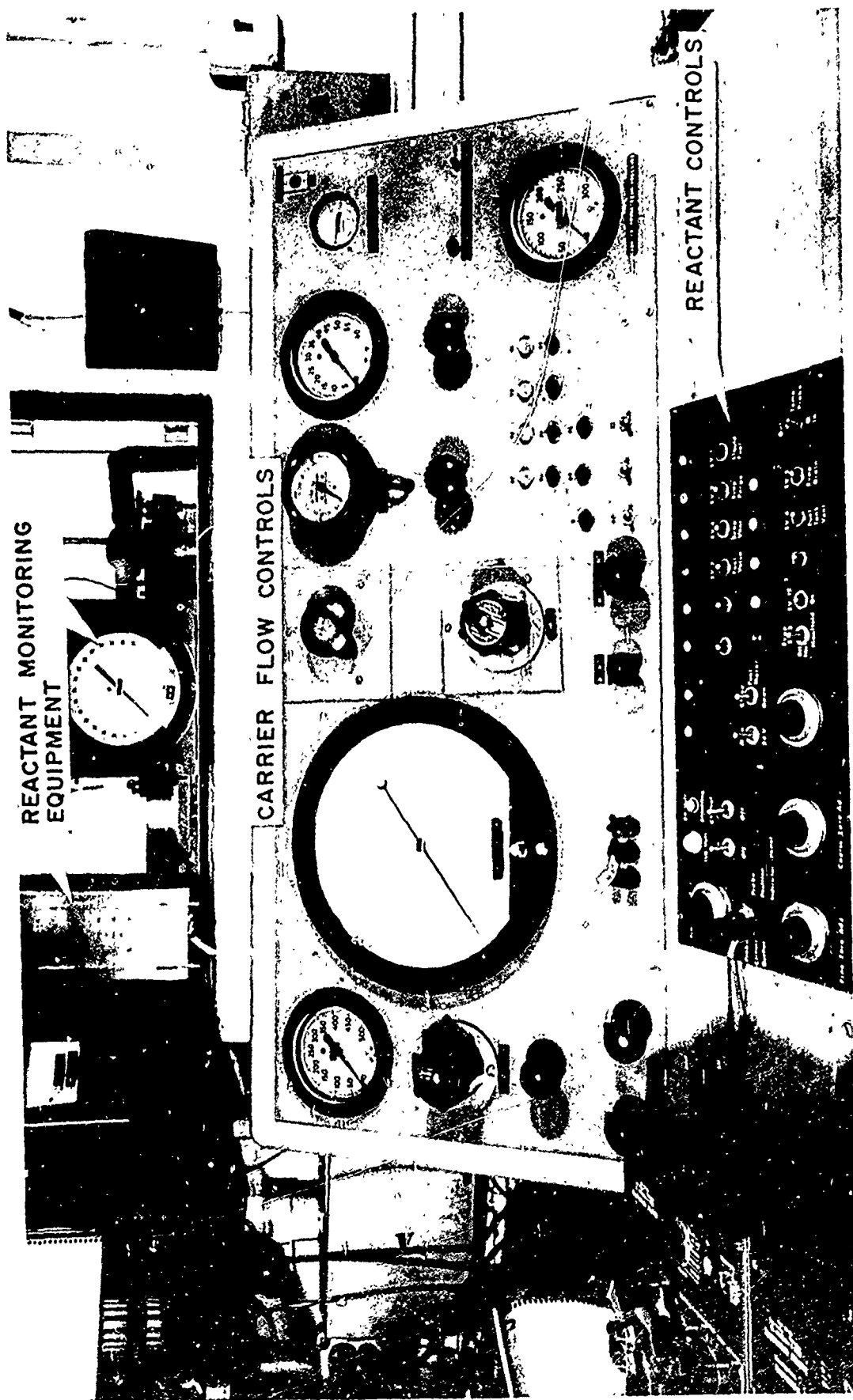
FLOW REACTOR CONTROL INSTRUMENTATION

FIGURE 2.4

609 P-6 72

SAMPLING & TEMPERATURE PROBE

REACTOR ASSEMBLY

TRAVERSE MECHANISM

HEAT EXCHANGERS

HEATER POWER CONTROL

EVAPORATOR SYSTEM

BURNER SYSTEM
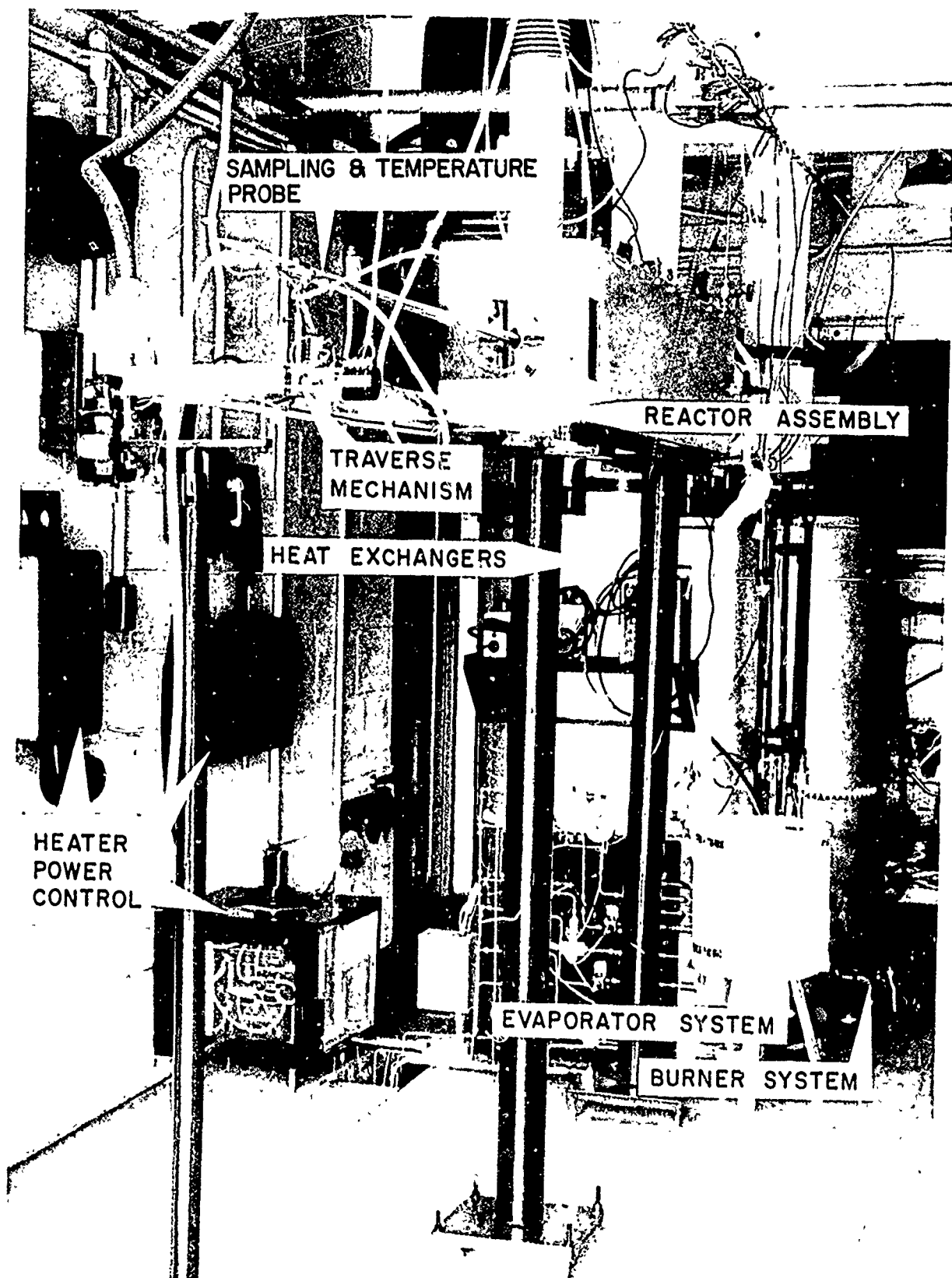
FLOW REACTOR INSTRUMENTATION

FIGURE 2.5

2.2.1 Reactor Assembly

A cut-away drawing of the reactor assembly is presented in Figure 2.6. The main reactor tube (illustrated in Figure 2.7) consists of a 10 cm diameter cylindrical quartz tube with an adjoining conical inlet section. Cylindrical quartz reactor inserts of 5 and 7.5 cm diameter are available to reduce the cross-sectional area and increase the surface to volume ratio of the reactor section. Four capillary quartz tubes, equally spaced around the circumference of the entrance to the main reactor tube, provide uniform, high velocity injection of the reactant fuel. Reactant oxygen is added upstream of the reactor; rapid mixing and homogeneous distribution of the carrier, oxygen, and fuel are insured by the conical inlet section.

The main reactor is suspended in an oven constructed of 4 electrical resistance heating tubes, firebrick and insulation. The heating tubes (Figure 2.8) are constructed of Kanthal A-1 resistance wire, and adjustment of resistances in parallel with the two central heating tubes permit independent control of power input to the central regions of the oven. Adjustment of power input and parallel resistances is aided by Pt/Pt 13% Rh thermocouple monitoring instrumentation. Reaction zone parameters are measured by longitudinal extension of instrumentation probes along the central axis of the reactor tube from its exit.

FIGURE 2.6

REACTOR ASSEMBLY

PROBE

EXHAUST

ACCESS DOORS

OVEN HEATER TUBE

MAIN REACTOR TUBE

FIRE BRICK

INJECTOR TUBE

POWER TERMINALS

INSULATION

THERMOCOUPLE MONITOR (EXAMPLE)

FUEL

INLET TEMPERATURE MONITOR

CARRIER + OXYGEN

JP13 R 4247 72
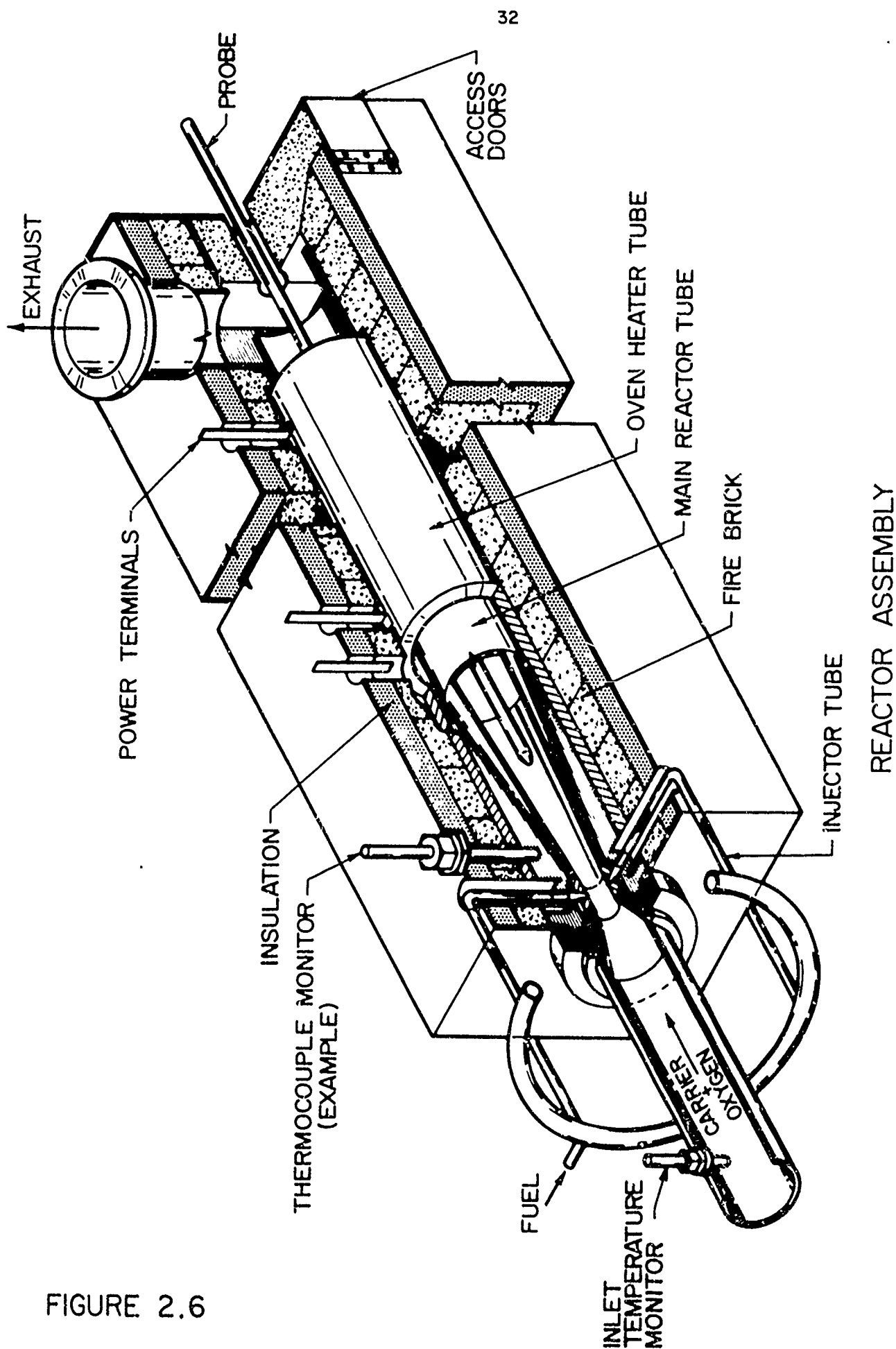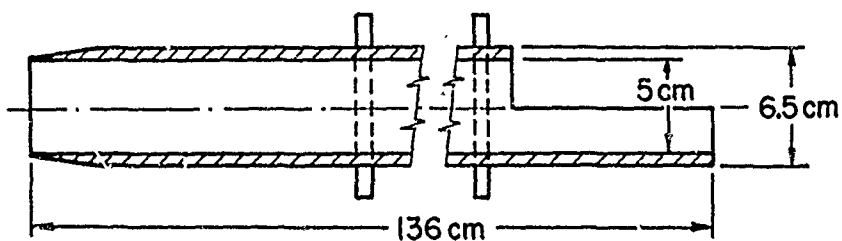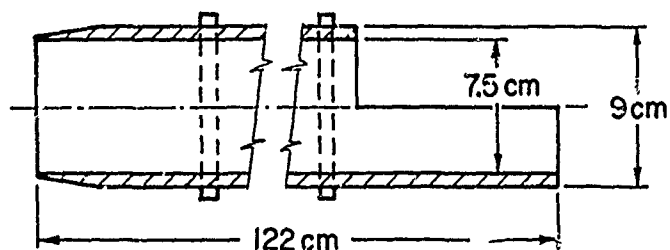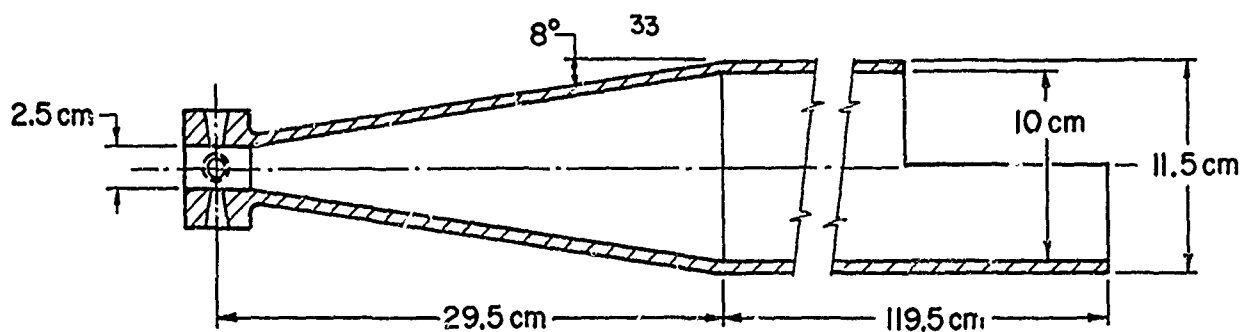
DIMENSIONAL SKETCH OF REACTOR TUBES
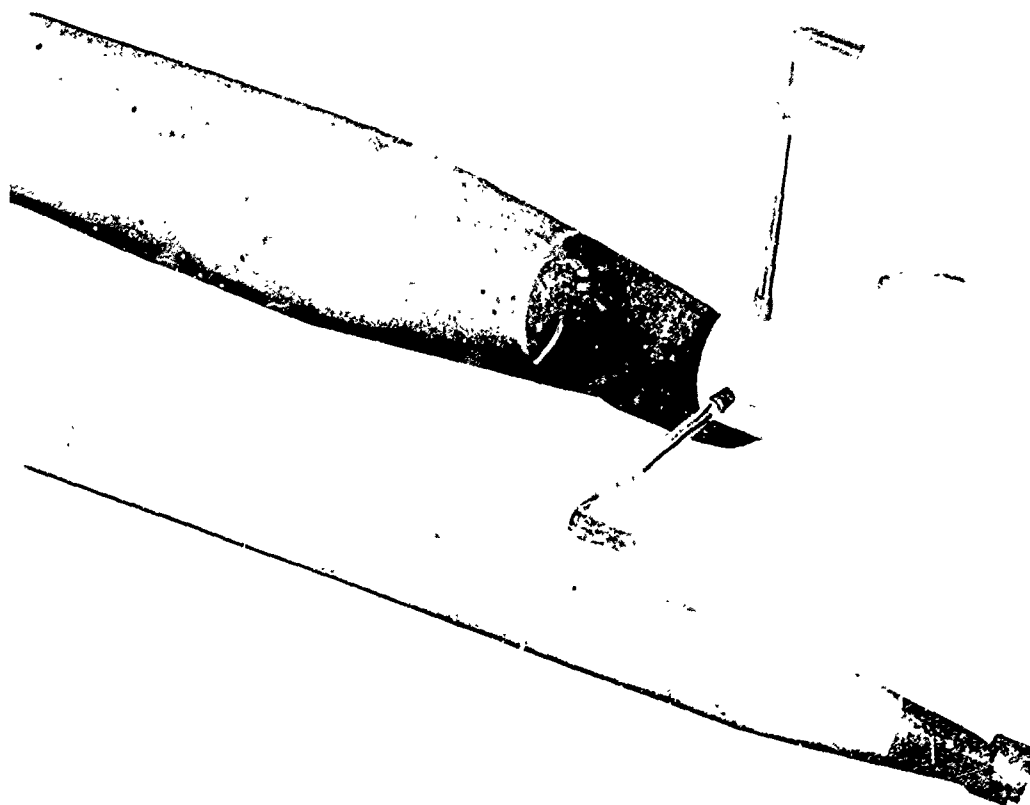
QUARTZ REACTOR TUBE ASSEMBLY

FIGURE 2.7

T/C   T/C   T/C   T/C

HEATER
TUBE

.5-5 Ω, 500 W

VARIAC SYSTEM
220 volt, 50 amps
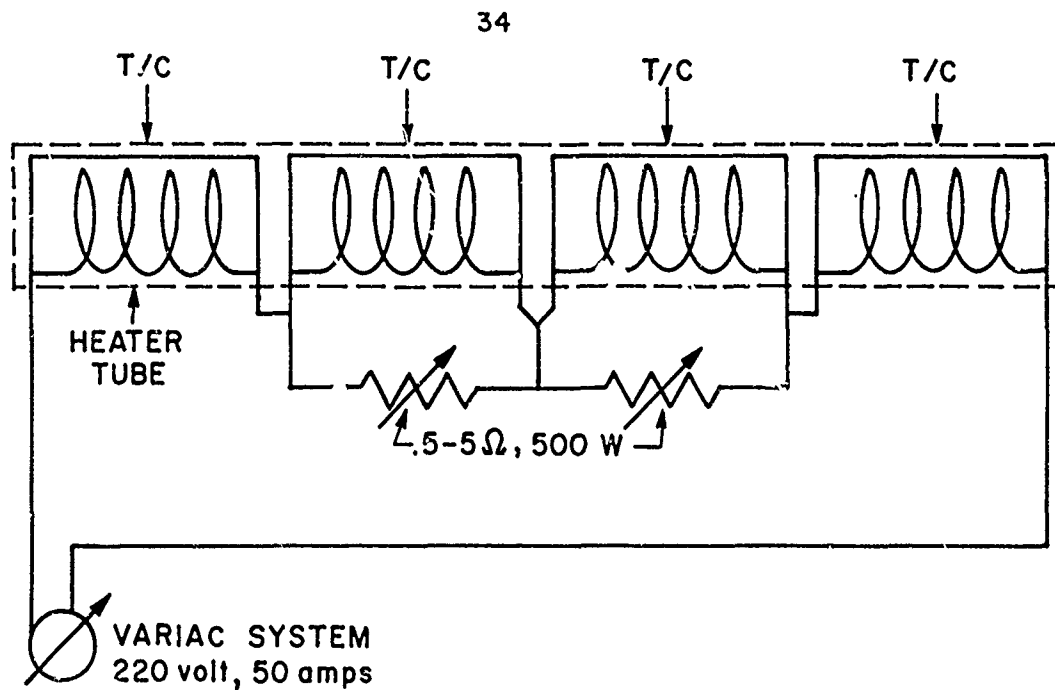
POWER SCHEMATIC

KANTHAL 13X HEATER TUBE

.5 Ω, 1300W MAX. OUTPUT
I.D.-5"   O.D.-6"
LENGTH-13"
MAX. TEMP. = 1325 °C

REACTOR OVEN HEATING SYSTEM

FIGURE 2.8

2.2.2 Probe Traverse Mechanism

Longitudinal positioning of thermocouple or gas sampling/thermocouple probes in the reaction zone is controlled by a probe trolley mechanism (see Figure 2.5). The traverse mechanism electronics consisting of relays, an electromagnetic brake and a synchronous motor provide for two modes of operation:

(1) Continuous traverse mode

A constant velocity traverse of the entire length of the reactor tube at 2.0 cm/sec is convenient for monitoring adjustment of carrier and reactor wall temperatures, and measuring longitudinal reaction temperature profiles of a chemical reaction. The latter information along with initial carrier, fuel, and oxidizer flow rates are all that is necessary for analysis of reactions which can be characterized as in Appendix A.

(2) Cyclic traverse mode

Control of power and electromagnetic impulse braking of the probe drive mechanism result in a move/hold cycle which can be repeated over the entire length of the reactor tube. Cycle movement and hold time are continuously variable from 1.5 to 12 $\pm$ .2 cm and 1 to 60 $\pm$ .5 seconds respectively. Such operation permits acquisition of point chemical sample and temperature data at equidistant positions through the reactor tube and is made necessary by the finite response time of the chemical sampling system.

The longitudinal position of an instrumentation probe relative to the fuel injection ports is determined by voltage drop measurements across a linear resistance pot coupled to the probe drive mechanism. The voltage drop is displayed on a Hewlett-Packard Model 3440A digital voltmeter; overall accuracy of the position measurements is within $\pm$ .1 cm. (This should be compared to an overall length of a reaction zone of greater than 60 cms.)

2.2.3 Carrier Flow System

The carrier system provides the necessary energy and controls for maintaining the temperature and flow of an inert carrier gas to the flow reactor assembly. A schematic of the flow system is presented in Figure 2.9.

Energy is supplied to the carrier gas (usually nitrogen or air) by two ceramic packed bed heat exchangers connected in series and constructed similarly to those used in the investigations of Sawyer. The heat exchangers are pre-heated to temperatures approaching $1500^{\circ}K$ by two (independent) propane/air heating systems. One of the burner systems is illustrated in Figure 2.10. The hot carrier gas is delivered to the reactor assembly through an inlet section constructed of Inconel tubing and heated by Kanthal A-1 electrical resistance heating ribbon. A number of injection ports are provided in the inlet section for addition of oxidizer or other reactants (e.g., water vapor in the carbon monoxide oxidation). Pt/Pt-13% Rh thermocouple instrumentation
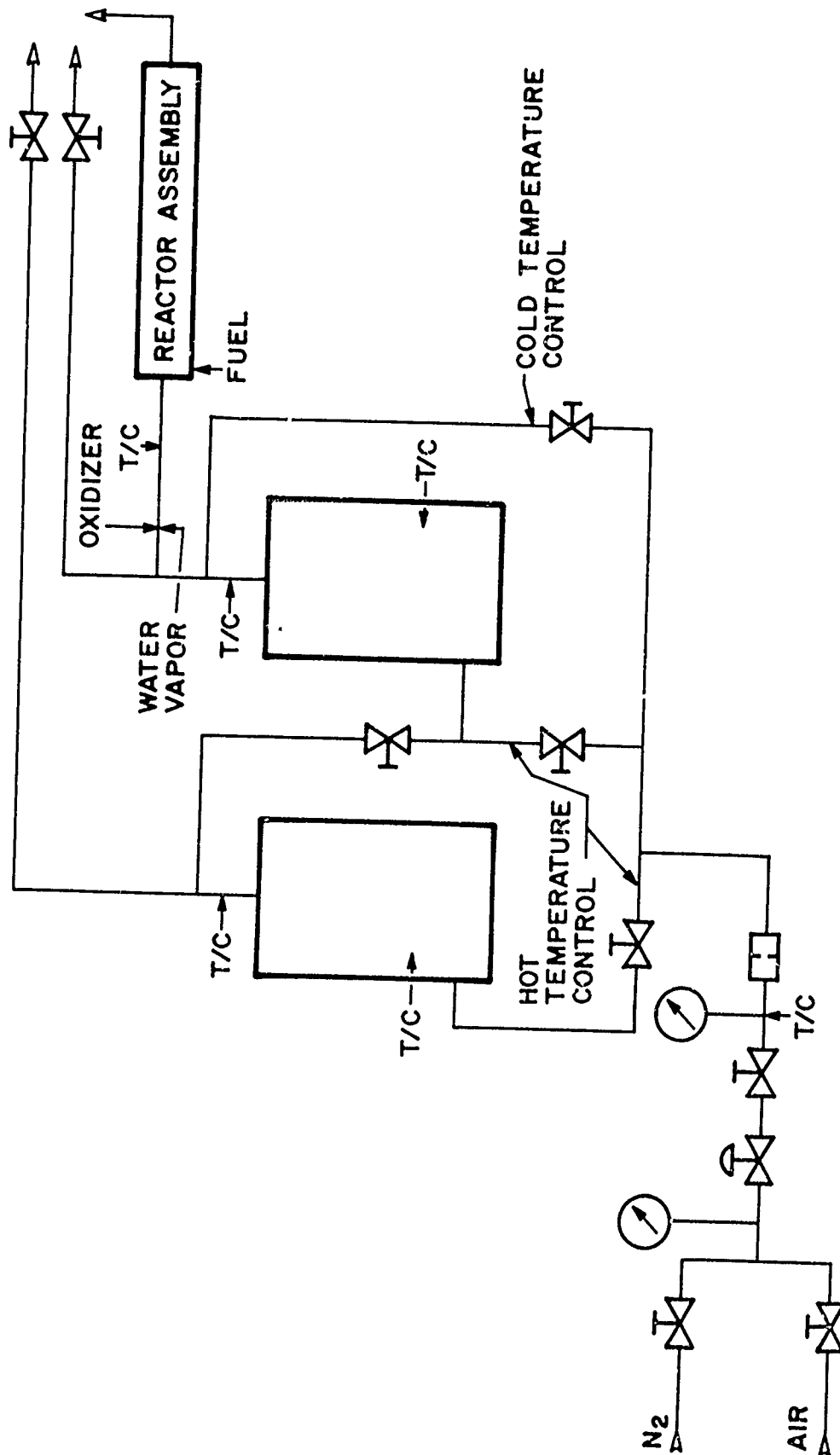
CARRIER SYSTEM FLOW SCHEMATIC

FIGURE 2.9

BLOCK
COOLING
FLOW

BURNER NO. 416-14
(ECLIPSE FUEL ENG. CO.)

AIR
HIGH PRESS.

AIR
LOW PRESS.

PROPANE

T/C

Ⓐ

Ⓐ

Ⓐ
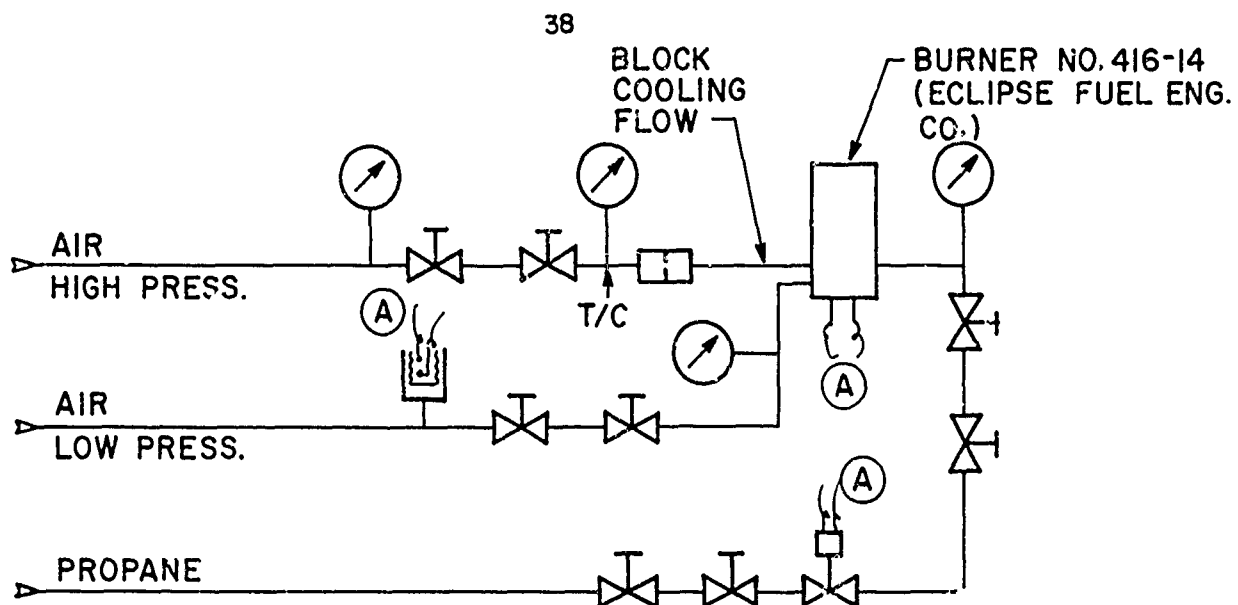
NOTE:
Ⓐ SAFETY CIRCUIT.
NO AIR PRESS. NO FUEL FLOW
NO IGNITION SOURCE NO FUEL FLOW
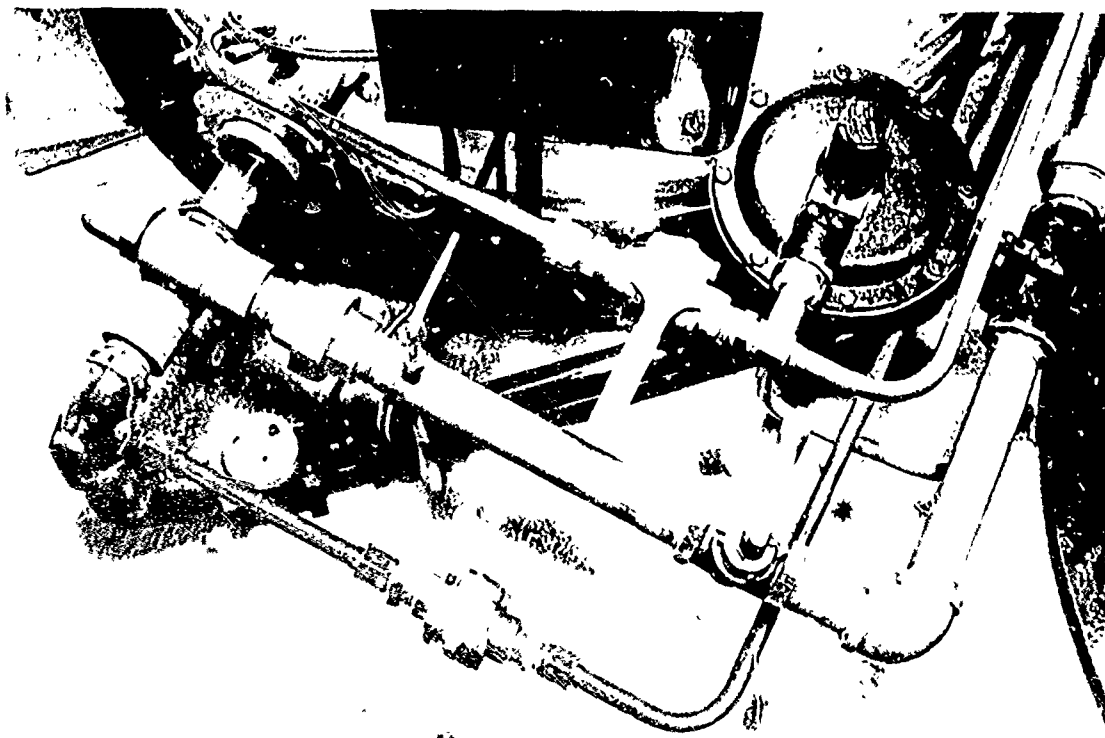
BURNER SYSTEM

FIGURE 2.10

is employed to continuously monitor the temperature of the carrier gas/oxidizer/catalyst mixture as it enters the mixing section of the reactor assembly. Adjustments of the mixture inlet temperature are achieved through by-passing of a controlled fraction of the carrier gas to the exit of the second heat exchanger. Manual adjustment of the by-pass flow was found adequate to control the time averaged inlet temperature to $\pm$ 1°K relative. Total carrier gas flow rate is controlled by a regulator/needle valve arrangement and is measured by a critical orifice technique.

2.2.4 Reactant Flow Systems

The reactant flow systems control and determine the flow rates of fuel and oxygen to the flow reactor. Since the reactants used in the present studies are stable, gaseous compounds under standard conditions, the handling problems created by the hazardous liquid reactants used by Sawyer and Eberstein are avoided. Though it was not necessary for the present studies, an evaporator system has been developed to supply gaseous fuels in the higher hydrocarbon kinetic studies. The flow schematics of the gaseous oxygen and fuel supply systems are presented in Figure 2.11.

Oxygen is added to the inert carrier gas through one of the available ports in the reactor inlet section. The flow rate is controlled by a pressure regulator/needle valve assembly, and the rate is measured using critical flow orifice
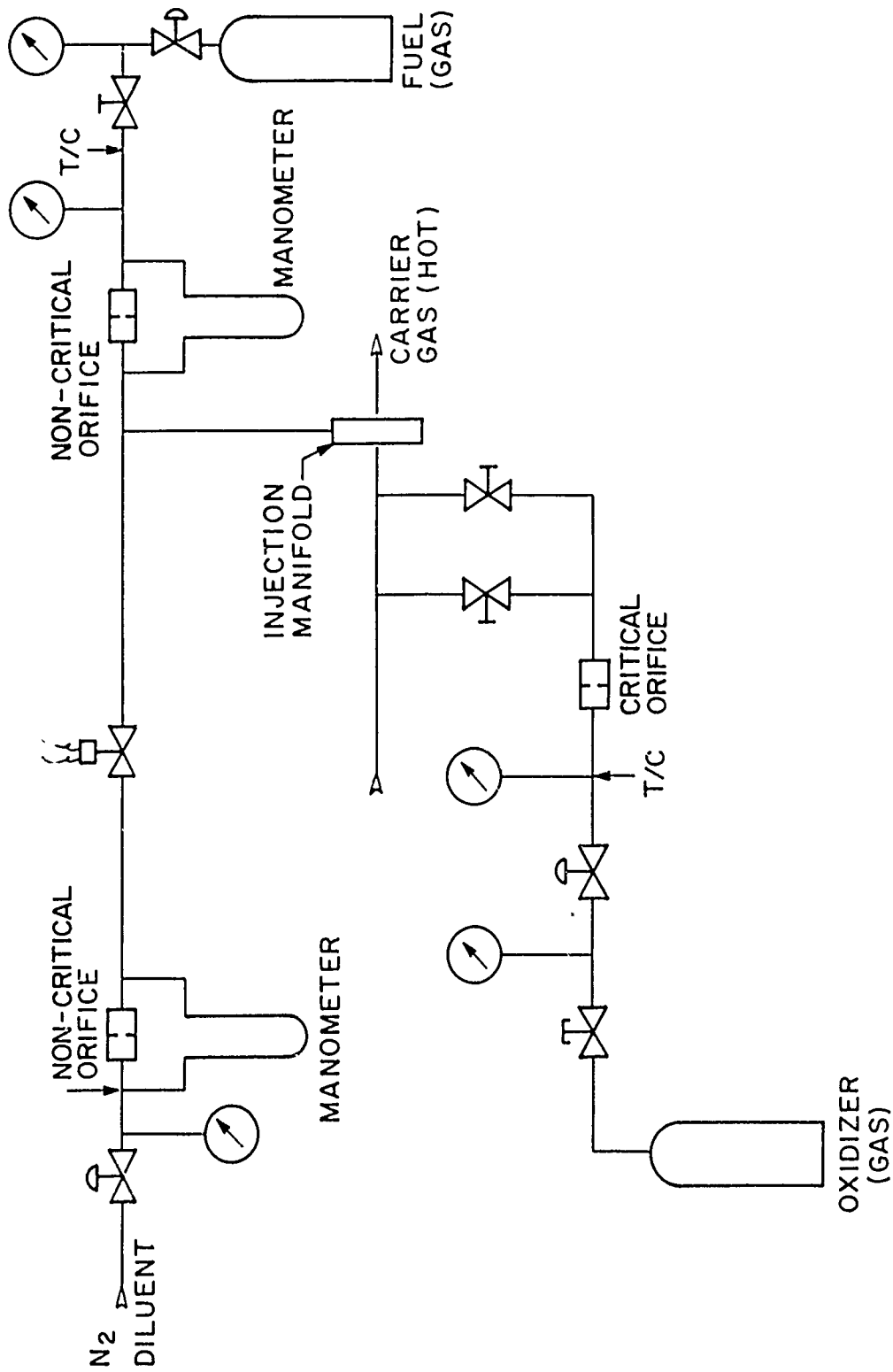
REACTANT FLOW SCHEMATIC

FIGURE 2.11

instrumentation calibrated in this laboratory. Oxygen concentrations greater than 20% are achieved by replacing the nitrogen carrier gas with air.

Gaseous fuel is supplied to the capillary quartz injector tubes in the reactor assembly. Injection velocity of the reactant fuel can be increased by addition of diluent nitrogen to improve mixing with the carrier gas/oxygen mixture entering the conical inlet section of the reactor tube. Fuel and diluent nitrogen flows are controlled by pressure regulator/ needle valve assemblies and are measured by non-critical flow orifice instrumentation calibrated in this laboratory.

2.3   Experimental Procedure

Though the type of measurements necessary to characterize the kinetics will depend on the particular reaction studied, a common run procedure of the flow reactor itself can be recognized.

This run procedure includes pre-heating of the heat exchangers, and adjustments of inlet and reactor heater power to establish and control temperatures near the range at which experiments are to be conducted. Because of the large thermal inertia of the system, temperature stabilization requires from 4 to 6 hours. Final adjustments are monitored by the inlet temperature measurements and longitudinal thermocouple traverse measurements of the reactor tube. Such measurements are illustrated in Figure 2.12.

FIGURE 2.12

FLOW REACTOR
TEMPERATURE PROFILE,
NO REACTION

RUN 180

DISTANCE (cm)

TEMPERATURE (MILLIVOLTS)

N_2 INJECTION
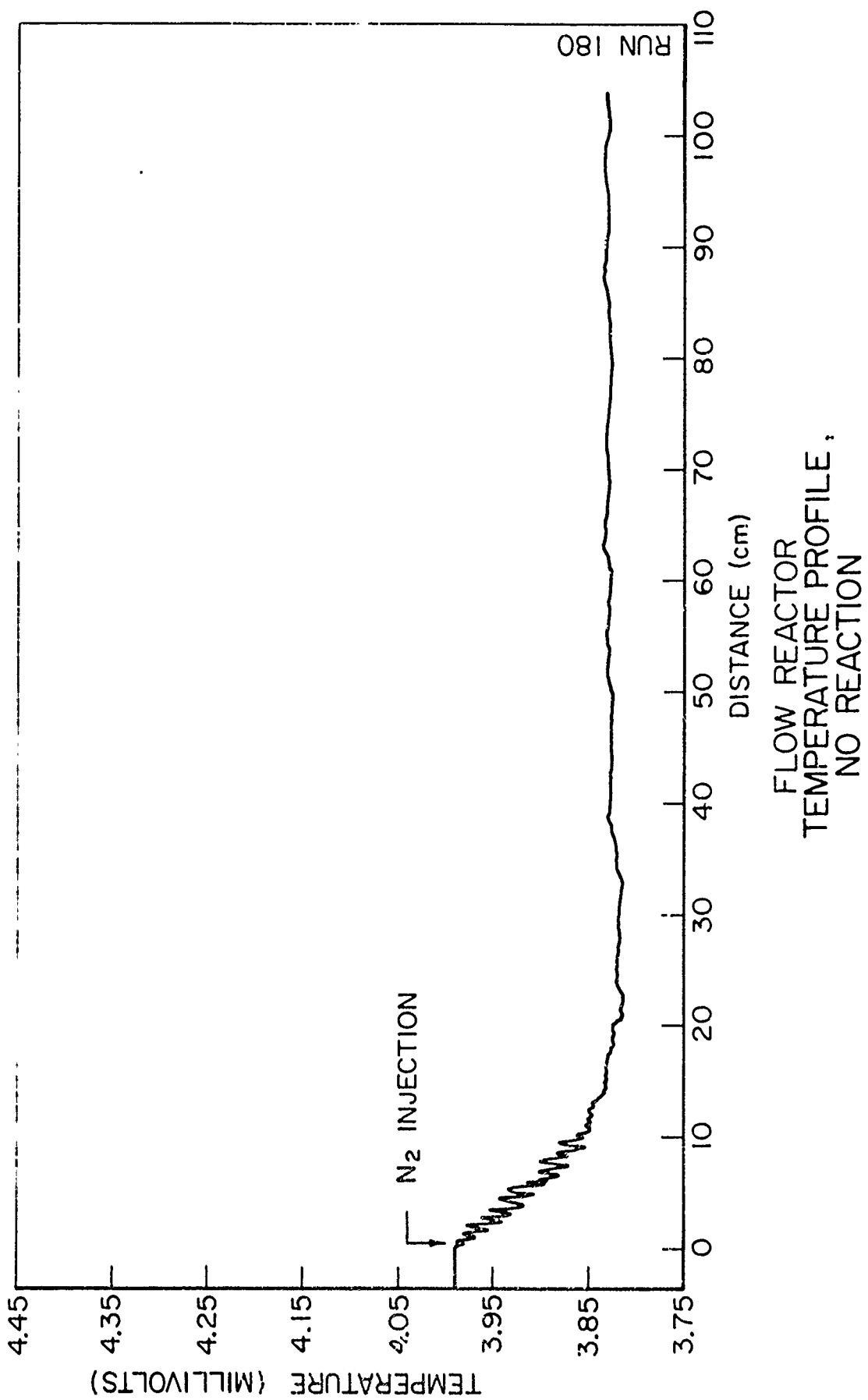
After shut-down of the propane/air heating systems
and a twenty-minute air-purge of the system to eliminate all
contaminants, the chosen carrier (air or nitrogen), fuel, and
oxygen flow rates are adjusted and a reaction temperature pro-
file similar to Figure 1.4 results. Measurements of the reac-
tion zone can then be made using the proper probe instrumenta-
tion.

2.4   Experimental Variables

Necessarily, the merit of the final results will
depend not only on the accuracy of these experimental measure-
ments, but also on the degree to which one is able to approxi-
mate the theoretical assumptions (summarized on Page 25)
which facilitate reduction of the data. Thus, these assump-
tions and their experimental approximation bear some discus-
sion.

The assumptions of a constant pressure-perfect gas
reacting media have been adequately discussed by Eberstein
and Sawyer; however, the steadiness, one dimensionality and
adiabaticity of the reaction zone have been re-investigated
in the present work, since the chemical sampling process re-
quires these conditions to exist over more extended periods
of time (than did the temperature profile measurements alone).
One dimensionality of the reaction zone was investigated by
measurement of both velocity and temperature at radial loca-
tions across the reactor tube. Results illustrated in
Figures 2.13 and 2.14 are for a Reynolds numbers (10^3-10^4)
in the range of those achieved during experiments.
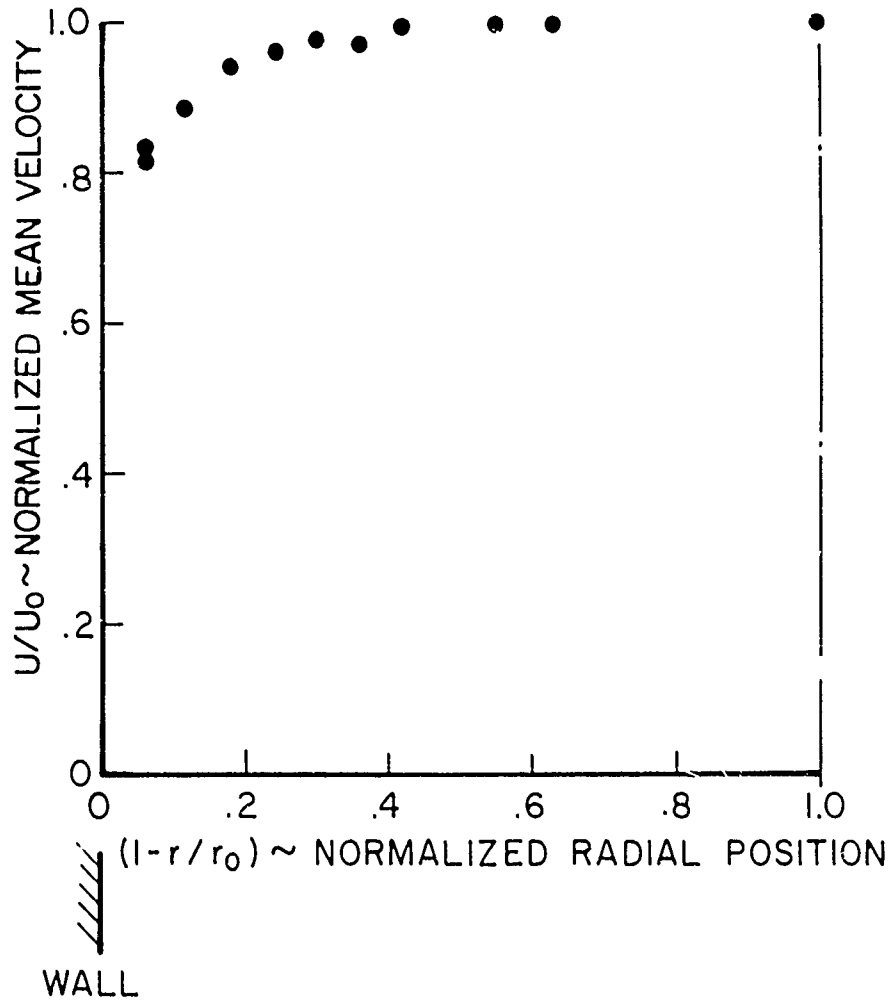
CONDITIONS:

- DUCT DIAMETER ~10 cm
- CARRIER ~ N_2
- REYNOLDS NUMBER ~ 10^4
- AXIAL LOCATION ~100 cm FROM MIXING
  NOZZLE INJECTION PORTS
- INLET TEMPERATURE ≈ 500 °K

EXPERIMENTAL RADIAL VELOCITY PROFILE

FIGURE 2.13

EXPERIMENTAL RADIAL TEMPERATURE PROFILE

FIGURE 2.14

Quasi-steadiness of the reaction zone was investigated by measurement of the reaction temperature at a stationary axial position over an extended period of time. A position near the end of the reaction zone was chosen so that changes in losses to the reactor walls and shifts in equivalence ratio and initial temperature should be most noticeable. The results of Figure 2.15 show that the reaction zone may be considered "steady" for times approaching 15 minutes. The most sensitive parameter is the reaction initial temperature which must be continuously monitored and adjusted (slowly) at the inlet to the reactor assembly. The near adiabaticity and quasi-steadiness of the reactor wall temperatures are realized from the design of the reactor assembly (see Figure 2.6). Suspension of the reactor tube within a reactor oven of large thermal inertia permits most of the temperature increase of the gas to be adjusted in the surrounding air gap, and reactor wall temperatures rapidly equilibrate to within $10^{\circ}C$ of the reacting gas temperature (for total gas temperature rises less than $100^{\circ}K$).

An estimation of the resulting change in longitudinal temperature gradient due to this non-adiabaticity of the wall can be obtained by extension of the analysis of Eberstein [15] (Pages 51-52 in [15]).

Using the generalized one dimensional energy equation for laminar flames,

(diffusion)   (convection)   (energy release)

$$-A\varepsilon \frac{d^2T}{dx^2} + \rho v A C_p \frac{dT}{dx} = \frac{dQ}{dt}$$
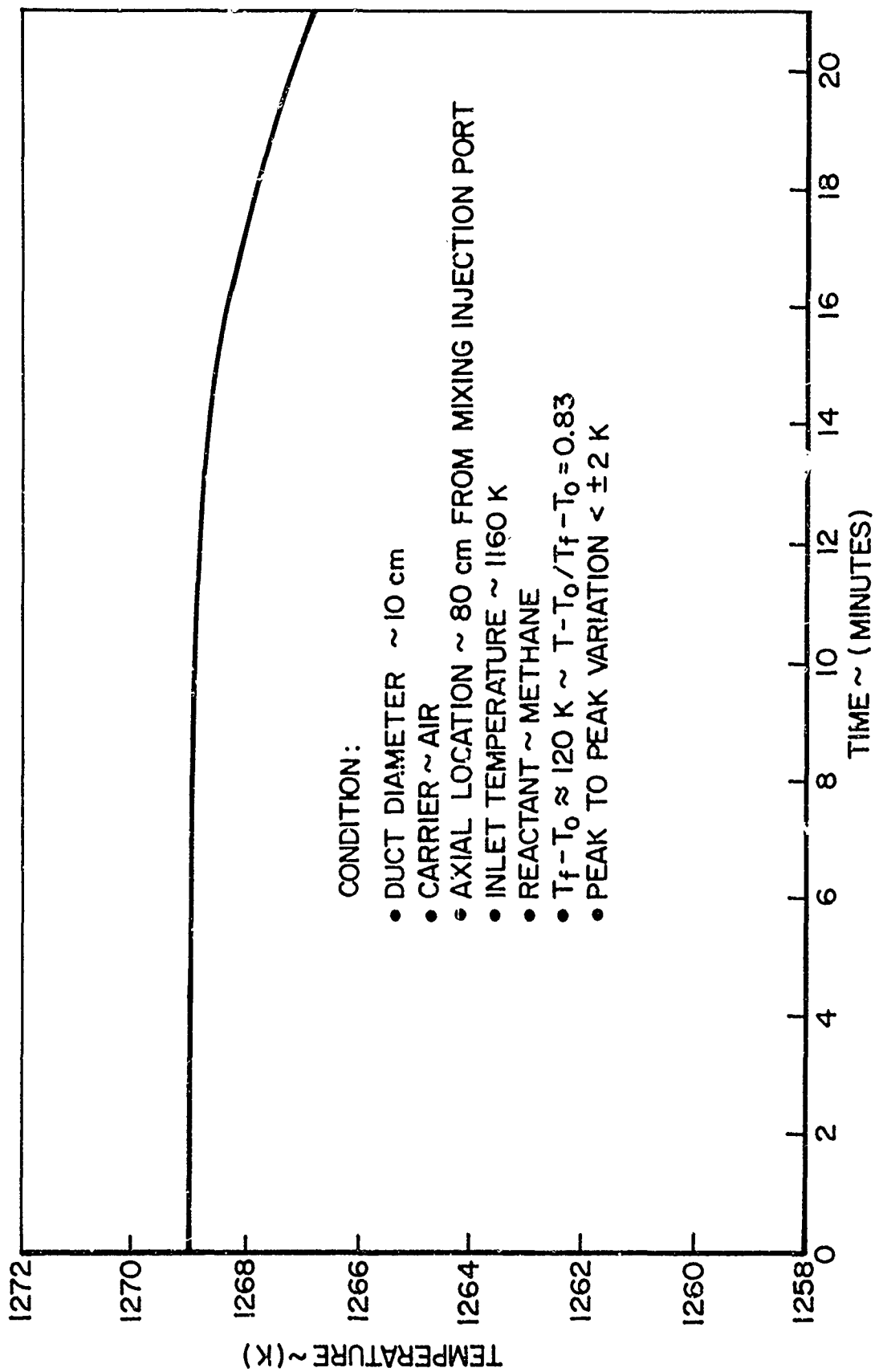
QUASI STEADINESS OF TURBULENT REACTION ZONE

CONDITION:
- DUCT DIAMETER ~ 10 cm
- CARRIER ~ AIR
- AXIAL LOCATION ~ 80 cm FROM MIXING INJECTION PORT
- INLET TEMPERATURE ~ 1160 K
- REACTANT ~ METHANE
- $T_f - T_0 \approx 120$ K ~ $T - T_0 / T_f - T_0 \approx 0.83$
- PEAK TO PEAK VARIATION < ± 2 K

TIME ~ (MINUTES)

TEMPERATURE ~ (K)

FIGURE 2.15

JP 15   R 4274   7z

with the laminar diffusion coefficient replaced by the

eddy diffusivity (ϵ), Eberstein re-wrote the relation in

the form

$$\frac{dT}{dx}\Big)_{ad} = \frac{dT}{dx}\Big)_{meas}(1+\beta L) \quad \text{where} \quad \beta L \equiv -\frac{\epsilon A}{\overset{\circ}{m} C_p}\frac{d^2 T}{dx^2}\Big/\frac{dT}{dx}\Big)_{meas}$$

β thus expresses the percent difference between adiabatic

$(\frac{dT}{dx}\Big)_{ad}$) and measured $(\frac{dT}{dx}\Big)_{meas}$) temperature gradients

resulting from longitudinal diffusion. Similarly, a term

for the loss of energy to the reactor walls can be included

and the expression can be written as:

$$\frac{dT}{dx}\Big)_{ad} = \frac{dT}{dx}\Big)_{meas}\left(1+\beta L+\beta w\right) \; ; \; \beta w \equiv \frac{2\pi \lambda}{\overset{\circ}{m} C_p} \, h_f \frac{(T_{gas} T_{wall})}{dT/dx)_{meas}}$$

As done by Eberstein, $h_f \, \& \, \epsilon$ can again be estimated from [7]

$$\frac{\epsilon}{\lambda} = \frac{h_f d}{\lambda} = 0.021 \left(Re\right)^{0.8} \left(P_r\right)^{0.4}$$

and for the typical numbers,

$Re = 10^4$ $d = 10\,cm = 2\lambda$

$P_r = .73$ $\overset{\circ}{m} N_2 = 35\,gm\,sec^{-1}$

$\lambda_{N_2} = 1.7 \times 10^{-4}\,cal\,cm^{-1}\,sec^{-1}\,K^{-1}$ $Cp N_2 = 0.29\,cal\,gm^{-1}\,K^{-1}$

$\left(\begin{array}{c}T_{gas}-T_{wall} \simeq 10K \\ \text{for} \\ T_{gas}-T_{oven} \simeq 125K\end{array}\right)$ $\frac{dT}{dx} = 2\text{-}4\,Kcm^{-1}$

one obtains,

$$|\beta L| \lesssim 1 \times 10^{-2}$$
$$\beta w \lesssim 2 \times 10^{-2}$$

Thus, it is seen that both longitudinal energy diffusion and losses of energy to the reactor wall contribute less than 3% to departure of the longitudinal temperature gradient (at any position in the reaction zone) from the adiabatic condition. This is very important to the thermal analysis technique and is also of some relevance to the assumption of one-dimensionality used in simplifying the analysis. Similar conclusions can be drawn concerning the relevance of longitudinal mass diffusion since energy and mass are always nearly proportional. Further, it is worth noting that all molecules, radicals, and atoms behave similarly (as far as diffusion is concerned) since the turbulent diffusivity is independent of the physical character of the species, and accounts for the major diffusive effect. This is in large contrast to the laminar flame where very light (and reactive) species such as [H] are by far the most mobile.

As discussed in Section 2.1, Glassman and Eberstein have theoretically argued that turbulence and mixing do not effect the kinetics. Sawyer's results experimentally vindicate these arguments since, (1) the kinetic measurements were not observed to be a function of the Reynold's number (turbulence), and (2) kinetic data taken from hydrogen/oxygen reactions which had initiated well before reactant mixing was complete show no effect of the upstream mixing phenomena on the downstream kinetics. Longitudinal mixing profiles

through the reactor tube have been taken by injecting methane
into nitrogen carrier, and the results summarized in Figure 2.16
show that under all conditions mixing is complete within the
conical inlet section in times less than 3 msec. (Reaction
times are not less than 50 msec.) Thus, it is concluded that,
providing results are shown not to be dependent on Reynold's
number, the approximations necessary to simplify analysis of
the flow reactor data are reasonable and do not introduce
gross errors to the experiment.

2.5 Experimental Limitations

The range over which experimental variables can be
varied is limited by both the mechanical structure and the
experiment. Sawyer has adequately discussed these limita-
tions and his summary is reproduced here (Table 2.1) with
some changes as to the operational limitations of the mechan-
ical structure.
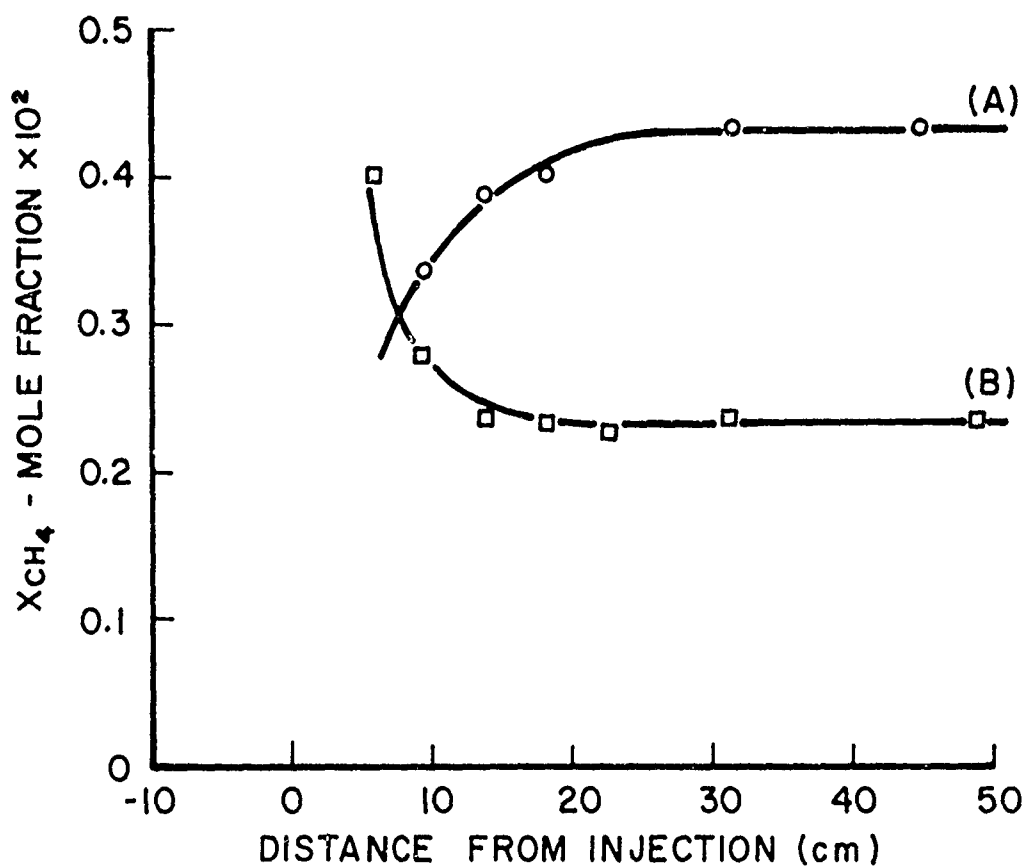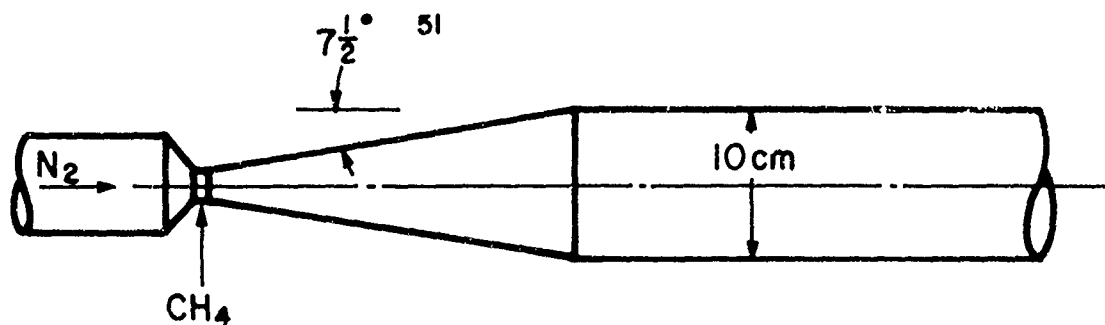
CONDITIONS:
- DUCT DIAMETER ~ 10 cm
- REYNOLDS NUMBER ~(A)-3×10³, (B)-6×10³
- INLET TEMPERATURE ~ 1173 K
- SAMPLING MEASUREMENTS ALONG AXIS OF FLOW

EXPERIMENTAL TURBULENT MIXING OF
METHANE IN NITROGEN CARRIER

FIGURE 2.16

SUMMARY OF FLOW REACTOR
EXPERIMENTAL OPERATING LIMITATIONS

pressure   1 (atm)

total gas density $.9-1.3 \times 10^{-5}$ (moles cm^{-3})

flow Mach number   less than .1

duct diameter   5-10 (cm)

duct length, overall   150 (cm)

reaction zone   about 100 (cm)

temperature   to 1450 (K)

flow velocity   400-5000 (cm sec^{-1})

Reynolds number (diameter)   3500-35000

stay time   20-250 (milliseconds)

mixing time   1-10 (milliseconds)

reaction time   10-250 (milliseconds)

time available for kinetic
  measurements $<$ 15 (minutes)

TABLE 2.1

CHAPTER 3 - INSTRUMENTATION
FLOW REACTOR KINETIC MEASUREMENTS

Assessment of the chemistry occurring within the turbulent flow reactor will require measurement of the longitudinal temperature profile through the reaction zone, and, where the assumptions of Appendix A are not valid, this must be supplemented by measurement of at least some of the longitudinal chemical specie profiles. Suitable precision of these measurements will necessitate not only an accurate chemical analysis technique, but assurance that the samples analyzed are truly representative of the reacting gas mixture at the positions from which they were removed. While for continuous analysis techniques only the effects of the sampling itself must be considered, here, effects of storage (before gas chromatographic analysis), and transfer to the analysis instrument are important as well.

In the following sections of this chapter, pertinent design and operational information on the instrumentation constructed to make these thermal and chemical measurements in the flow reactor will be discussed.

3.1   Reaction Temperature Measurement

Measurement of temperature within the reaction zone is achieved by extension of a thermocouple longitudinally through the zone, very near the axis of the flow.

Construction of the probe has been refined from that used in previous investigations, and a detail of the new probe design is presented in Figure 3.1.

9 mm OD QUARTZ HEAVY WALL
SUPPORT TUBE

ALL SURFACES COATED
WITH THIN SHEATH
OF SILICA

$\frac{3"}{4}$

CERAMABOND
CEMENT

99% ALUMINA
INSULATOR

$\frac{5"}{8}$

FUSED METAL BEAD

.010" WIRE

.0015" Pt 30% Rh/Pt 6% Rh
THERMOCOUPLE WIRE
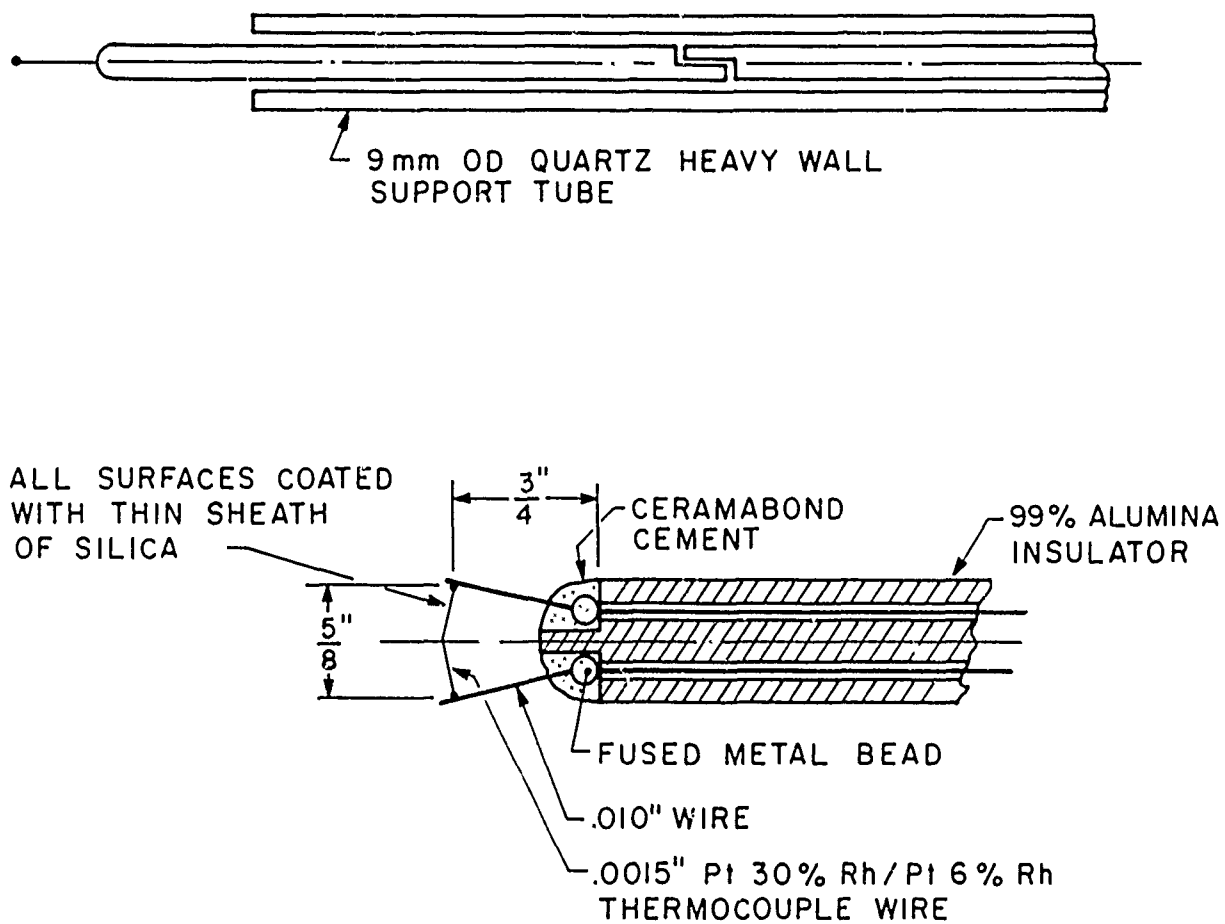
THERMOCOUPLE PROBE DESIGN

FIGURE 3.1

The probe support sheath is constructed of 9 mm heavy wall quartz tubing, and thus the thermal expansion problems (such as warpage) associated with an uncooled stainless steel design are eliminated. More importantly, the use of quartz also removes the possible catalytic effects which may arise from the presence of hot stainless steel surfaces.

Ten one-thousandth inch diameter lead wire of identical composition to that of the actual junction wire extends the length of the probe and is contained in twin bore, 99% alumina insulators. Each wire is held stationary at the entrance to the alumina nearest the thermocouple junction, by a fused bead enclosed in 501 Ceramabond Cement. The actual thermocouple junction is formed from .0015 inch wire fused to the .010 inch lead wire, and junction bead diameters are kept as near the same diameter as the junction wire as possible (always less than 2 wire diameters).

3.1.1 Corrections

A number of possible physical and chemical effects are present which can cause the actual undisturbed temperature of the reacting flow and the temperature measured by the probe to be different.

(i) Conduction

Conduction to or from the thermocouple junction from hotter or to colder regions of the junction and lead wires can cause steady state temperatures at the junction to be different from the bath temperature. This problem is not

of significant consequence in the present measurements since the junction wire extends from the junction, normal to the flow, and the temperature of the reacting gas is both radially uniform and changes only slowly longitudinally.

(ii) Radiation

Radiation losses from the junction to a cold surrounding atmosphere could be notable at reaction temperatures near $1200^{\circ}K$. However, the junction sees only the surrounding hot reactor walls which are at temperatures within $10-20^{\circ}K$ of the reacting gas (see Section 2.21). Radiative temperature corrections can be crudely approximated (as in [30]) by considering a sphere of diameter d, at steady state temperature Tc, immersed in a gas of thermal conductivity λ and temperature Tg ($Tg > Tc$). By equating the energy radiated to the surrounding environment to that transferred to the sphere from the gas ($Re_{sphere} < 1$):

$$T_g - T_c = \epsilon \sigma d \, \frac{Tc^4 - Tw^4}{2\lambda}$$

Using upper limit values for conditions in the turbulent flow reactor, i.e., $\lambda = 10^4 \, ERG \, cm^{-1} sec^{-1} K^{-1}$, $\epsilon = 1.0 \, \xi$

$$\sigma = 5.65 \times 10^{-5} \, ERG \, cm^{-1} K^{-4} sec^{-1}$$
$$Tw = 1200 K \, , \, T_g = 1220 \, K$$

$$T_g - T_c \doteq 1.5 \, K$$

Thus, the radiation correction is seen to very small and relatively constant.

(iii)   Stagnation Corrections

Mach number of the flow is not large enough to make this correction significant.

(iv)   Catalysis

The principal chemical disturbance of the probe is the promotion of catalytic reaction on the junction wire surfaces, particularly since most high temperature thermocouple measurements are made with nobel metals. Catalysis effects in laminar flame temperature measurements have been described by Friedman and Burke [17] and Kaskan [31]. They attribute spuriously high temperature measurements and hysterisis in measured temperature profiles to catalytic reactions occurring on the exposed thermocouple surfaces. (Similar disturbances have been noted in diffusion flames studies in this laboratory [32]). Encapsulation of the thermocouple metal surfaces with a thin sheath of silica was shown to significantly reduce the observed effects. However, Cookson, et. al. [3] has shown that removal of catalysis problems is not a sufficient condition for complete elimination of all chemical effects. They demonstrated that recombination reactions within the thermocouple boundary layer can also cause measurement errors, and these errors can be reduced or extrapolated out by decreasing the (coated) junction to the smallest possible diameter.

Silica coatings have been applied to thermocouple probe junctions in previous turbulent flow reactor studies to minimize catalysis. However no direct evidence of the

problem as been previously noted. Hysteresis of the measured
profiles has never been significant, but destruction of the
junction (from proposed high catalytic heat release on the
wire surface) has been attributed to degradation of the non-
catalytic coating. In the present research, the following
experiments have clearly shown that the integrity of the
silica coating is more important than previously realized,
and that its degradation need not necessarily result in destruc-
tion of the thermocouple junction itself.

Using the methods described in Appendix A, thermal
analysis measurements were carried out on a high temperature
methane/air reaction zone. It was recognized that the analysis
technique might yield incorrect rate data; however, any depen-
dence of measurements from the same reaction zone on the probe
junction coating character would be clearly indicative of
catalysis effects.

A thermocouple probe junction of .0015 inch diameter
Pt 30% Rh/Pt 6% Rh wire was coated with a thin silica sheath
by immersing it in a propane/air flame seeded with hexamethyl-
disiloxane (see Figure 3.2a). A second thermocouple probe
(uncoated) was immersed in the flame for the same period of
time without coating compound added (see Figure 3.2b). Two
sets of measurements were made with the coated thermocouple
probe. After the first set of measurements, slight physical
flexure of the junction was applied to "crack" the coating
(see Figure 3.2c). Comparison of the resulting second set
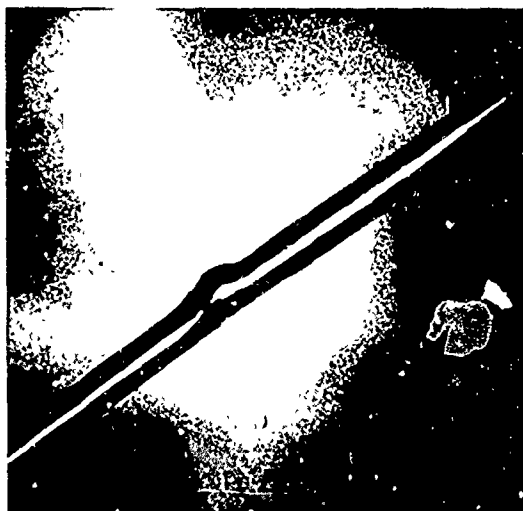
a SILICA COATED
THERMOCOUPLE JUNCTION
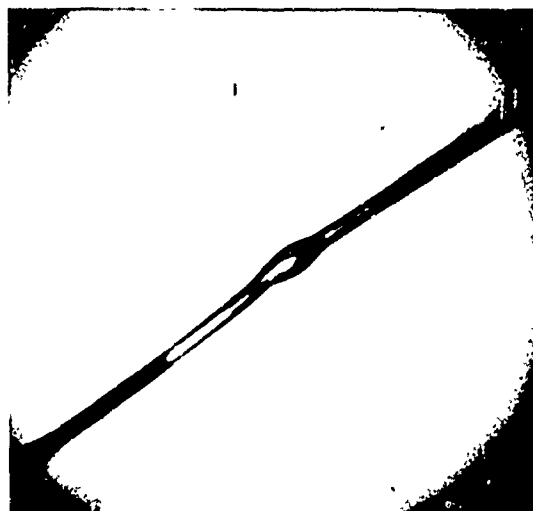
b UNCOATED THERMOCOUPLE
JUNCTION
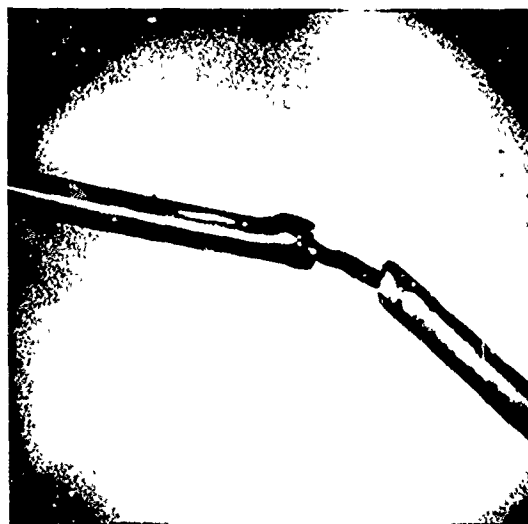
c SILICA COATED
THERMOCOUPLE JUNCTION
(ARTIFICIALLY CRACKED)

THERMOCOUPLE JUNCTION CATALYSIS EXPERIMENTS
MICROSCOPIC PHOTOGRAPHS OF PT 6% Rh/PT 30% Rh,
.0015 INCH DIAMETER JUNCTIONS

FIGURE 3.2

of measurements to those with the silica coating intact are shown in Figure 3.3. Note the shift in "thermal analysis" rate with the physical character of the coating. Comparison of the results of the "cracked" probe with those of the un-coated probe (Figure 3.4) demonstrate the strong effect of the slightest degradation in the protective silica coating. It should be noted that throughout all the tests, no changes in the physical character of the temperature profile (hysteresis, temperature oscillation) were observed.

The decisive conclusion is that any available metallic thermocouple surface in the vicinity of the junction can cause serious error in the resulting temperature measurements. Following the above tests, pre- and post-run microscopic inspections of the thermocouple silica coating (similar to those shown in Figure 3.2) were carried out in each flow reactor experiment. For those experiments in which a defective (chipped or cracked) coating was noted, the results were immediately discarded.

3.1.2 Resolution

Spatial resolution of thermocouple measurements in a low Mach number flow has been estimated to be about 10 diameters [30] of the thermocouple junction; this is approximately 5×10^{-3} cm in the present experiments. This dimension is extremely small compared to the dimensions of the flow reactor and is also insignificant in comparison to the positional accuracy of the thermocouple probe measurements ($\pm$ .1 cm).

$$\frac{d[CH_4]}{dt} = [CH_4]^{.7}[O_2]^{.8} \, 10^A e^{-E/RT}$$

COATED PROBE DATA

ARTIFICIALLY "CRACKED" PROBE DATA

$1000/T \sim (°K)^{-1}$

LOG_{10} (RATE CONSTANT) $(MOLE/cm^3)^{-1.5}(sec)^{-1}$
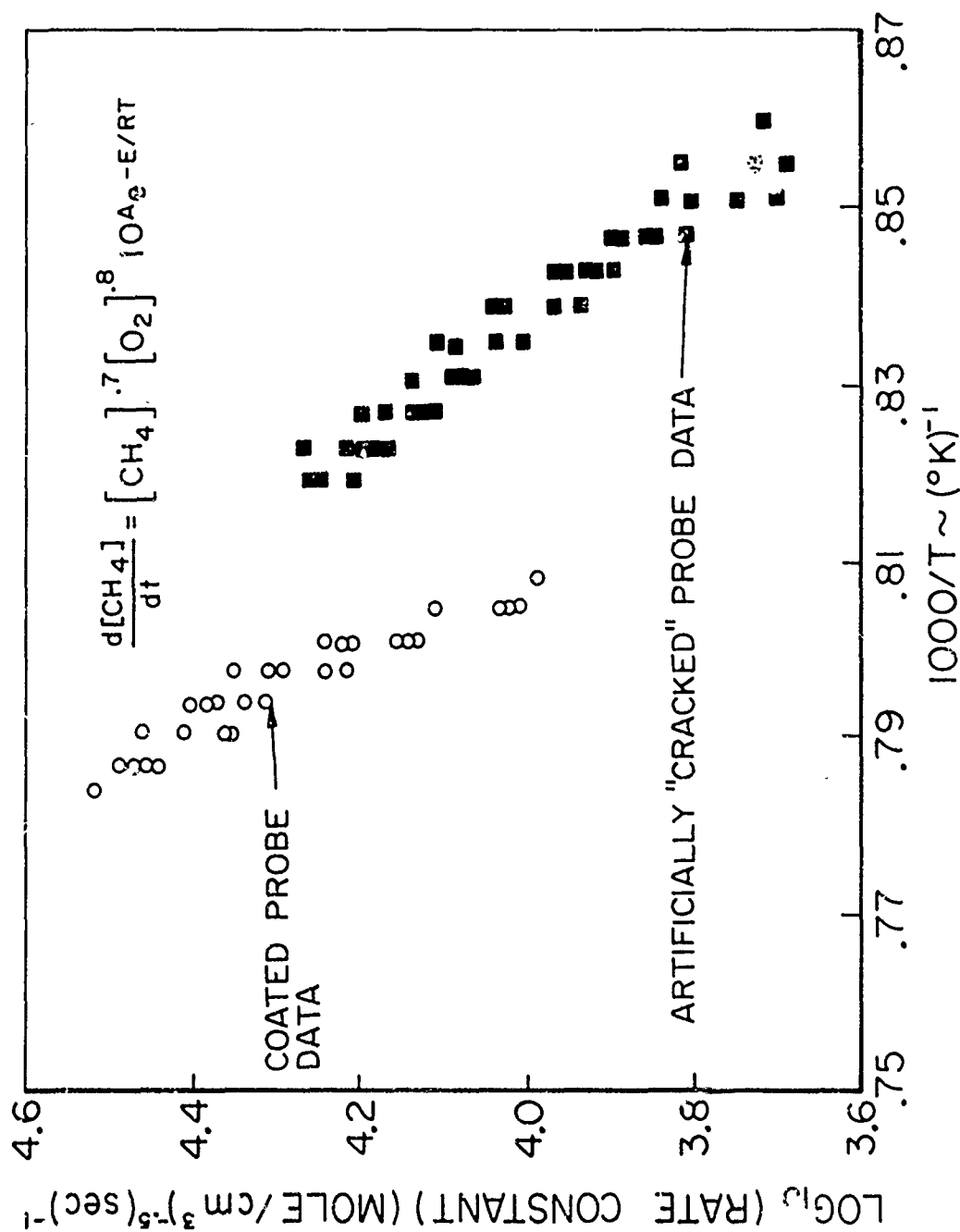
TEMPERATURE PROBE CATALYSIS
COMPARISON OF "COATED" & "CRACKED" RESULTS

FIGURE 3.3
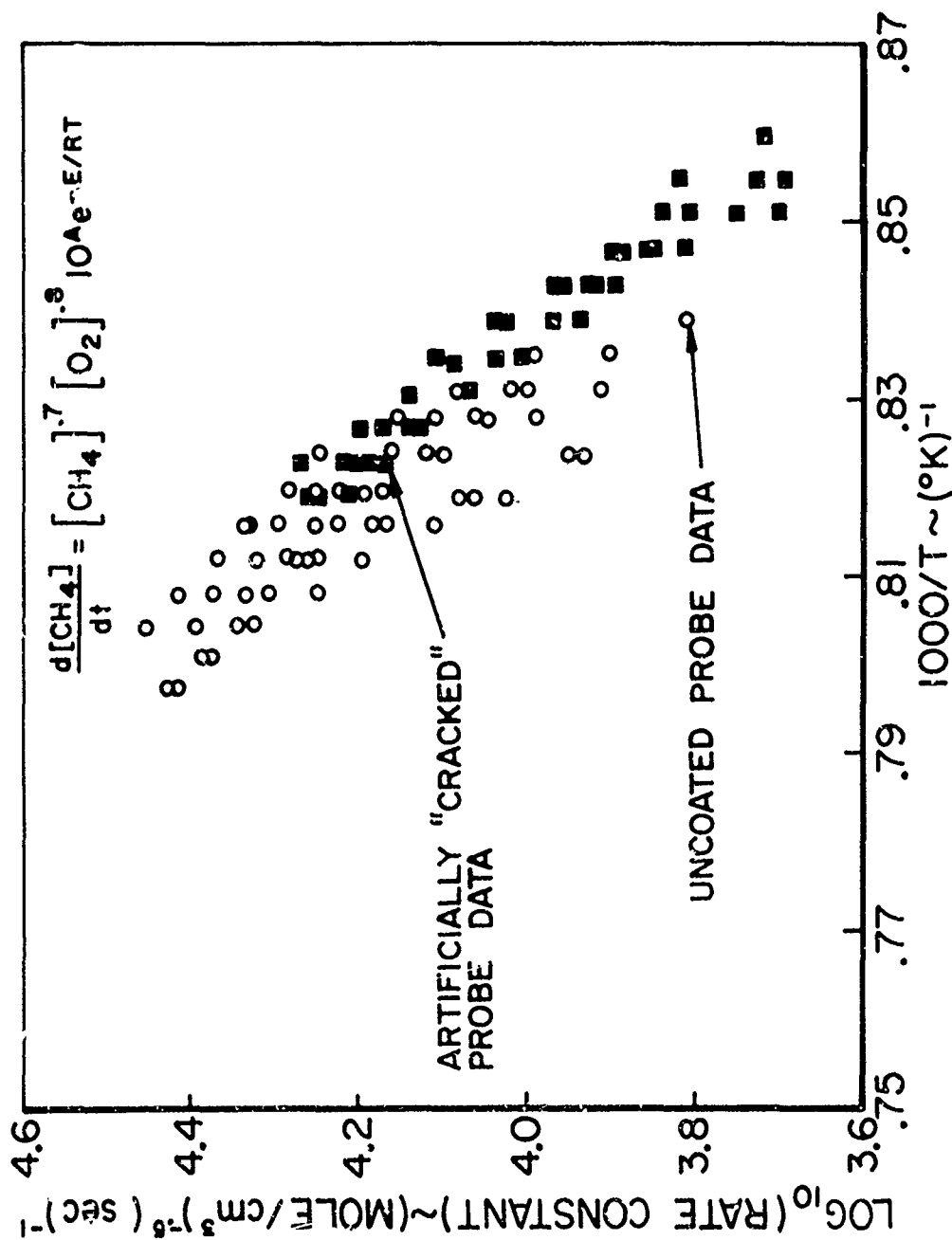
TEMPERATURE PROBE CATALYSIS
COMPARISON OF "CRACKED" & UNCOATED RESULTS

FIGURE 3.4

3.1.3 Electrical Circuitry

All temperature measurements were made with thermo-
couple probes constructed of Platinum 30% Rhodium/Platinum
6% Rhodium thermocouple wire supplied by Englehard Industries
(the higher percentages of Rhodium result in improved structural
characteristics). Response calibrations were determined by
the company on all wire used. Departure from the NBS standard
calibration tables [34] was so small that these tables were
used to interpret all measurements.

Measuring circuitry is presented in Figure 3.5.
Voltage output from the thermocouple junction is referenced
by an ice bath reading and is displayed on a Speedomax strip
chart recorder. The recorder is biased by a Leeds & Northrup
potentiometer so that a pen deflection of 10 inches/mv is
possible. This corresponds to an accuracy of measurements
of approximately $\pm$ .5 K; however, turbulent fluctuations are
normally of the order of $\pm$ 2K. Response characteristics of
the system are limited by the recorder (1 sec. full scale).

3.2   Chemical Measurements

Development of chemical measurement techniques for
the turbulent flow reactor must be considered a major contri-
bution of this research. Addition of chemical measurements
to previously available experimental parameters will permit
extension of the basic turbulent flow reactor technique to
detailed study of reaction systems which have not been
researched (even on an overall basis) previously. Further,
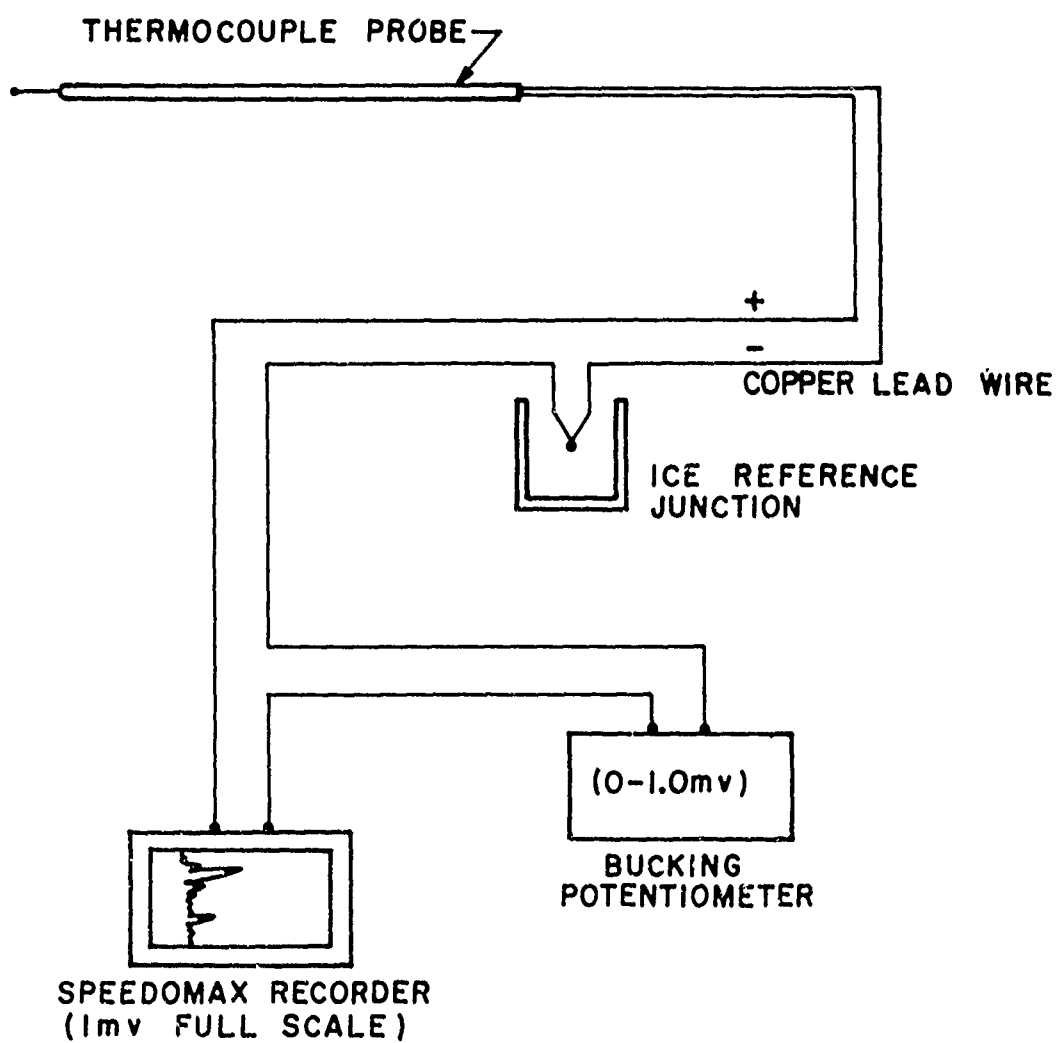
THERMOCOUPLE PROBE MEASURING CIRCUITRY

FIGURE 3.5

accurate and more complete chemical characterization of reactions will be extremely helpful in developing detailed mechanisms through computer modeling, and it will sometimes permit numerical evaluation of elementary rate constants.

Fristrom, et. al. [20,30,35,36] and Friedman and Cyphers [37] have discussed at length problems associated with chemical measurements of simple hydrocarbon reactions in low pressure flames, and Burgoyne and Hirsch [21], Pratt [22], and Kozlov [23] have addressed themselves to methane/oxygen chemical studies in laminar flow reactors of small dimension.

While it would be expected that the non-dispersive infrared (NDIR) or mass spectrometric (MS) techniques used in these studies would be adequate for study of these same reactions in the turbulent flow reactor, it is the purpose of this research to develop techniques which can also be extended to study the higher hydrocarbon oxidations. Chemical responses of the above techniques are not specific enough to be independently useful in description of such complex chemistry, and additional chemical analyses must be performed by one or more of the exhaustive techniques (gas chromatography, wet methods, orsat analysis). Long analysis times compared to those for MS or NDIR are common to all of these latter techniques. Thus, a chemical sampling technique must:

(i) isolate a flow of reactive media from a specific point in the reaction environment,

(ii)   prevent further chemical interaction of the
contained species,

(iii)   transport the sample flow, intact, to an
analysis instrument (or suitable storage
facility).

If exhaustive analyses are to be performed, the storage
facility must assure the stability of the sampled chemical
composition until analysis can be completed.

Tiné [38], in his review of the above mentioned
works and other chemical researches on propulsion devices
(ramjets, rockets, etc.), points out a critical difference
between laminar chemical studies and the present research.
It has often been assumed (without justification) that the
random variations in the distributions of chemical concen-
tration gradients in turbulent flows do not adversely effect
the sampled composition. It is likely that such an assump-
tion would not be tenable in flows containing steep gradients,
large scales and high intensities of turbulence. However,
in the turbulent flow reactor the turbulence is both uniform
and of small scale and gradients are small. Many turbulent
eddies pass the sampling position during the response time
of the sampling system (approximately the sample system
volume/sampling volume flow rate), and compositional varia-
tions of many eddies are effectively averaged. Thus, the
necessary condition for kinetic interpretation of the sampled
composition is that the mean rates of change of concentrations

with distance and the rates of change of the mean concentra-
tions with distance are the same. In this light, Glassman
and Eberstein [9,10] have discussed the relative effects of
temperature and concentration fluctuations in the turbulent
flow reactor. For reaction mechanisms with reasonably large
apparent activation energies ($>$ 10 kcal/mole), they found
that temperature fluctuation effects predominate, but are,
in fact, small enough to be neglected.

With these introductory remarks in mind, attention
may be turned to discussion of the versatile sampling and
analysis equipment and techniques developed for turbulent
flow reactor chemical analyses.

Instrumentation will be discussed under two major
subject areas:

     (1)   chemical sampling instrumentation composed of

          (i) that necessary for chemical sampling
              in the flow reactor

          (ii) facilities for storage of samples for
              exhaustive analysis.

     (2)   analysis instrumentation

3.3   Chemical Sampling System

There are no simple means of relating chemical
composition measurements at two axial locations (recall the
reaction zone is one-dimensional) in the flow reactor if
significant changes occur in the reaction zone during acquisi-
tion of the samples. Likewise, the number of variables which
control the reaction zone creates obvious disadvantages in

attempting to re-establish the same experimental conditions
to procure further chemical information. Thus it is best to
treat the reaction zone established in each flow reactor run
as a complete experiment. Further, it must be kept in mind
that the quasi-steady character of the variables controlling
the zone will limit the available time in which meaningful
chemical sampling results can be procured. Chemical informa-
tion can be achieved by sampling simultaneously or by reposi-
tioning the same sampling probe at several axial locations.
Kozlov [23], using the former technique, positioned a number
of sampling taps at several locations in his reactor wall.
This approach must be strongly questioned since residence
times in the flow boundary layer differ significantly from
those in the core of the flow. Further, results may be
seriously effected, if not completely vitiated, by possible
heterogeneous reactions occurring on the hot reactor wall.
Simultaneous operation of several sampling devices in the
core of the flow offers no better solution, for the resulting
fluid mechanical and chemical disturbances of the reacting
media would be unacceptable.

If repositioning a single sampling probe is to be
a satisfactory solution, the response time of the overall
sampling system to changes in chemical composition as the
probe is moved must be short. (If this is not so, the
number of sampling positions sufficient to characterize the
zone cannot be achieved before significant change in the

reaction variables occur.) This obviously requires that the volume of the sampling system be minimized and that the volume flow rate of the sample stream be as large as possible (i.e., the system pressure be as low as possible). Adsorption equilibration of the surfaces contacted by the sample stream as its chemical composition changes is also of importance. Evaluation of trace specie concentrations will be completely invalidated if this process is not rapid. Surface material is important in controlling this rate of equilibration. Fristrom and Westenberg [30] recommend surfaces of Teflon as opposed to glass or stainless steel, and they estimate the equilibration times to be the order of a few seconds (com-pared to the order of minutes for glass or steel). It is obvious that turbulent flow conditions through the sampling system and heating of the system surfaces would also be beneficial.

Figure 3.6 is a schematic of the constructed sampling system. Continuous sample flow is established by a vacuum source of variable pumping rate, and system pressures are maintained below 10 cm Hg. By operating at these low pres-sures, the expected partial pressure levels of high boiling point compounds are reduced below their vapor pressures (at room temperature); and, thus, condensation is prevented. Chosen line diameter and flow rates assure turbulent flow conditions and system volume flush times of less than 500 msecs. Where possible, surfaces contacted by the sample flow are constructed
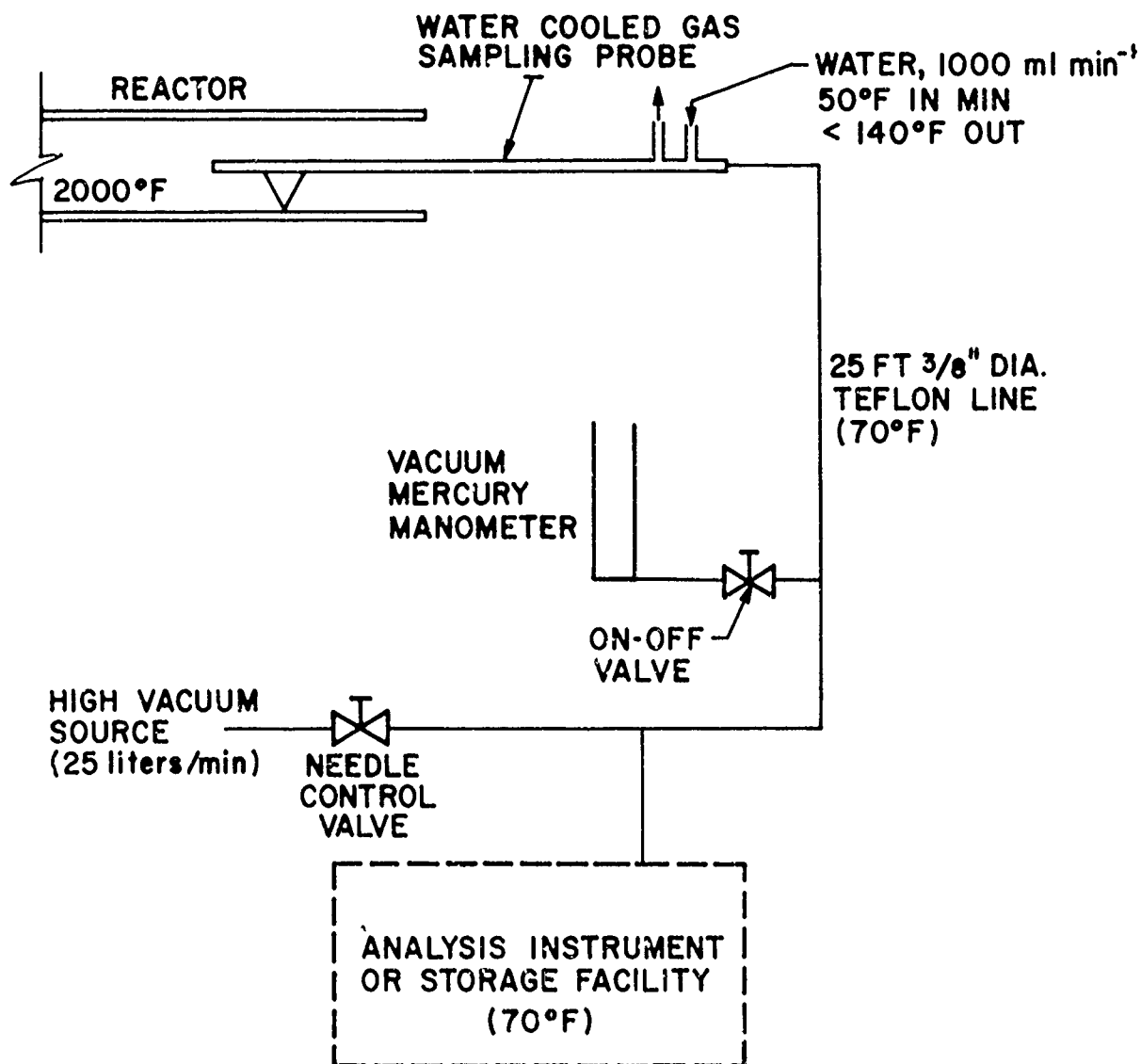
GENERAL SCHEMATIC OF SAMPLING SYSTEM

FIGURE 3.6

of Teflon. Though the present system is unheated, provisions have been made for this condition to be added if it becomes necessary.

The sampling probe itself is constructed of 304 stainless steel and is illustrated in Figure 3.7. Water cooling is necessary to insure its structural integrity. A flow rate of 1000 ml/min is adequate to restrict the coolant temperature increase to less than $40^{\circ}C$ under all sampling conditions. Convection cooling of the sample flowing through the central capillary is the primary method used to quench the chemistry of the sampled stream. The chemical quenching time (τ_q) can be envisioned as the time necessary to reduce the sample flow temperature from the free stream value (T_1) to a lower temperature (T_2), the "quenching temperature". For a capillary tube of diameter (d) and wall temperature (T_w), Beal and Grey [39] have estimated from the empirical relation:

$$\tau_q = \left(\frac{1}{1.75\,\pi}\right)^{3/2} \left(\frac{\pi d^2}{4}\right) \left(\frac{P\lambda}{\nu}\right) \left[\frac{T_1 - T_2}{\frac{T_1 + T_2}{2} - T_w}\right]^{3/2} \; {}^*$$

They have chosen T_2 as about 1120R (620K); at this temperature, recombination reactions are much faster than radical-molecule reactions, and very reactive species (radicals) will be rapidly eliminated from the environment. The quenching process is especially effective because of the third body property of the cold metal walls.

---

*It is interesting to note that the quenching time is independent of the sample flow rate.

COOLANT

.37"D.

11"

$79\frac{1}{2}$"

41°

.016"D.

.16"

COPPER TIP
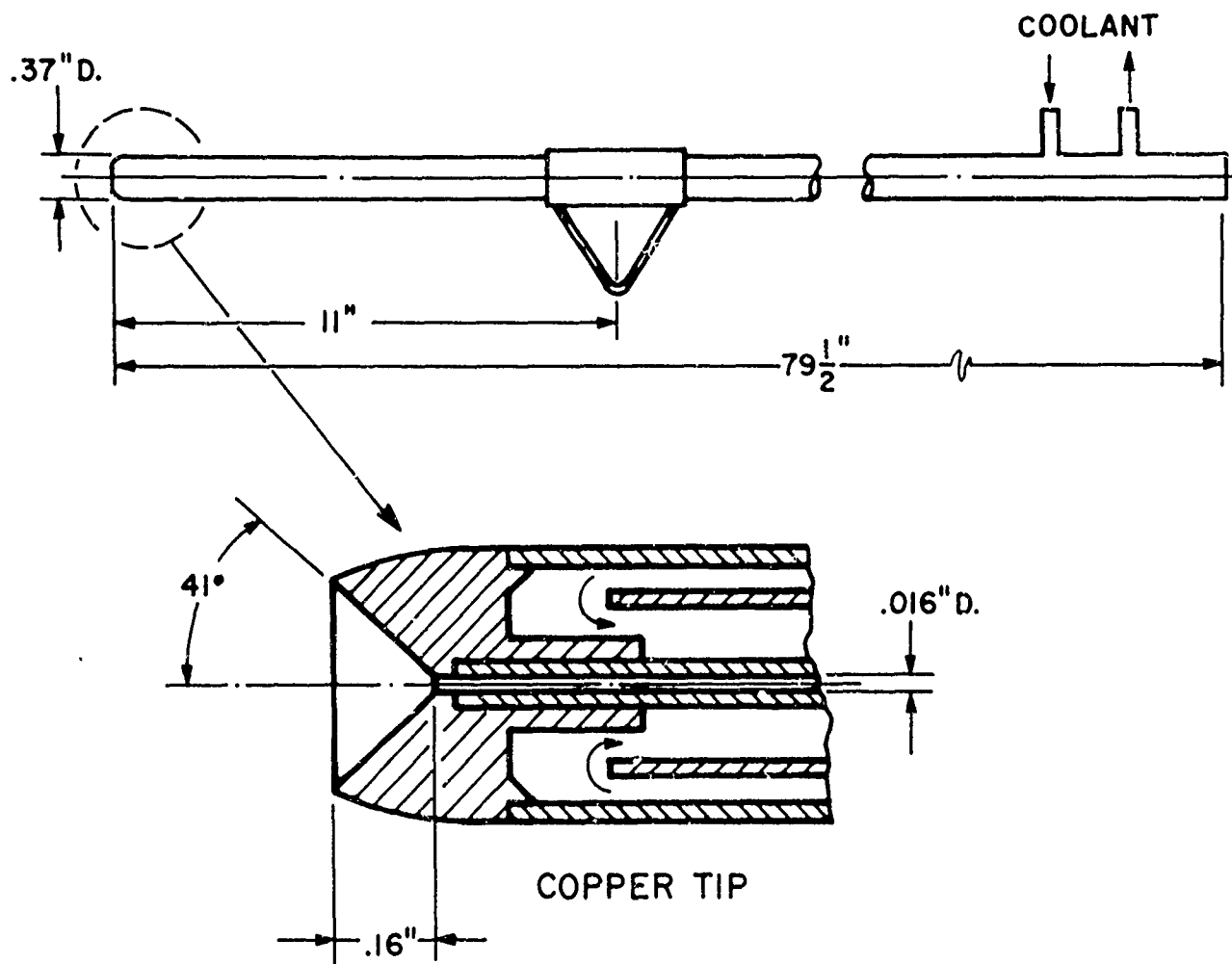
CONSTRUCTION: STAINLESS STEEL
WATER COOLING, 1000 ml/min
MAXIMUM SAMPLE FLOW-450cc/min

GAS SAMPLE PROBE DESIGN

FIGURE 3.7

With: ν = 168×10^{-5} ft^2 sec^{-1}

P_r = .75

d = 1.32×10^{-3} ft (.016 in)

T_1 = 2520R (1400K)

T_w = 600R (320K)

τ_q $\doteq$ 50 μ secs.

Halpern and Ruegg [40] have suggested that convection cooling must be supplemented by some other quenching method (expansion or dilution) to achieve suitable quenching in low pressure laminar flame studies. However, at the temperatures and pressures realizable in the turbulent flow reactor, convection cooling is adequate for freezing stable species. (Typical times for half reaction of these species in the flow reactor are about 30,000 μ secs.) Necessarily the unstable species (atoms and radicals) will recombine to form stable products during the quenching process. However, even if concentrations of these unstable species were several orders of magnitude greater than their equilibrium values at 1000°K, stable product concentrations would not be changed significantly by their recombination.

Water cooling of the probe is also beneficial in the elimination of possible hot metal surfaces from the reaction zone which might be conducive to acceleration of

must insure that sufficient sample is trapped to complete the required analysis and that compositional changes which might occur during storage are negligible. In addition to adsorption and condensation, slower processes such as polymerization, photochemical and heterogeneous reactions and atmospheric contamination can produce sample degradation.

Condensation can be prevented (as it was in the primary sampling system) by heating of the sample and by low pressure storage. However, low pressure storage introduces the possibility of atmospheric leakage into the sample vessels. Even if small, when integrated over lengthy storage times, its effect could be devastating.

Fristrom and Westenberg [30] recommend that storage containers be lined with Teflon or polyethelyne to minimize adsorption effects. No successful method of lining containers to be used at sub ambient pressure is available. Furthermore, Papa [42] has shown polyethylene to be one of the more chemically active surfaces, producing rapid degradation of some chemical species. Thus, complete construction of containers of polyethelyne is not judicious, and it would be prohibitively expensive to use Teflon. A compromising choice of material appears to be one of high surface smoothness and low porosity, (such as glass) which, if necessary, can be heated to decrease surface adsorption.

Concerning polymerization, photochemical, and other reactive types of sample degradation, Dimitriades, et. al., [43]

the reaction. In contrast, the outer cool surfaces of the probe enhance only recombination (quenching) reactions.

Aerodynamic disturbances of the flow are minimized by extension of the sampling probe (and parallel ther ocouple probe) from the exit of the reactor by the traverse system discussed in Section 2.22. The tip of the probe has also been aerodynamically shaped. Fristrom, et. al. [35] (experimentally) and Rosen [41] (theoretically) have considered the displacement of the sampling position caused by the rate of sample withdrawal through a probing device. Direct extension of their results to this work (because of turbulent effects) does not appear feasible. However, the parameters which control the magnitude of the mean displacement (such as free stream mean velocity, sampling volume flow rate, probe radius, etc.) are constant throughout the reaction zone. Thus, it would appear that any mean displacement would also be constant and therefore unimportant, since all sampling position measurements are used only in a relative, not absolute, sense. (See Appendix B.)

3.3.1 Chemical Sample Storage

As described earlier, the more exhaustive chemical analysis techniques are time consuming and are generally incapable of being used with continuous sampling. Thus, to the previously described system must be added a mechanism to trap and store a discrete gas volume from each sampled position in the reaction zone. Design of such storage facilities

must insure that sufficient sample is trapped to complete the required analysis and that compositional changes which might occur during storage are negligible. In addition to adsorption and condensation, slower processes such as polymerization, photochemical and heterogeneous reactions and atmospheric contamination can produce sample degradation.

Condensation can be prevented (as it was in the primary sampling system) by heating of the sample and by low pressure storage. However, low pressure storage introduces the possibility of atmospheric leakage into the sample vessels. Even if small, when integrated over lengthy storage times, its effect could be devastating.

Fristrom and Westenberg [30] recommend that storage containers be lined with Teflon or polyethelyne to minimize adsorption effects. No successful method of lining containers to be used at sub ambient pressure is available. Furthermore, Papa [42] has shown polyethylene to be one of the more chemically active surfaces, producing rapid degradation of some chemical species. Thus, complete construction of containers of polyethelyne is not judicious, and it would be prohibitively expensive to use Teflon. A compromising choice of material appears to be one of high surface smoothness and low porosity, (such as glass) which, if necessary, can be heated to decrease surface adsorption.

Concerning polymerization, photochemical, and other reactive types of sample degradation, Dimitriades, et. al., [43]

concluded that storage system design cannot under any circum-
stances assure universal elimination of these effects. Thus,
as each new reaction study is initiated in the flow reactor,
storage stability of chemical species suspected to be formed
in the reaction should be investigated.

Trapping and storage apparatus constructed in this
research are displayed in Figures 3.8 and 3.9. Up to twenty
individual sample containers may be mounted in the sampling
and storage rack (Figure 3.8). The rack is installed in the
primary sampling system immediately upstream of the vacuum
source; it permits part of the primary sample flow to be
diverted (independently) to and/or through any one of the
storage containers. Surfaces contacted by the primary sample
flow are glass or Teflon, and all vacuum connections are made
with nylon Ultra Torr high vacuum fittings. The structure
of the rack is made of plexiglass. By using electrically
non-conducting construction materials, detection of vacuum
leaks can be easily performed with high voltage discharge
techniques.

Each individual sample container is approximately
200 ml in volume and is constructed of pyrex (Figure 3.9).
Ultra vacuum port valves are located at opposing ends of the
cylindrical body. These valves were chosen because of their
extremely low leak rate (usable in vacuums to 10^{-9} Torr) and
because sealing can be performed by "dry" "O" ring fittings.
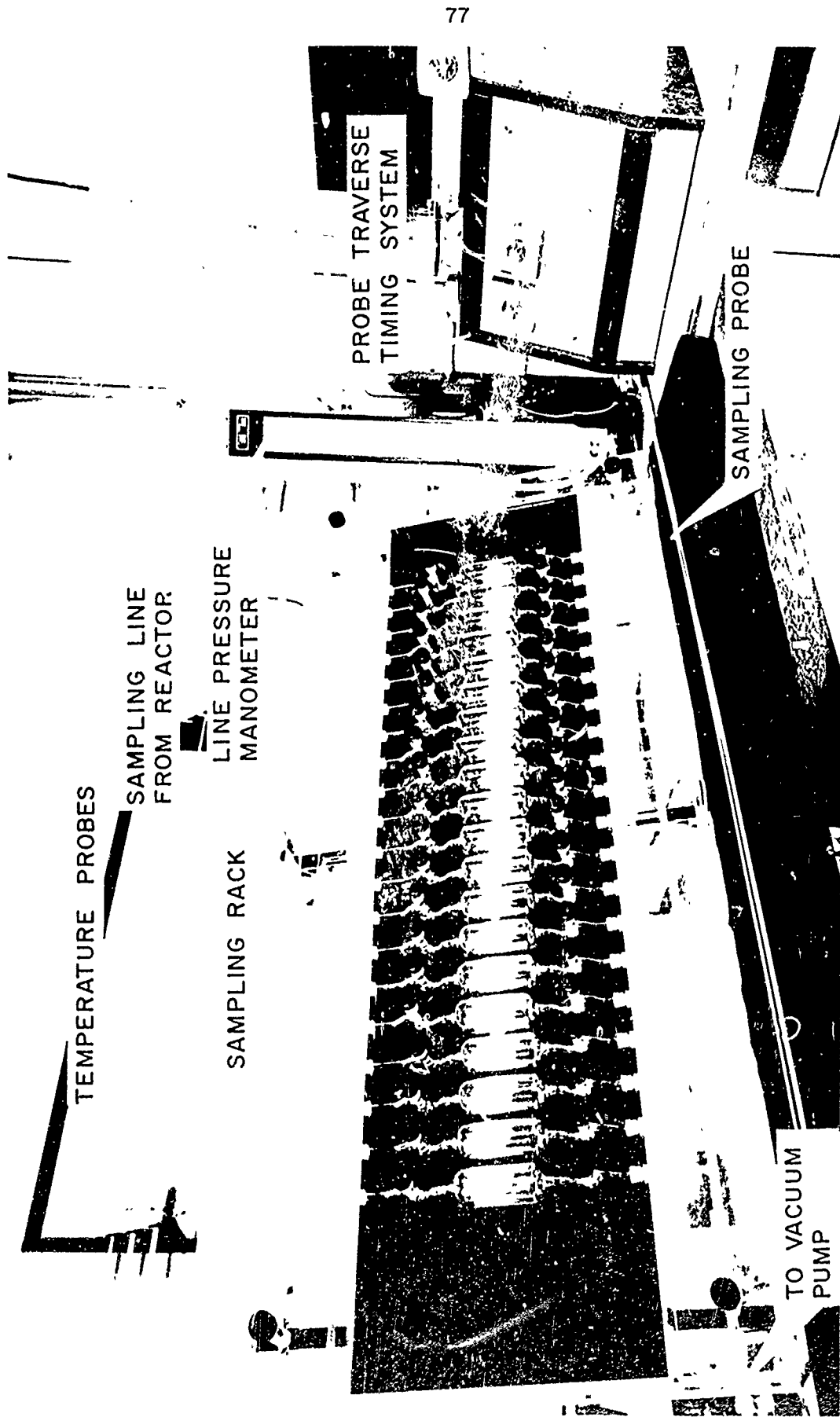
GAS SAMPLING APPARATUS

FIGURE 3.8
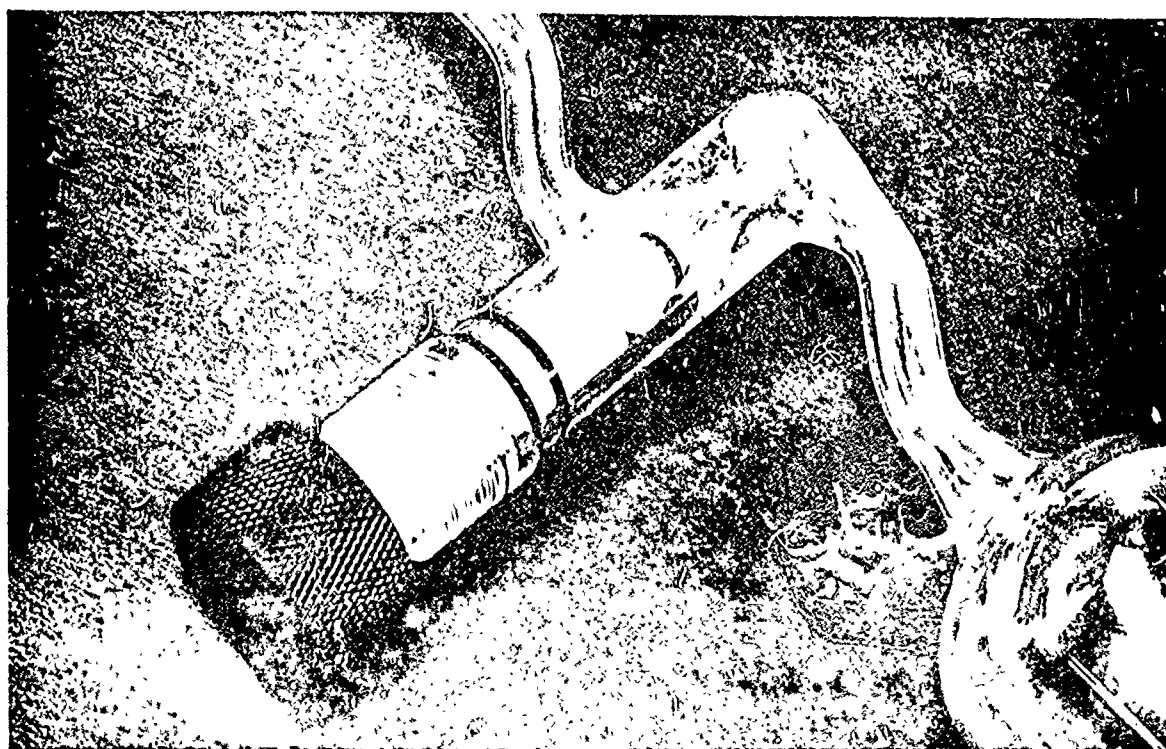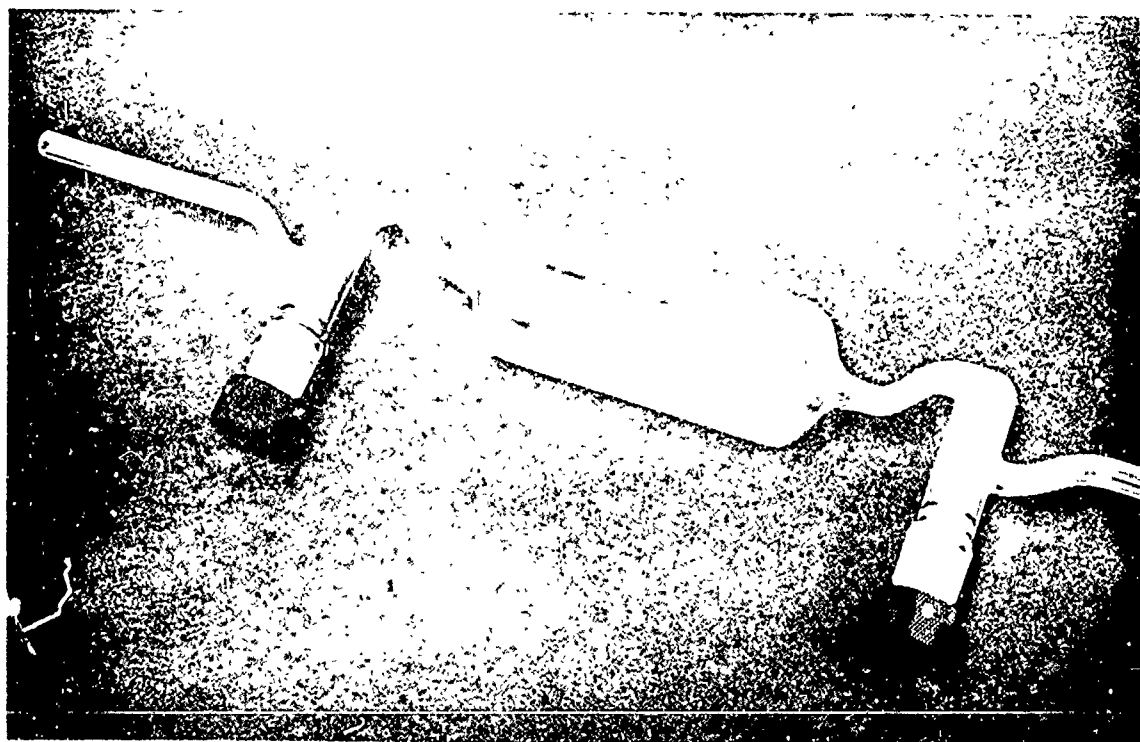
GAS SAMPLING BOTTLE

FIGURE 3.9

In general vacuum seals requiring the use of greases (silicone, apeizon, etc.) should not be used in chemical gas analysis systems. Jeffery and Kipping [44] point out that vacuum greases are known absorbers of hydrocarbons, particularly those in the alkene and alkyne series. Thus, concentrations of these species in a contained sample might be degraded.

3.3.2 Sampling System Procedures

General operating procedures for the complete chemical sampling system are as follows:

(i) Before an experimental flow reactor run is made, the complete sampling system (primary system and storage system) is flushed with dry helium, heated to $80^{\circ}C$, sealed, and then maintained at vacuum pressures less than 1 micron for several hours. Port valves of the containers are closed in this evacuated state.

(ii) After a reaction zone has been stabilized in the turbulent flow reactor (see Chapter 2), the sampling system flow is initiated and line pressures are adjusted between 2 and 10 cm Hg.

(iii) The probe traverse system, with sample and temperature probes properly mounted, is activated in the cycle mode. (Movement distances are generally chosen to divide the reaction zone into 20 equal parts.)

(iv) As the probe reaches a sampling position, the holding timer is activated, and the sample system is permitted to flush approximately 50 times with the flowing sample composition ($<$ 15 seconds).

(v) Following this, part of the primary sample flow is manually diverted to and then through a sample container. The container is permitted to flush approximately 4 times.

(vi) Port valves are manually closed, trapping a volume of sample at the previously set system pressure.

(vii) The traverse system timers cycle and the probes are moved to the new sampling position.

Operations (iv) through (vii) are repeated until all sample containers are expended. After conclusion of the run the sampling system (external to the containers) is sealed and pumped to pressures less than 1 micron. Each container is removed immediately before its analysis and is otherwise stored at high vacuum in the rack. Construction of the sample containers insure that under these conditions all leakage during storage will be out of, rather than in to, the containers. Also, during storage, light sources in the sampling room are extinguished to eliminate energy sources for photo chemical reactions.

3.4 Chemical Analysis

Gas Chromatography (GC) has evolved from the early researches of Martin and James [45] to become the most commonly used exhaustive gas analysis technique. The small amounts of sample necessary, the rapidity with which analysis can be completed, and the ease with which detector signals can be registered and repeated all have played a role in establishing

this general acceptance. The most distinct advantage of GC
is the speed of analysis relative to other extensive tech-
niques. Each sample injection permits a qualitative and
quantitative identification of the contained compounds; and,
sensitivity (detection limit), with some detector systems, can
be as small as 1 part per billion. Further, GC offers the
possibility of easily detecting isomers of the same compound,
which by other methods is extremely difficult or impossible.

The major disadvantage common to all extensive
analysis techniques is that analysis times are lengthy and
generally necessitate sample storage. In many cases, a
manner of storage in which the sample composition is satis-
factorily maintained cannot be found, and accuracy of analyses
is therefore questionable.

A theoretical treatment of the gas-liquid and gas-
solid separation phenomena which gas chromatography employs
is rarely of direct help to the researcher (at least at
present) and will therefore not be discussed here. See
[46-54]. It is, however, felt that a very brief de-
scription of the technique is worthwhile.

An instrumental flow system similar to that of
Figure 3.10(a) is basic to all GC's. It includes a carrier
source, an oven containing the GC column which will perform
the component separation, and a detector which responds to
some physical or chemical character of the species to be
determined. A small amount of the sample to be analyzed is
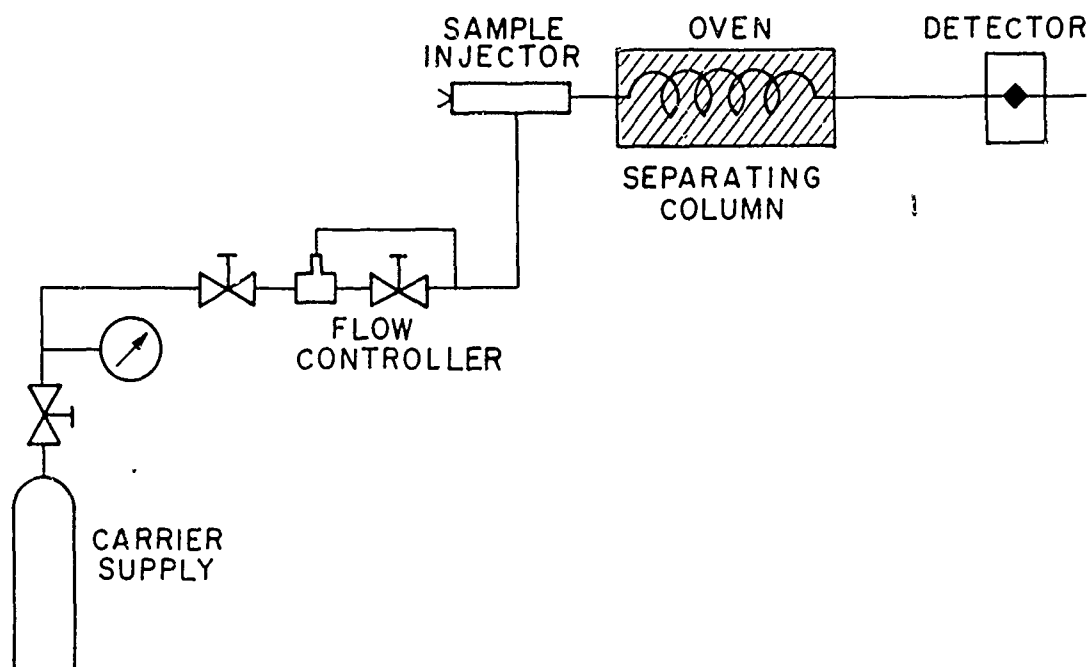
(a) BASIC GAS CHROMATOGRAPH FLOW SYSTEM
FOR ISOTHERMAL OPERATION
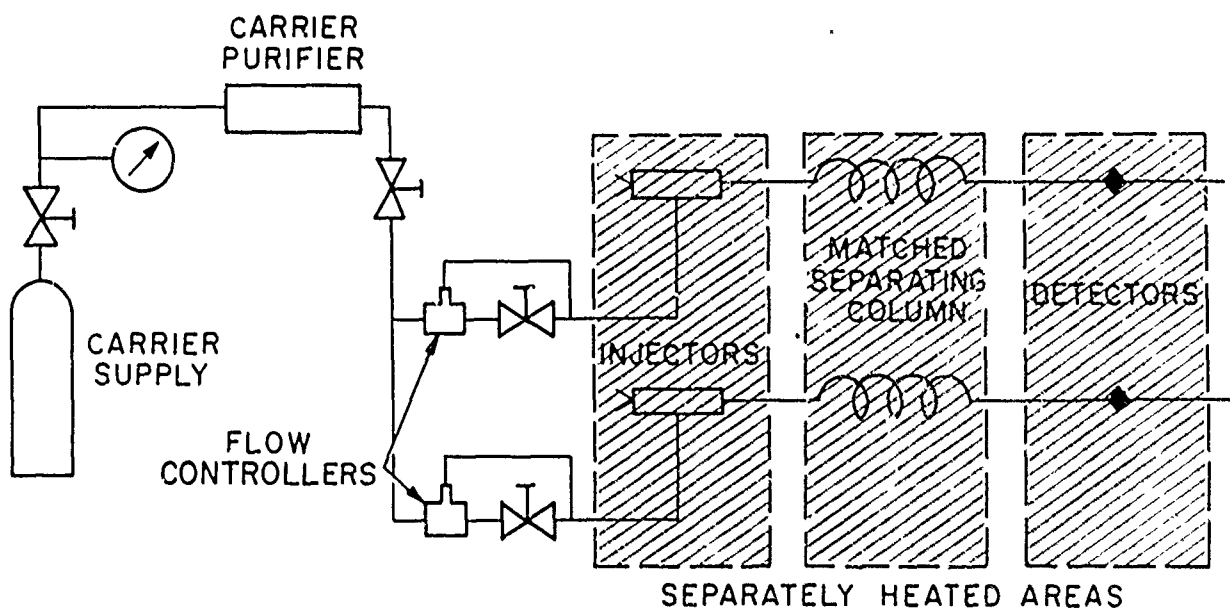
(a) GAS CHROMATOGRAPH SYSTEM FOR TEMPERATURE
PROGRAMMED GAS CHROMATOGRAPHY

CHROMATOGRAPH FLOW SCHEMATICS

FIGURE 3.10

injected into the flowing carrier upstream of the separating column. As this gas volume passes through the column, each contained chemical component moves at a rate determined by its physical or chemical affinity for the "packing" material within the column. Substances having differing affinities will "elute" from the columns at different times. Those having nearly the same or identical affinities will elute, "unresolved" (at or nearly at the same time), and some components may be totally impeded in the column and not elute at all (e.g., CO_2 does not pass through molecular seive packings). Compounds with different retention times (time from injection to elution of the maximum concentration of the specie) will elute as binary mixtures with the carrier, and their presence can be quantitatively sensed by a suitable detector. In some cases, a selective detector (one which responds to only a special family of compounds) will permit quantitative detection of compounds which elute with one or more other compounds to which the detector is insensitive.

Every chemical specie has a characteristic retention time which is a function of the specific column packing, carrier flow rate and molecular weight, and the column pressure and temperature. Of these, the more critical variables are column packing and temperature. To present, no single packing material has been found which would permit complete separation of all possible species in a sample mixture. Thus, several partial analyses on different column materials are

generally necessary. Special methods of performing these multiple analyses have aided in reducing total analysis times; however, no single innovation has been as effective as temperature programming. Temperature programmed gas chromatography (TPGC) requires an instrumental flow system as in Figure 3.10(b). The detector output of the reference system is opposed to the primary analysis system. This minimizes detector signal drift from column "bleed" (loss of liquid coating on packing material and re-adjustment of adsorption/absorption) during temperature programmed operation.

If a single column material is operated under isothermal conditions, efficient separation of compounds is generally limited to those having boiling points within 50K of one another. At low isothermal operating temperatures (see Figure 3.11) the higher boiling point compounds will have extremely long retention times. Their elution bands (peaks) will be very broad, and there will be a resulting loss in apparent detector sensitivity. At high isothermal operating temperatures, the low boiling point compounds will elute very rapidly with similar retention times, and the resulting peaks will not be well resolved. However, by enclosing the column in an oven which can undergo a temperature excursion as the analysis is proceeding, all compounds will elute well resolved with nearly the same band (peak) width in a much shorter time. Each peak will be much more amenable to accurate measurements. Although closely spaced peaks will not be better resolved than

ISOTHERMAL OPERATION, LOW TEMPERATURE

ISOTHERMAL OPERATION, HIGH TEMPERATURE

INSTRUMENT RESPONSE (ARBITRARY UNITS)

TEMPERATURE (ARBITRARY UNITS)

TIME (ARBITRARY UNITS) →
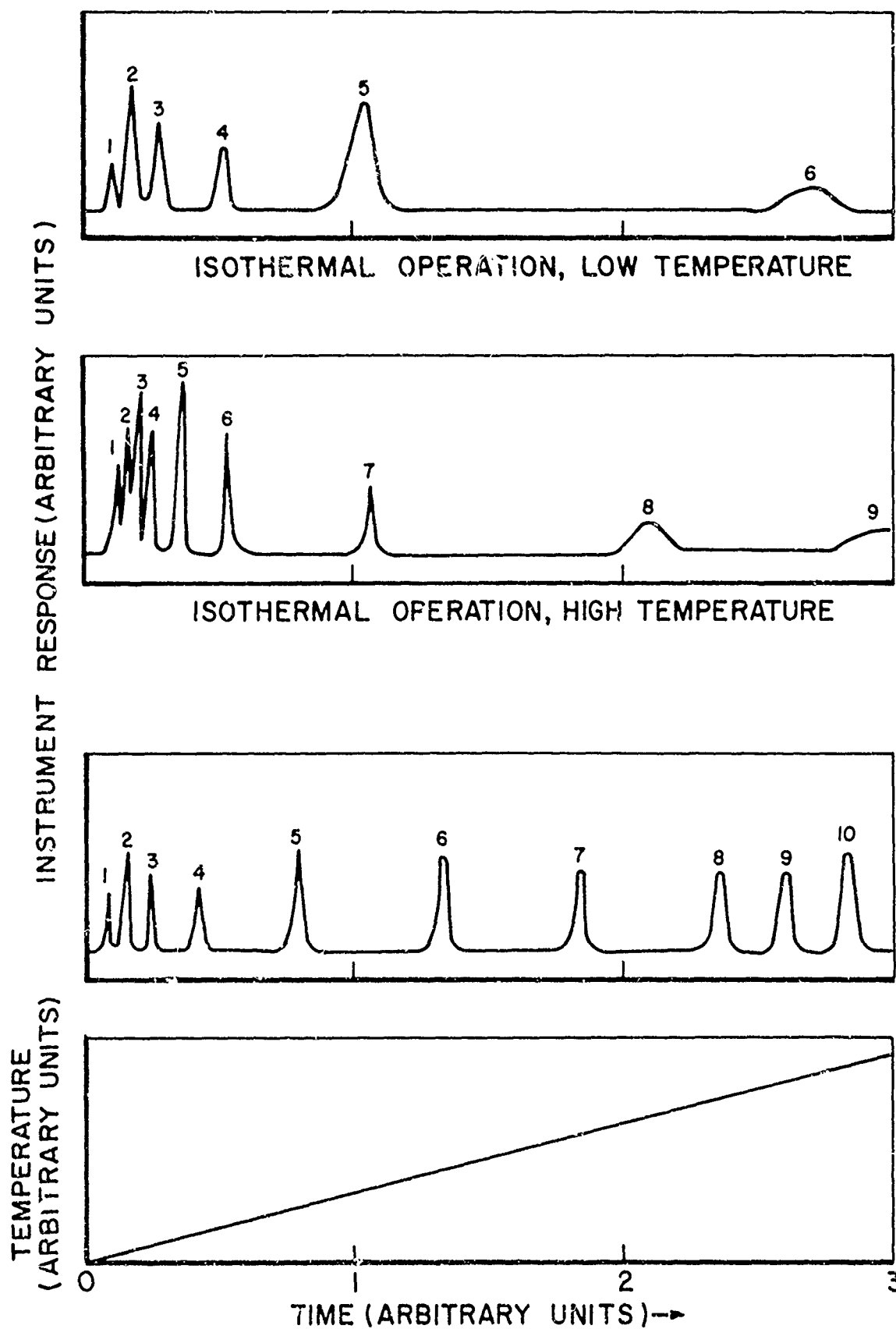
TEMPERATURE PROGRAMMED OPERATION
SEPARATION CHARACTERISTICS
AND COLUMN TEMPERATURE.   FIGURE 3.11

JP13 R 4258 71

they would be under isothermal operation, separation of all pairs will approach the best attainable at any temperature.

A complete review of TPGC is beyond the scope of this work, as it has become in itself a subject of major dimension. (For further information, see [54].)

3.5   Instrumentation

In general, the precision of gas chromatographic techniques is determined not only by the method of analytical separation, but by the repeatability and accuracy of the sample injection system, the type(s) of sensing detector(s), and the way in which each detector output is used to determine quantitative and qualitative information. Discussion of each and every of the available choices of these particular aspects is beyond the scope of the present work, and the reader is referred to the following references [44,51,54].

In the following paragraphs the accepted methodology and instrumentation in each of the above mentioned areas will be briefly described. Basic analysis instrumentation is composed of a number of equipment modules available for the Hewlett Packard 7624A research gas chromatography system. Photographs of the instruments and the developed support equipment are presented in Figures 3.12 - 3.14.

The Hewlett Packard (HP) 7624 gas chromatograph provides the researcher with the necessary equipment for general gas analysis by state of the art techniques. Column oven and electronic design permits isothermal or matrix

SAMPLE TRANSFER AND
SUPPORT INSTRUMENTATION

CRYOGENIC COOLANT
STORAGE (LIQUID N₂)

SAMPLE TRANSFER
PRESSURE MONITOR

SAMPLE TRANSFER
VACUUM SOURCE

HEWLETT PACKARD 7624A
RESEARCH GAS CROMATOGRAPH

6109   P - 13   72
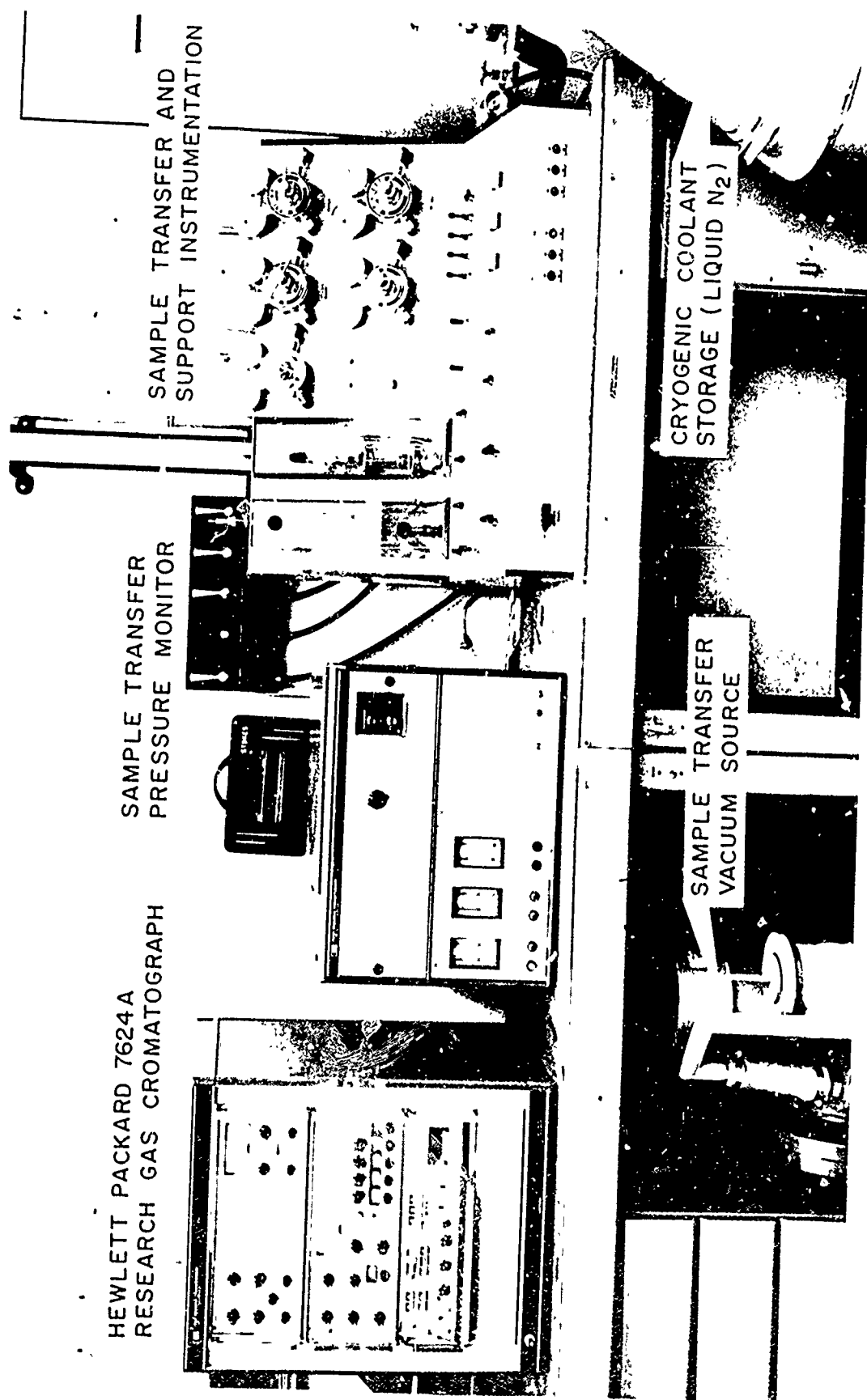
CHROMATOGRAPHIC CHEMICAL ANYLISIS SYSTEM

FIGURE 3.12
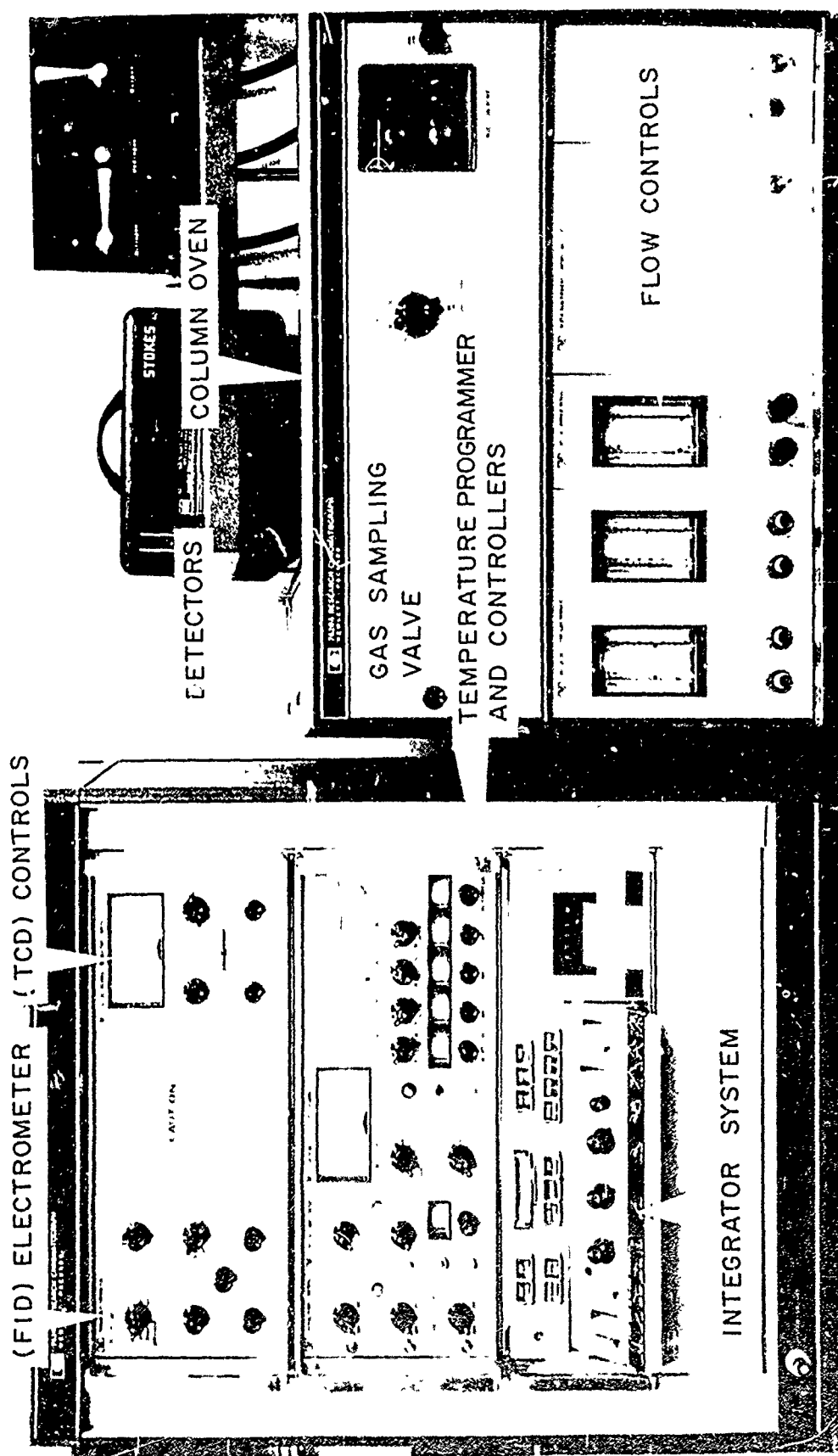
GAS CHROMATOGRAPH INSTRUMENTATION

FIGURE 3.13
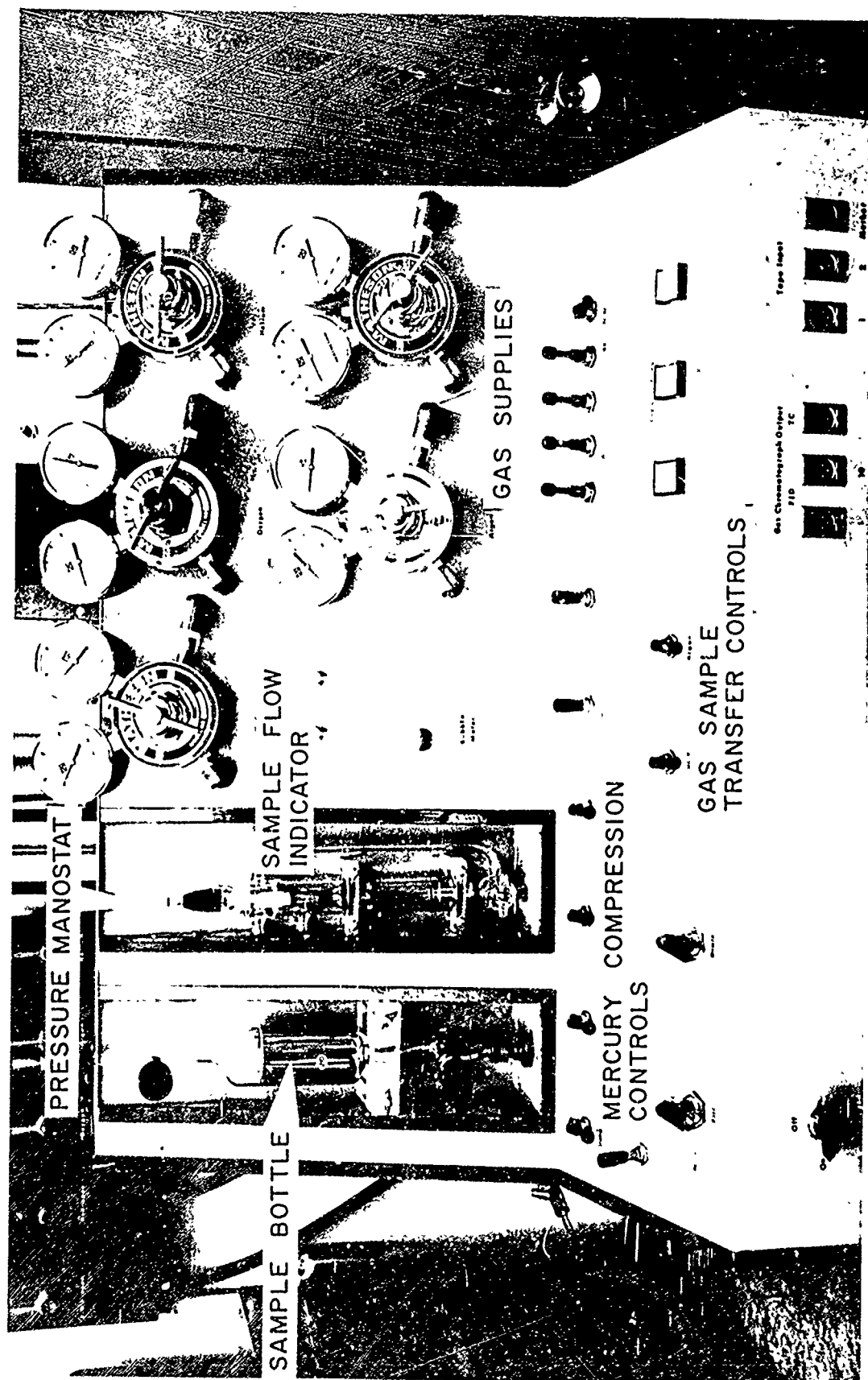
GAS SAMPLE TRANSFER SYSTEM

FIGURE 3.14

temperature programming analysis from cryogenic temperatures (to -95°C) to 500°C. Dual column operation for all column sizes from those for preparatory use to capillary open tubular techniques is available, and simultaneous series or parallel operation of up to two detector systems is possible. More detailed information on the 7624 basic system and the additional module components mentioned in the following discussion can be found in [55].

3.5.1 Separation Techniques

Of prime importance in the chemical analysis of the turbulent flow reactor studies is efficiency in consumption of time and sample. Reduction of sample storage time can be of critical importance to accuracy of the experiment, and design considerations of the sampling procedure severely limit the amount of raw sample available to complete extensive analytical study. Choice of the separation technique (way in which sample components are separated for detection) is most important in conservation of these quantities.

History has demonstrated that the basic GC unit (i.e., single column, direct sample injection) is of proven reliability in quantitative analysis, and temperature programming has significantly increased the information available with each analysis on a single column material. But multiple separations on several column materials are generally required to complete the more exhaustive analyses. Introduction of fluid mechanical complexities - sample splitting,

subtractive column treatment, multi stage separation (column switching), back flushing - to speed separations, significantly shorten extensive analysis times. However, these methods are generally accompanied by inherent decreases in the precision of the results, the magnitude of which will depend on the complexity of the chosen analytical design. Selection of the separation technique itself is very dependent on the species expected to be important in the analysis.

With regard to the turbulent flow reactor experiments, each new area of study will most likely involve new or additional species of importance and, thus, a new or modified separation technique. In reference to the present studies, the separation of the permanent gases, simple alkanes and alkenes, and some of the simple hydrocarbon oxygenates are of specific interest. Many partial separations of these compounds have been described in the literature [56]. Complex flow systems [57] or multiple sample injections would thus be necessary for complete analysis. With introduction of commercial equipment capable of cryogenic temperature programming (Perkin Elmer, 1967; Hewlett Packard, 1969) and development of column packing materials consisting of porous polymer beads, a simple GC system which would have the necessary separation characteristics appeared plausible.

Baum [58] first described the use of porous polytehylene as a low temperature packing support, and Hollis [59] introduced the use of polyaromatic porous polymer bead columns for separation of gaseous mixtures containing water. By

operating the column at $-78^{\circ}C$, he demonstrated the separation of the permanent gases (H_2, N_2, O_2, Ar, CO). Similar separations have been performed in this laboratory on porous polymer beads (Poropak Q and Chromosorb 102) by using a cryogenic temperature program (see Figure 3.15). However, these materials alone do not resolve the C_2 and C_3 hydrocarbons (C_2H_2, C_2H_4, C_2H_6, C_3H_6, C_3H_8), and trace analysis of CH_2O is impaired due to the very strong peak tailing of water. Development of other porous column packing materials and comparisons of their chromatographic properties [60] indicated that composite columns of these materials could solve these problems.

Extensive effort was necessary to develop a successful column and reduce baseline drift to acceptable levels during cryogenic programming. However, a resulting composite column packing of two types of porous polymer beads and a matrix temperature program was determined which separates H_2, N_2, O_2, A_r, CO, CH_4, CO_2, C_2H_4, C_2H_2, C_2H_6, CH_2O, H_2O, CH_3OH mixtures. With selective detection, amounts of C_3H_8 and C_3H_6 can also be quantitatively analyzed, if quantitative detection of water and CH_2O are unimportant. The simpler fluid mechanical design and temperature programming significantly improve experimental precision while conserving the time necessary for analysis. Further, the same separation technique will be useful in studies of other of the simpler hydrocarbon oxidations in addition to that of methane.

THERMAL CONDUCTIVITY DETECTOR:
260 ma @ 130 °C

12 ft DUAL COLUMNS, 80/100 MESH, POROPAK Q

HELIUM FLOW RATE OF 50 ml/min

TEMPERATURE PROGRAM: -95°C TO -75°C
@ 2%/min, -75°C TO 150°C @ 30%/min

SAMPLE SIZE, 1/2 cc @ 1/2 atm

PEAKS

1) 4 % HYDROGEN
2) NITROGEN BALANCE
3) 2 % ARGON
4) 8 % CO
5) 2 % CH_4
6) 8 % CO_2
7) WATER

TIME (MINUTES)
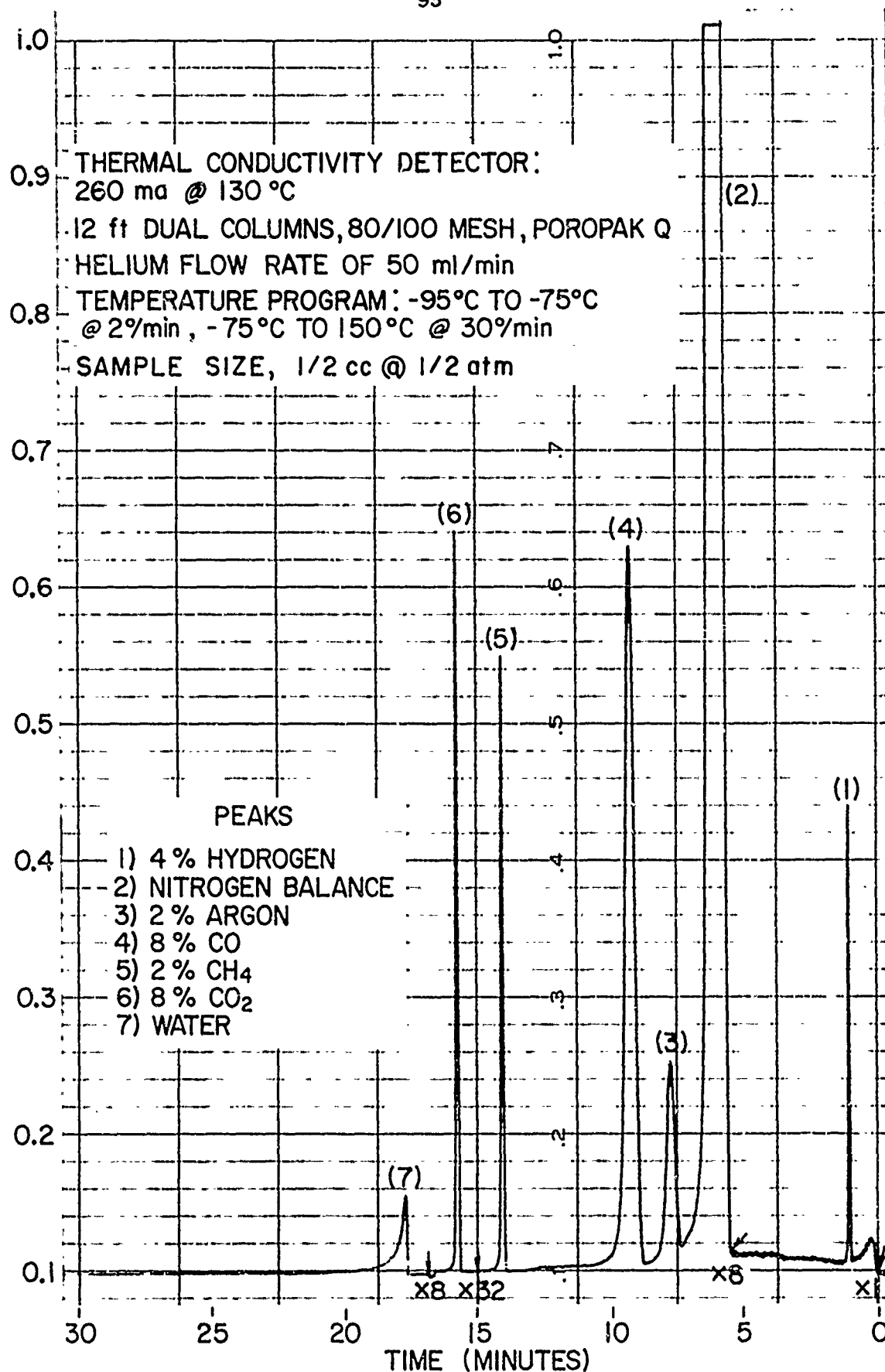
EXAMPLE OF CRYOGENIC TEMPERATURE PROGRAMMED
SEPARATION OF PERMANENT GASES

FIGURE 3.15

Details of the composite column design, temperature program, other operating conditions, and component retention times are deferred to Chapter 4.

3.5.2 Detection Methods

In the present work, two detector systems are applied: (1) the thermal conductivity detector (TCD), a "universal" detection technique, and (2) the flame ionization detector (FID), a "selective" detection method particularly suitable for sensing hydrocarbon species. Clear description of other available detection methods can be found in [44] or [51]. In comparison, the chosen techniques have better stabilities (limited instrumental signal drifts) and wider linear dynamic ranges. (Linear dynamic range is the ratio of the largest to smallest concentration to which the detector will respond in a linear fashion.) Selection of carrier gas is not important to their operation, but does significantly alter their responses.

3.5.2.1 The Thermal Conductivity Detector

The TCD fulfills the need for a detection scheme responsive to all chemical compounds (i.e., universal detection method). It belongs to the class of differential detectors which measure some physical property of the separated gaseous components. The use of this detector is particularly important for determination of chemical compositions which contain the permanent gases (CO, CO_2, N_2, O_2, H_2, etc.).

The TCD essentially compares the thermal conductivity of the carrier/specie mixture to that of the pure carrier.

For binary mixtures, such a measurement is indicative of the concentration of the detected component. It is clear that the specific response of the detector is related to the magnitude of the thermal conductivity difference between the carrier and the species to be sensed, and this fact dictates the choice of carrier. For heavier molecular species ($\lambda \propto 1/\sqrt{mw}$), a very light carrier gas such as helium or hydrogen produces the best responses. However, detection of one of these latter gases in a carrier of the other has limited sensitivity, and anomalous results occur as the mixture ratio changes over a wide range [61].

Response is also a strong function of the construction of the detector cell itself. Recent developments at Hewlett Packard show promise of achieving sensitivities near those of the FID [62] in future instruments. Pertinent design data for the Hewlett Packard (HP) Model 7645A TCD used in these studies are presented in Table 3.1 along with typical sensitives for some common compounds.

3.5.2.2 Flame Ionization Detector

Ionization detectors operate on the proportionality of charged particle concentration and electrical gas conductivity. The flame ionization detector (FID) creates ions from the component eluting from the GC column by combining the effluent with a flow of hydrogen and burning the mixture in oxygen or air.

THERMAL CONDUCTIVITY DETECTOR
MODEL 7645A SPECIFICATIONS
From Reference [55]

TYPE DETECTOR

Four filament detector (two filaments per cartridge).
High sensitivity DPS split spiral, flow thru.

OPERATING TEMPERATURE

Ambient to 425°C. Typical heat-up time to 350°C in four hours.

TYPE FILAMENTS

Tungsten-Rhenium, passivated for greater protection against oxidation damage.

FILAMENT REPLACEMENT

Readily changed filament cartridges.

FILAMENT PROTECTION

Automatic pressure switch (detector protector) to cut off current when carrier pressure falls. (Cut off pressure between 4-8 psig).

RECOMMENDED CARRIER GAS

Helium from 5-200 ml/min (up to 350 ml for prep work.)

CELL VOLUME

0.72 cc per two filament cartridge.

FLOW SENSITIVITY

Relatively insensitive to flow change: ½ mV for flow change of one stream from 30 to 150 ml/min. at 150 ma and 350°C.

TEMPERATURE REGULATION

Power proportional temperature controller with platinum sensor; independently heated buffer.

TYPICAL NOISE

± 1/4% at following conditions: 150 ma, attenuation IX, detector isothermal at 350°C.

TYPICAL DRIFT

± 4%/hr. at following conditions: 150 ma attenuation IX, detector isothermal at 350°C.

TABLE 3.1(a)

TYPICAL TCD DETECTOR SENSITIVITIES
AT HIGH FILAMENT
CURRENT OPERATION
From Reference [63]*

CONDITIONS: Filament current 290 ma
1 ml sample volume.
Helium carrier gas 40 ml/
minute.

Gas	Minimum Detectible Limit
	(PPM)
H_2	300
O_2	4
N_2	8
CO	5
CO_2	5
CH_4	11

*Relative response information of many other compounds can be found in [64,65].

TABLE 3.1(b)

The degree of ionization (response) of a specie is dependent in most cases on the number of carbon atoms it contains. Upon introduction of the FID in 1958, it was assumed that thermal ionization was the operating mechanism. More recent evidence indicates this plays only a minor role. Sternberg, et. al., [66] give a comprehensive discussion of the presently proposed theories.

Table 3.2 presents pertinent operational data for the (HP) Model 7635A FID Detector and, also, a list of compounds giving little or no response by this technique. This selective detection property can be important in determining hydrocarbons in incompletely resolved mixtures of one or more of the above compounds. Hydrocarbon sensitivity of this detector is approximately 1000 or more times greater than that available with present TCD designs.

3.5.3 Sample Injection System

Precision of the complete analytical system is to a large degree determined by the way in which the sample is introduced into the GC. Repeatability of the injection process is obviously important. However, one of the conditions for maximizing chromatographic response is that the sample transfer technique must also be as rapid as possible, avoiding contamination or dilution and interfering as little as possible with the flow of carrier gas.

FLAME IONIZATION DETECTOR
MODEL 7635A SPECIFICATIONS
From Reference [55]

TYPE

Dual detector unit

OPERATING TEMPERATURE

Ambient to $500^{\circ}C$ - platinum
feedback for temperature
control

JETS

Dual - each isolated with
operating potential of 350
VDC

LINEAR OPERATING RANGE

Over 10^6 with propane
sample

SENSITIVITY

40 millicoulombs/grams
of carbon with hydro-
carbon sample and oxy-
gen as combustion gas
(10 mc with air)

FLAME IGNITION

Pushbutton flame ignitor
for both flames

COMPOUNDS GIVING SMALL
OR NO RESPONSE IN THE
FLAME DETECTOR*

He	CS_2	NH_3
Ar	COS	CO
Kr	H_2S	CO_2
Ne	SO_2	H_2O
Xe	NO	$SiCl_4$
O_2	N_2O	$SiHCl_3$
N_2	NO_2	SiF_4
	CH_2O	

*Other response information pertaining to many other com-
pounds can be found in [65].

TABLE 3.2

Precision of the experiment can clearly be improved by averaging the results of several measurements (sample injections). If only small quantities of the sample are available, each transfer of sample to the GC therefore must waste as little as possible.

Transfer from storage to the GC instrument involves one of two processes: direct injection into the carrier gas stream by hypodermic needle or transfer by constant volume by-pass sampling loops. The former system is obviously difficult with gaseous systems and generally offers poor precision. Sample transfer systems of the latter design have been detailed in [44]. The utility of valve systems employing by-pass transfer loops was recognized early in the development of sample transfer devices. The basic function of the sample valve is to reproducibly transfer a fixed volume of continuously flowing or stored sample into the carrier gas stream by interchanging two loops of matched volume. However, with external calibration techniques (i.e., measurement of integrated response to a known pre-determined concentration of the specie to be calibrated), constant volume transfer is not a sufficient condition. For precise results, repeatability in the number of moles transferred is important. In view of the perfect gas equation, this means that the pressure and temperature of the transfer process must also be fixed. Temperature control is easily achieved by heating

the sampling transfer valve. Control of the transfer system pressure has previously been accomplished by manometer or transducer measurements or by diluting a known amount of sample with inert to a specific pressure. Both of these methods are inapplicable in the present situation. Conventional pressure measurements necessitate that a significant amount of sample be wasted in each transfer, thus limiting the possible number of repetitive analyses. Further, dilution techniques are not amenable to trace analysis of the permanent gases.

To solve this dilema, a novel, simple, minimum volume method which accurately repeats transfer pressure, volume, and temperature has been devised. A schematic of the transfer system is presented in Figure 3.16. Volume and temperature of the transferred sample is controlled by a HP Model 19021A heated gas sampling valve. Transfer volume (loop) sizes of .5, 1, 2, 5, 10 and 20 ml are available, and temperature can be accurately controlled to $\pm$ 2K in the range 40-200°C. Volume of the transfer system is less than 1 ml (excluding the loop volume). By first applying a hard vacuum to the transfer system and then filling it with sample to the desired pressure, minimum waste of sample is assured.

Transfer pressure is controlled by a cartesian manostat/check valve arrangement which does not add further waste volume to the system and controls pressure to $\pm$ 1 mm Hg.
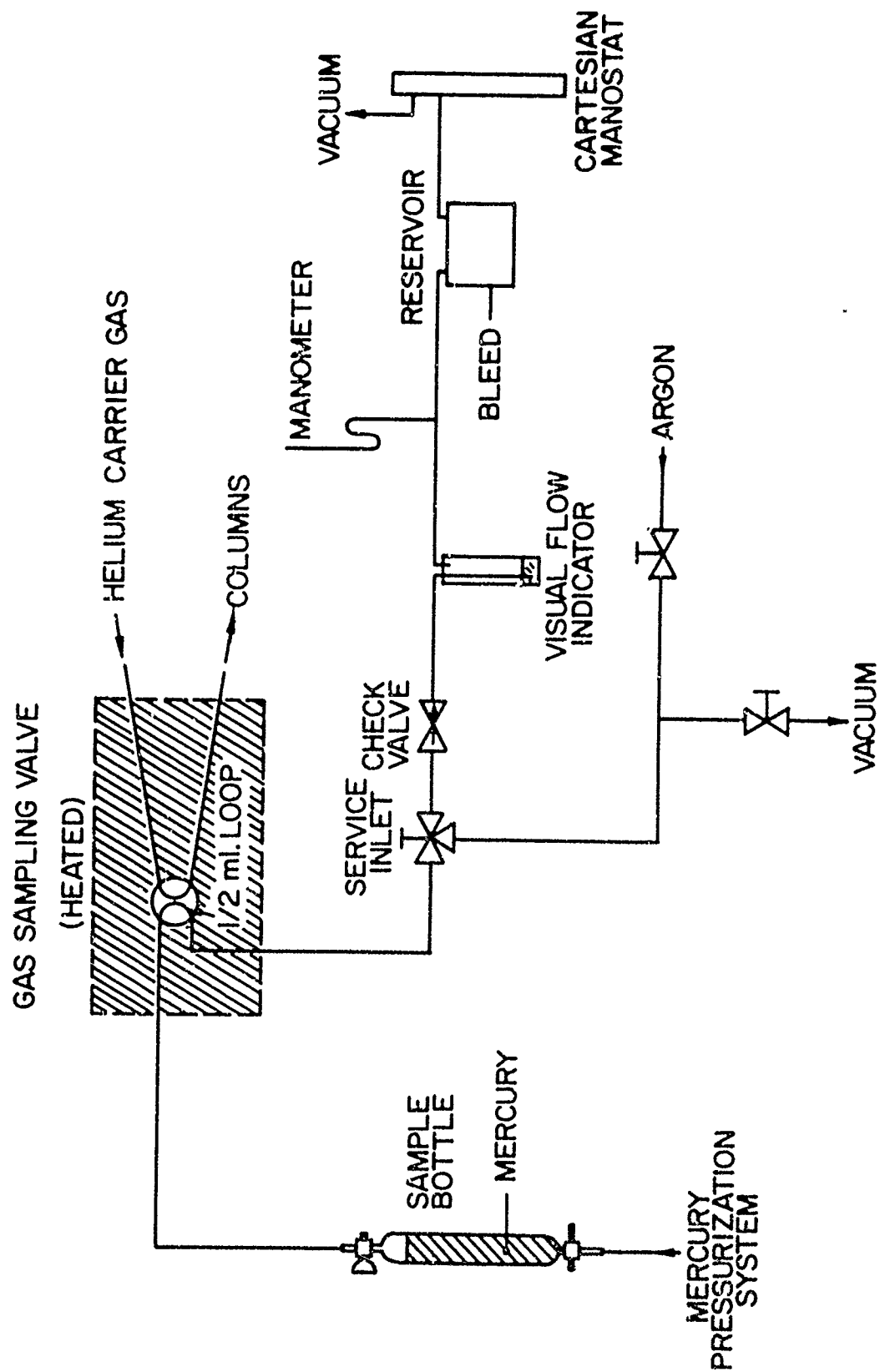
GAS CHROMATOGRAPH SAMPLE TRANSFER SYSTEM

FIGURE 3.16

For samples stored at pressure below that controlled by the manostat, a mercury displacement system for compressing the stored sample to pressures greater than .7 atmospheres has been devised. Mercury displacement can be used without effecting sample composition, providing the sample does not contain nitrogen dioxide or hydrogen sulphide and the compressed pressure does not exceed that level which produces condensation. Available choices of system pressure and sample loop volume can successfully eliminate the latter problem.

3.5.4 Chromatographic Data Reduction Techniques

Required relative precision and the immense amount of data expected in these experiments necessitate the use of automatic data handling.

All detector output data is integrated electronically to give both retention time and area response of each sensed compound. The sophisticated electronics of an HP Model 3370A Integrator provide automatic correction of null voltage shift (baseline drift), selective independent triggering sensitivity of beginning and end of each sensed peak, determination of peak maximum elution time (retention time), and area assignment to incompletely resolved components. Complete specifications of the instrument can be found in [67]. Goland and Peterson [68] have reviewed the performance characteristics of the 3370A integrator and conclude that, even with considerable overlap of peaks, error in area determination and allocation averages less than 1%. In well resolved cases,

relative precision was found to be better than .5%.

Detector outputs are continuously monitored on a Texas Instrument dual channel variable range, variable zero recorder and are also fed to the 3370A integrator system. Output of the 3370A integrator (retention time, peak area) are printed on paper tape, and manually transferred to computer cards. Computer reduction of this "raw" data is accomplished by the program described in Appendix B.

CHAPTER 4   EXPERIMENTAL MEASUREMENTS

The developed instrumentation and chemical measurement techniques described in the preceding two chapters have been applied to two (interrelated) high temperature reaction studies: the reaction of methane with oxygen and the reaction of carbon monoxide (in the presence of hydrogeneous compounds) with oxygen. In addition to supplying a logical starting point and basis for future (proposed) experimental efforts on the higher paraffin oxidation reactions, these two studies provide sufficient opportunity to evaluate the developed experimental techniques.

Both oxidation mechanisms have been studied extensively by kineticists over a wide range of experimental conditions using diverse experimental techniques; thus, some comparative results are available. However, additional measurements from these turbulent flow reactor experiments are capable of much more than re-development or substantiation of previous results. More complete chemical description of the reactions in a simple fluid mechanical environment (one dimensional, no diffusion, adiabatic) must be considered as new and significant results. The direct kinetic interpretations of such results will be most useful in computer modeling of complete kinetic mechanisms, and it is unfortunate that such analytical studies were not plausible in the time available for this research. However, it will be seen that the

overall kinetic interpretations of the turbulent flow reactor results (and other more particular interpretations of the data) offer qualitative and quantitative support to important and sometimes different conclusions concerning the oxidation mechanisms, their interrelated character, and previously published results. The new overall rate results will also be shown to be of importance to engineering design considerations.

Although it was not an original motivating factor in the decision to study these two particular reactions, one further benefit of the results should be emphasized. While it has been shown that the thermal analysis method will not be applicable to complex kinetic reactions in which significant build up of intermediaries (stable or unstable) appear, the facility with which simpler reactions can be studied urges one to reconsider its use in such circumstances.

The carbon monoxide (water)/oxygen kinetics satisfy the necessary assumptions for use of the thermal technique; and, thus, independent chemical and thermal analysis studies of this reaction offer a unique opportunity to establish their relative precision in the same experimental environment. Further, independent studies of the methane/oxygen reaction will give some quantitative picture to the departures expected when the assumptions necessary to the thermal analysis method are not well modeled.

4.1 Experimental Methods

Thermal analysis and chemical measurements were performed on both the CH_4/O_2 and $CO(H_2O)/O_2$ reactions. Chemical measurements and their results were emphasized and thermal measurements were conducted primarily for the previously described comparisons. The end result of either of these experimental methods is simultaneous definition of reactant and product (and in the chemical method, intermediary) mean concentrations, mean rates of change of concentrations (with time), and mean temperature at specific axial locations in the turbulent reaction zone. On an overall basis of study, each point measurement is considered completely independent of all others, while the mechanistic approach must consider an inherent relationship among all of the measurements in the same reaction zone.

4.1.1 Preliminary Measurements

Each "run" of the turbulent flow reactor is characterized by a complete traverse of the instrument probe(s) through the reaction zone and measurements of the carrier flow rate, reactant flow rates and the reaction zone temperature profile. For thermal runs, continuous traverse of a temperature probe is adequate. For chemical analysis runs, the chemical sampling and temperature probes are incrementally repositioned through the zone, the location of each sampling position being recorded. All tests are accompanied by continuous monitoring and control of the reactor inlet temperature.

4.1.2   Thermal Analysis Studies

The above preliminary measurements provide the initial reactant concentrations, the mean (one dimensional) velocity at any axial location, and the mean temperature and mean temperature gradient (with distance) at each axial location in the flow reactor. Appendix A adequately describes how these quantities can be used to calculate the concentrations and rate of change of concentration (with time) of products and reactants at each point in the flow reactor.

4.1.3   Chemical Analysis Studies

Since the (stable) chemical species in the $CO(H_2O)/O_2$ reaction also occur in the oxidation of CH_4, the same method of analyzing the chemical samples taken from the flow reactor in the latter study can be employed in the former one.

The cryogenic temperature programming technique described in Section 3.5.1 was used together with simultaneous detection by TCD and FID systems. Effluent from the column was split in a volume flow ratio of 2 to 1, FID/TCD. Operating parameters for the GC instrument, GC Integrator, and sample transfer system are summarized in Table 4.1. Retention data, lower detectible limit, and approximate responses (μ volt-sec/100 ppm specie) for pertinent species are enumerated in Table 4.2.

GAS CHROMATOGRAPH OPERATING CONDITIONS

Column Conditions

Type Packing

	Flow Rate (cm^3-min^{-1})		Carrier Gas
A Column	30.0	80/100 Mesh, 6 ft. Porapak R, 6 ft. Porapak Q, 1/8 ir S.S.	Helium
B Column	30.0	80/100 Mesh, 12 ft. Porapak R, 1/8 in. Stainless Steel	Helium

Detector Conditions

Thermal Conductivity Detector (TCD)

Bridge Current	270.	mamps
Oven Temperature	130.	°C
Auxiliary Temp.	125.	°C

Flame Ionization Detector (FID)

Hydrogen	40.	cm^3 min^{-1}
Oxygen	500.	cm^3 min^{-1}
Auxiliary	40.	cm^3 min^{-1}
Temperature	250.	°C

Temperature Program(s)*

Start °C	Pinj min	Rt 1 °C min⁻¹	Lv 1 min	Temp 1 °C	Rt 2 °C min⁻¹	Lv 2 min	Temp 2 °C	Rt 3 °C min⁻¹	Lv 3 min	Temp 3 °C	RCV °C	Comments
-95.	0.	4.	0.	-62.	30.	2.	40.	8.	0.	65.	160.	General PG, all species
140.	0.	0.	0.	0.	0.	0.	0.	0.	0.	0.		0. H$_2$O & CH$_2$O

(column header Rt 1: $°C$ min^{-1}; Rt 2: $°C$ min^{-1}; Rt 3: $°C$ min^{-1})

Miscellaneous

Sample Vol.	0.5	cm^3		
Sample Temp.	110.0	°C	Inj. Port. Temp.	160.0 °C
Sample Press.	38.0	cm hg	Split Ratio	2.0 TC/FID

Integrator Parameters**,+

Prog.Inpt.	Noise Suppression	Up Sens. mv min⁻¹	Down Sens. mv min⁻¹	Brst.Time min	Peak Summation	FNT	RHR
1 TCD	3.00	0.10	0.03	0.00	0.00	NO	1000.00
2 TCD	3.00	0.10	0.03	0.10	0.00	NO	0.10
3 TCD	1.00	0.03	0.01	0.00	0.00	NO	0.10
4 FID	4.00	0.10	0.03	0.10	0.00	NO	0.10

* See Reference [55]
** See Reference [67]
+ General Analysis: PRG(1) & PRG(4)
  H2O & CH2O: PRG(3)

Table 4.1

Pertinent Chemical Analysis Data[*]

Chemical Specie	Retention Time ($\pm 2\%$) (Min)	Detector Used	Lower Detectible[+] Limit (ppm)	Approximate Response (μvolt-sec/100 ppm)
H_2	1.50	TCD	300	5
N_2	5.05	TCD	-	175
O_2	5.80	TCD	-	180
A_r	6.50	TCD	-	100
CO	7.60	TCD	80	145
CH_4	11.60	FID	1	1015
CO_2	14.10	TCD	40	190
C_2H_4	16.20	FID	.1	1940
C_2H_2	16.90	FID	1	910
C_2H_6	17.50	FID	.1	2080
C_3H_6	19.60	FID	.05	3050
C_3H_8	21.40	FID	.05	3150
CH_2O‡	2.20	TCD	-	130
H_2O‡	2.50	TCD	-	110
CH_3OH‡	4.00	FID	-	820

*For Gas Chromatograph Conditions of Table 4.1

‡Analyzed using second temperature program

+If not listed, it was not estimated

Table 4.2

Several important points relative to chemical analysis measurements should be mentioned.

(i) The high polarity of several compounds, notably water and methanol, produces significant broadening of the eluted peaks, and, therefore, inferior lower limits of detection and response, even with temperature programming. Due to this fact and adsorption of water on the sample bottle and transfer system walls, measurements of water were not very reproducible. It will be seen later that this problem could be successfully circumvented by initial water flow measurements in the reactor and calculation of the water concentration from atom conservation principles among the other stable species detected.

(ii) Although C_3H_6 and C_3H_8 elution times occur during the broadened elution band of water, selective quantitative detection of these species is possible on the FID.

(iii) One might erroneously conclude that, since detector responses (both FID & TCD) have wide linear dynamic ranges, single point calibration techniques are sufficiently accurate to determine absolute concentrations. This, however, is true only when species can be sufficiently resolved that peak overlapping and/or tailing does not interfere with integrator detection. Such interference was investigated for all possible species by dilution of an initial mixture with air or helium and noting changes in the relative measured responses of the detector/integrator system. Notable departure from linear response occurs for carbon-monoxide because of overlapping

with the tail of the oxygen or argon peaks. The resulting
non-linear response was repeatable for oxygen concentrations
between .5% and 20% and all expected carbon monoxide concentra-
tions and was accounted for in determination of the absolute
carbon monoxide level in each sample analyzed. The non-
linearity is accurately represented by the curve depicted
in Figure 4.1, and it was independent of the TCD filament
current level.

(iv) As noted in Section 3.3.1, each specie which might be
present in the sample to be analyzed should be checked for
adsorption or chemical reaction effects which could result
in sample degradation during storage and analysis. Experi-
mentally, all species present in the methane/oxygen reaction
system, excluding CH_2O and H_2O (previously discussed), showed
no sample degradation properties during storage and analysis
periods exceeding 72 hours. Investigations of a mixture of
H_2O, CH_2O and CH_3OH exhibited a slow degradation of the
relative response of CH_2O with time. Slow polymerization of
CH_2O to tri-oxymethelyne or paraformaldehyde can occur at
room temperature when water is present [69]. Wall [70] claims
that 100% depolymerization and re-formation of CH_2O can be
obtained by heating the polymers to temperatures in excess of
$150^{\circ}C$. However, Sperling and Toby [71] have shown that slow
pyrolysis of CH_2O can occur at these temperatures. There is
also some evidence that CH_2O can be photochemically decomposed
and/or oxidized at room temperature.
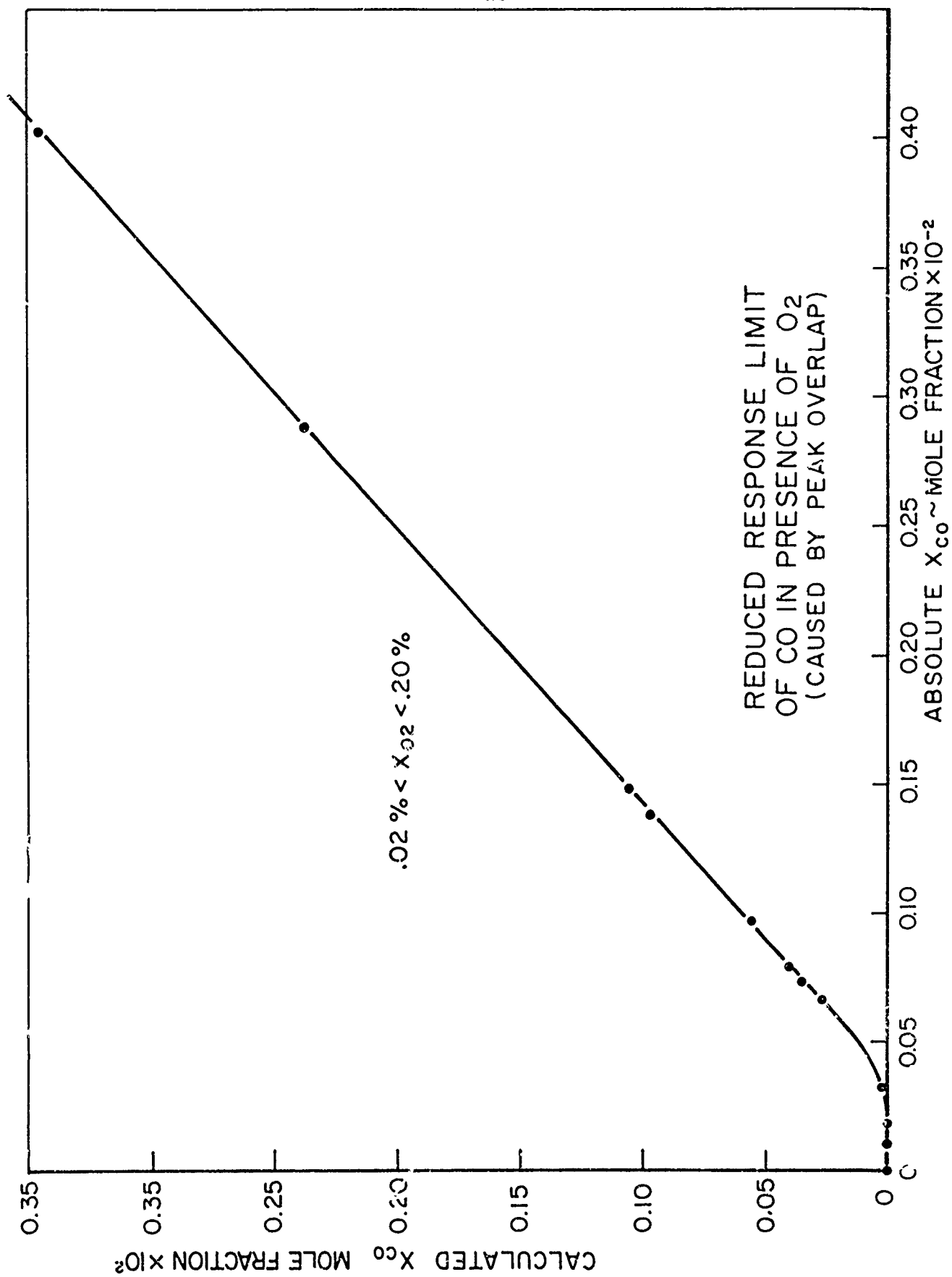
FIGURE 4.1

All of these facts were taken into account in trying to discover a reasonable way to store gaseous CH_2O without degradation, but at present no technique offers more than 80-90% recovery of the original concentration. However, it was definitely established that all decay processes were very slow, too slow in fact to occur during the actual sampling process. Attempts were made to perform rapid analysis for formaldehyde in the methane/air reaction before significant degradation could occur. Detected concentration levels were of the same order as the lower detection limit, and reproducible profile measurements of CH_2O were not plausible. This level of CH_2O was also confirmed by auxiliary analysis techniques (see Page 182) and observed total carbon balance of other detected species.

(v) Because all experiments necessarily had to be conducted with amounts of oxygen largely in excess of the stoichiometric level (see Page 178), it was plausible and simpler to calculate the oxygen present in each sample from initial flow measurements in the flow reactor and atom conservation among the stable species present.

4.1.3.1 Calibration of Chemical Analysis System

Calibration of the complete G.C. analysis system (except for CH_2O, CH_3OH, H_2O) was performed by one point response measurements to primary standard certified calibration mixtures obtained from the Matheson Co. (Table 4.3).

Calibration Standard Mixtures[†]

Mixture One

Specie	Mole Percentage
METHANE	$1.01 \pm .02$
CARBON MONOXIDE	$1.98 \pm .02$
CARBON DIOXIDE	$1.99 \pm .02$
ETHYLENE	$0.99 \pm .02$
ETHANE	$0.99 \pm .02$
PROPANE	$1.00 \pm .01$
NITROGEN	Balance

Mixture Two

ETHYLENE	$2.01 \pm .02$
ETHANE	$2.00 \pm .02$
ACETYLENE	$2.00 \pm .02$
NITROGEN	Balance

Mixture Three

PROPYLENE	$2.01 \pm .02$
PROPANE	$2.02 \pm .02$
NITROGEN	Balance

[†]Mixtures made by weight measurements, Matheson Gas Products,

Table 4.3

Proportional relations (with a correctional function for CO) were used to calculate concentrations of the detected species.

The certified calibration mixtures were produced by actually weighing the specific components in each mixture. Accuracy of the mixtures was independently verified by Gollab Analytical Services.

Several calibrations were performed before, during, and after the complete analysis of a flow reactor run to account for detector response drift or changes in sample transfer pressure or temperature settings. Calibration responses never varied by more than 2% during any 72 hour period. Repeatability of the sample analysis system response over such a time period is illustrated by the calibration responses shown in Table 4.4.

4.1.3.2   Data Reduction

Calculations of concentration and concentration gradients with distance were aided by computer techniques. Calculation of gradients from integral functions is a degenerate process, a fact which is especially true for gradients to be calculated from incremental data. A computer program which calculates concentrations, concentration gradients (with time), temperature, and velocity at each sampled position in the flow reactor has been developed and the employed methodology, together with explanatory notes and examples of output are presented in Appendix B.

REPEATABILITY OF CHEMICAL ANALYSES*

Area Count in μvolt-seconds

Time hrs.	CO 1.98%	CH$_4$ 1.01%	CO$_2$ 1.99%	C$_2$H$_2$ 0.99%	C$_2$H$_6$ 0.99%	C$_3$H$_8$ 1.00%
0	2808×10^1	1123×10^2	3479×10^1	2158×10^2	2149×10^2	3414×10^2
12	2809×10^1	1139×10^2	3430×10^1	2185×10^2	2175×10^2	3456×10^2
24	2807×10^1	1146×10^2	3417×10^1	2201×10^2	2188×10^2	3470×10^2
36	2790×10^1	1125×10^2	3420×10^1	2190×10^2	2176×10^2	3446×10^2
48	2825×10^1	1131×10^2	3442×10^1	2168×10^2	2147×10^2	3461×10^2
60	2815×10^1	1142×10^2	3465×10^1	2176×10^2	2190×10^2	3468×10^2
72	2830×10^1	1128×10^2	3418×10^2	2105×10^2	2180×10^2	3421×10^2

* Analyses of mixture 1 over 72 hour period with gas chromatograph conditions of Table 4.1

Table 4.4

4.2 Reactant Gases and Carrier

The reactants and carrier gases used in these turbulent flow reactor studies and facts concerning their chemical purities are presented in Table 4.5. All gases (excluding the G.C. carrier gas) were used as received from the manufacturer, without further purification. The chosen G.C. carrier gas (helium) was purified by a quartz diffusion cell technique [72] to levels greater than 99.99995% minimum. (All contaminants are hydrogen and neon.) This ultra purity proved to be necessary for removal of ghost peaks resulting from the cryogenic PTGC techniques in the chemical analysis procedure.

The purity of reactant and flow reactor carrier gases are considered sufficiently high for contaminants (except possibly water or hydrogen formed water) to be in-effective in changing kinetic observations. Since water is one of the primary reaction products in the methane/oxygen reaction, contaminant levels of H_2O are negligible. Additions of water by direct atomization in the carrier inlet section during all carbon monoxide/oxygen reaction studies produced water levels sufficiently high for contaminant levels to be neglected.

4.3 Overall Correlation Methods

The concept of overall (global) reaction kinetics and its use is a direct result of the complexity of most

REACTANTS AND CARRIER GASES

Gas	SPECIFICATIONS Supplier	Composition (Vol %)
Carriers		
Air	In House Compressor	N_2 78 *
		O_2 - 20.8
		Ar - .93
		CO_2 - 660 ppm
Nitrogen	Air Reduction Inc. (Liquid)	$N_2 >$ 99.8
		O_2 - .02
Reactants		
Methane	Matheson (Ultra Pure Grade)	$CH_4 >$ 99.97% *
		$CO_2 <$ .001
		$O_2 <$ .001
		$N_2 <$ .003
		$C_2H_6 <$ .0046
		$C_3H_8 <$ .0005
Carbon Monoxide	Matheson (Cp Grade)	$CO >$ 99.5% *
		$O_2 <$ .04
		$CO_2 <$ .07
		Ar $<$ .005
		$CH_4 <$ .004
		HC $<$ .003
		$FE(CO)s$ None
		$H_2O <$ .01
Oxygen	Air Products (Extra Dry)	$O_2 >$ 99.5
		Ar $<$ .45
		$N_2 <$ .05

*Analysis supplied by supplier; others are typical compositions.

Table 4.5

chemical reactions and the complicated fluid mechanical situations in which some knowledge of heat release or chemical rates is necessary (ram jets, rocket engines, gas turbines, etc.). The assumption invoked is that the course of chemical kinetic events may be described in terms of a few of the main reactants and products (C_i) in a functional relation with much the same form as an elementary reaction process. Typically, the equation is of the form:

$$\frac{d[C_i]}{dt} = k_{ov} \prod_{i=1}^{m} [C_i]^{m_i} \qquad 4.1$$

k_{ov} , the overall specific rate constant, is expressed in the Arrhenius form

$$k_{ov} = 10^A e^{-E/RT}$$

The n_i's are defined as the orders of reaction with respect to C_i, and m is termed the overall reaction order. 10^A and E are termed the overall frequency factor and activation energy respectively.

The relation implies nothing about the actual kinetic mechanism (in terms of elementary reactions), although the parameters in the strictly empirical relation sometimes are governed by a single elementary step (or a number of steps) which basically control the rate of the chemical process. Under what circumstances such an overall correlation is usable is largely dependent on both the kinetic mechanism to which it is applied and the physical environment in which the

process is occurring. As mentioned earlier Levy and Weinberg [6] have shown that the approximation is not generally applicable in flames ; however, this fact may not arise from the chemistry itself, but from the physical structure and diffusive character of the flame. Where a particular rate-determining step or sequence in the true chemical reaction mechanism occurs and the physical circumstances of the application are similar to those in which the expression was derived, the overall approximation is a valid and vastly simplifying idea. However, extension of such a correlation to experimental conditions outside the range studied should always be done with some reservation.

Eberstein [15] and Sawyer [16] have described and used several methods to express the turbulent flow reactor data in the overall approach of equation 4.1. The values of the constants n_i, A, and E are unknown and are generally determined by considering them as unknown dependent variables of the equation.

The most direct approach to evaluate n_i, A, and E is as follows:

(i) Holding T and all C_i's constant except for C_α, note the dependence of $\frac{dC}{dt}_1$ on C_α. (The slope of a plot of ln $\frac{d[C_1]}{dt}$ versus ln $[C_\alpha]$ will give n_α.)* Repetitive application of this technique will determine all of the n_α's.

*Linearity of the slope will to some extent verify the validity of the chosen functional dependence (Equation 4.1).

(ii)   having determined all of the n_i's, evaluate

A and E from the resulting plot of $\ln(k_{ov})$

versus T^{-1}.

$$k_{ov} = \frac{d[c_i]}{dt} \frac{1}{\prod\limits_{i=1}^{m} [c_i]^{m_i}}$$

Unfortunately it is usually difficult or impossible
to hold all parameters except one concentration (C_α) in-
variant.   An indirect method of achieving this is to conduct
experiments with those parameters in large excess.   Then

$$\frac{d[c_i]}{dt} = K_1 [C_\alpha]^{m_\alpha} \; ; \; K_1 = K_1(T)$$

is approximately true again, and n_α may be determined as
before.   As evidenced by the study of the methane oxidation,
this method is also not always plausible.   There, although
the fuel order can be determined by running with excess
oxygen, the reaction could not be studied with fuel in large
excess.   If only two concentration dependencies are assumed
(fuel and oxidizer), the oxidizer order might be determined
by conducting experiments at constant temperature and account-
ing for the determined fuel order.   However, in practice, it
will be shown that in the methane oxidation this solution is
also implausible.

In such a situation Sawyer concludes that one must
rely on statistical techniques to determine the missing orders
and A and E.   Eberstein [15] and Sawyer [16] have suggested

that the standard deviations or the percent standard devia-
tion (respectively) will achieve their minimum values when
the correct orders have been found. There appears to be
little or no theoretical basis for these arguments since

from

$$k_{ov} = 10^A e^{-E/RT}$$

$$\frac{dk_{ov}}{k_{ov}} = dA \ln 10 - \frac{dE}{RT}$$

$$\frac{\sigma k_{ov}}{k_{ov}} \approx \sigma A \ln 10 - \frac{\sigma E}{RT}$$

Because of this coupling, σE and σA or $\frac{\sigma E}{E}$ and $\frac{\sigma A}{A}$
independently do not reflect either minimum deviation in k_{ov}
or correct choice of reaction orders. Further, the degree
of coupling is unknown.

An alternative technique, which has apparently
been previously overlooked, was used in the present studies.
If one considers the relation

$$\frac{d[F]}{dt} = k_{ov}[F]^a [O]^b$$

F = fuel

O = oxidizer

and conducts at least one set of experiments with excess
concentrations of either F or O at constant temperature,
the order of either F or O (a or b) can be determined. A
second set of experiments in which T is varied (with the
same concentration in excess) will determine E. For example,
consider oxidizer to be in large excess and the fuel order

as already determined. Then,

$$\frac{d[F]}{dt} = 10^{A'} e^{-E/RT} [F]^{a}$$

$$10^{A'} = 10^{A} [O]^{b} \quad ; \quad b \text{ arbitrary}$$

The intercept of a plot of $\ln\left(\frac{d[F]}{dt} / [F]^{a}\right)$ vs. $\frac{1}{T}$ will be variable; however, if the assumed functionality is correct, E should be independent of the choice of b. Having determined a and E, a third set of experiments in which F, O, and T are varied over the widest range possible are conducted. The correct choice of b will be that which results in the above value of E when this last data set is plotted on a $\ln(k_{ov})$ vs $\frac{1}{T}$ scale. All data sets can then be combined with the determined values of a and b to obtain the correct value of A and a better value of E.

Further clarification of the principles of the approach will be demonstrated in the next chapter.

CHAPTER 5 - THE REACTION OF CARBON MONOXIDE AND OXYGEN IN THE PRESENCE OF WATER

As mentioned earlier, the "wet" carbon monoxide oxidation has been studied extensively by many investigators over a wide range of experimental conditions. The noted sensitivity of the reaction to the presence of water has long been recognized. According to Freidman and Cypher [73], the accelerating effect of water on the rate of disappearance of CO was first studied by H. B. Dixon as early as 1880.

Work previous to 1951 (summarized by Lewis and Von Elbe [74]) dealt mainly with the so called "dry" $CO-O_2$ reaction and its transition from a slow reaction to one of explosive character. It was established that the $CO-O_2$ reaction system exhibited first and second order limits of explosion similar to the hydrogen oxygen reaction, but at much higher temperatures and pressures. Further, it was proposed that the second pressure limit was controlled by a second-order chain branching reaction and a third-order termination process. Though the accelerating effect of water was noted, the supposed independence of the second explosion limit from water led investigators to propose that the terminating and branching reactions involved only species containing C and O. Later work of Gordon, et. al. [75,76] and Hoare and Walsh [77] indicated dependence of the second pressure limit on both water and surface and the more recent work of Dickens, Dove, and Linnett [78] showed the limit to be even more sensitized than previously

thought. Though these works continued to propose limiting kinetics involving only species containing C and O, Brokaw [79] has recently shown that in shock tube experiments lasting only a few tenths of a millisecond, as little as 20 ppm of water would severely alter the observed kinetics. Thus, he concluded it not unreasonable that levels of 1 ppb or less of water could completely dominate the slower, low temperature kinetic observations of other workers. Furthermore, Brokaw proceeded to develop a second limit mechanism involving hydrogeneous species and concluded that the question of whether the observed second limit was due to traces of hydrogeneous materials remained plausible. In any case, it is this fast (explosive) reaction of carbon monoxide and oxygen in the presence of water or other hydrogeneous compounds that is of interest in the combustion of hydrocarbons and, therefore, is of concern in the present work.

5.1 Turbulent Flow Reactor Results

Turbulent flow reactor reaction rate measurements were obtained in a 10 cm diameter reactor tube with nitrogen or air as the carrier gas. Water vapor was added to the flow at a known rate by direct atomization into the carrier stream in the reactor inlet section. Thus, water concentrations could be determined from this and other preliminary measurements (Section 4.1.1). Five chemical analysis runs and approximately 25 thermal analysis runs were conducted. The range of experimental parameters covered in each study are presented in

Table 5.1. An attempt was made to cover a range of parameters similar to those occurring in the methane oxidation studies of Chapter 6.

5.1.1 Chemical Analysis Results

Typical chemical rate profile data for a chemically analyzed turbulent flow reactor run are presented in Figure 5.1.[*] The impressive degree to which the total carbon contained in the reaction is accounted for at each sampled position should be noted. In this experimental run, oxygen was in large excess (20%); and, thus, its concentration could be considered constant. Calculation of the oxygen concentration profile for experimental runs with low initial oxygen levels was much simpler and as accurate as its actual analytical measurement. Thus, oxygen consumed was approximated from

$$CO + 1/2 \ O_2 \longrightarrow \ CO_2 \quad ie$$

$$X_{O_2 \ Consumed} = 1/2 \ X_{CO_2 \ Formed} \qquad \text{5.1}$$
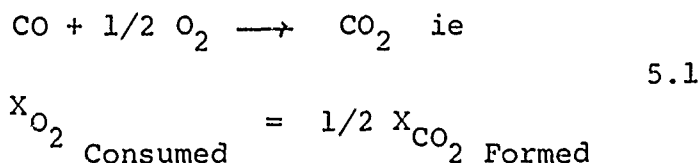
As in previous studies, recognizing the sensitivity of the CO/O_2 reaction to H_2O, an overall correlation of the rate data in the form

$$\frac{d[CO]}{dt} = k_{ov} \ [CO]^a \ [H_2O]^b \ [O_2]^c$$

$$k_{ov} = 10^A e^{-E/RT} \qquad \text{5.2}$$

was attempted.

---

[*]Tabulated results for the concentration profile, concentration gradient profile, and temperature at each sampled position of Figure 5.1 are presented as one of the examples in Appendix B.

RANGE OF EXPERIMENTAL PARAMETERS
FOR STUDIES OF THE $CO(H_2O)/O_2$ REACTION

	Thermal Analysis	Chemical Analysis
X^o_{CO}	.006 .025	.004 - .016
X^o_{CO}	.10 .20	.006 .20
ϕ (Equivalence Ratio)	.04 - .4	.04 - .5
X_{H_2O}	.001 - .015	.0013 - .025
Duct Diameter	10 cm	10 cm
Pressure	1 atm	1 atm
Temperature	1050 - 1220K	1030 - 1160

Table 5.1

129

FIGURE 5.1

CHEMICAL COMPOSITION OF SPREAD
MOIST CARBON MONOXIDE - AIR REACTION
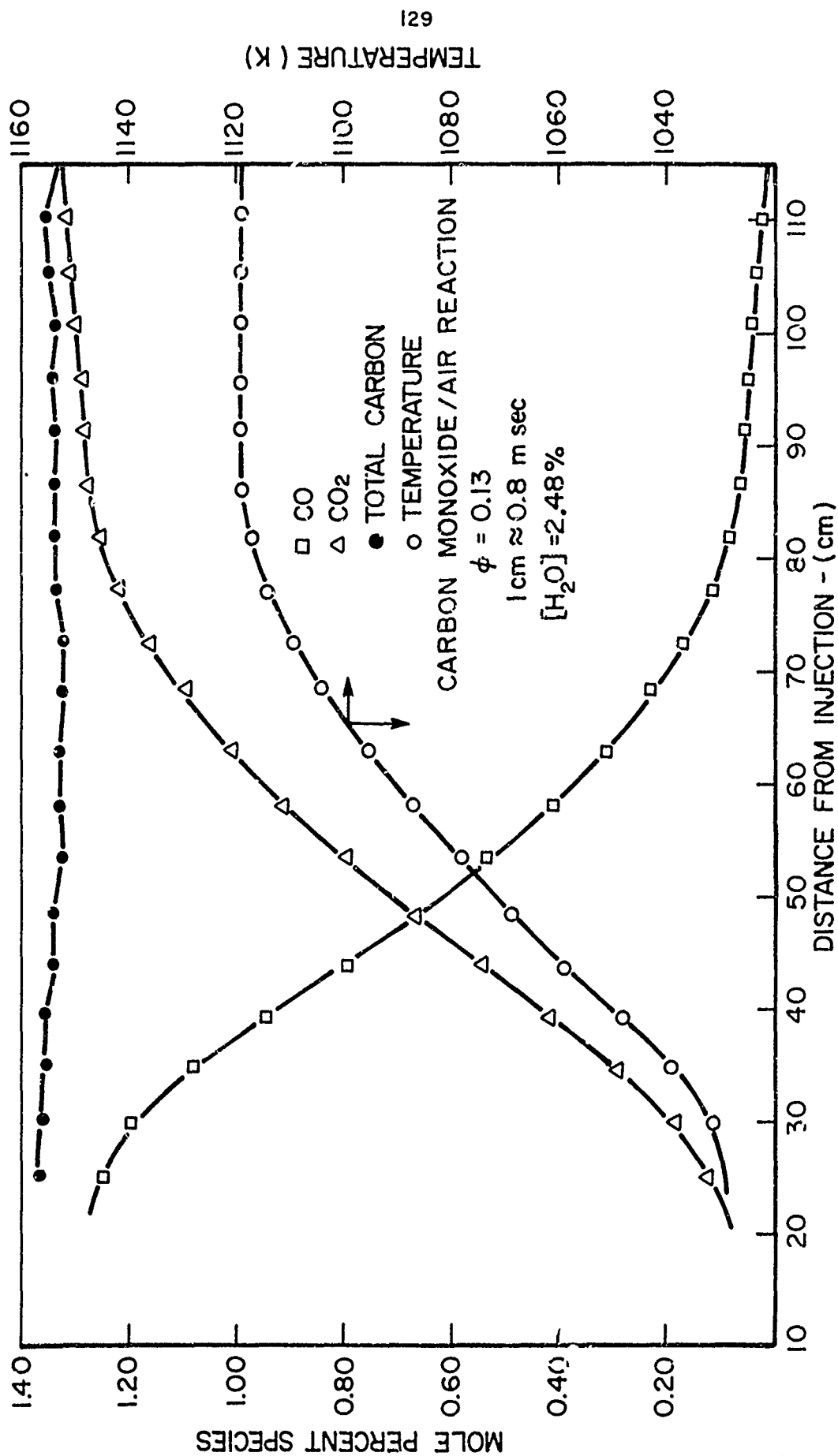
Determination of the experimental reaction orders, a, b, c, offers a clear demonstration of the methods proposed in the closing paragraphs of Section 4.4.

The reaction order with respect to CO was determined in a highly diluted CO/air reaction with a small amount of water added (.1%). As a result of the low heat release per mole of CO consumed,

$$CO + 1/2\ O_2 \longrightarrow CO_2 - 59\ \frac{kcal}{mole} \qquad 5.3$$
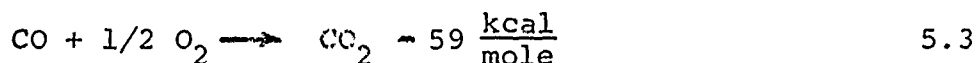
the temperature through the diluted reaction zone was essentially constant. A log-log plot of $\frac{dX_{CO}}{dt}$ vs. X_{CO} is presented in Figure 5.2, and the demonstrated linear slope defines the fuel reaction order, a. as 1.0.

Consider, now, a second flow reactor run with CO/air and a constant water concentration. By adding larger amounts of CO (1.6%), the temperature through the reaction zone is no longer constant. If arbitrary values are assigned to the undetermined reaction orders, $k_{ov} = k_{ov}$ (b,c) can be determined from

$$k_{ov} = \frac{d[CO]}{dt}\ \mathcal{K}\ e^{-E/RT}\frac{1}{[CO]^{1.0}} \qquad 5.4$$

$$\mathcal{K} = 10^A/[H_2O]^b\ [O_2]^c\ ;\ b,\ c\ \text{Arbitrary}$$

On a semi-log scale of log k_{ov}(b,c) vs. T^{-1}, the data should exhibit a straight line if $\frac{d[CO]}{dt}$ and T are truly related in an exponential fashion. A linear least square fit of
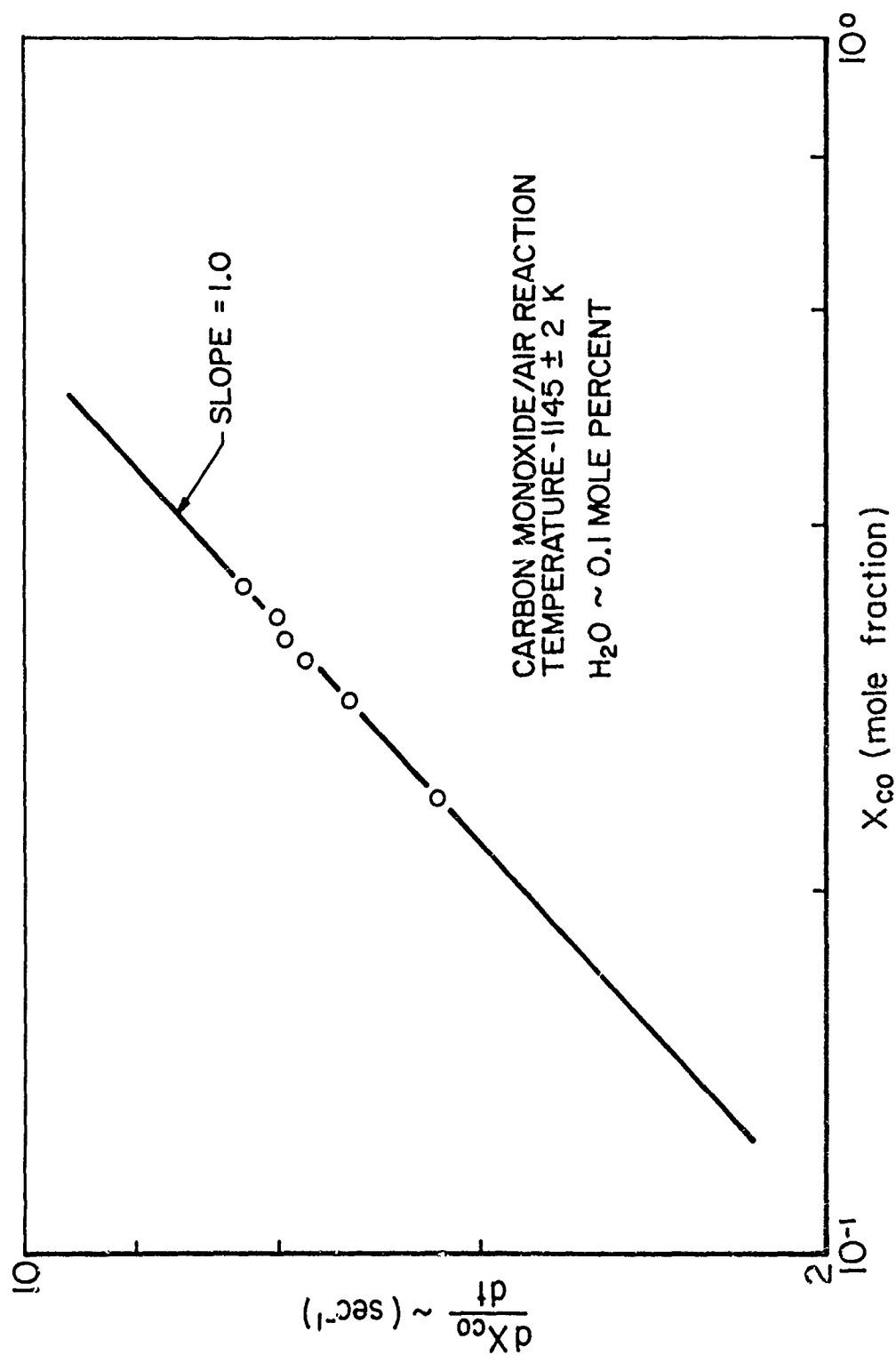
CARBON MONOXIDE
OVERALL REACTION RATE STUDY
CARBON MONOXIDE ORDER DETERMINATION

FIGURE 5.2

such data will yield values of $\mathcal{K}$ and E. The value of $\mathcal{K}$
will be dependent on the choices for b and c. However, in
view of the fact that $[H_2O]$ and $[O_2]$ are effectively constants
in this experiment, E should remain invariant. Exemplary
data from the above described experiment is shown in Figure
5.3. The linear least square value of E was found to be
40.0 $\pm$ 2.0 kcal/mole. Negligible variation of E occurred
for different choices of b and c. Thus, E has been de-
termined without complete knowledge of all of the concentra-
tion dependences. With additional experimental data, the
above values of E and a can be used to calculate b, c,
and finally A. The value of E can then be further refined
if desired.

Proceeding to the determination of b, consider a
set of data consisting of rate measurements of the $CO(H_2O)/O_2$
reaction in air. Further, require that the temperature
range studied be as large as possible. Near one extremity
of the temperature range, experiments are conducted with low
water concentrations; at the other end, experiments with high con-
centrations of water are made. Fundamentally, this is the
natural chain of events necessary to study the largest tempera-
ture range possible (as long as $b \neq 0$). If Equation 5.4 is
again applied to the data (b and c arbitrary) and the result-
ing values of $\log k_{ov}$ are forced to be represented by a linear
least square relation in T^{-1}, it will be observed that while
E remains independent of c, the determined E will be a
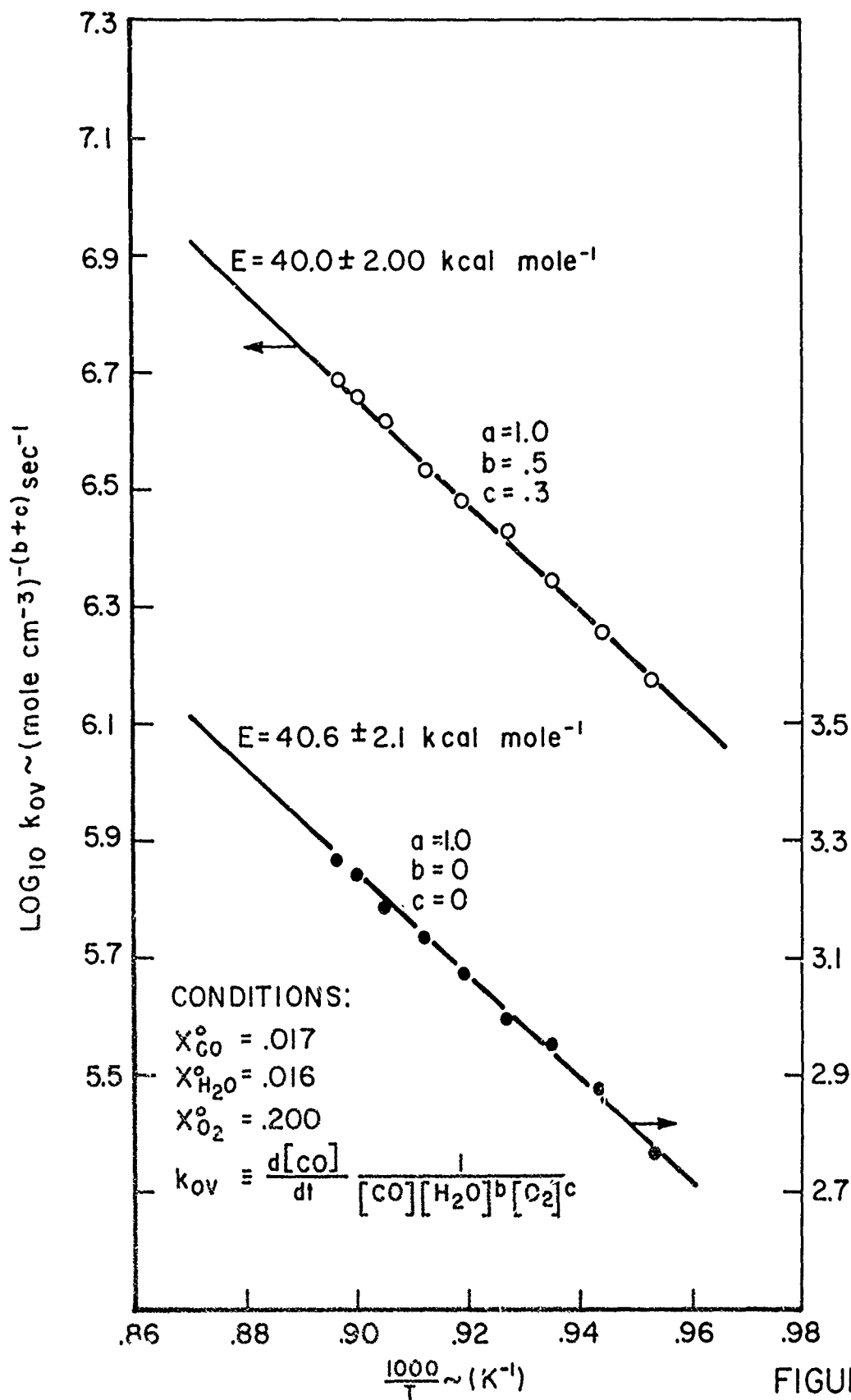
FIGURE 5.3

DETERMINATION OF E FOR THE REACTION OF $CO(H_2O)/O_2$

function of the choice of b. Following this procedure, the
E dependence on b described in Figure 5.4 was found for the
$CO(H_2O)$/air reactions. Note that for b = 0.5, the determined
value of E is the same as that found in the previous analysis
Thus, if both sets of experiments are to be satisfied by
Equation 5.2, a = 1.0, b = 0.5, E = 40 $\frac{kcal}{mole}$, and c and A
remain to be determined.

The oxygen reaction order was found in a similar
way from experimental flow reactor runs in which T and CO, H_2O,
and O_2 concentrations varied. Again it is advantageous to con-
duct high and low oxygen concentration experiments at opposed
extremities of the studied temperature range. The calculated
dependence of E on c resulting from a forced linear
least square fit of log k_{ov} (from Equation 5.4, b ≡ 0.5) vs.
T^{-1} is displayed in Figure 5.4. A unique value of c = 0.25
produced the same value of E determined above.

All the above data sets were then combined and
analyzed by Equation 5.4 with the above determined reaction
orders (a = 1.0, b = 0.5, c = 0.25). The resulting data are
displayed in Figure 5.5. Linear least square fit of the com-
plete data determined

$$A = 14.59 \qquad \sigma A = .25$$
$$E \text{ (refined value)} = 39.95 \text{ kcal/mole} \qquad \sigma E = 1.25 \frac{kcal}{mole}$$

Thus, the experimental correlation is complete.

$$\frac{-d[CO]}{dt} = 10^{14.6 \pm .25} e^{40,000 \pm 1,250/RT} [CO] [H_2O]^{0.5} [O_2]^{0.25}$$

$$5.5$$
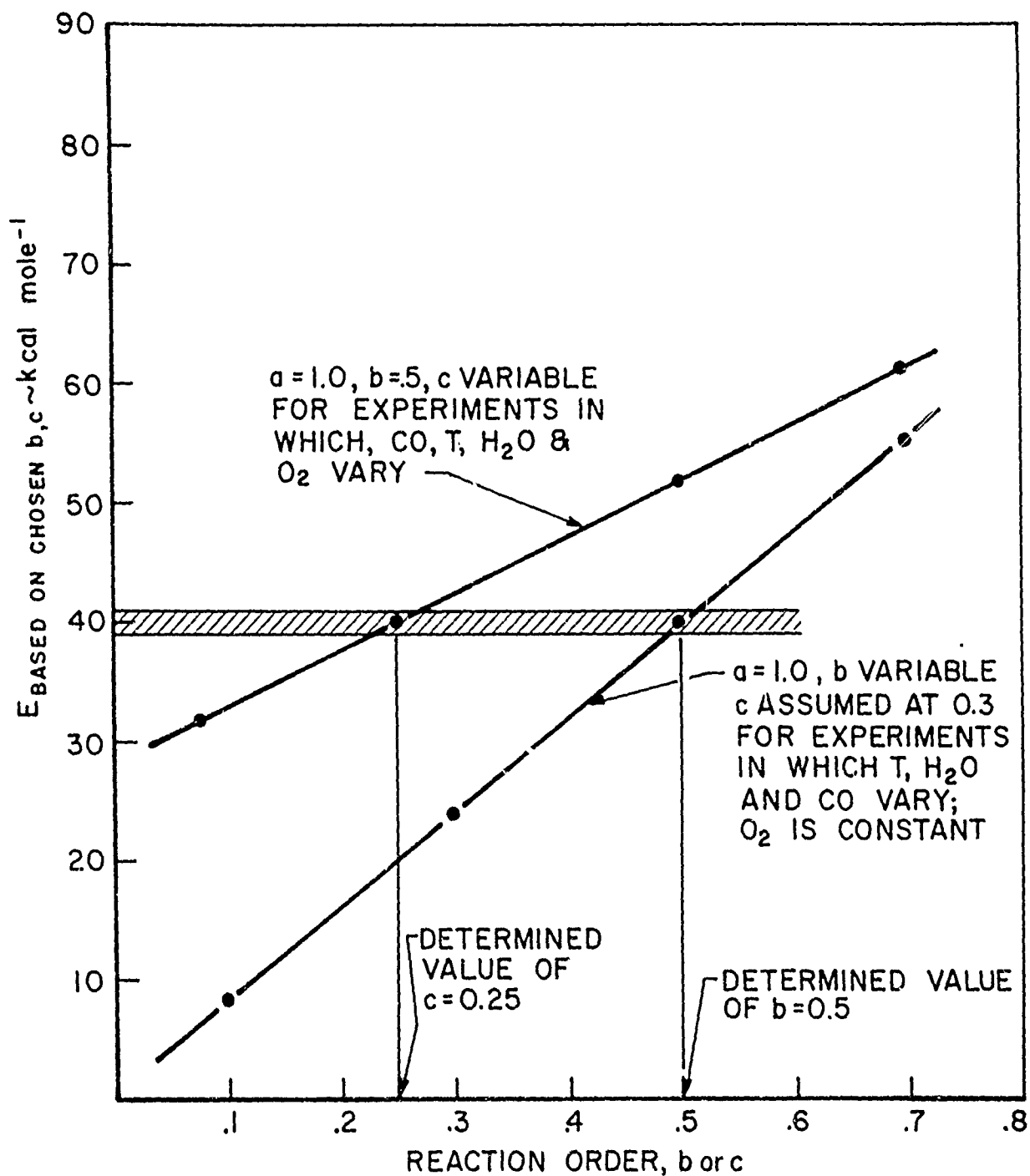
DETERMINATION OF OXYGEN AND WATER
REACTION ORDERS FOR CO $(H_2O)/O_2$ REACTION

FIGURE 5.4
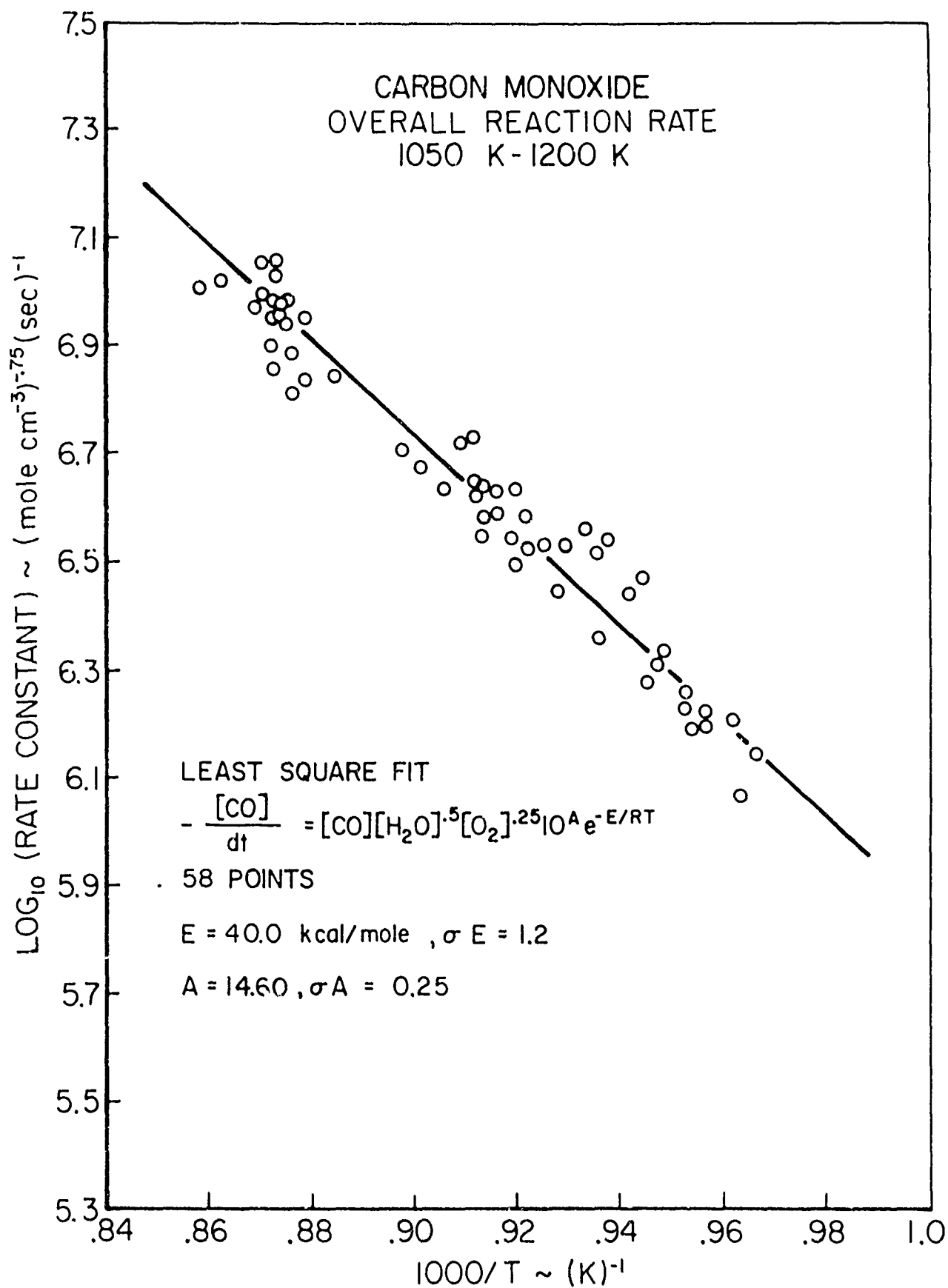
FIGURE 5.5   CHEMICAL·ANALYSIS TECHNIQUE

It is seen that the combination of experimental
control of variables in the turbulent flow reactor experi-
ments with some simple insight into the overall correlation
relation and linear least square techniques determine
the reaction orders, a, b, c, and A and E. This is accom-
plished in a much simpler fashion than more complex statis-
tical approaches, and the procedure evaluates one of the more
important parameters (E) immediately. While errors estimated
by statistical programs give no way of suggesting improvement
in the experimental approach, this method points directly to
which parameters are determined with least precision. The
slopes of the generated dependences of E with reaction orders
are directly related to the studied range of each of the species
represented in the correlation and the range of temperature
investigated. It is these slopes, along with the standard
deviation of the value of E, that control the precision to
which each order is estimated. Precision of order determination
should degenerate as the calculated orders approach zero, but, in
fact, the determined order then becomes less important.

Finally, it should be noted that the efficiency of
the method is quite good. Only five reactor runs and approxi-
mately 58 points of data were necessary to complete the corre-
lation. Obviously, the precision of the experiment could be
improved at any one of the several steps in the process by adding
more data, but the above results indicate this to be unnecessary.

5.1.2   Thermal Analysis Results

As discussed earlier in the thesis, the thermal analysis approach offers significant advantages over chemical analysis when the kinetics are simple enough to be modeled well by the thermal approach.   The $CO(H_2O)/O_2$ reaction should satisfy the necessary assumptions for its application, and comparison of thermal results with the chemical results of the previous section will quantitatively establish the validity of the thermal approach.   Using the same reaction orders determined in the chemical analysis experiments, measurements of $\dfrac{d[CO]}{dt}$, $[CO]$, $[O_2]$ and T from thermal analysis results were correlated.   The stoichiometric relation used (Equation A-5) was

$$CO + 1/2 \;\; O_2 \longrightarrow CO_2 \;\; - 59 \text{ kcal/mole CO consumed}, \qquad 5.6$$
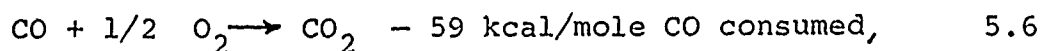
and $[H_2O]$ was again calculated from initial flow measurements to the reactor.   Results are presented in Figure 5.6.   Note that the thermal and chemical predictions of $[CO]$, $[O_2]$, and $\dfrac{d[CO]}{dt}$ compare very well and that the correlations lie well within their standard deviations.   The thermal analysis measurements were conducted over a slightly higher temperature range and, therefore, verify that the measurements are acceptable over the wider temperature range 1220K to 1050K.   This is a very good confirmation that the previously described adiabatic design of this turbulent flow reactor operates effectively and that the thermal approach is indeed a valid experimental technique.

CARBON MONOXIDE
OVERALL REACTION RATE
1025 K - 1225 K

LEAST SQUARE FIT OF
CHEMICAL ANALYSIS DATA

$$-\frac{d[CO]}{dt} = [CO][H_2O]^{.5}[O_2]^{.25} 10^{14.6} \exp\left(\frac{-40000}{RT}\right)$$

LEAST SQUARE FIT

$$-\frac{d[CO]}{dt} = [CO][H_2O]^{.5}[O_2]^{.25} 10^A e^{-E/RT}$$

136 POINTS

E = 39.23 kcal/mole, $\sigma E = 1.00$

A = 14.46, $\sigma A = 0.19$

LOG$_{10}$ (RATE CONSTANT) ~ (mole cm^{-3})$^{-.75}$(sec)$^{-1}$

1000/T ~ (K)$^{-1}$
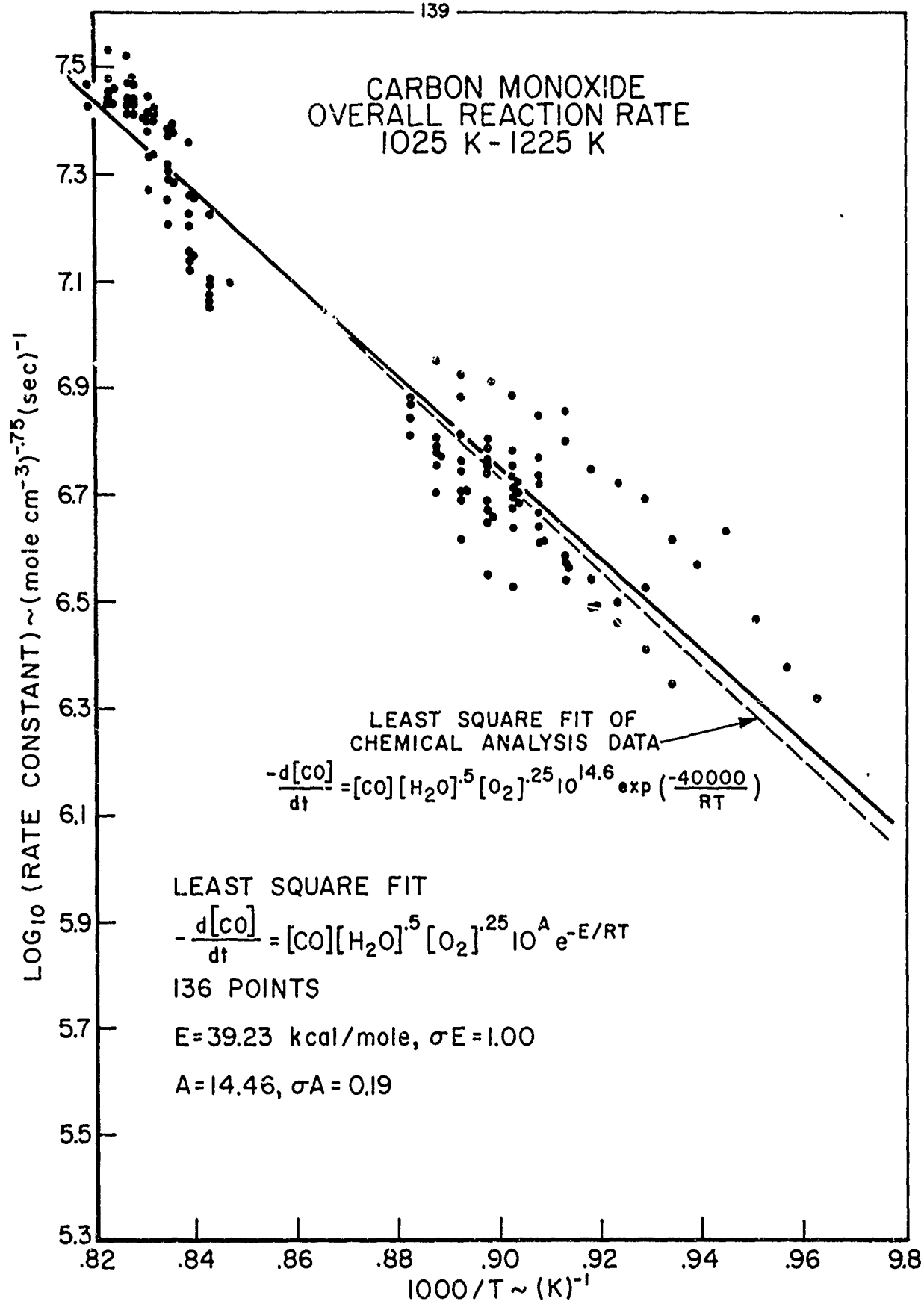
THERMAL ANALYSIS TECHNIQUE

FIGURE 5.6

5.2 Other Measurements of Overall Rate Parameters

A summary of previously available complete reaction rate correlation data is presented in Table 5.2. The data result from four separate experimental areas:

(i) burning rate measurements of $CO(H_2O)/O_2(N_2)$ flames

(ii) chemical sampling of $CO(H_2O)/O_2(N_2)$ flames and the afterburning regions of hydrocarbon (HC) flames

(iii) stirred reaction measurements of the $CO(H_2O)/O_2$ reaction and the hydrocarbon reactions of propane and methane

(iv) a laminar flow reactor study of $CO(H_2O)/O_2$ reaction

With respect to all of the data:

(1) There is unanimous agreement on the first order dependence of the oxidation rate of carbon monoxide independent of the method of study or the chemical reaction in which the measurements were made.

(2) The reaction dependence on water was expressed through concentration terms and does not appear to influence the temperature dependence of the reaction. With the exception of Fenimore and Jones [81], the above studies as well as several others [86-90] have concluded the reaction order with respect to water to lie between .2 and .6. More recent empirical determinations, exclusive of burning rate measurement

SUMMARY OF OVERALL RATE PARAMETERS FOR MOIST CARBON MONOXIDE OXIDATION

$$-\frac{d[CO]}{dt} \equiv c[CO]^a [H_2O]^b [O_2]^c e^{-E/RT} \text{ moles cm}^{-3} \text{ sec}^{-1}$$

Investigator	Ref	Temp Range (K)	Press (atm)	Technique	C	E kcal/mole	a	b	c
Friedman & Cyphers	73	2010		Burning Velocity Measurements in CO(H2O)/O2 Flames	5.3×10^9	20	1	.5	0
Sobolev	80	1900-2400	1	(A) Burning Velocity Measurements in CO(H2O)/O2 Flames	9.5×10^7	30	1	0	0
				(B) Sampling Afterburning Zone, CO(H2O)/O2 Flames	2.7×10^5	27	1	0	0
Fenimore & Jones[1]	81	1700-2000	1	Sampling Afterburning Zone, Hydrocarbon Flames	1.2×10^{12}	24	1	1 (0)	0 (1)
Nemeth & Sawyer	82	1800-2000	1	Sampling Afterburning Zone, Hydrocarbon Flames	2×10^{11}	24.6	1	.5	.25
Hottel, et.al.	83	1280-1535	.25-1	(A) Stirred Reactor CO(H2O)/O2 Reaction	1.2×10^{11}	16	1	.5	.3
		1550-1800	.6-1	(B) Stirred Reactor C3H8/O2 Reaction	8.7×10^{11}	16	1	.5	.3
Williams & Hottel	84	1450-1750	.6	Jet Stirred Reactor Methane Oxidation	1.8×10^{13}	25	1	.5	.5
Levrov	85	1063-1593	1	Jet Stirred Reactor CO(H2O)/O2 Reaction	1.8×10^{12}	28.3	1	.5	.25
Kozlov[2]	23	970-1370	1	Laminar Flow Reactor CO(H2O)/O2 Reaction	$\dfrac{1.04\times10^{12}}{T^{2.5}}$	32	1	.5	.25

TABLE 5.2

Investigator	Ref	Temp Range (K)	Press (atm)	Technique	c	E kcal/mole	a	b	c
This Work	-	1050-1200	1	Turbulent Flow Reactor $CO(H_2O)/O_2$ Reaction	3.9×10^{14}	40	1	.5	.25

NOTES:

[1]Fenimore & Jones find (b=0, c=1) when $[H_2O]$ is large, (b=1, c=0) when $[H_2O]$ is small

[2]Kozlov's concentrations are expressed as mole fraction, not as mole cm^{-3}

TABLE 5.2 (cont'd.)

experiments, have more reliably defined "b" near 0.5, and are in agreement with the present result.

(3)   The dependence of the rate on oxygen has been concluded to vary with oxygen concentrations by several investigators.   In oxygen deficient systems Sobolev [80], Fenimore and Jones [81] and Hottel, et. al. [83] suggest a dependence of nearly first order.   However, for systems in which available oxygen concentration is above 3%, these same references, as well as Freidman and Nugent [92], conclude the oxygen order to be very near zero (c = 0.0-0.25).   No such variation in oxygen reaction order was noted in the present work. Lavrov [85] reports that his determined orders are constant and result from experiments with:

$$x^o_{CO} \quad - \quad .01 \quad - \quad .86$$
$$x^o_{O_2} \quad - \quad .09 \quad - \quad .85$$
$$x^o_{H_2O} \quad - \quad .00189 \quad - \quad .102$$
$$T \quad - \quad 1063K \quad - \quad 1593K$$

To date, his studies would appear to cover the widest investigated range of experimental parameters.

(4)   Determined overall pre-exponential constants and activation energies are in wide disagreement.   Levy and Weinberg [6] have shown that little fundamental chemical significance should be attached to chemical constants determined using flame theory.   Thus, the parameters of Sobolev [80] and Freidman and Cypher [73] resulting from flame theory calculations after Zeldovich, Frank-Kamenetsky and Semenoff [91]

should be viewed with some skepticism. Furthermore, several other studies, notably those of Kozlov [23] and Németh and Sawyer [82], did not empirically determine the reported reaction orders but accepted the values of these previous flame measurements.

The low values of temperature dependence (16 kcal/mole) of Hottel, et. al. [83] are particularly curious in light of the value obtained from the similar technique of Lavrov [85] (28.3 kcal/mole). Also, Kydd and Foss [93] have concluded the temperature dependence of the $CO-(H_2)O_2$ reaction in a stirred reactor to be 38 kcal/mole.

Some further insight can be gained from comparison of the rates of oxidation of CO calculated by the overall expressions listed in Table 5.2. For the comparison, common concentrations of reactants which had been studied in each of the researches were employed and results are displayed in Figure 5.7.

To be noted first is that the present research predicts CO oxidation rates within a factor of five of Hottel, et. al. [83] and within a factor of 2 of Kozlov [23] and Lavrov [85] over their respective temperature ranges. It should be emphasized that these are all of the available studies of the $CO(H_2O)/O_2$ reaction not employing flame theory or hydrocarbon combustion.

It is apparent that, though pre-exponential and temperature dependence constants vary considerably among

COMPARISON OF AVAILABLE OVERALL
RATE PREDICTIONS FOR
CO(H_2O)/O_2 REACTION

FIGURE 5.7
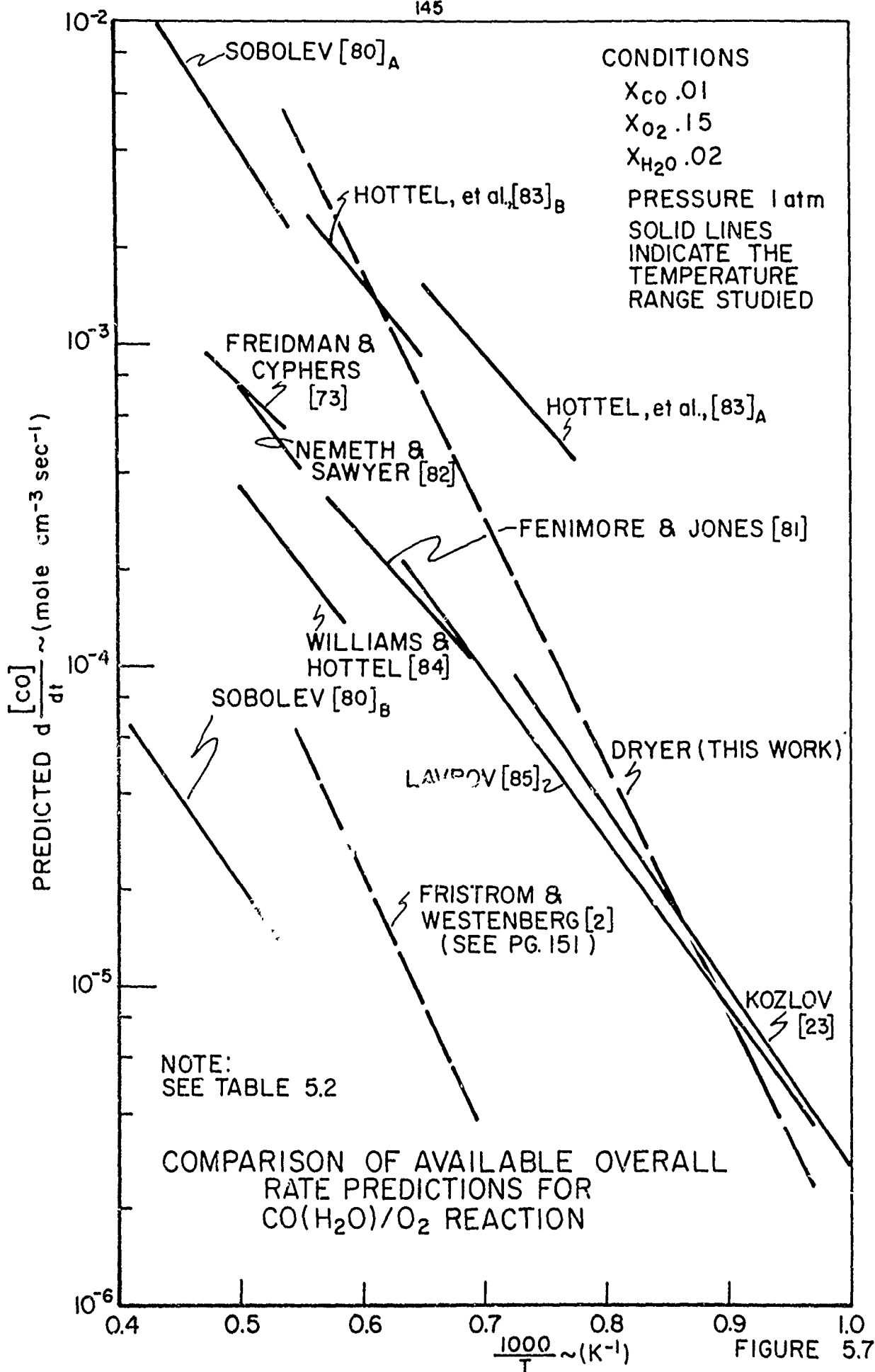
these studies, the combination of parameters from each work produce comparable rate results. Thus, the incongruity of the parameters of Hottel, et. al [83] would appear to be due purely to his limited range of investigation. A similar conclusion might be in order in the case of the present work since its determined temperature dependence is significantly larger than other studies. However, estimation of temperature dependence in the other studies could not be nearly as accurate, since all employed average isothermal concepts and did not make precise temperature measurements.

Secondly, it is apparent that there is some difference in the oxidation of CO in hydrocarbon combustion and in the $CO(H_2O)/O_2$ reaction. Fenimore and Jones [81], Németh and Sawyer [82] Hottel et al. [83] , Williams and Hottel [84] , and Friedman and Cyphers [37] observe slower rates of combustion of CO in hydrocarbon oxidation than would be predicted from results on the $CO(H_2O)/O_2$ reaction. This lower rate is not reflected in different reaction orders or temperature dependence, but largely in a smaller pre-exponent in the overall rate equation.

5.3 General Mechanism and Relation to Overall Measurements

The slow oxidation of carbon monoxide in environments devoid of hydrogeneous species and its critical sensitivity to their presence can be interpreted on a more elementary kinetic level as meaning that the principal oxidation process is carried out by radical species containing hydrogen.

In light of early kinetic measurements of Avromenko and Lorentzo [94] (now known to be erroneous) it was proposed that the principal oxidation route was

$$CO + OH \rightleftharpoons CO_2 + H \quad (1) \text{ (see footnote)}$$
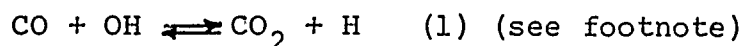
Early work of Friedman and Cyphers [73] substantiated that the rate of oxidation of CO was proportional $[OH]_{eq}$. More recently, Singh and Sawyer [95] have experimentally verified a proportionality with [OH] through absolute measurements in afterburning regions of ethane and ethylene flames.

Consideration of the possible alternative reactions

$$CO + O + M \rightarrow CO_2 + M \quad (2)$$

and

$$CO + O_2 \rightarrow CO_2 + O \quad (3)$$
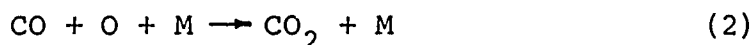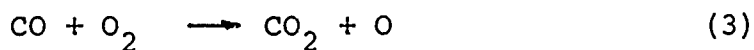
show them to be very slow relative to reaction (1) and mechanistically, they cannot account for the pronounced effect of addition of hydrogen containing species to reacting mixtures of CO and O_2.

Lewis and Von Elbe [74] have proposed one other elementary oxidation route,

$$CO + HO_2 \rightarrow CO_2 + OH - 76 \frac{kcal}{mole} \quad (4)$$

---
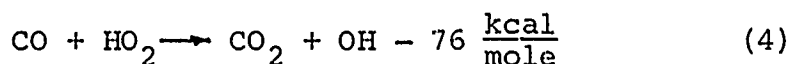
*Elementary kinetic reactions will be consecutively numbered throughout the thesis in order of their introduction. The elementary specific rate constant for each reaction will be subscripted as follows: k_{if} or k_{ir} will refer to the "forward" or "reverse" specific rate constant for reaction i. Similar notation will be used in denoting the apparent activation energy (E_{if} or E_{ir}) and the pre-exponential factor (C_{if} or C_{ir}) for each reaction. A complete tabulation of all elementary reactions and the associated k_{if}'s will be found in Appendix C. Reverse rate constants can be determined through equilibrium considerations. The direction(s) of arrows in the equation or the reaction number followed by "f" or "r" signifies the reaction direction(s) under discussion.

The importance of this reaction has been a matter of question for many years, yet no direct measurements of k_{4f} presently exist. Its possible contribution to the conversion of CO to CO_2 has been argued most recently by Wilson [96] in connection with the apparent discrepancy in measured rates for reaction (1) in flames and in low temperature experiments (see next section). Flame studies have considered the route unimportant, while Baldwin [97] has attributed about half of the formation rate of CO_2 in explosion limit studies to reaction (4). Further, Wilson [96] claims that values of k_{1f} obtained from measurements of k_{1r} and equilibrium considerations generally fall appreciably lower than the so-called direct measurements of the forward reaction.

However, other experimental and theoretical arguments would indicate reaction (4) to be an unlikely principal route of oxidation to which these effects can be attributed. Baldwin [98] has estimated E_{4f} at about 24 kcal/mole and concludes a maximum value for C_{4f} of 5.8×10^{13} cm^3 $mole^{-1} sec^{-1}$. At 1000K this would suggest an upper limit for k_{4f} of 5×10^8 cm^3 $mole^{-1}$ sec^{-1}. Baldwin [97] has also reported a value for $\frac{k_{4f}}{k_{5f}}$,

$$HO_2 + H_2 \longrightarrow H_2O_2 + H \tag{5}$$

at 773K of 9.5. With Baulsch and Drysdale's evaluation of k_{5f} [99],

$$k_{5f} \approx 9.6 \times 10^{12} \exp\left(- \frac{24000}{RT}\right)$$

and the above estimate of E_{4f},

$$k_{4f}\bigg|_{T \approx 1000K} \approx 10^7 \text{ cm}^3 \text{ mole}^{-1} \text{ sec}^{-1}$$

However, k_{1f} is of the order of $1\text{-}4 \times 10^{11}$ cm^3 mole^{-1} sec^{-1} at 1000K (see next section). Thus, $[HO_2]$ would need to be $10^3 - 10^4$ larger than $[OH]$ for reaction (4) to compete effectively with reaction (1). But $[HO_2]/[OH] \approx 10^{-2}\text{-}10^{-3}$ at thermodynamic equilibrium and atmospheric pressure (and $T \sim 1000K$). Such a large inversion of this ratio in lean oxidation reactions appears to be unlikely. Kaskan [100] has shown $[OH]$ to exceed equilibrium by a factor of 10^1 to 10^3. Thus, $[HO_2]$ would need to exceed its equilibrium concentration by factors of $10^6 - 10^{10}$ to make reaction (4) competitive. This does not appear plausible in view of the rapidity of reactions such as

$$HO_2 + HO_2 \longrightarrow H_2O_2 + O_2 \qquad (6)$$

$$H_2O_2 + M \longrightarrow 2OH + M \qquad (7)$$

$$HO_2 + OH \longrightarrow H_2O + O_2 \qquad (8)$$
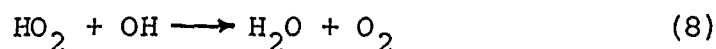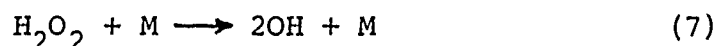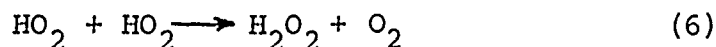
which can destroy HO_2. Baldwin [98] estimates k_{6f} at 10^{21} cm^3 mole^{-1} sec^{-1} at 773K. Kaufman [101] , Foner and Hudson [102], Baldwin [97] and Schofield [103] estimate $k_{8f} \approx 10^{12}$ cm^3 mole^{-1} sec^{-1} at 300K. Furthermore, the results of Meyer [104] on the H_2O_2 decomposition reaction (900-1400K) show $[HO_2]$ to be less than 10^{-1} times $[OH]$, and this decomposition supposedly exhibits enhanced relative concentrations of HO_2.

Furthermore, it will be seen in the following section that reverse and forward measurements of k_1 and discrencies in high and low temperature measurement of k_{1f} can be resolved without introduction of secondary oxidation paths for CO (such as (4)). Other experimental evidence refuting previous suspicion of the importance of reaction (4) in the methane oxidation will be presented in Chapter 6.

With reaction (1) the remaining primary mechanism for formation of CO_2 in the oxidation of CO, it is apparent that factors controlling the level of [OH] must account for the empirically derived overall rate expression. This can be confirmed to some extent by the following simple arguments first proposed by Fristrom and Westenberg [2].

If one considers the situation of very small amounts of CO reacting in a hot environment rich in water and oxygen, the levels of [OH], [O], and [H] should be very near those established by thermodynamic equilibrium, that is, from the equilibrium formation reactions

$$H_2 + \tfrac{1}{2}O_2 \underset{\xrightarrow{\hspace{1cm}}}{\overset{K_{P_{H_2O}}}{\rightleftharpoons}} H_2O \qquad\qquad 5\text{-}7$$

$$\tfrac{1}{2}O_2 + \tfrac{1}{2}H_2 \underset{\xrightarrow{\hspace{1cm}}}{\overset{K_{P_{OH}}}{\rightleftharpoons}} OH \qquad\qquad 5\text{-}8$$

$$[OH] = [OH]_{eq} = \frac{K_{P_{OH}}}{K_{P_{H_2O}}^{1/2}} \; \frac{[H_2O]^{\frac{1}{2}}\,[O_2]^{\frac{1}{4}}}{(RT)^{\frac{1}{4}}} \qquad\qquad 5\text{-}9$$

The concentration of [H] would be small and, neglecting the reverse reaction of (1),

$$-d \frac{[CO]}{dt} = k_{1f} \, [CO] \, [OH]$$

It would follow that

$$-\frac{d[CO]}{dt} = \frac{k_{1f} \, K_{P_{OH}}}{(RT)^{\frac{1}{4}} K_{P_{H_2O}}^{\frac{1}{2}}} \, [CO] \, [H_2O]^{\frac{1}{2}} \, [O_2]^{\frac{1}{4}} \qquad 5.10$$

Expressing data for $K_{P_{OH}}$ and $K_{P_{H_2O}}^{\frac{1}{2}}$ from JANAF Tables [105] in Arrenhius form,

$$\frac{K_{P_{OH}}}{(RT)^{\frac{1}{4}} K_{P_{H_2O}}^{\frac{1}{2}}} = 10^{.87} \exp \frac{-38,400}{RT} \qquad 5.11$$

and using the Baulsch and Drysdale evaluation for k_{1f} [99]

$$k_{1f} = 10^{11.74} \exp\left(- \frac{1080}{RT}\right) cm^3 \, mole^{-1} \, sec^{-1} \qquad 5.12$$

$$-\frac{d[CO]}{dt} = 10^{12.61} \exp\left(- \frac{39,480}{RT}\right)[CO] \, [H_2O]^{\frac{1}{2}} \, [O_2]^{\frac{1}{4}}$$

Fristrom and Westenberg [2] report the derived expression (Equation 5.12) as

$$-d \frac{[CO]}{dt} = 4 \times 10^{13} \, [CO] \, [H_2O]^{\frac{1}{2}} \, [O_2]^{\frac{1}{4}} \, e^{\frac{-45,000}{RT}} \qquad 5.13$$

The differences in pre-exponential constant and temperature dependence are due primarily to revised estimates for the expression for k_{1f}.

It is interesting that these same reaction orders are found in many of the experimental studies summarized in Table 5.2. In fact, the present work, which deals only with oxygen and water rich reaction environments, also exhibits the same temperature dependence (Equation 5.6) as found in Equation 5.12. However, it should be noted that Equation 5.12 predicts rates of oxidation of CO (see Figure 5.7) 100 times slower than the present work and 10-100 times slower than all of the other experimental investigations presented in Table 5.2.

Such a large discrepancy in rate cannot be attributed to the value of k_{1f} used in Equation 5.12; numerous experimental measurements of this rate constant do not scatter by more than a factor of 10. Thus, the level of [OH] in the experiments must be in the order of 100 times greater than that determined by thermodynamic equilibrium. That [OH] might achieve concentrations this far above that at thermodynamic equilibrium, $[OH]_{eq}$, is not unreasonable. Several investigators including Sugden, et al. [106, 107] , Schott [108,109] , and Kaskan [100] have experimentally shown $[OH] > [OH]_{eq}$ by one to three orders of magnitude in hydrogen-oxygen flames and shock tube studies; furthermore, Kaskan [110] has shown $[OH] > [OH]_{eq}$, $[O] > [O]_{eq}$ in atmospheric hydrogen/air flames seeded with carbon monoxide.

Sugden, et al. [106,107] and Schott [108,109] have attributed this super-equilibrium phenomena to the balanced* rapid reactions,

---

*A balanced elementary reaction is defined by Sugden [106] as one in which the forward and reverse reactions are in equilibrium with each other but not necessarily with other reactions.

$$H + O_2 \rightleftharpoons OH + O \qquad (9)$$

$$O + H_2 \rightleftharpoons OH + H \qquad (10)$$

$$OH + H_2 \rightleftharpoons H_2O + H \qquad (11)$$
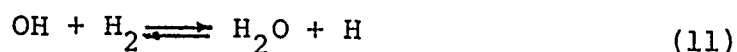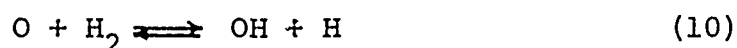
The general assumption is that these reactions achieve a "partial equilibrium" among themselves before the slower recombination reactions,

$$(H, OH, O) + (H, OH, O) + M \rightarrow \begin{pmatrix} stable \\ products \end{pmatrix} + M \qquad (12)$$
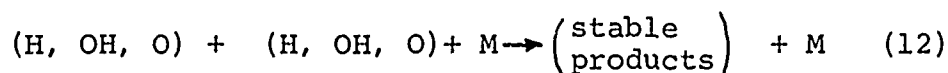
can contribute to the equilibrium mechanism and reduce the radical concentrations to values appropriate to equilibrium products. Initially, Schott [108] suggested that the partial equilibrium values of radical species represented practical upper limits to the maximum concentrations reached by [OH] and the other reaction intermediates; later work of Schott and Hamilton [109] indicated that H_2-O_2 mixtures far from stoichiometric conditions could initially produce concentrations of one or more of the chain carrier species considerably above partial equilibrium levels. However, chain carrier concentrations were seen to approach partial equilibrium later in the reaction.

Analytical solutions of a mechanism involving the reactions (9)-(12) have been attempted in connection with the CO oxidation. Hottel, et al. [83] combined these reactions and reaction (1) to attempt explanation of the low temperature dependence and varying reaction orders observed in their stirred

reactor studies. Though some favorable comparisons could be made in the trends predicted by the analytical model, no closed numerical comparisons were possible. In light of Lavrov's work [85] (see Page 143), agreement might have been fortuitous. It should also be noted that, though reactions (9)-(12) may be in partial equilibrium, they do not by themselves offer the only possible mechanistic routes for destruction or creation of [OH]. Kaskan [100] has commented that the balanced reaction

$$H_2O + O \rightleftharpoons OH + OH \tag{13}$$
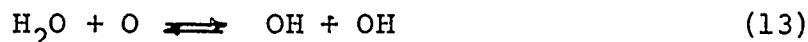
is equivalent to a combination of the balanced reactions (10) and (11). However, reaction (13) might offer additional contributing terms to the net [OH] production of a reaction mechanism. In fact, from the evaluations of Baulsch and Drysdale [99],

$$\frac{k_{13f}}{k_{10f}} \approx 3.4 \; \exp\left(- \; \frac{8550}{RT}\right)$$

or

$$\frac{k_{13f}}{k_{10f}} > 4 \times 10^{-2} \quad \text{for } T > 1000K$$

For the ratios of $\frac{[H_2O]}{[H_2]}$ generally observed in the present work and reported by Hottel, et al. [83],

$$\frac{[H_2O]}{[H_2]} \approx 10^{+1} - 10^{+2} ,$$

reaction (13) can add significant branching in the production of [OH] from O atoms.

At any rate, it would appear that analytical modeling of the overall rate expressions of Table 5.2 must be relegated to numerical integration of a reasonably complex mechanism on a computer. This conclusion is substantiated by the results of Singh and Sawyer [95] which experimentally show [OH] to be somewhere between the thermodynamic and partial equilibrium values, and not necessarily approaching either value. Furthermore, the contributions of the HO_2 radical to the CO oxidation, cannot be neglected. Although its direct reaction with CO is unlikely, at high pressures $[HO_2]$ can be relevant to production of [OH]. The reaction

$$H + O_2 + M \longrightarrow HO_2 + M \tag{14}$$
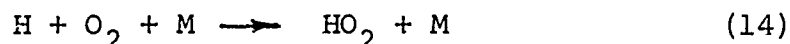
can compete quite favorably with

$$H + O_2 \longrightarrow OH + O , \tag{9}$$

From Baulsch and Drysdale [97]

$$\frac{k_{9f}}{[M] \cdot k_{14f}}_{\text{(for } M = N_2)} \approx 6 \times 10^{-2} \; RT \; \exp\left(\frac{-17,800}{RT}\right)$$

and at atmospheric pressure and 1000K

$$[M] \cdot \frac{k_{9f}}{k_{14f}} \approx .6$$

Furthermore, due to the rapidity of reactions (6)-(8), reaction (14) cannot in itself be considered a termination step.

Thus, even a crude elementary mechanism of the CO oxidation must include:

$$CO + OH \rightleftharpoons CO_2 + H \tag{1}$$

$$H + O_2 \rightleftharpoons OH + O \tag{9}$$

$$H + O_2 + M \rightleftharpoons HO_2 + M \tag{14}$$

$$H + H_2O \rightleftharpoons H_2 + OH \tag{11}$$

$$O + H_2 \rightleftharpoons OH + H \tag{10}$$

$$O + H_2O \rightleftharpoons OH + OH \tag{13}$$

some reactions such as:

$$HO_2 + HO_2 \rightleftharpoons H_2O_2 + O_2 \tag{6}$$

$$H_2O_2 + M \rightleftharpoons OH + OH + M \tag{7}$$

$$HO_2 + OH \rightleftharpoons H_2O + O_2 \tag{8}$$

$$HO_2 + H_2 \rightleftharpoons H_2O_2 + H \tag{15}$$
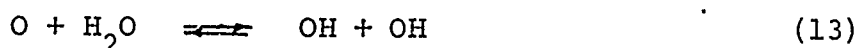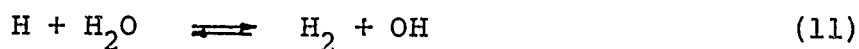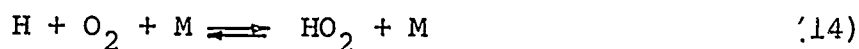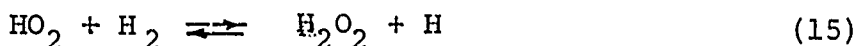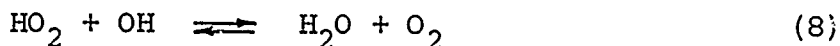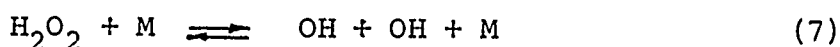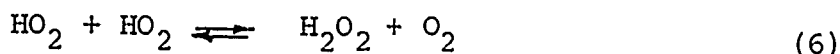
and the terminating reactions:

$$(H, OH, O) + (H, OH, O) + M \rightarrow \text{stable products} + M \tag{12}$$

$$(HO_2) \xrightarrow{wall?} \text{stable products} \tag{1}$$
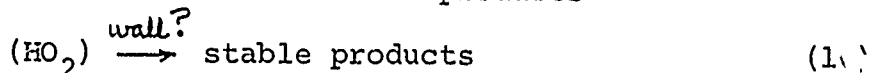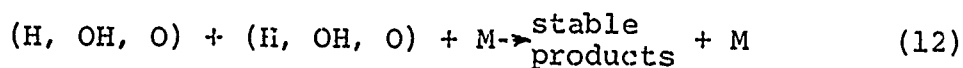
Browne, et al. [111] have used a most complex mechanism involving 28 such reactions to analytically model density profiles (with time) in shock heated mixtures of H_2, CO and O_2. Though favorable comparisons with experimental measurements were obtained, many of the elementary kinetic parameters and even the number of elementary reactions do not appear to be unique. Some of the rate constants were completely unknown, while others are defined only to within $\pm$ 50% (relative). No reactions involving H_2O_2 were used in the mechanism. It

would appear to this author that further computer modeling
would be worthwhile, and that overall kinetic measurements
presented in this section, along with chemical profile and
rate data similar to Figure 5.1, will be of great help in
evaluating which elementary reactions are important to the
mechanism.

5.4 Some Observations on the Reaction $CO + OH \longrightarrow CO_2 + H$

As discussed in the previous section, reaction (1)

$$CO + OH \longrightarrow CO_2 + H \qquad (1)$$
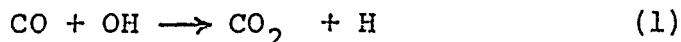
apparently offers the only primary route by which CO_2 is
formed in the $CO(H_2O)/O_2$ reaction. Likewise, in the oxida-
tion of hydrocarbons, there is no other reaction, except
possibly,

$$CO + HO_2 \longrightarrow CO_2 + OH \qquad (4)$$
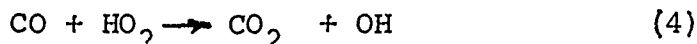
which could compete successfully with reaction (1). Thus,
if k_{1f} is known, and T, $[CO]$, and $\dfrac{d[CO_2]}{dt}$ are measured,
reaction (1) can be used to accurately estimate the concen-
tration of $[OH]^*$. For this reason, reaction (1) has achieved
great importance in kinetic studies of other elementary reac-
tions involving $[OH]$; and, thus, assignment of suitable kinetic
parameters (C_{1f} and E_{1f}) to this hydroxyl radical reaction has
been a long standing problem.

A summary of experimental data on reaction (1f)

---

*Provided that reaction (1f) may be neglected or is suitably
taken into account.

is presented in Figure 5.8.[*]

Early high temperature results (Fristrom and Westenberg [2, 112] , Fenimore and Jones [113]) and the work of Avramenko [94] resulted in an evaluation by Fristrom and Westenberg [30, 112] of C_{1f} and E_{1f} as

$$k_{1f} = 6 \times 10^{12} \ \exp\left(\frac{- \ 7700}{RT}\right)$$

However, following the consistent room temperature measurements of three laboratories (Dixon-Lewis, et al. [114] , Wilson and Westenberg [115] , Greiner [116], Wilson and O'Donovan [117]) and, in light of the errors in Arvamenko's work [94] found by Kaufman and DelGreco [118] , Dixon-Lewis, et al. [114] re-evaluated the description of k_{1f} as

$$k_{1f} \ = 3.1 \times 10^{12} \ \exp\left(\frac{-600}{RT}\right)$$

Following this, several critical surveys (Wilson [119], Schofield [103] , Baulsch and Drysdale [99]) have repeatedly concluded the temperature dependence of k_{1f}, E_{1f}, to be very

---

[*]Many experiments (e.g., References [114,124-127] evaluate k_{1f} relative to k_{11r} where k_{11r} is the rate constant for

$$H_2O + H \rightleftharpoons H_2 + OH \qquad (11)$$

Recent experimental data for k_{11r} [122,129] at temperatures in close proximity to those of each CO experiment were used to re-evaluate these k_{1f}'s and the new values are plotted in Figure 5.8.
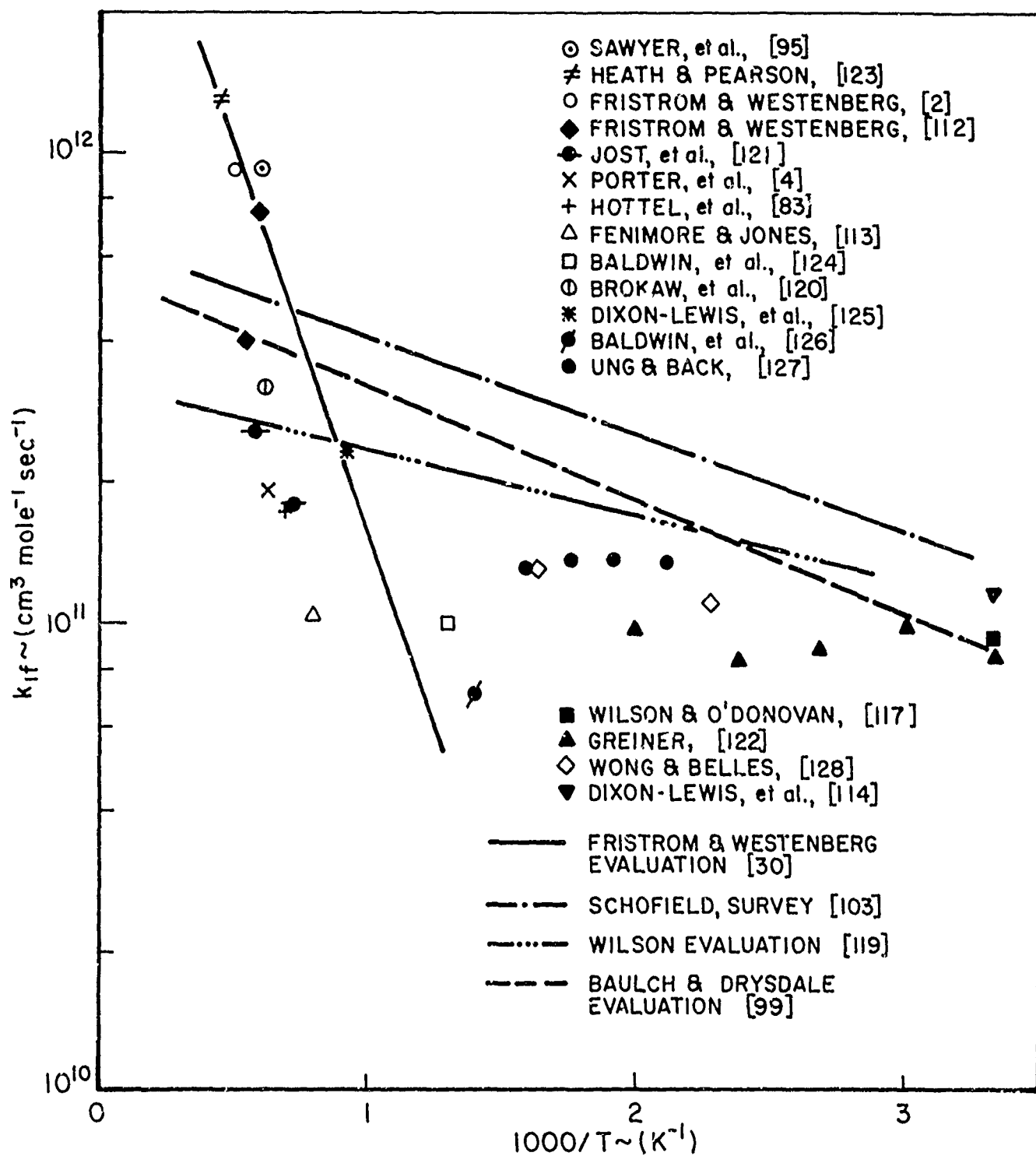
AVAILABLE EXPERIMENTAL MEASUREMENTS
OF THE SPECIFIC RATE CONSTANT, k_{1f}, FOR
$CO + OH \rightarrow CO_2 + H$

FIGURE 5.8

small, in spite of the large temperature dependence which
continued to be experimentally found above 1000K (Jost,
et al. [121], Brabbs , et al. [120]).

This difference between low and high temperature
results has generally been attributed to experimental diffi-
culties incurred in the high temperature measurements. How-
ever, Wilson [96], has concluded that experimental errors
alone could not account for the order of magnitude difference
between high temperature measurements and the extrapolation of
the precise results of Greiner [122] near room temperature.
Wilson [96] advanced two other possible explanations for the
observed discrepancies: either the reaction does not follow
the classical Arrenhius temperature dependence of

$$k_{ij} = C_{ij} \; T^n \exp \frac{E_{ij}}{RT} \qquad \begin{array}{l} i = 1, 2 \ldots \ldots \\ ; \; j = 5, n \end{array} \qquad \text{5.13}$$

$$n, \; C_{ij}, \; E_{ij} \quad \text{constant}$$

or there are competing CO reactions which are not properly
accounted for in the experimental analyses summarized in Figure
5.8. Finding that including the pre-exponential temperature
dependence of $T^{\frac{1}{2}}$ did not improve the discrepancy, he pursued
the possibilities of other competing reactions. However, it
might be argued that the specific rate constant, while not con-
forming to classical kinetics, (Equation 5.13) might be ex-
plained by absolute reaction rate theory. Thus, in the present
work, the temperature dependence of reaction (1) has been
analytically investigated using transition state theory (see

Laidler [130] or Benson [131]). In contrast to the classical approach, transition state theory predicts a temperature dependence of the form

$$k_{ij} = C_{ij} \ Q_{ij}(T) \quad \exp \ \frac{-Eo_{ij}}{RT} \ ; \ \begin{array}{l} i = 1,2 \cdots \\ j = 5, n \end{array} \quad 5.14$$

$$C_{ij}, \ Eo_{ij} \quad \text{constant}$$

where Eo_{ij} is the activation energy barrier between reactants and products in their zero point vibrational states, and $Q_{ij}(T)$ is the pre-exponential temperature dependence resulting from the various degrees of freedom of the reacting species and the activated complex. The constant, C_{ij}, includes all non-temperature dependent terms such as the symmetry number, moments of inertia, etc. It was not the intention of this work to theoretically evaluate C_{lf} but simply to estimate the pre-exponential temperature dependence $Q_{lf}(T)$. Therefore, the characteristics of the activated complex that must be known are the structure (linear or non-linear) and the vibration frequencies. The vibration frequencies of the activated complex, HOCO $^{\neq}$, for reaction (1) can be estimated in two ways:

(i) The vibrational structure of HOCO $^{\neq}$ can be envisioned as similar to the species HONO. The cis- and trans-forms of this molecule have been examined spectroscopically (Herzberg [132]); necessarily, this approach will yield results only for an assumed non-linear HOCO $^{\neq}$ complex.

(ii) Both linear and non-linear vibrational struc-
tures of HOCO$^{\neq}$ can be estimated by the char-
acteristic frequency method of Bennewitz and
Rossner [133,134].

The estimated fundamental vibration frequencies of
HOCO$^{\neq}$ resulting from these two approaches are presented in
Table 5.3.

The formulation for $Q_{1f}(T)$ will depend on the assumed
structure of the complex. For the non-linear activated complex

$$Q_{1f}(T) = \frac{1}{T} \frac{Q_V^{\neq}(T)}{Q_V^{OH}(T)Q_V^{CO}(T)} \qquad 5.15$$

where $Q_V(T)$ are the vibrational partitition functions (excluding
the zero point vibrational energy contributions) and where
$Q_V^{\neq}(T)$, the vibrational partitition function of the activated
complex, HOCO$^{\neq}$, excludes the vibrational mode along the
reaction coordinate. Independent of the structure, the missing
vibrational mode was assumed to be the frequency, ν_1, (Table
5.3) which can be attributed primarily to the stretching of the
O-H bond. However, for the linear activated complex, the 1/T
dependence in Equation 5.15 becomes $1/T^{3/2}$ (one less rotational
degree of freedom) and $Q_V^{\neq}(T)$ will include one additional vibra-
tional degree of freedom, ν_7. For example, using the average
of the cis,trans values of the $\nu_2 - \nu_6$ frequencies for the HONO
model, and the fundamental vibration frequencies of OH and

ESTIMATED FUNDAMENTAL VIBRATION FREQUENCIES
FOR THE ACTIVATED COMPLEX, HOCO

i. Using Fundamental Frequencies of HONO

(ν in cm^{-1})

	ν_1	ν_2	ν_3	ν_4	ν_5	ν_6	ν_7
Cis	3426	1639	1370	856	620	638	---
Trans	3590	1698	1264	793	548	544	---
Average	3510	1664	1317	825	584	591	---

ii. Using Characteristic Frequencies of HOCO$^{\neq}$

	ν_1	ν_2	ν_3	ν_4	ν_5	ν_6	ν_7
Non-Linear	3500	1740	1030	1350	780	1120	---
Linear	3500	1740	1030	1350	780	1120	1083

TABLE 5.3

CO (Herzberg [135]),

$$Q_{1f}(T)(\text{HONO MODEL}) \equiv Q'_{1f}(T) = \frac{1}{T}\left[\frac{\left(1-e^{\frac{-5370}{T}}\right)\left(1-e^{\frac{-3125}{T}}\right)}{\left(1-e^{\frac{-2400}{T}}\right)\left(1-e^{\frac{-1899}{T}}\right)\left(1-e^{\frac{-876}{T}}\right)\left(1-e^{\frac{-852}{T}}\right)}\right] \qquad 5.16$$

Similar expressions result for the non-linear and linear characteristic frequency models of HOCO $^{\neq}$

$$Q_{1f}(T)(\text{NONLINEAR}) \equiv Q''_{1f}(T) = \frac{1}{T}\left[\frac{\left(1-e^{\frac{-5370}{T}}\right)\left(1-e^{\frac{-3125}{T}}\right)}{\left(1-e^{\frac{-1500}{T}}\right)\left(1-e^{\frac{-1940}{T}}\right)\left(1-e^{\frac{-1120}{T}}\right)\left(1-e^{\frac{-1610}{T}}\right)}\right] \qquad 5.17$$

$$Q_{1f}(T)(\text{LINEAR}) \equiv Q'''_{1f}(T) = \frac{1}{T}\left[\frac{\left(1-e^{\frac{-5370}{T}}\right)\left(1-e^{\frac{-3125}{T}}\right)}{\left(1-e^{\frac{-1500}{T}}\right)\left(1-e^{\frac{-1940}{T}}\right)\left(1-e^{\frac{-1120}{T}}\right)\left(1-e^{\frac{-1610}{T}}\right)\left(1-e^{\frac{-1510}{T}}\right)}\right] \quad 5.18$$

In addition to the formulation of $Q_{1f}(T)$ (Q'_{1f}, Q''_{1f} or Q'''_{1f}), C_{1f} and Eo_{1f} (Equation 5.14) must be determined to obtain the analytical description of k_{1f}. These constants could be theoretically estimated, or alternatively, Equation 5.14 could be least square fitted to the experimental data

of Figure 5.8. However, it should be re-emphasized that the intention of this work is to attempt some reconciliation of the experimentally observed temperature dependence in the high and low temperature regimes. Thus, it was decidedly easier and just as effective to parametrically vary Eo_{1f} over a reasonable range and to choose C_{1f} such that the analytical k_{1f} (for the chosen Eo_{1f} and form of $Q_{1f}(T)$) fitted the experimental data at the most investigated value (temperature = 300K):

$$k_{1f} \text{ calculated} \Big|_{T=300K} \equiv 8.5 \times 10^{10} \text{ cm}^3 \text{ mole}^{-1} \text{sec}^{-1}$$

The resulting analytical expressions could then be extrapolated to the high temperature regime for comparison with experiment.

The analytical results obtained for the three assumed models of the HOCO $^{\neq}$ activated complex are presented in Figures 5.9-5.11. Comparison of analytical and experimental results are presented in Figure 5.12. The agreement of the transition state theory results with experimental data is most promising. It might be suspected that the assumed structure (linear or non-linear) of the HOCO $^{\neq}$ complex would be of some concern. Westenberg and Wilson [115(b)] have argued that a linear complex might be more likely on the basis that the polyatomic product of the reaction, CO_2, was linear. However, another intuitive argument could be that a linear product could form from a non-linear complex, but not vice-versa. The above comparison (Figure 5.12) makes the question rather academic as far as the displayed temperature dependence is concerned.

The formula shown in the figure:

$$k_{1f} = \frac{C_{1f}}{T}\left[\frac{\left(1-e^{\frac{-5370}{T}}\right)\left(1-e^{\frac{-3125}{T}}\right)}{\left(1-e^{\frac{-2400}{T}}\right)\left(1-e^{\frac{-1899}{T}}\right)\left(1-e^{\frac{-1188}{T}}\right)\left(1-e^{\frac{-876}{T}}\right)\left(1-e^{\frac{-852}{T}}\right)}\right]\exp\left(\frac{-E_{0_{1f}}}{RT}\right)$$
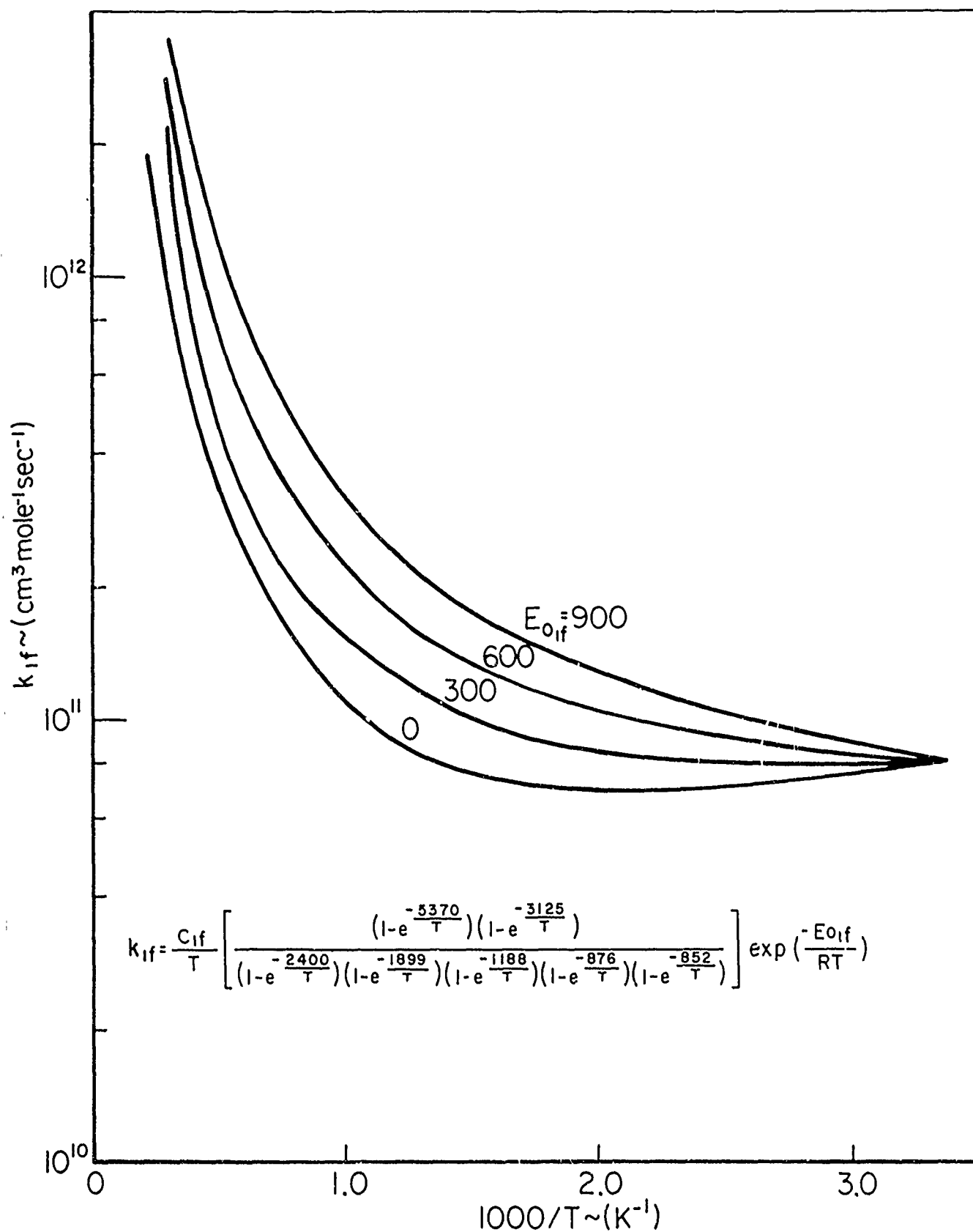
TEMPERATURE DEPENDENCE OF k_{1f}
HONO MODEL NON-LINEAR COMPLEX

FIGURE 5.9

$$k_{lf} = \frac{C_{lf}}{T^{3/2}} \left[\frac{(1-e^{\frac{-5370}{T}})(1-e^{\frac{-3125}{T}})}{(1-e^{\frac{-1500}{T}})(1-e^{\frac{-1940}{T}})(1-e^{\frac{-1120}{T}})(1-e^{\frac{-1610}{T}})(1-e^{\frac{-1610}{T}})} \right] \exp\left(\frac{-E_{0lf}}{RT}\right)$$

$k_{lf} \sim (cm^3 \ mole^{-1} \ sec^{-1})$

$E_{0lf} = 900$

600

300

0

$1000/T \sim (K^{-1})$

JF 13 R 4229 71
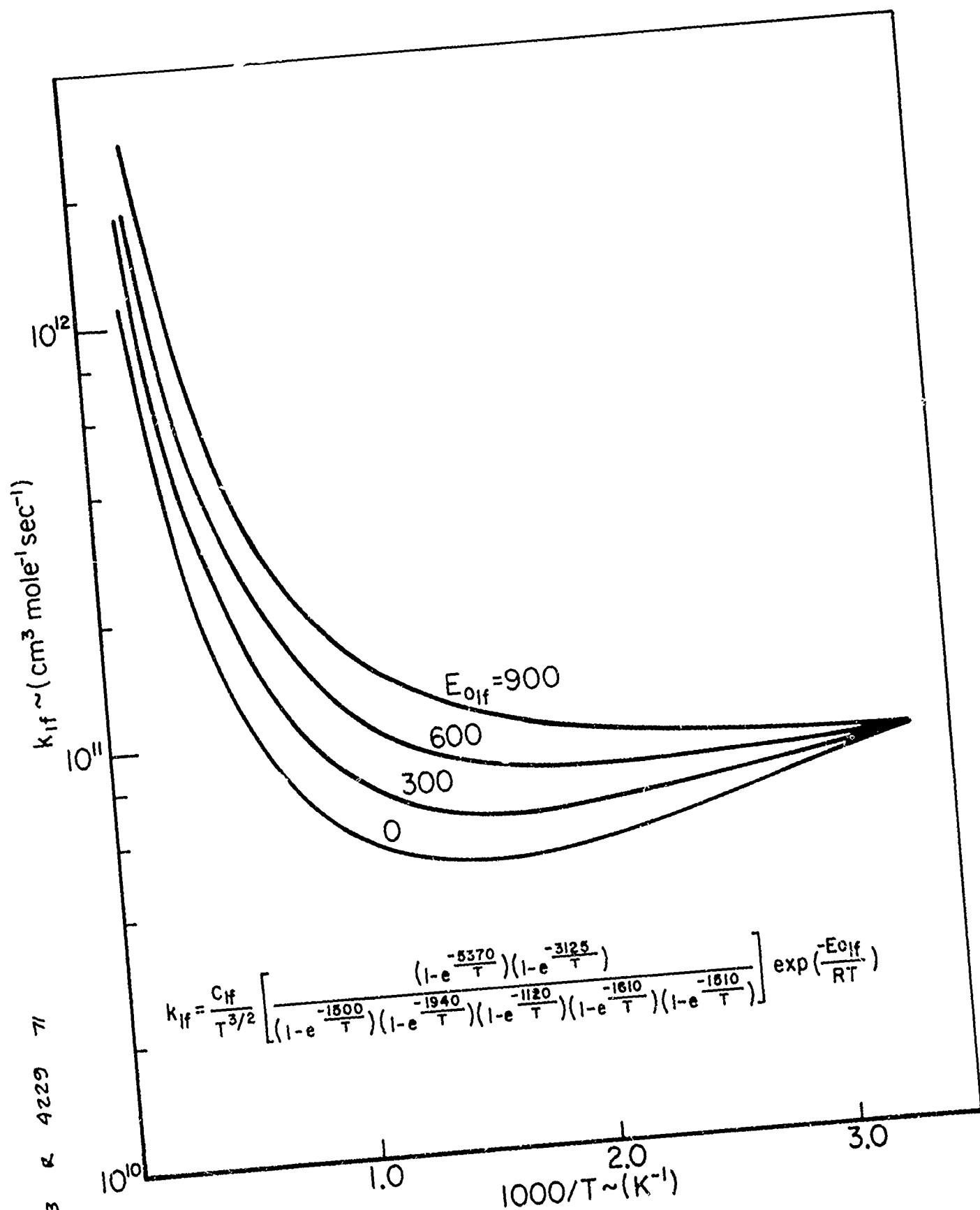
TEMPERATURE DEPENDENCE OF k_{lf}
CHARACTERISTIC FREQUENCY MODEL LINEAR COMPLEX
FIGURE 5.10
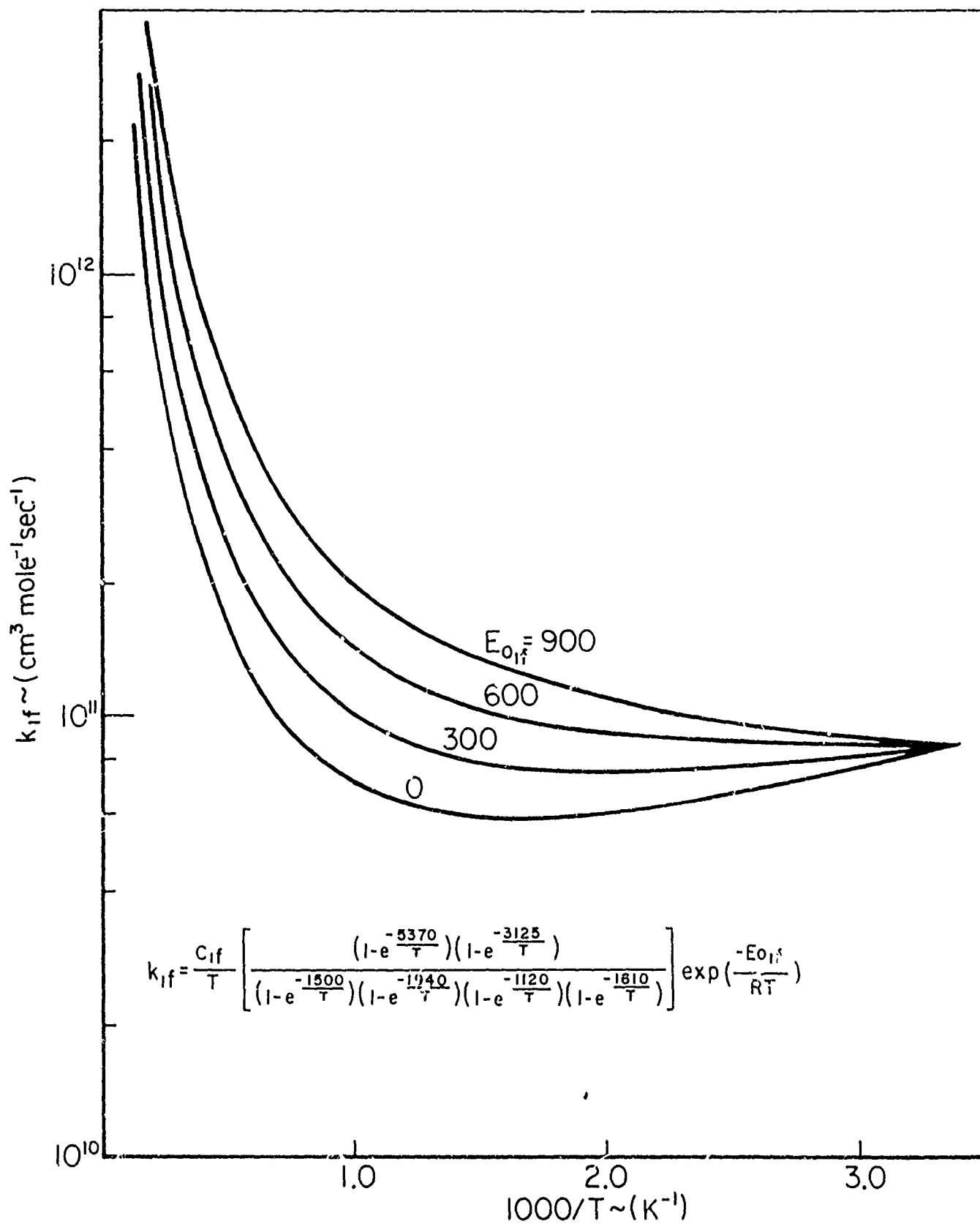
$$k_{1f} = \frac{C_{1f}}{T}\left[\frac{\left(1-e^{\frac{-5370}{T}}\right)\left(1-e^{\frac{-3125}{T}}\right)}{\left(1-e^{\frac{-1500}{T}}\right)\left(1-e^{\frac{-1940}{T}}\right)\left(1-e^{\frac{-1120}{T}}\right)\left(1-e^{\frac{-1610}{T}}\right)}\right]\exp\left(\frac{-E_{0_{1f}}}{RT}\right)$$

TEMPERATURE DEPENDENCE OF k_{1f}
CHARACTERISTIC FREQUENCY MODEL NON-LINEAR COMPLEX
FIGURE 5.11

SEE FIGURE 5.8 FOR
SOURCES OF
EXPERIMENTAL DATA

—— HONO MODEL
$Eo_{1f} = 0$ cal mole^{-1}

---- ENVELOPE OF ALL
ANALYTICAL RESULTS
(FIGURES 5.9-5.11),
$Eo_{1f} = 0-900$ cal mole^{-1}

$1000/T \sim (K^{-1})$

COMPARISON OF ANALYTICAL AND
EXPERIMENTAL RESULTS FOR REACTION (I),
$CO + OH \rightarrow CO_2 + H$
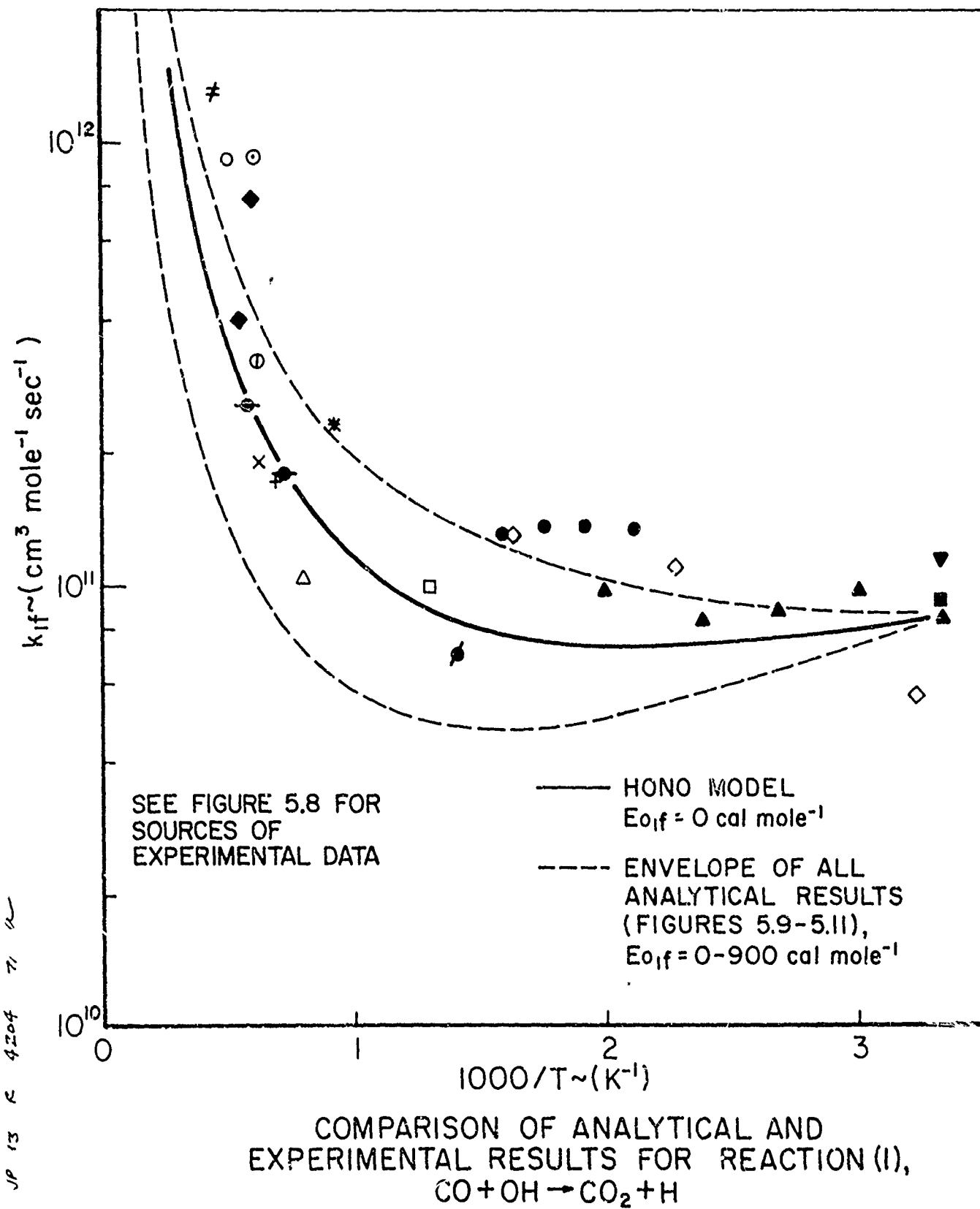
FIGURE 5.12

Results are seen to be slightly dependent on the choice of Eo_{1f}. At room temperature, $Q_{1f}(T)$ in all cases (Equation 5.16-5.18) contributes much less to the temperature dependence of k_{1f} than the exponential term, Eo_{1f}. The measurements of Greiner [122] at 300-500K indicate this temperature dependence to be (in exponential form) 230 ± 140 cal mole^{-1}. In light of this low value, Eo_{1f} must surely lie in the range 0-900 cal mole^{-1}. Furthermore, if Eo_{1f} is sufficiently small, $Eo_{1f} < 200$ (Equation 5.16), $Eo_{1f} < 400$ (Equation 5.17), $Eo_{1f} < 600$ (Equation 5.18), a negative temperature dependence of k_{1f} near room temperature is observed. Although Greiner [122] concludes the temperature dependence to be positive, his data (see Figure 5.8) could equally support a slightly negative relationship. Furthermore, if one were to observe reaction (1) over a limited temperature range and attribute all temperature dependence to the Arrhenius term in expression 5.13 (ie $n \equiv 0$), one would calculate an apparent value for the activation energy, E_{1f}. But, this is exactly what has been done in several of the independent experimental investigations reported in Figure 5.8. An analytical similitude can be obtained by estimating the mean slope of one of the expressions in Figures 5.9-5.11 over a short temperature range. Analytical calculations for the HONO model with $Eo_{1f} = 0$ cal/mole (Figure 5.12, solid line) are compared to experimental results in Table 5.4. It is interesting to note that the magnitudes of both the analytical and experimental apparent activation energies are similar and increase with

Comparison of Observed and Analytical Apparent
Activation Energy, E_{1f}, Equation 5.13(N=0)

Ref.	Temp. Range	Reported Experimental Apparent E_{1f}	Estimated Analytical Apparent E_{1f}
	(Deg. K)	(cal/mole)	(cal/mole)
[122]	300 - 500	230 ± 140	-230
[129]	300 - 610	1200	+200
[121]	1380 - 1720	4700	5200
[120]	1300 - 1900	3700	5800
[4]	1600	8700	5800

TABLE 5.4

increasing temperature.

In summary, although Wilson [96] correctly concluded that the experimental data on

$$CO + OH \longrightarrow CO_2 + H \tag{1}$$
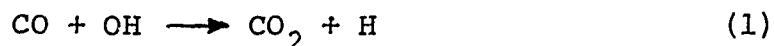
does not conform to classical kinetic interpretation, this work shows that absolute reaction rate theory can account for the entire difference in low and high temperature observations. The true activation energy of reaction (1) may be very near zero, but the temperature dependence of the specific rate constant can be substantial at high temperatures. Thus, to explain experimental measurements, there is no need or supportive evidence for any other elementary reactions such as

$$CO + HO_2 \longrightarrow CO_2 + OH \tag{4}$$
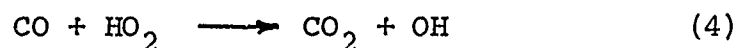
contributing to CO_2 formation at high temperature.

Furthermore, it is important to emphasize that, when a specific rate constant relation is used over large temperature ranges (as in kinetic computer modeling of combustion processes), the inclusion of more than the classical pre-exponential temperature dependence of the specific rate constant may be essential. This is particularly true when Eo_{ij} is very small.

Considering that the high temperature experimental measurements on reaction (1) may be better than most have previously thought, data on several other hydroxyl reactions which

have been comparatively studied should be reviewed. This will become more evident in the next chapter during discussion of the reactions contributing to disappearance of CH_4 in the oxidation of methane.

CHAPTER 6 - OXIDATION OF METHANE AT HIGH TEMPERATURES

Since the initial work of Bone and Gardiner [136], numerous researches have been performed on the reaction of methane and oxygen at low temperatures. However, relatively few studies, other than those in flames (e.g., Van Tigglen, et. al. [137], Westenberg and Fristrom [2], Dixon-Lewis and Williams [3]) have investigated the complete oxidative reaction at temperatures greater than 900K. This fact is due in part to experimental difficulties arising from the macroscopic chemical character of the methane-oxygen reaction.

As with all high temperature hydrocarbon-oxygen reactions, the chemistry proceeds through two distinct phases. There is an initial slow reaction stage accompanied by little or no energy release which is generally referred to as the induction period. During the induction phase, reaction centers important to chain branching build up to levels necessary to cause explosion (fast reaction). In the case of methane oxidation, this initial reaction phase has been studied in both shock tubes (Skinner and Ruehrwein [138], Asaba, et. al. [139], Miyama and Takeyama [140], Glass, et. al. [141], Seery and Bowman [142], Higgen and Williams [143]) and flow reactors (Loyd [144], Mullins [145], Németh and Sawyer [146]*).

---

*If one reviews the experimental data of Németh and Sawyer [146], one finds that they have characterized only the initial reaction stage, i.e., the induction kinetics.

The induction period is abruptly followed by a highly exothermic reaction phase during which the remaining hydrocarbon fuel is rapidly consumed. The final distribution of products is a function of equivalence ratio and temperature and is generally considered to proceed through the sequential oxidation process,

$$CH_4 \xrightarrow{O_2} H_2O + CO \xrightarrow{O_2} CO_2 + H_2O.$$
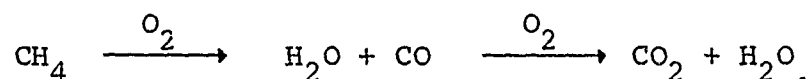
While Brokaw [147] has shown that induction time for higher paraffins (kerosene and iso-octane) accounts for less than 20% of the total reaction time (induction time plus exothermic reaction time), induction period chemistry can in some cases completely dominate the reaction time for methane and oxygen. Shock tube experiments of Seery and Bowman [142] and Bowman [148] clearly show that induction time accounts for 20%-90% of the reaction time; thus, experimental methods employing residence time measurements (Burgoyne and Hirsch [21] and Kozlov [23]) may under some circumstances characterize, to a large extent, only the induction period kinetics.

However, it is the secondary, highly exothermic phase of the reaction that is important in most practical design situations. For example, in turbine combustor systems, recirculation of hot, partially burned gases provides the ignition source for continuous operation. These hot gases will contain some of the necessary reaction centers for chain branching, and thus the fluid mechanics will significantly reduce or eliminate the induction period phase of the reaction. The post-induction phase of the oxidation

will remain largely uneffected, and thus this reaction time will be the characteristic parameter of importance in choosing the combustor volume. Furthermore, this same chemistry will be of interest in the oxidative reaction of higher paraffins where induction times are more nearly a function of fuel pyrolysis than of direct reaction.

Thus, it was the intention of this study to deal primarily with the post induction phase kinetics of the methane-oxygen reaction. Turbulent flow reactor experiments were conducted in 5 and 10 cm diameter reactor tubes with nitrogen or air as carrier. Both chemical analysis and thermal analysis experiments were conducted. Thermal analysis measurements were obtained during construction and testing of the chemical sampling and analysis systems, and they provided guidance for the ensuing chemical studies. The thermal data also offer an interesting comparison for the chemical results. As in the preceding chapter, a summary of the range of parameters studied in each case are presented in Table 6.1. It should be noted immediately that experimental results were obtained over a limited range of equivalence ratio ($\phi < 0.6$). This fact is due to the strong dependence of the $CH_4^- O_2$ induction time on equivalence ratio. Through shock tube experiments, Seery and Bowman [142] have emperically correlated the induction time, τ'_{iND}, as

$$\tau'_{iND} = [O_2]^{-1.6} [CH_4]^{+0.4} \; 7.65 \times 10^{-18} \; e^{\left(\frac{+51,400}{RT}\right)} \; \text{(sec)}$$

6.1

RANGE OF EXPERIMENTAL PARAMETERS FOR
STUDIES OF THE CH_4/O_2 REACTION

	Thermal Analysis	Chemical Analysis
$X^O_{CH_4}$	.005　.013	.005 - .009
$X^O_{O_2}$	.02　- .20	.025 - .20
ϕ (Equivalence Ratio)	.05　- .500	.05　- .55
Duct Diameter	10 cm	5-10 cm
Pressure	1 atm	1 atm
Temperature	1200 - 1400K	1100 - 1400K
Additive Experiments	None	CO and/or H_2O

Table 6.1

While τ_{IND} was qualitatively observed to follow these concentration dependences in this study, it will be shown later that the time necessary to complete the exothermic phase of the reaction, τ_{ox}, was inversely effected by the methane concentration. Thus, as the equivalence ratio was increased, the induction time increased while the exothermic reaction time decreased. As $\phi = 0.6$ was approached, flow velocities had to be considerably reduced to complete the reaction in the length of the reactor duct; and, at these lower velocities, the exothermic reaction was not sufficiently spread, i.e., longitudinal diffusion and conduction effects were no longer negligible.

It should be mentioned that Equation 6.1 predicts induction times two to four times longer than those experimentally observed in the flow reactor. It is not clear that mixing effects occurring in the initial stages of the reaction accounted for this discrepancy; but for this reason, reaction time measurements should not be used to study the induction period kinetics in flow reactors.

The following sections of this chapter will present, discuss, and compare the turbulent flow reactor measurements of the methane oxygen reaction and those of other investigators. The qualitative results of this study will be presented and discussed first, and this will be followed by presentation of the emperical correlation and discussion of results of the methane disappearance rate and carbon dioxide production rate.

The concluding section of the chapter will discuss the relevance of these qualitative and quantitative observations to the description of the elementary reaction mechanism.

6.1   Qualitative Chemical Observations

Typical chemical analysis results for reaction of methane and air at two different initial temperatures are presented in Figures 6.1 and 6.2[*]. Illustrated here are the concentration profiles for the major species CH_4 CO, and CO_2, and minor species C_2H_4 and C_2H_6. Minor species other than C_2H_4 and C_2H_6 were present; however, carbon atom summations for the above mentioned compounds were always within 3-5% of the carbon initially present as CO_2 (in compressed air) and CH_4. CH_2O was observed in the gas chromatographic analysis; however, sensitivity and repeatability of analyses were such that, at such low concentration levels, no specie profile could be constructed. Hydrogen was also known to be present (Burgoyne and Hirsch [21] and Pratt [22]); however, its concentration did not rise above the lower detection limit of the detector system (300 ppm).

That the CH_2O concentration accounted for most of the total carbon discrepancy was confirmed by cryogenic sample concentration. Sample flow at the position of maximum carbon deficiency was passed through a cryogenic trap for a period of fifteen minutes. After returning the trap to room temperature and adding ultra purity helium to raise the total

---

[*]Tabulated results for concentration, concentration gradient and temperature at each sampled position of Figures 6.1, 6.2 are presented in one of the computer output examples in Appendix B.

TEMPERATURE ~ (K)

1195

1175

1155

1135

1115

MOLE PERCENT SPECIES

0.6

0.5

0.4

0.3

0.2

0.1

0

0.005

0

○ CO_2
□ CH_4
△ CO
● TOTAL CARBON
▲ TEMPERATURE

1 cm ≈ 1.7 m sec
Φ ≈ 0.05
10 cm dia. DUCT

○ C_2H_4
□ C_2H_6

CO_2

CO

T

CH_4

30 40 50 60 70 80 90 100 110 120 130

DISTANCE FROM INJECTION - (cm)
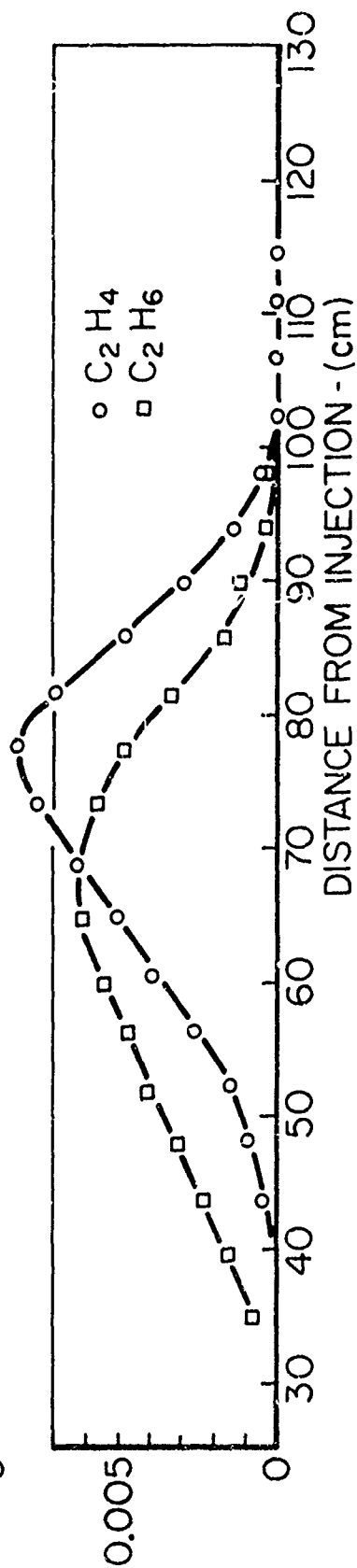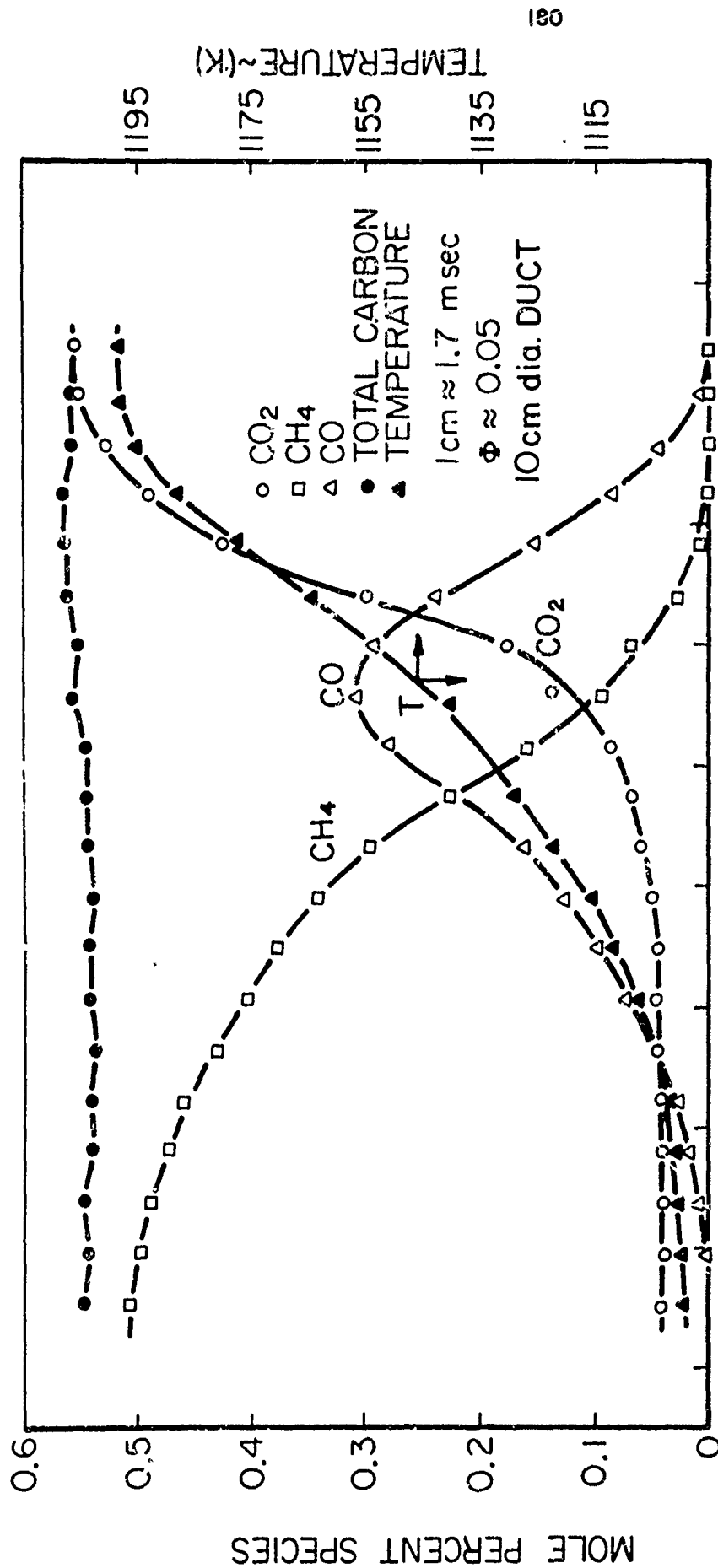
CHEMICAL COMPOSITION OF SPREAD METHANE - AIR REACTION
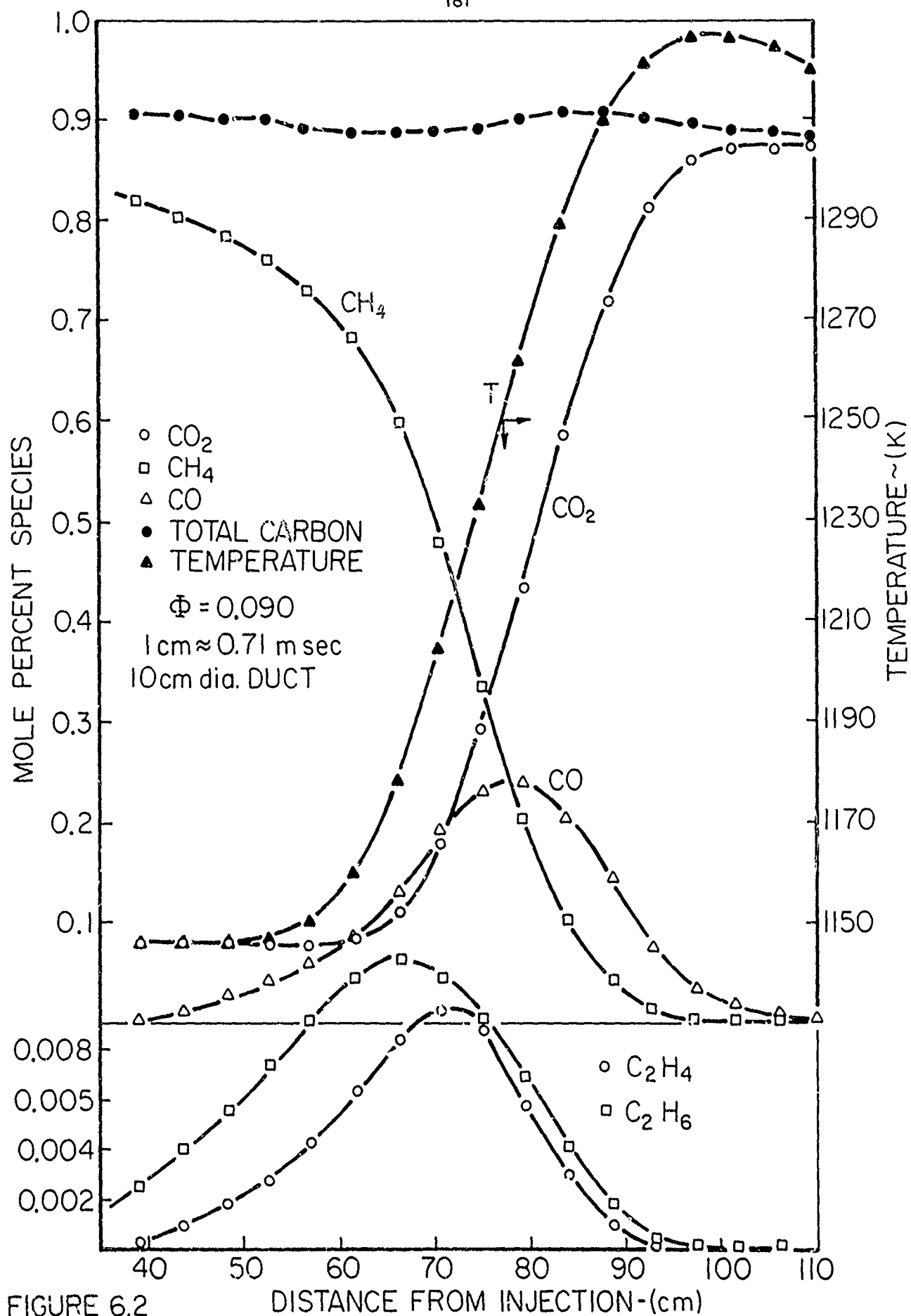
FIGURE 6.1

FIGURE 6.2

CHEMICAL COMPOSITION OF SPREAD METHANE-AIR REACTION

pressure of the sample, the sample concentration factor was evaluated by the ratio of CO_2, C_2H_4 and C_2H_6 in the concentrated sample to amounts in a sample taken before the cryogenic trap. Hydrocarbons other than CH_2O were detected on the gas chromatograph analysis system. CH_2O and H_2O_2 concentrations were evaluated by spectrophotometric methods using chromotropic acid (Bricker and Johnson [149]) and titaneous sulphate (Egerton, et. al. [150]), respectively. Results of one of the analyses are presented in Table 6.2. Addition of these measurements reduced error in total carbon balance to less than 2%.

In light of these results, it was feasible to calculate H_2O and O_2 concentration and gradient profiles from hydrogen and carbon atom balances and the initial concentrations of CH_4 and CO_2 (when air was used as carrier).

These chemical measurements have several interesting features which may be compared with the qualitative methane oxidation studies of Burgoyne and Hirsch [21] and Pratt [22].

First, it is apparent that total carbon discrepancies reported in both of these studies were a result of undetected C_2 hydrocarbons. Each study argued that these compounds (as well as others) might be responsible; however, the employed analysis techniques were not selectively sensitive to C_2H_6 and C_2H_4.

The noted C_2H_4 was almost certainly a secondary reaction product of the oxidation of C_2H_6, and C_2H_6 most likely resulted from recombination of methyl radicals formed

CRYOGENIC SAMPLE CONCENTRATION RESULTS
ON THE METHANE/AIR REACTION

Experimental Conditions

Concentration Factor:

based on: CO_2 - 95.5

C_2H_4 - 115.

C_2H_6 - 97.0

reaction temperature   1200K

X^OCH_4 - .005

Minor Specie	Maximum Concentration (PPM)	Analysis Instrument
CH_2O	100	(1)
C_2H_6	60	GC(FID)
C_2H_4	40	GC(FID)
CH_3OH	5	GC(FID)
C_2H_2	1	GC(FID)
C_3H_6	.01	GC(FID)
C_3H_8	.01	GC(FID)
H_2	300	GC(FID) *
H_2O_2	1	(2)

Notes:

(1) Spectrophotometry, Reference [149]

(2) Spectrophotometry, Reference [150]

* Not detected. Figure is instrument lower detection limit.

Table 6.2

from CH_4. It is, however, somewhat surprising that these C_2 hydrocarbons reached concentration levels comparable to that of the intermediary, formaldehyde. It is possible that significant amounts of methane may pass through this C_2 oxidation route.

A more interesting observation in the present studies is the accelerated formation of carbon dioxide (relative to methane disappearance) with increasing temperature. This is reflected in Figures 6.1 and 6.2 as a decrease in the relative maximum concentration of carbon monoxide at increasing reaction temperatures. At an initial temperature of 1100K (Figure 6.1), carbon monoxide concentration maximizes at 60% of the total carbon, while at a higher initial temperature (Figure 6.2), maximum carbon monoxide concentration is less than 30% of the initial methane concentration. Carbon dioxide formation remains suppressed in the initial stages of the oxidation at higher temperature, but less methane has disappeared before CO_2 formation becomes significant. These observations are in great contrast to those of Burgoyne and Hirsch [21] and Pratt [22]. Both studies concluded CO_2 formation to be strongly inhibited by the presence of methane or its oxidation products until nearly all the initial fuel had disappeared. No definitive experimental explanation for this discrepancy is apparent. However, maximum relative formaldehyde concentrations in both of these studies were two to three times that found in the present work, and Burgoyne and Hirsch [21] have shown conclusively

that CH_2O strongly inhibits the oxidation of carbon monoxide. There is not an obvious reason for the lower concentrations of CH_2O; however, it is interesting to note that both of the studies mentioned above were in laminar flow reactors with surface to volume ratios as much as two orders of magnitude larger than those in the present work. Although experimental results of this work indicated little effect of surface to volume ratio[*], it was not possible to deduce if surface effects may have been present at the much larger surface to volume ratios of Burgoyne and Hirsch [21], Pratt [22], or Kozlov [23]. These authors have conclusively shown surface construction material and conditioning to have no effect on measured parameters; however, no evidence was presented to indicate that the presence of a surface did not effect the reaction.

6.2   Disappearance Rate of Methane

The overall disappearance rate of methane in the post-induction phase of the oxidation was empirically correlated using the procedures described in Chapter 4 and employed in Chapter 5. The chemical analysis and thermal analysis results will be presented and discussed separately, and the section will be concluded with a critical discussion and comparison of similar overall measurements of other investigators.

---

[*]section 6.2.1

6.2.1 Chemical Analysis Results

Experimental data from the 10 cm diameter reactor duct was experimentally correlated by the functional relation

$$-\frac{d[CH_4]}{dt} = k_{ov} [CH_4]^a [O_2]^b = 10^A e^{-E/RT} [CH_4]^a [O_2]^b \qquad 6.2$$

The fuel reaction order was evaluated from several methane-air experiments with varying initial temperatures and methane concentrations. A log-log plot of $d\frac{[CH_4]}{dt}$ versus $[CH_4]$, at constant temperature is presented in Figure 6.3, and the demonstrated linear slope defined the fuel reaction order, a, as 0.7. The fuel reaction order was observed to be independent of temperature.

These same experiments were also employed to estimate the overall activation energy, E, for determination of the oxygen reaction order, b. Each methane-air experiment was treated separately, and Figures 6.4-6.6 are representative of the semi-log plots of k_{ov}, determined from Equation 6.2 (a = 0.7, b arbitrary) versus T^{-1}. The overall activation energy in the post-induction phase reaction was determined as 49 ± 2.0 kcal/mole. E was observed to be relatively independent of the assumed oxygen reaction order, b.

It should be emphasized that the two reaction stages discussed earlier are clearly visible in Figures 6.4-6.6 and that the induction kinetics do not exhibit the same parameter dependencies as the post-induction phase reaction. Sufficient data was not available to evaluate the induction phase reaction orders and temperature dependence, but it
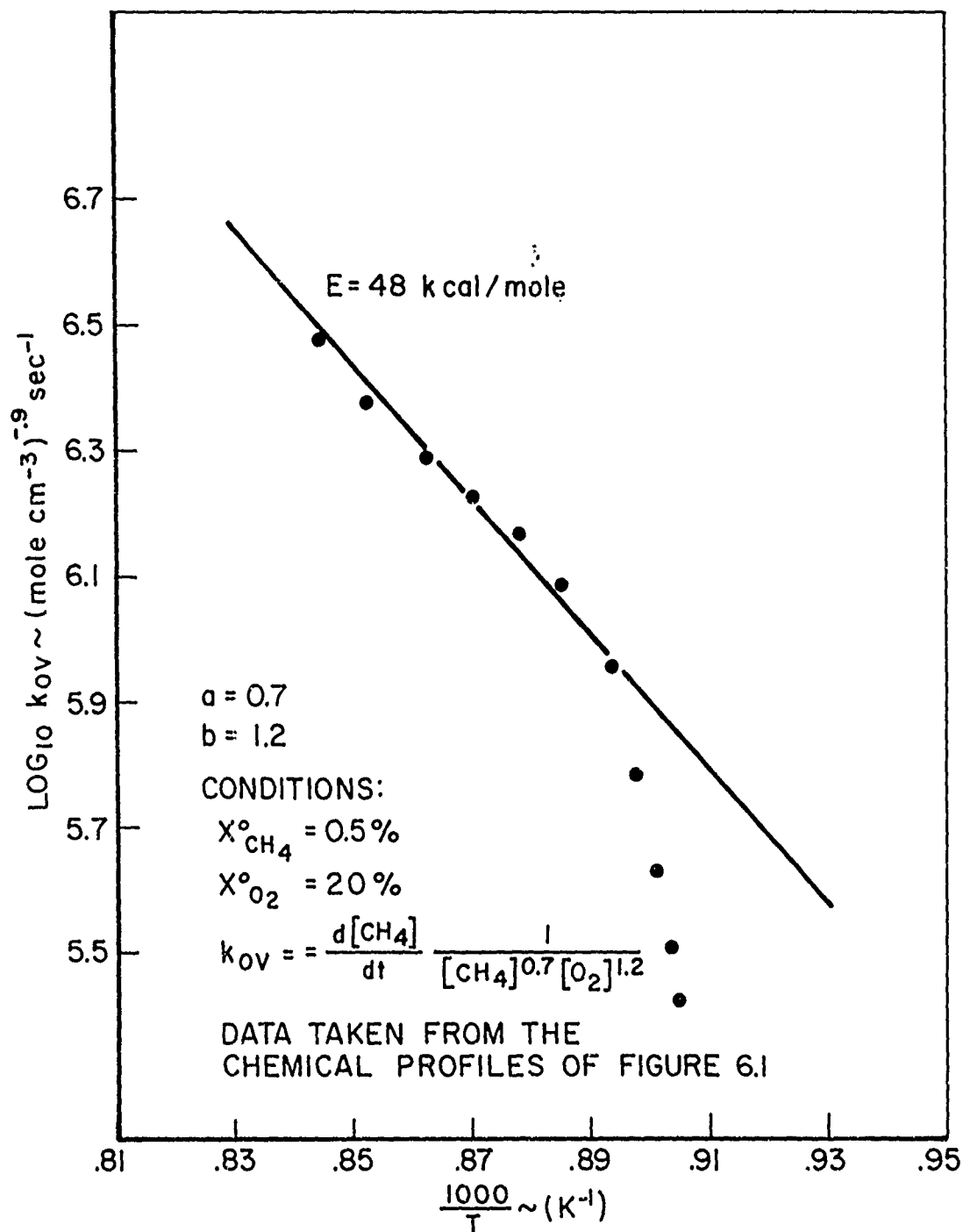
METHANE/OXYGEN
OVERALL REACTION RATE STUDY
METHANE ORDER DETERMINATION

SLOPE = 0.7

METHANE/AIR DATA
TEMPERATURE : 1205 ± 2 K

$[CH_4] \sim$ (mole cm^{-3})

$\dfrac{d\ [CH_4]}{dt} \sim$ (mole cm^{-3} sec^{-1})

FIGURE 63

DETERMINATION OF E FOR REACTION OF CH_4/O_2

FIGURE 6.4
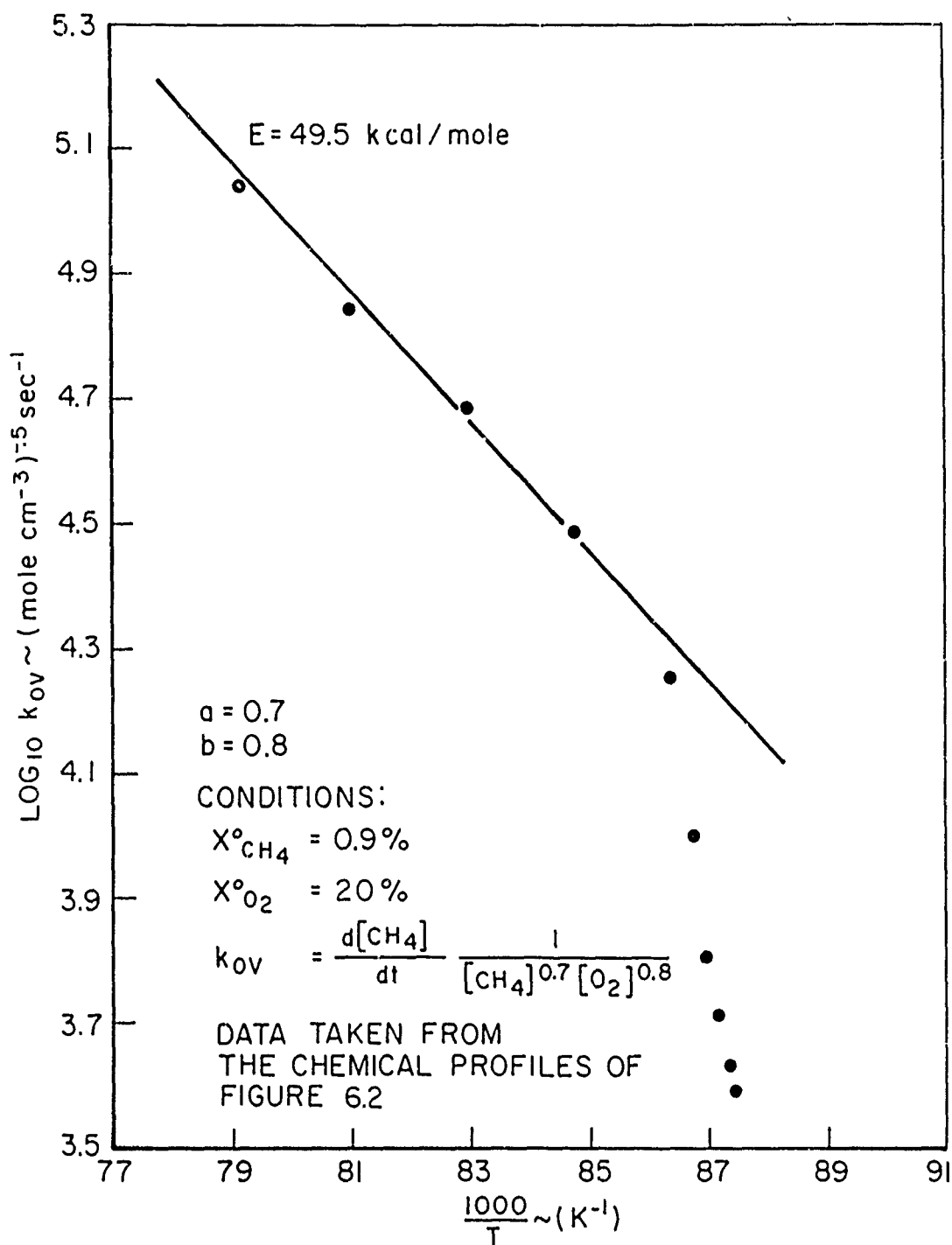
DETERMINATION OF E FOR REACTION OF CH_4/O_2

FIGURE 6.5
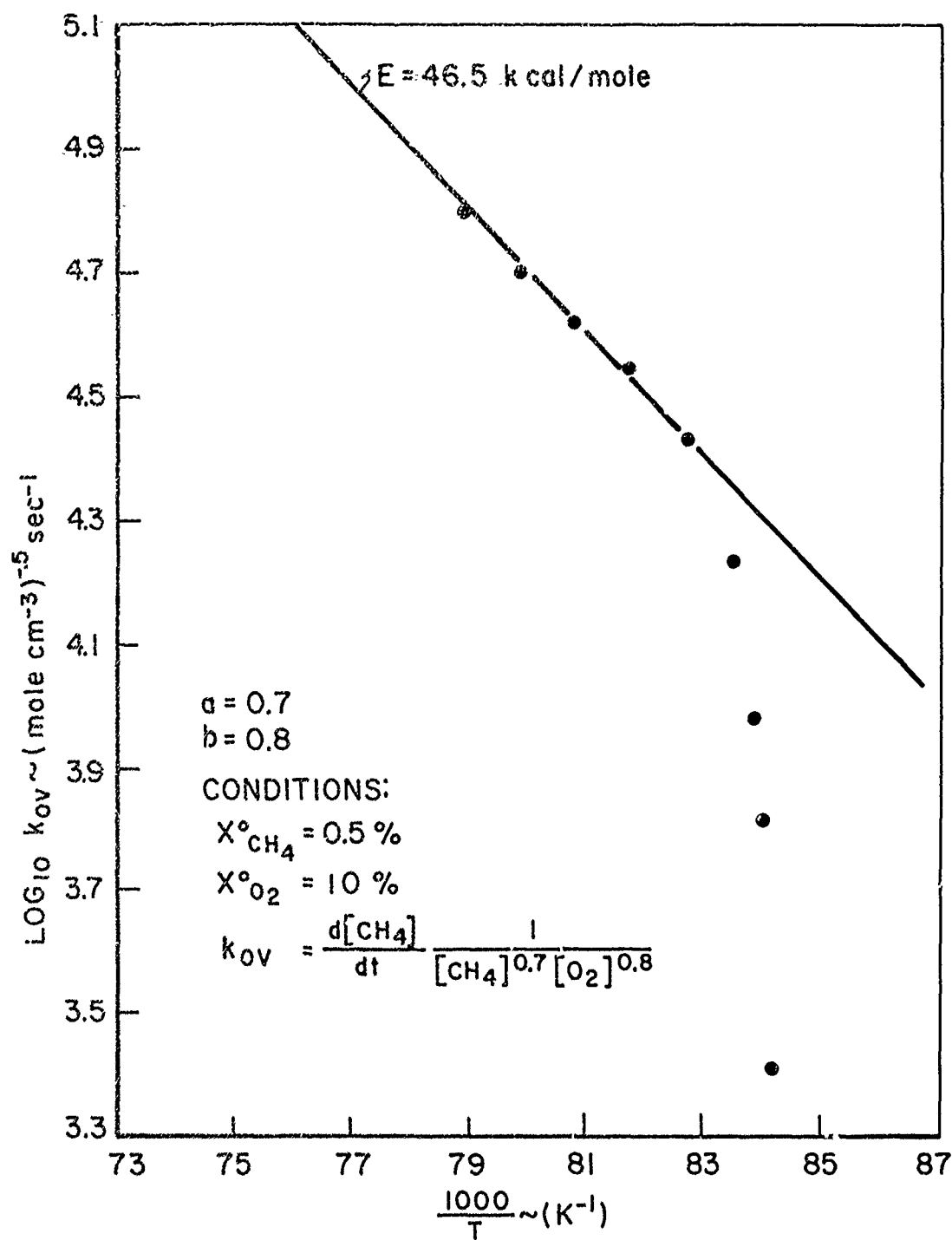
DETERMINATION OF E FOR REACTION OF CH_4/O_2

FIGURE 6.6

should be noted that it is feasible to study the induction oxidation reaction in a manner similar to the above. However, it is interesting that expressions with reaction orders and temperature dependence similar to those in Equation 6.1 fitted the available data reasonably well.

The methane-air reaction data were combined with experiments in which initial oxygen concentration was varied between 2 and 20%, and the determined value of a and estimate of E were used to evaluate the oxygen reaction order. The apparent overall activation energy determined from linear least square fits of data to Equation 6.2 (a = 0.7, b arbitrary) are plotted as a function of the assumed oxygen reaction order in Figure 6.7. A value of b = 0.8 $\pm$ .1 was found to reproduce the previous estimate of E.

All 10 cm diameter reactor duct data were linear least square fitted to Equation 6.2 with a = 0.7 and b = 0.8 to obtain A and E. The result is displayed in Figure 6.3 and determined the overall rate of methane disappearance to be best represented by

$$\frac{d[CH_4]}{dt} = 10^{13.2 \pm .20} \exp\left(\frac{-48,400 \pm 1,200}{RT}\right) [CH_4]^{0.7} [O_2]^{0.8}$$

$$\text{mole cm}^{-3} \text{ sec}^{-1} \qquad 6.3$$

Limited results of methane-air reaction experiments conducted in the 5 cm diameter reactor duct are presented in Figure 6.9. The rate of disappearance of methane was found to be independent of changes of surface to volume ratio over the range of study available in the turbulent flow reactor.
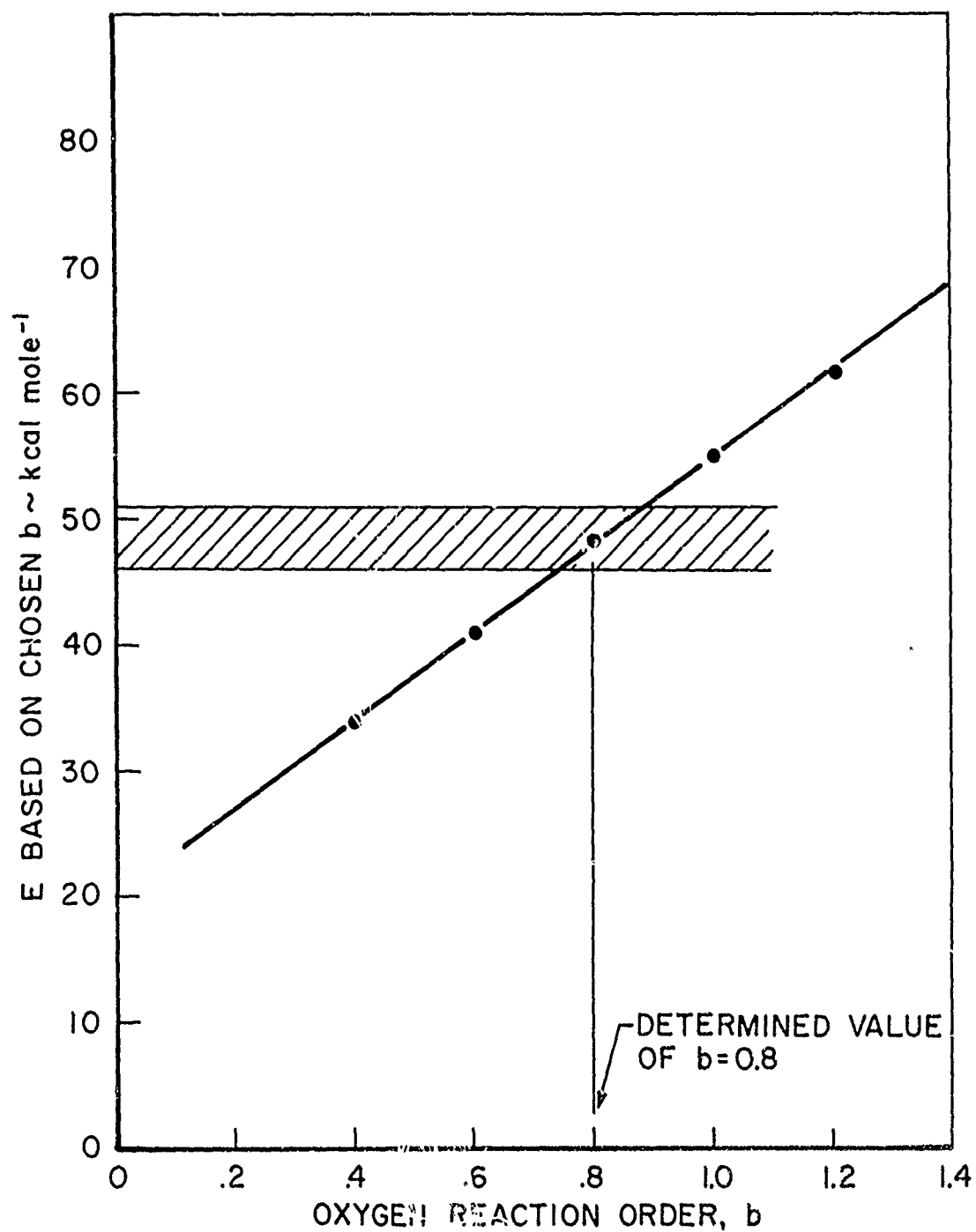
DETERMINATION OF OXYGEN REACTION ORDER FOR
CH_4 / O_2 REACTION

FIGURE 6.7

METHANE/OXYGEN
OVERALL REACTION RATE
1100 K – 1400 K
(10 cm DIA. DUCT)

LEAST SQUARE FIT

$$-\frac{d[CH_4]}{dt} = [CH_4]^{.7}[O_2]^{.8}10^A e^{-E/RT}$$

50 POINT

E = 48.4 kcal/mole, σE = 1.20

A = 13.2, σA = 0.20

y-axis: LOG_{10} (RATE CONSTANT) ~ (mole cm^{-3})$^{-.5}$ sec^{-1}

x-axis: $\frac{1000}{T}$ ~ (K^{-1})

CHEMICAL ANALYSIS TECHNIQUE

FIGURE 6.8

METHANE/OXYGEN OVERALL
REACTION RATE

EFFECT OF SURFACE ON METHANE
OXIDATION RATE

DATA CORRELATED AS

$$-\frac{d[CH_4]}{dt} = [CH_4]^{.7}[O_2]^{.8}10^A e^{-E/RT}$$

LEAST SQUARE FIT
10 cm DUCT DATA

METHANE/AIR REACTION DATA

5 cm REACTOR DUCT
INITIAL FUEL ~ 0.5 MOLE PERCENT

LOG_{10} (RATE CONSTANT) ~ (mole cm^{-3})$^{-5}$ sec^{-1}

1000/T ~ (K)$^{-1}$

CHEMICAL ANALYSIS TECHNIQUE

FIGURE 6.9

JP 13 K 4233 71

6.2.2　Thermal Analysis Results

It was discussed earlier in the thesis that over the temperature range available in the flow reactor, the methane oxygen reaction does not generally meet the necessary assumptions for application of the thermal analysis technique. It should be recalled that the major difficulty was that the primary oxidation of methane to carbon monoxide and the ensuing oxidation of carbon monoxide occur simultaneously to an extent dependent on the reaction temperature, and this situation is further complicated by the induction period reaction. Essentially, this meant that no fixed stoichiometric relation of reactants going to products (Equation A-5) can be developed to fit the reaction, and it is evident from the chemical results displayed in Figures 6.1 and 6.2 that departure from a one-step reaction is most severe at lower reaction temperatures. If the methane oxidation was tentatively treated as a one-step reaction,

$$CH_4 + 2O_2 \longrightarrow CO_2 + 2 H_2O - 192 \frac{kcal}{mole}$$
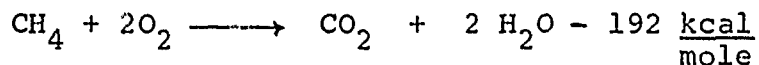
would be the necessary stoichiometric relation (Equation A-5). Reduction of thermal analysis data using this expression and correlation techniques similar to those used in the Section 6.1.2 resulted in the least square fitted data displayed in Figure 6 10. The determined overall reaction orders were the same as those found in the chemical analyses. However, the resulting overall temperature dependence was in wide disagreement, and the overall rate correlation produced average

METHANE-OXYGEN OVERALL
REACTION RATE
1200-1400 K
(10 cm dia. DUCT)

LEAST SQUARE FIT OF
CHEMICAL ANALYSIS DATA

$$\frac{-d[CH_4]}{dt} = [CH_4]^{0.7}[O_2]^{0.8} 10^{13.2} \exp\left(\frac{-48,400}{RT}\right)$$

LEAST SQUARE FIT

$$\frac{d[CH_4]}{dt} = [CH_4]^{.7}[O_2]^{.8} 10^A e^{-E/RT}$$

397 DATA POINTS
E = 62.5 kcal/mole , σE = 1.01
A = 15.3 , σA = .17

LOG_{10}(RATE CONSTANT) ~ (mole cm^{-3})$^{-.5}$ sec^{-1}

1000/T ~ (K)$^{-1}$

THERMAL ANALYSIS TECHNIQUE

FIGURE 6.10

JP 13   4157   63
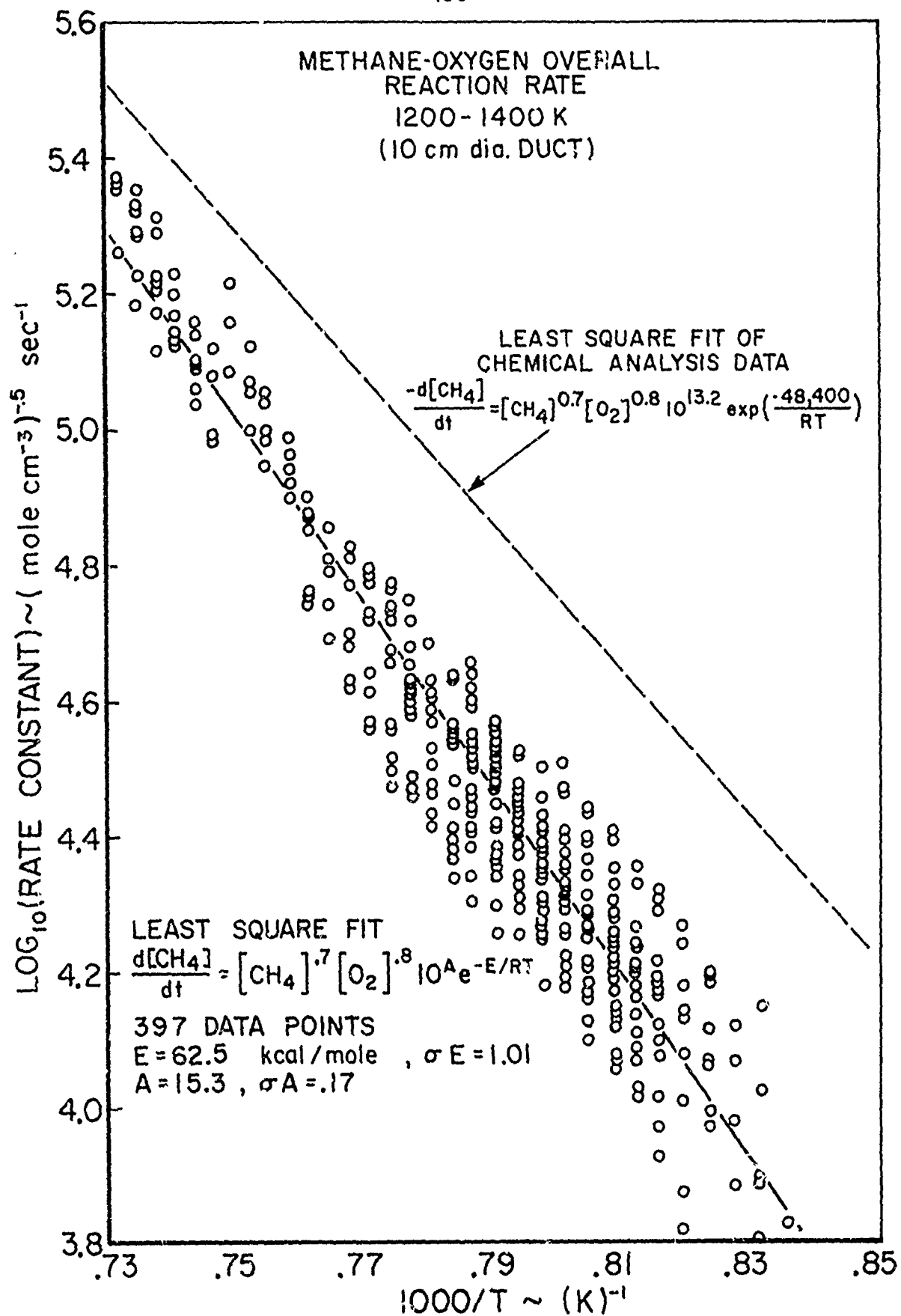
disappearance rates of methane which were significantly lower than those measured chemically. Thus, the crucial character of the one-step kinetic assumption is vividly pointed out.

However, it is interesting to note that above 1300K, chemically and thermally determined rates of disappearance of methane become comparable. This is undoubtedly due to the relative acceleration of the carbon monoxide oxidation as higher reaction temperatures are attained, i.e., the departure from a pseudo one-step oxidation reaction is becoming smaller. Thus, over some temperature range above 1300K, the post-induction phase methane oxidation is well approximated by one-step reaction kinetics, and this fact can greatly simplify application of chemical kinetics in practical design situations requiring one to calculate the rate of heat release.

6.2.3 Comparison with Other Work

Available correlated results of the methane disappearance rate, including that from this study, are presented in Table 6.3. To be noted first is that while the concentration dependences in the works of Van Tigglen, et.al. [137], Kozlov [23] and Németh and Sawyer [146] are in agreement among themselves, they are opposed to this work and that of Williams and Hottel [84]. In the light of earlier arguments concerning the induction phase kinetics of the methane oxidation, and their observed behavior in the present work, the contrast in orders may be attributed to the relative importance of induction phase and post induction phase kinetics

SUMMARY OF OVERALL RATE PARAMETERS FOR
DISAPPEARANCE RATE OF METHANE IN THE
OXIDATION REACTION OF METHANE

$$\frac{-d[CH_4]}{dt} = c[CH_4]^a [O_2]^b e^{-E/RT} \quad \text{moles cm}^{-3}\text{ sec}^{-1}$$

Investigator	Ref	Temp Range (K)	Technique	C	E kcal/mole	a	b	Press (atm)	Equiv-alence Ratio
Van Tigglen, et. al		1750-2000	Laminar Flame Burning Rate Measurements	-	38.	-.4	1.4	1.0	-
Kozlov[1]	23	1200-1350	Isothermal Laminar Flow Reactor	$\frac{7\times10^8}{T}$	60.	-.5	1.5	1.	Lean
Németh and Sawyer	14	1182-1282	Laminar Flow Reactor	6×10^{10}	59.	-.4	1.4	1.	Lean
Williams and Hottel[2]	84	1450-1750	Jet Stirred Reactor	5.3×10^{18}	57.	1.0	0.5	.3-.8	.5-.8
This Work	--	1100-1400	Turbulent Flow Reactor Chemical Sampling	1.6×10^{13}	48.4	0.7	0.8	1.	.05-0.6

NOTES:

(1) Kozlov's concentrations are expressed as mole fractions, not as mole cm^{-3}.
(2) also shows a dependence on [H$_2$O] of [H$_2$O]$^{\frac{1}{2}}$

TABLE 6.3

in each of the experimental studies. Where induction phase
kinetics played a dominant role in the experimental observa-
tions, the methane disappearance rate was found to be inhibited
by the presence of methane; where the post-induction phase
kinetics were dominant, methane was observed to accelerate
the methane disappearance rate. Indeed, the changing methane
reaction order observed by Kozlov [23] (0.65 at 973K, 0.0 at
1073K, -0.5 at 1223K, -0.5 at 1350K) is most likely a result
of an increasing dominance of the induction phase kinetics in
the observations as the reaction temperature was increased.

Kozlov [23] derived the overall methane reaction
orders from observations of the total methane-air reaction time,
τ_R , at isothermal temperature. τ_R is merely the sum of the
induction time, τ_{iND}, and the exothermic reaction time, τ_{ox} ,

$$\tau_R = \tau_{iND} + \tau_{ox}$$

But τ_i and τ_{ox} are inversely proportional to the average
rates of methane disappearance in the induction and post-
induction phase of the reaction. Therefore,

$$\tau_R = \frac{CONSTANT}{\left.\frac{d[CH_4]}{dt}\right|_{iND}} + \frac{CONSTANT}{\left.\frac{d[CH_4]}{dt}\right|_{ox}}$$

But, this study concludes

$$\left.\frac{d[CH_4]}{dt}\right|_{ox} = \mathcal{K}_{ox} [CH_4]^{0.7} e^{-E_{ox}/RT}$$

while Seery and Bowman [142] determined

$$\left.\frac{d[CH_4]}{dt}\right|_{iND} = \mathcal{K}_{iND} [CH_4]^{-0.5} e^{-E_{iND}/RT}$$

Thus, $\tau_{\lambda} = \mathcal{K}_i \left[CH_4\right]^{0.5} e^{+E_{iND}/RT} + \mathcal{K}_{ox} \left[CH_4\right]^{-0.7} e^{+E_{ox}/RT}$

$E_{iND} \gtrsim E_{ox}$, $\mathcal{K}_{iND} > \mathcal{K}_{ox}$. 6.4

At sufficiently low temperatures, the first term on the right side of Equation 6.4 would dominate, and the apparent overall methane reaction order would appear to be near 0.5. As the overall methane order was evaluated at higher isothermal temperatures, the second term would become more important, and over some range of temperature it is possible that the apparent overall methane reaction order would vary from near 0.5 to -0.7, similar to the observations of Kozlov [23].

Alternatively, the observations of Williams and Hottel [84] may have been primarily of the post-induction kinetics, the induction period effects being minimized by the fluid mechanical mixing of their jet stirred reactor. However, agreement with this interpretation may be somewhat fortuitous. Upon assumption that

$$CH_4 + OH \longrightarrow CH_3 + H_2O \qquad (17)$$
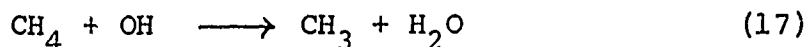
Was the primary mechanism for disappearance of methane and the supposed similarity of this kinetic situation to that of the carbon monoxide oxidation (see Chapter 5), Williams and Hottel [84] forced their experimental observations to fit the correlation expression

$$\frac{-d[CH_4]}{dt} = k_{ov} [CH_4]^{1.0} [H_2O]^{b} [O_2]^{c} .$$

i.e., the methane disappearance rate was forced to be first order in CH₄ and to depend on water. In the present work,

attempts to include a concentration dependence on water failed to yield correlations which were reasonable. Data were significantly scattered and apparent overall activation energies were unreasonably large (> 100 kcal mole). In light of these results, several methane/air experiments in which water was added to the initial reactant mixture were conducted. Figure 6.11 shows that the correlated methane disappearance rate in these experiments was independent of two orders of magnitude variation in initial water concentration. Thus, it was conclusively established that the overall rate of disappearance of methane is independent of the water concentration, and that the correlation expression and reaction orders assumed by Williams and Hottel [84] are incorrect. Thus, either [OH] is not governed by a mechanism similar to that in the $CO(H_2O)/O_2$ reaction, or reactions other than (17f) are important in determining the overall rate of disappearance of methane. The relevance of reaction (17f) to this disappearance rate will be discussed in a more detailed manner later.

6.3   Appearance Rate of Carbon Dioxide

It was shown in Chapter 5 that the oxidation of carbon monoxide proceeds primarily through the elementary reaction

$$CO + OH \longrightarrow CO_2 + H \tag{1}$$
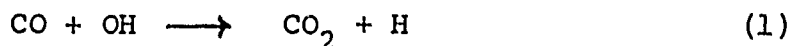
Thus, the formation rate of CO_2 and disappearance rate of CO were synonomous parameters. This conclusion is equally true in the high temperature oxidations of hydrocarbons. Also,

METHANE/OXYGEN OVERALL
REACTION RATE

EFFECT OF WATER ON METHANE
OXIDATION RATE

LEAST SQUARE FIT
OF 10 cm DUCT DATA

DATA CORRELATED AS

$$-\frac{d[CH_4]}{dt} = [CH_4]^{.7}[O_2]^{.8} \, 10^A e^{-E/RT}$$

O METHANE/AIR REACTION DATA

WATER ADDITION (10 cm DUCT DATA)
2-3 MOLE PERCENT
INITIAL FUEL ~ .5 MOLE PERCENT

LOG_{10} (RATE CONSTANT) ~ (mole cm^{-3})$^{-.5}$ sec^{-1}

1000/T ~ (K)$^{-1}$

CHEMICAL ANALYSIS TECHNIQUE

FIGURE 6.11
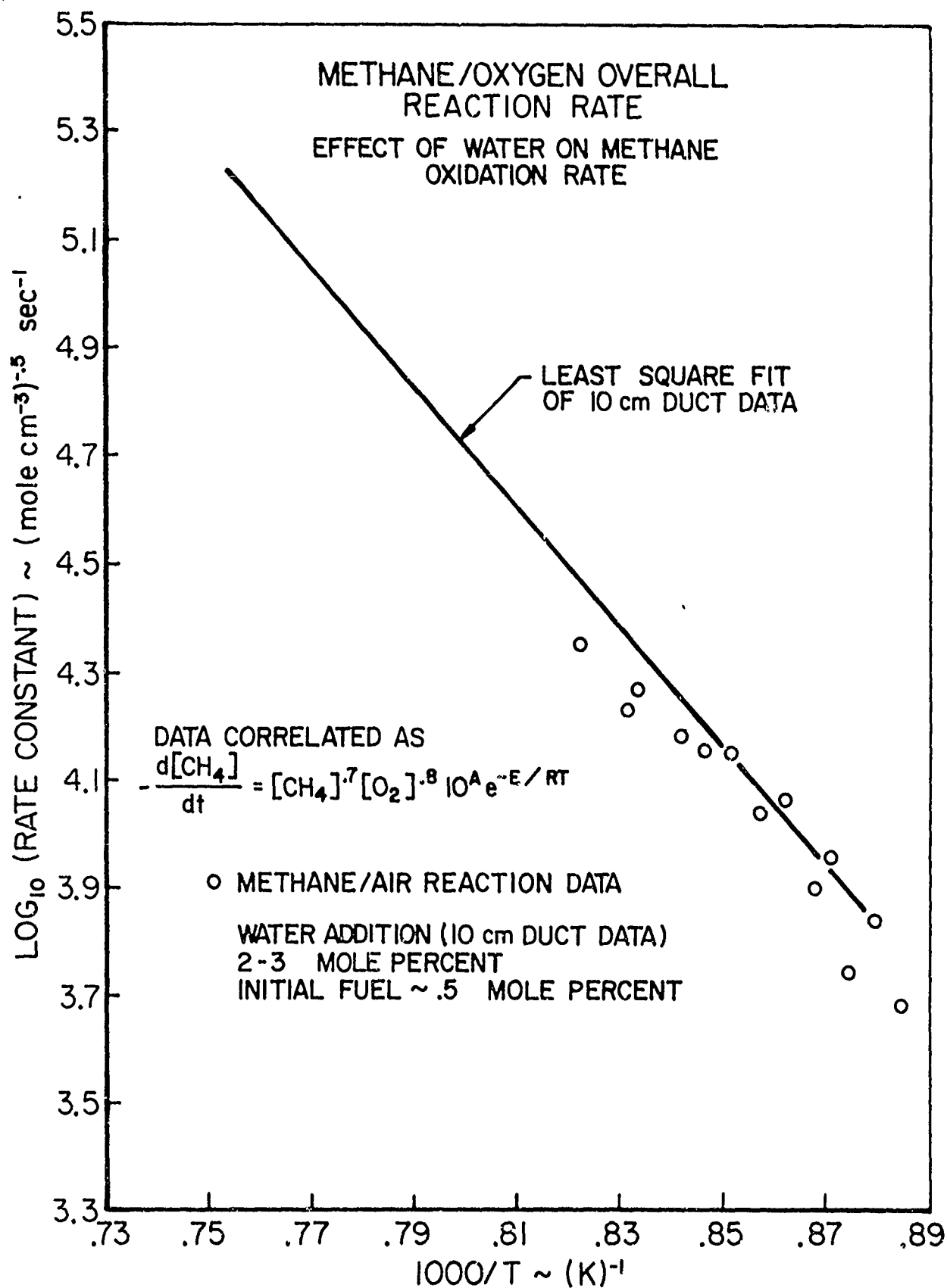
since reaction (1r) is not of importance (except near equilibrium), the net formation rate of CO_2 in the oxidation and the rate obtained from reaction (1f) should be the same, and thus,

$$\frac{d[CO_2]}{dt} = -\frac{d[CO]}{dt} = k_{1_f} [CO] [OH].$$

An overall rate correlation of $d[CO_2]/dt$ will depend on how [OH] responds to the concentrations of other species and temperature.

The rate of formation of CO_2 in the methane oxidation can be compared with that in the $CO(H_2O)/O_2$ reaction (Equation 5.5) by least square fitting the reaction data to the relation

$$\frac{d[CO_2]}{dt} = 10^A e^{\frac{-E}{RT}} [CO]^{1.0} [H_2O]^{0.5} [O_2]^{0.25} \qquad (5.5)$$

and comparing the resulting values of A and E (i.e., k_{ov}). This correlation of the CO_2 production rate data in the methane/oxygen reaction is presented in Figure 6.12, and the linear least square fit expression was found to be

$$\frac{d[CO_2]}{dt} = 10^{14.8 \pm .4} \exp\left(\frac{-42,900 \pm 2,250}{RT}\right) [CO]^{1.0} [H_2O]^{0.5} [O_2]^{0.25}$$

$$\text{mole cm}^{-3} \text{ sec}^{-1} \qquad (6.6)$$

While the reaction orders were not empirically determined. the small standard deviations of the values of A and E demonstrate that the concentration dependencies of Equation 6.5 fit the data rather well. However, Figure 6.13 shows that the average rate of CO_2 production and thus the calculated overall rate constant is some 3.5 times smaller in the methane

METHANE/OXYGEN OVERALL
REACTION STUDY
CARBON DIOXIDE PRODUCTION RATE
(1100K-1400K)

LEAST SQUARE FIT

$$\frac{d[CO_2]}{dt} = [CO][H_2O]^{.5}[O_2]^{.25}10^A e^{-E/RT}$$

62 POINTS

E = 42.9 kcal/mole , σE = 2.26

A = 14.76 , σA = 0.40

LOG$_{10}$ (RATE CONSTANT) ~ (mole cm^{-3})$^{-.5}$ sec^{-1}

1000/T ~ (K)$^{-1}$

CHEMICAL ANALYSIS TECHNIQUE

FIGURE 6.12

METHANE/OXYGEN - CARBON MONOXIDE/OXYGEN
REACTION STUDIES
COMPARISON OF CARBON DIOXIDE
PRODUCTION RATE

MOIST CARBON MONOXIDE/
OXYGEN REACTION
(EQUATION 5.5)

METHANE/OXYGEN
REACTION
(EQUATION 6.8)

DATA CORRELATED AS

$$\frac{d[CO_2]}{dt} = [CO][H_2O]^{.5}[O_2]^{.25}10^A e^{-E/RT}$$

REACTION	E kcal/mole	A	σE	σA
CH_4/O_2	42.90	14.76	2.26	0.40
CO/O_2	39.95	14.59	1.25	0.25

LOG_{10} (RATE CONSTANT) ~ (mole cm^{-3})$^{.5}$ sec^{-1}

1000/T ~ $(K)^{-1}$

CHEMICAL ANALYSIS TECHNIQUE

FIGURE 6.13

oxidation than in the $CO(H_2O)/O_2$ reaction. This same experimental phenomena was noted in the stirred reactor study of Williams and Hottel [84].

If the assumption that reaction (1f) accounts for the net rate of production of CO_2 in both reaction studies is correct, this decrease in rate must be attributed to lower available concentrations of [OH] in the methane oxidation.

This lower average concentration of [OH] must somehow be related to the presence of methane or its intermediary oxidation products. But Equation 6.5, the formula used to correlate the CO_2 production rate, contained no such concentration dependences. However, the neglected dependences must be small since the scatter in this correlation is not very large (see Figure 6.12).

This point is further substantiated by the results of a methane-sensitized $CO(H_2O)/air$ reaction. Small amounts of methane were added to a carbon monoxide reaction which contained large amounts of CO, H_2O and O_2. The CO_2 production rate data were correlated by expression 6.5, and the results are presented in Figure 6.14. The numbers in parentheses are the measured concentration of CH_4 at each data point.

It was observed that, as the methane disappeared, the CO_2 production rate increased from the average value found in the methane oxygen reaction (expressed by Equation 6.5) to that found in the $CO(H_2O)/O_2$ (Equation 5.5) reaction.

METHANE/OXYGEN OVERALL
REACTION STUDY
CARBON DIOXIDE PRODUCTION
CARBON MONOXIDE/METHANE/WATER/AIR REACTION

DATA CORRELATED

$$\frac{d[CO_2]}{dt} = [CO][H_2O]^{.5}[O_2]^{.25}10^A e^{-E/RT}$$

(0.0)

(0.5)

MOIST CARBON MONOXIDE
OXYGEN REACTION
(EQUATION 5.5)

(2.5)

(7.0)

(14)

FIGURES IN PARENTHESES
ARE ($X_{CH_4} \cdot 10^5$)

(24)

METHANE/OXYGEN
REACTION
(EQUATION 6.6)

(35)

(48)

INITIAL FUEL ~ (90% CO/10% CH$_4$)–
1.6 MOLE PERCENT

INITIAL WATER ~ 2.4 MOLE PERCENT

(60)
(72)
(84)
(95)

LOG_{10} (RATE CONSTANT) ~ (mole cm^{-3})$^{-.5}$ sec^{-1}

1000/T ~ (K)$^{-1}$
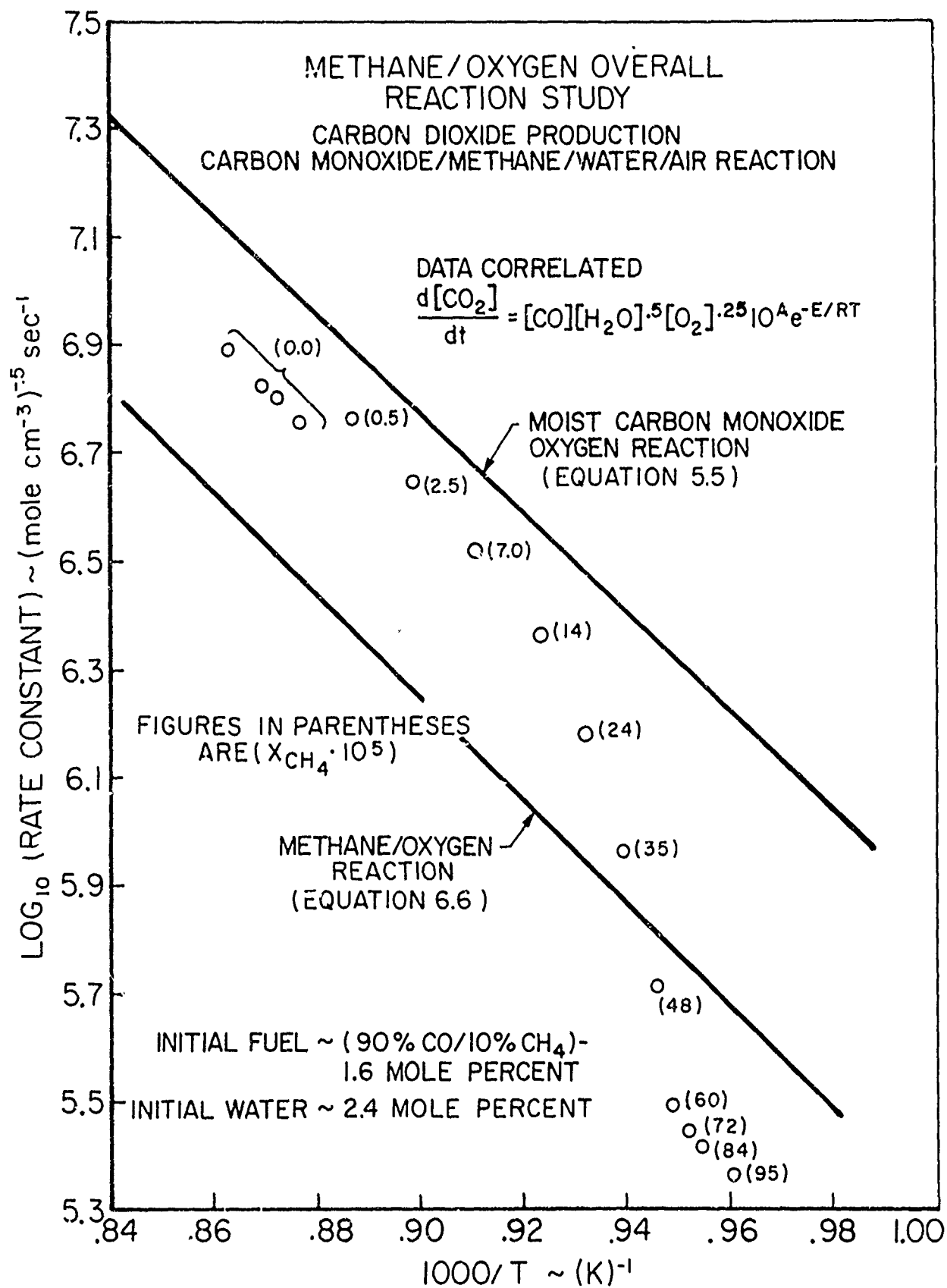
CHEMICAL ANALYSIS TECHNIQUE

FIGURE 6.14

That is, for a change of methane concentration over two
orders of magnitude, the rate of CO_2 production changed by
a factor of 3.5. In fact, above a ratio of $[CH_4]/[CO]$
.10, the CO_2 production rate remained depressed at the
average rate found in the methane-oxygen reaction study
and was independent of CH_4 concentration. Also, addition
of carbon monoxide to reacting CH_4/O_2 mixtures, while re-
ducing the induction time of the methane reaction, did not
change $\frac{d[CO_2]}{dt}$ from the expression found in the methane
oxidation alone.

Another interesting observation in this methane-
sensitized $CO(H_2O)/$ air reaction was that the rate of disap-
pearance of methane was considerably faster than that ob-
served in the methane/oxygen reaction experiments.
Figure 6.15 shows the methane disappearance rate correlated
for comparison with that in the CH_4/O_2 reaction (Equation
6.3). The observed difference in rate is approximately a
factor of 6.3, while the observed temperature dependence of
the rate is essentially unchanged. These results will be
own to be of importance in arguments concerning the oxida-
tion mechanism of CH_4 to be presented in the next section.

6.4   Mechanism of Methane Oxidation

The principal feature, as far as chemical kinetic
experiments are concerned, is the relation of experimental
observations to an elementary reaction mechanism. In this
respect, the methane-oxygen reaction has been thought to

METHANE/OXYGEN OVERALL
REACTION STUDY

METHANE OXIDATION RATE
CARBON MONOXIDE/METHANE/WATER/AIR REACTION

o METHANE/AIR REACTION DATA
IN CARBON MONOXIDE

INITIAL FUEL 90% CO/10% CH$_4$
1.6 MOLE PERCENT

LEAST SQUARE FIT
OF 10 cm DUCT DATA
(EQUATION 6.3)

DATA CORRELATED AS

$$-\frac{d[CH_4]}{dt} = [CH_4]^{.7}[O_2]^{.8} 10^A e^{E/RT}$$

$1000/T \sim (K)^{-1}$
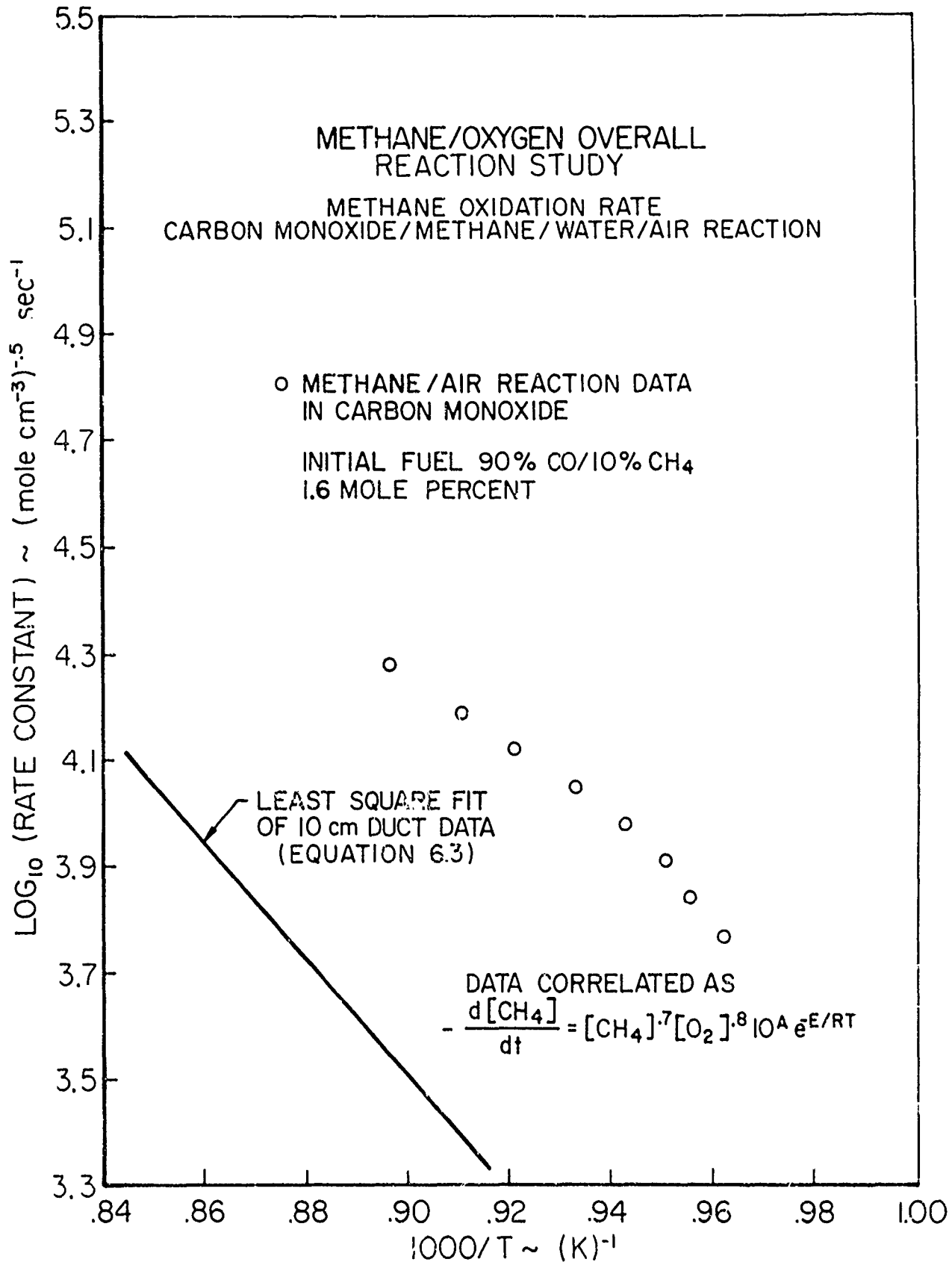
CHEMICAL ANALYSIS TECHNIQUE

FIGURE 6.15

exhibit two distinct regimes of chemical reaction, so different in character, that two basic reaction mechanisms have been proposed to describe them.

At low temperature (< 800K), the methane oxidation has been observed to be effected by surface material, extent, and condition (Egerton, et. al. [151], Hoare and Walsh [152]). Major products formed were carbon monoxide, water, and, depending on the temperature, some carbon dioxide. Intermediary products of formaldehyde, hydrogen peroxide, and methanol were formed, and their concentration relative to each other and to methane were observed to be dependent on surface activity.

Experiments including those of Burgoyne and Hirsch [21], Hoare and Walsh [153] and more recently Couze, et. al. [154] have shown drastic changes in the reaction character as the temperature increased from 700K to 900K and above. Intermediary formaldehyde and hydrogen peroxide reach maximum concentrations relative to methane near 800K (Meriaux, et. al. [155]), and surface material and activity become less important. These changes were observed to be accompanied by varying concentration and temperature dependences of the overall disappearance rate of methane.

Shtern [156] has summarized and discussed the "low temperature" experimental results and the mechanisms proposed to explain them. More recently, Franklin [157] has summarized the low temperature mechanism as:

$$CH_4 + O_2 \longrightarrow CH_3 + HO_2 \qquad (18)$$

$$M + CH_3 + O_2 \longrightarrow CH_3O_2^* + M \qquad (19)$$

$$CH_3O_2^* \longrightarrow H_2CO + H \qquad (20)$$

$$CH_3O_2^* + CH_4 \longrightarrow CH_3 + CH_3OOH \qquad (21)$$

$$CH_3OOH \longrightarrow CH_3O + OH \qquad (22)$$

$$CH_3O + CH_4 \longrightarrow CH_3OH + CH_3 \qquad (23)$$

$$CH_4 + OH \longrightarrow CH_3 + H_2O \qquad (17)$$

$$R + CH_3O \longrightarrow CH_2O + RH \qquad (24)$$

$$O_2 + CH_2O \longrightarrow HCO + HO_2 \qquad (25)$$

$$HCO + O_2 \longrightarrow HO_2 + CO \qquad (26)$$

$$HCO + OH \longrightarrow CO + H_2O \qquad (27)$$

$$HO_2 + CH_4 \longrightarrow H_2O_2 + CH_3 \qquad (28)$$

$$HO_2 + CH_2O \longrightarrow H_2O_2 + CHO \qquad (29)$$

$$HO_2, \; HCO \; \text{etc.} \longrightarrow \text{wall} \qquad (30)$$
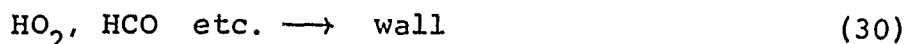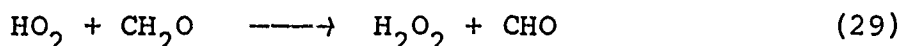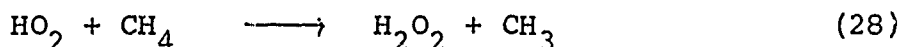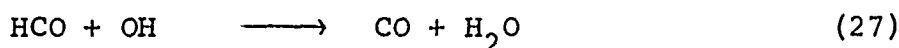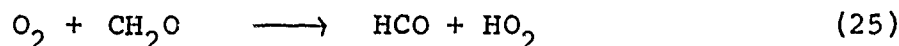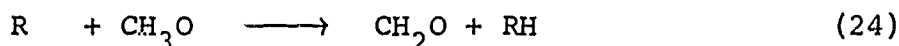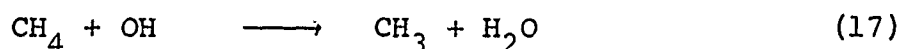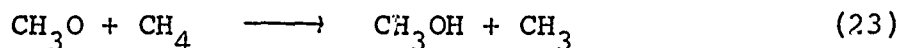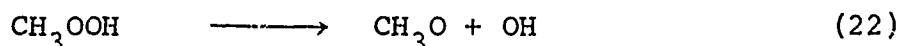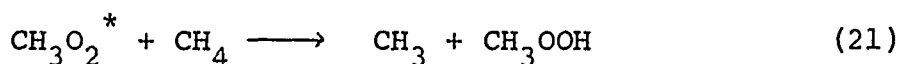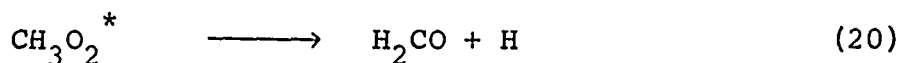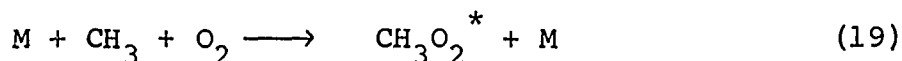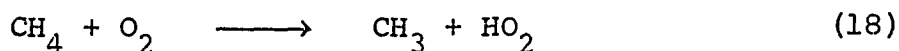
This is in general agreement with the mechanisms proposed by Semonov [158], Enikolopyan [159] and Minkoff and Tipper [160], except that Semonov [158] and others also consider the reaction

$$CH_2O + OH \longrightarrow HCO + H_2O \qquad (31)$$
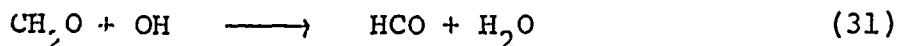
to be important.

The work of Westenberg and Fristrom [2,30] has been most influential in determining the presently accepted description of the "high temperature" reaction. The computer modeled mechanisms of Chintz [161], Seery and Bowman [142], Higgin and Williams [143] and Bowman [143] have all drawn from this work.

The work of Bowman [148] represents the most recent and extensively tested model and his proposed mechanism is as follows:

$$CH_4 + M \rightleftharpoons CH_3 + H + M \qquad (32)$$

$$CH_4 + OH \Longrightarrow CH_3 + H_2O \qquad (17)$$

$$CH_4 + O \rightleftharpoons CH_3 + OH \qquad (33)$$

$$CH_4 + H \rightleftharpoons CH_3 + H_2 \qquad (34)$$

$$CH_3 + O_2 \rightleftharpoons HCO + H_2O \qquad (35)$$

$$HCO + OH \rightleftharpoons CO + H_2O \qquad (27)$$

$$HCO + M \rightleftharpoons H + CO + M \qquad (36)$$

$$CO + OH \rightleftharpoons CO_2 + H \qquad (1)$$

$$H + O_2 \rightleftharpoons O + OH \qquad (9)$$

$$O + H_2 \rightleftharpoons H + OH \qquad (10)$$

$$O + H_2O \rightleftharpoons OH + OH \qquad (13)$$

$$H + H_2O \rightleftharpoons H_2 + OH \qquad (11)$$

$$H + OH + M \rightleftharpoons H_2O + M \qquad (12)$$

$$CH_3 + O \rightleftharpoons HCO + H_2 \qquad (37)$$
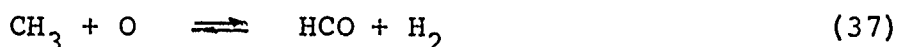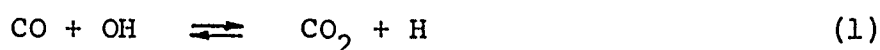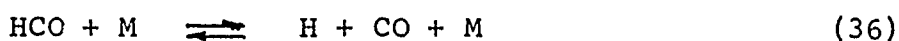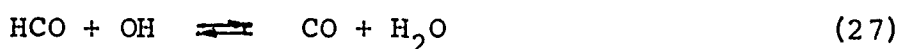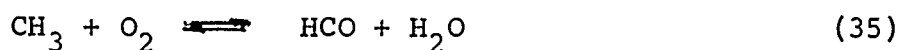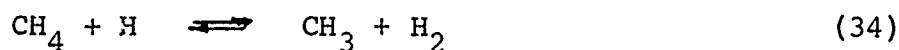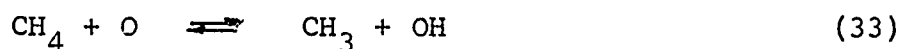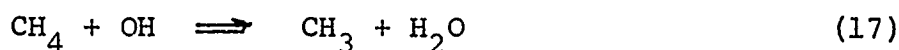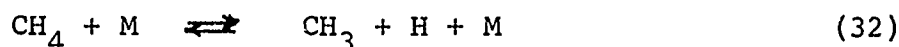
As clearly stated by Bowman [148], while all of the reactions included in this mechanism were essential for description of his experimental results, the mechanism may be incomplete and non-unique.

To be noted immediately is the absence of reactions involving HO_2 or, if you will, the complete dominance of the $H_2 - O_2$ chain carrying and branching reactions. Fristrom and Westenberg [30] eliminated HO_2 from the mechanism for low-pressure methane-oxygen flames by proposing

$$CH_4 + O_2 \longrightarrow CH_3 + HO_2 + 55 \text{ kcal} \qquad (18)$$
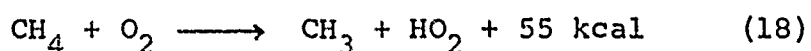
to be the principal source of $[HO_2]$. This reaction was shown to be too slow to account for even a minor portion of the observed methane disappearance rate. However, at the higher pressures of this work and those normally employed in combustion processes, the reaction

$$H + O_2 + M \longrightarrow HO_2 + M \qquad (14)$$
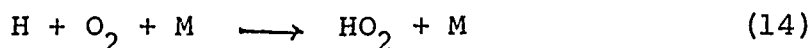
occurs at a rate of comparable magnitude with the $H_2 - O_2$ branching reaction

$$H + O_2 \longrightarrow OH + O \qquad (9)$$

at least to 1100K.[*] Thus, in these works, it would appear that the role of HO_2 cannot be eliminated by claiming insufficient sources of $[HO_2]$.

Furthermore, it is interesting to note that no formation or destruction reactions of CH_2O explicitly appear in the "high temperature" mechanism of Bowman [148]. Seery and Bowman [142] claim that the reaction

$$CH_2O + OH \longrightarrow HCO + H_2O \qquad (31)$$
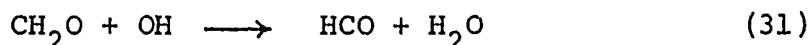
is so fast above 1400K, that CH_2O is extremely short lived, and any reaction forming CH_2O, in effect, forms HCO and H_2O.

6.4.1 Relevance of Low and High Temperature Mechanisms to This Work

It is clear that some compromise of the low and high temperature mechanisms must be pertinent to the methane-oxygen reaction at the temperatures and pressures of interest in this work and in common combustion processes.

---

[*] see Figure 6.21.

As indicated in the previous paragraphs, under
these conditions, the role of HO_2 in the reaction may be of
some significance. This conclusion is supported by the de-
tected presence of H_2O_2 in this work and that of Pratt [22].
The results of Chapter 5 suggested

$$CO + HO_2 \longrightarrow CO_2 + OH - 63 \text{ kcal} \tag{4}$$
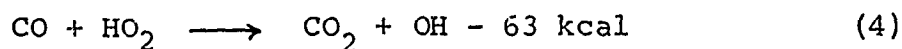
to be too slow relative to reaction (1f) to be important.
However, $[HO_2]$ may be of some consequence to the methane and
formaldehyde disappearance rates through

$$CH_4 + HO_2 \longrightarrow CH_3 + H_2O_2 + 12.3 \text{ kcal} \tag{28}$$
$$CH_2O + HO_2 \longrightarrow HCO + H_2O_2 - 12.7 \text{ kcal} \tag{29}$$
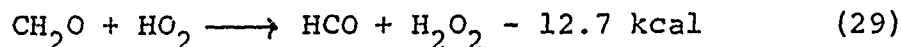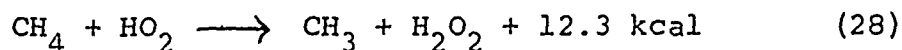
In view of the endothermicity of reaction (28f), it is not
likely to be rapid in comparison to reactions (17f), (33f)
and (34f). Thus, the most important role of HO_2 may be
reaction (29f) and changes in the rate of chain branching in
the mechanism from competition of reactions (14f) and (9f).
However, it should be emphasized again that reaction (14f)
is not a chain terminating reaction since reactions (6) - (8)
should be rapid at these high temperatures.

Secondly, the detected presence of CH_2O necessitates
the inclusion of reaction (31) and some mechanism for CH_2O
formation. While it is clear that CH_2O must be a product of
oxidation of CH_3 radicals, the experimental evidence of
Baldwin, et. al. [162,163] indicates that it does not result
directly from the bimolecular reaction

$$CH_3 + O_2 \longrightarrow H_2CO + OH$$
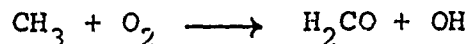
as proposed by some earlier works (Minkoff and Tipper [160], Hoare [164]). Baldwin, et. al. [162,163] suggest the reaction proceeds through

$$CH_3 + O_2 + M \longrightarrow CH_3O_2 + M \qquad (33)$$
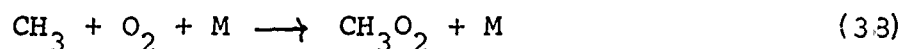
with much of the CH_3O_2 decomposing back into CH_3 and O_2. The remaining fraction of CH_3O_2 oxidizes with some other specie (or decomposes) to form CH_2O

$$CH_3O_2 \longrightarrow CH_2O.$$
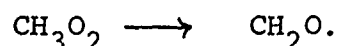
Thus, since the oxidation of CH_3 radicals is such a difficult process, Baldwin, et. al. [162,163] suggest that methyl radicals may recombine

$$CH_3 + CH_3 \longrightarrow C_2H_6. \qquad (39)$$

and a significant fraction may ultimately be destroyed by an oxidation route through C_2H_6. The present experimental results support this contention (C_2H_6 and C_2H_4 were detected species), and thus the reactions

$$C_2H_6 + H \longrightarrow C_2H_5 + H_2 \qquad (40)$$
$$C_2H_6 + OH \longrightarrow C_2H_5 + H_2O \qquad (41)$$
$$C_2H_6 + O \longrightarrow C_2H_5 + OH \qquad (42)$$
$$C_2H_5 \longrightarrow C_2H_4 \longrightarrow CO$$
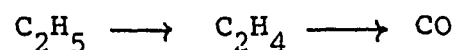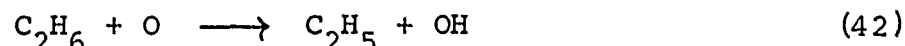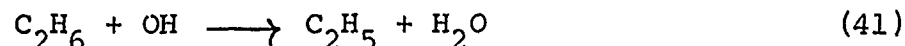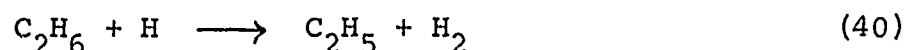
must also be considered. However, none of the arguments of Baldwin, et. al. [162,163] rule out the possibility of

$$CH_3 + O \longrightarrow H_2CO + H - 67 \text{ kcal} \qquad (37)$$
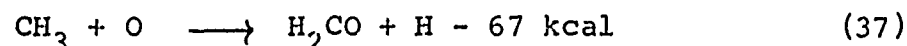
suggested by Fenimore and Jones [1] and included in the "high" temperature mechanism of Bowman [148].

Thus it is clear that the complete reaction mechanism for the methane oxidation near 1000K and atmospheric pressure is most complex and, at present, remains ambiguous. However, with the aid of the present experimental results and those of other workers, several important conclusions can be drawn concerning the reactions important to the methane disappearance rate.

6.4.2 Some Observations on the Disappearance Mechanism of Methane

The discussions in the preceding paragraphs have suggested the reactions

$$CH_4 + OH \longrightarrow CH_3 + H_2O \qquad (17)$$

$$CH_4 + HO_2 \longrightarrow CH_3 + H_2O_2 \qquad (28)$$

$$CH_4 + M \longrightarrow CH_3 + H + M \qquad (32)$$

$$CH_4 + O \longrightarrow CH_3 + OH \qquad (33)$$

$$CH_4 + H \longrightarrow CH_3 + H_2 \qquad (34)$$
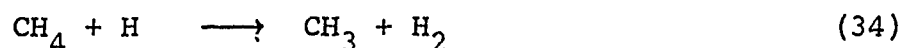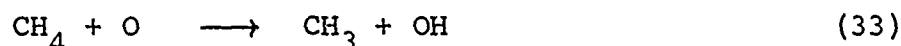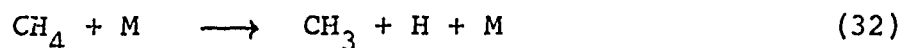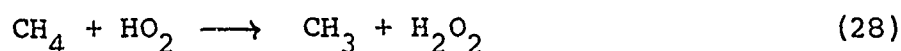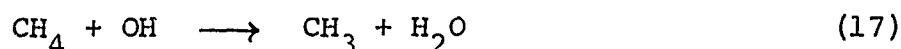
compose the most general mechanism for the depletion of methane in the presence of oxygen near 1000K. However, many studies, including those of Pratt [22], Williams and Hottel [84], Hoare [169], and Fristrom, et. al. [30,166] have suggested [OH] to be the primary reactant with methane in oxygen rich environments [reaction (17f)]. In view of a large excess of oxygen, it was argued that hydrogen atom concentration was very low in comparison with [OH] and [O] because of the rapidity of reactions (9f) and (14f). Furthermore, the works of Fenimore and Jones [1] and Wong and Potter [165] suggested that, even at flame temperatures,

reaction (33f) was considerably slower than (17f). Thus, reaction (17f) remained as the primary mechanism by which methane disappeared.[*] This assumption, in combination with experimental measurements of the methane concentration and disappearance rate in high temperature reactions, has been repeatedly used to evaluate the specific rate constant for reaction (17f). Interpretation of these results necessarily involved determination of the hydroxyl radical concentration, and a majority of studies have used the rate of conversion of CO to CO_2 simultaneously occurring in the reacting environment for this purpose. Assuming reaction (1f) to be the primary mechanism through which CO_2 was formed,

$$[OH] = \frac{1}{k_{1f}[CO]} \frac{d[CO_2]}{dt} . \qquad 6.7$$

Thus, providing all of the above assumptions were correct, the simply determined experimental measurements of the function

$$\delta^{\ell} \equiv \frac{d[CH_4]}{dt} \cdot \frac{1}{[CH_4]} \quad [CO] \quad \frac{1}{\frac{d[CO_2]}{dt}} \qquad 6.8$$

---

[*]Reactions (28f) and (32f) were not considered in the above works. It is clear that reaction (32f), with a specific rate constant given by

$$k_{32f} = 1 \times 10^{18} e^{\frac{-88,000}{RT}} \quad cm^3 \, mole^{-1} \, sec^{-1}$$

will be very slow in comparison to molecule-radical reactions. Furthermore, it may be argued that the large endothermicity of reaction (28f), 12.4 kcal, would suggest that this reaction is also slow.

would represent the ratio of the specific rate constants for reactions (17f) and (1f), i.e.,

$$\gamma^{\ell} = \frac{k_{17f}}{k_{1f}} = \gamma^{\ell} \text{ (T) only} \qquad 6.9$$

However, the studies of Wilson and Westenberg [115], and Dixon-Lewis and Williams [3] concluded that this technique must be applied with some reservations. Both of these works combined experimental measurements of the func-tion, γ^{ℓ}, with independent measurements of k_{17f} and k_{1f}, at room temperature,[*] to determine the temperature dependence of the ratio of k_{17f}/k_{1f}. The experimental data presented in these studies is summarized in Figure 6.16. It is clear that the measurements of γ^{ℓ} are not collectively well represented by the interpretation

$$\gamma^{\ell} = \frac{k_{17f}}{k_{1f}} = \frac{C_{17f}}{C_{1f}} e^{\frac{-E_{17f} + E_{1f}}{RT}} \qquad 6.10$$

Recognizing this fact, Wilson and Westenberg [115] and Dixon-Lewis and Williams [3] proceeded to discard measurements of γ^{ℓ} by Pratt [22], Hoare [169] and Blundell [170]. Reaction (4f)

$$CO + HO_2 \longrightarrow CO_2 + OH \qquad (4)$$
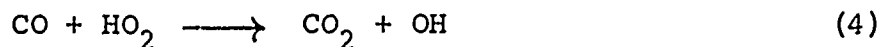
was assumed to contribute significantly to the formation of CO_2 in these studies, and thus Equation 6.7 was concluded to be an incorrect method for determining [OH]. The remaining

---

[*]Wilson [96] has concluded that the experimental techniques employed in obtaining these measurements permitted the results to be most precise.

FRISTROM , [166]
FENIMORE AND JONES [1]
WILSON , et.al., [167]
DIXON – LEWIS, et. al., [114,3]
BALDWIN, et. al., [168]
HOARE [169]
BLUNDELL [170]
PRATT [22]
WILSON , et. al., [115][1]
GREINER [171][1]

WILSON & WESTENBERG [115],
EVALUATION, 1967
DIXON – LEWIS & WILLIAMS [3],
EVALUATION, 1967

$CH_4 + OH \xrightarrow{k_{17f}} CH_3 + H_2O$

$CO + OH \xrightarrow{k_{1f}} CO + OH$

$\gamma \equiv \dfrac{d[CH_4]}{dt} \cdot \dfrac{1}{[CH_4]} \cdot [CO] \cdot \dfrac{1}{\dfrac{d[CO_2]}{dt}}$

1. FROM INDEPENDENT, ABSOLUTE MEASUREMENTS
OF k_{17f} AND k_{1f}

AVAILABLE EXPERIMENTAL MEASUREMENTS
OF γ AND k_{17f}/k_{1f}

γ OR k_{17f}/k_{1f}

$1000/T \sim (K^{-1})$

FIGURE 6.16

experimental measurements were fit to Equation 6.10 to obtain

$$\frac{k_{17f}}{k_{1f}} \approx 85 \ e^{\frac{-4500}{RT}} \quad ,$$

and Wilson and Westenberg [115] employed the expression for k_{1f} obtained by Dixon-Lewis, et. al. [114][*] to evaluate k_{17f} as

$$k_{17f} = 2.9 \times 10^{13} \ e^{\frac{-5000}{RT}} \quad cm^3 \ mole^{-1} \ sec^{-1}$$

In response to these works, the primary importance of [OH] and reaction (17f) in oxygen-rich methane flames, the assumed contributions of reaction (4f) to the production of CO_2 at lower temperatures, and the suggested complications in the measurements of Pratt [22], Hoare [169] and Blundell [170] have gained wide and unchallenged acceptance (Drysdale and Lloyd [172], Wilson [96], 1970). However, the full significance of the recent measurements of k_{17f} by Greiner [173] has not been recognized. Using flash-photolysis-kinetic-spectroscopy techniques, Greiner [173] studied reaction (17f) over the temperature range 300-500K to obtain

$$k_{17f} = 3.32 \times 10^{12} \ e^{\frac{-3772}{RT}} \quad cm^3 \ mole^{-1} \ sec^{-1} \ .$$

It was evident that at flame temperatures this expression predicted values of k_{17f} nearly an order of magnitude smaller than those determined by Fristrom [166], Fenimore and Jones [1], Wilson, et. al. [167] and Dixon-Lewis, et. al. [3], and Wilson [96] concluded that this discrepancy could not be

_____

[*]shown to be erroneous, see Section 5.4.

attributed to experimental sources of error in flame studies
or in the work of Greiner [173]. Wilson [96] suggested that
either the reaction does not follow an Arrhenius temperature
dependence, or there are competing reactions which have not
been properly accounted for in the analyses. However, it
was concluded that no clear explanation of the disagreement
was available.

That similar discrepancies in measurements of k_{1f}
were adequately explained by absolute reaction rate theory
(see Chapter 5) suggested these methods might be useful in
the description of reaction (17f). No experimental data were
available to estimate the fundamental vibration frequencies
of the $CH_4OH^{\neq}$ activated complex; however a characteristic
frequency, non-linear model was developed using the proce-
dures discussed in Section 5.4, i.e.,

$$k_{17f} = C_{17f} \ Q_{17f}(T) \ \exp \frac{-Eo_{17f}}{RT}$$

$$Q_{17f}(T) = \frac{1}{T^{3/2}} \frac{Q_V^{\neq}(T)}{Q_V^{OH}(T) \ Q_V^{CO}(T)} \ .$$

The values of Eo_{17f} and C_{17f} were chosen such that the analytical
k_{17f} fit the experimental data of Greiner [173], and the results
are presented in Figure 6.17. Comparison with the experimental
data summarized in Figure 6.16 necessitated that an analytical
model also be chosen for k_{1f}. The results of Figure 6.17 were
combined with the HONO model of reaction (1f), $Eo_{1f} = 0$, (see
Figure 5.12) and the analytical ratio, k_{17f}/k_{1f}, was compared

$$k_{17_f} = \frac{C_{17_f}}{T^{3/2}} \ \frac{\left(1-e^{\frac{-1510}{T}}\right)\left(1-e^{\frac{-4320}{T}}\right)}{\left(1-e^{\frac{-5040}{T}}\right)\left(1-e^{\frac{-1940}{T}}\right)^2\left(1-e^{\frac{-1650}{T}}\right)^3} \ \exp\left(\frac{-E^0_{1f}}{RT}\right)$$

TEMPERATURE DEPENDENCE OF k_{17_f}
CHARACTERISTIC FREQUENCY MODEL, NONLINEAR COMPLEX
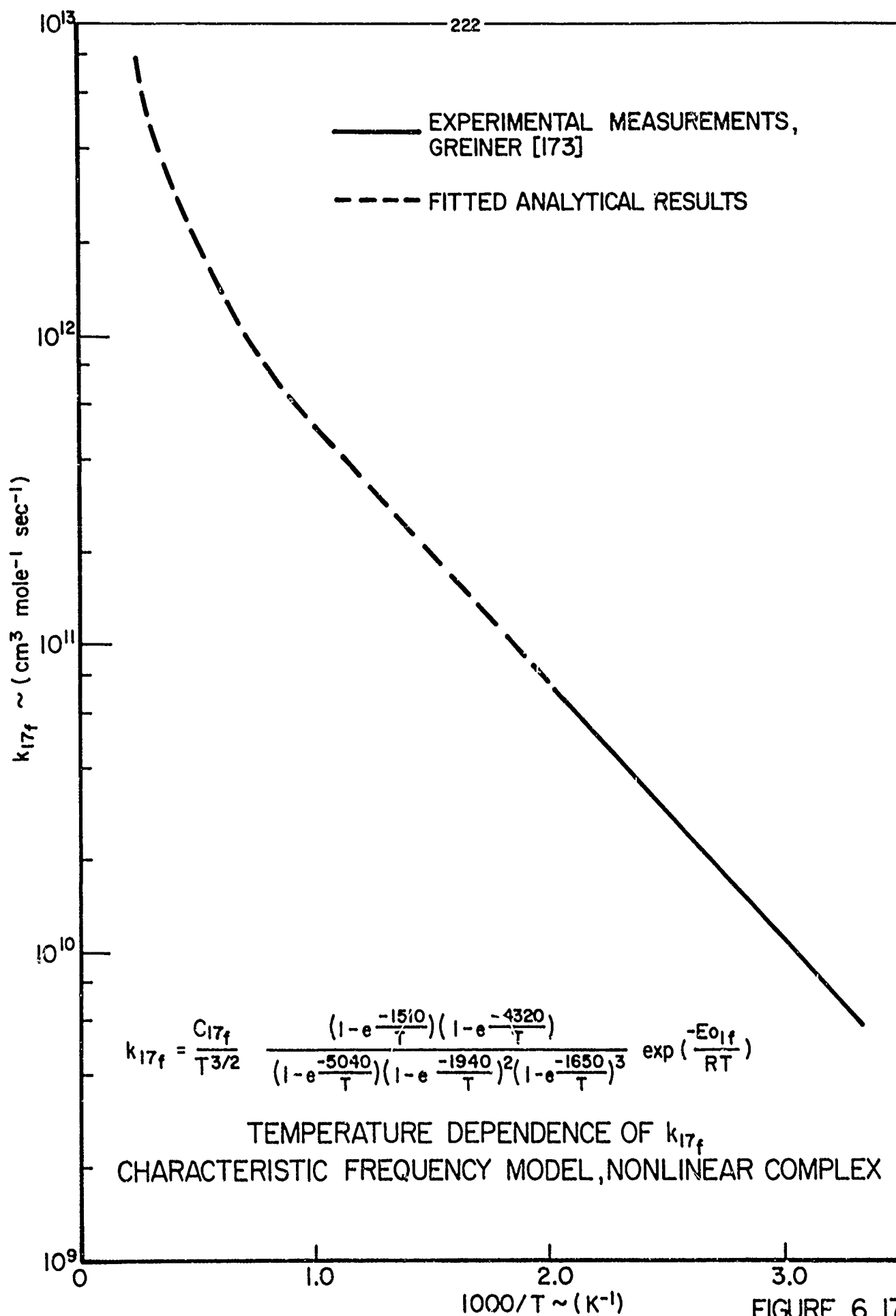
FIGURE 6.17

with the experimental results (see Figure 6.18). The developed model for the pre-exponential temperature dependence of k_{17f} could not explain the discrepancy between the data of Greiner [122,173] and flame temperature measurements of γ^ℓ. In fact, those data discarded by Wilson and Westenberg [115], Dixon-Lewis and Williams [3] and Drysdale and Lloyd [172] were in close agreement with both the analytical model and the low temperature results of Greiner [122,173]. Furthermore, experimental measurements of γ^ℓ in the present work (see Figure 6.19) conclusively indicated dependences on parameters other than temperature. These dependences could not be explained by supposed contributions of reaction (4f) to the formation of CO_2. It should be recalled that reaction (14f) is one of the primary sources of $[HO_2]$ in these experiments. Thus, if reaction (4f) was important, γ^ℓ should decrease with increasing concentrations of oxygen, and this conclusion is in direct opposition to experimental results displayed in Figure 6.19.

Thus it is suggested that reactions competing with (17f) may not have been properly accounted for in oxygen-rich flame studies. Investigation of this hypothesis required descriptions of k_{33f} and k_{34f} as functions of temperature. Fortunately, Herron [174] has critically evaluated k_{33f}, and Kurylo and Timmons [175] have recently used very precise experimental techniques to evaluate k_{34f}. These evaluations and those of k_{17f} (Greiner [173], Wilson and Westenberg [115], Drysdale and Lloyd [172]) are summarized in Figure 6.20.

TEMPERATURE DEPENDENCE OF k_{17f}/k_{1f}
USING CHARACTERISTIC FREQUENCY MODELS
FOR NONLINEAR ACTIVATED COMPLEXES

FIGURE 6.18

--- EXPERIMENTAL MEASUREMENTS GREINER [122,173]

—— ANALYTICAL MODEL

$CH_4 + OH \xrightarrow{k_{17f}} CH_3 + H_2O$

$CO + OH \xrightarrow{k_{1f}} CO + OH$

$\gamma \equiv \dfrac{d[CH_4]}{dt} \cdot \dfrac{1}{[CH_4]} \cdot [CO] \cdot \dfrac{1}{\dfrac{d[CO_2]}{dt}}$

SEE FIGURE 6.16 FOR SOURCES
OF EXPERIMENTAL DATA

Y OR k_{17f}/k_{1f}

$1000/T \sim (K^{-1})$
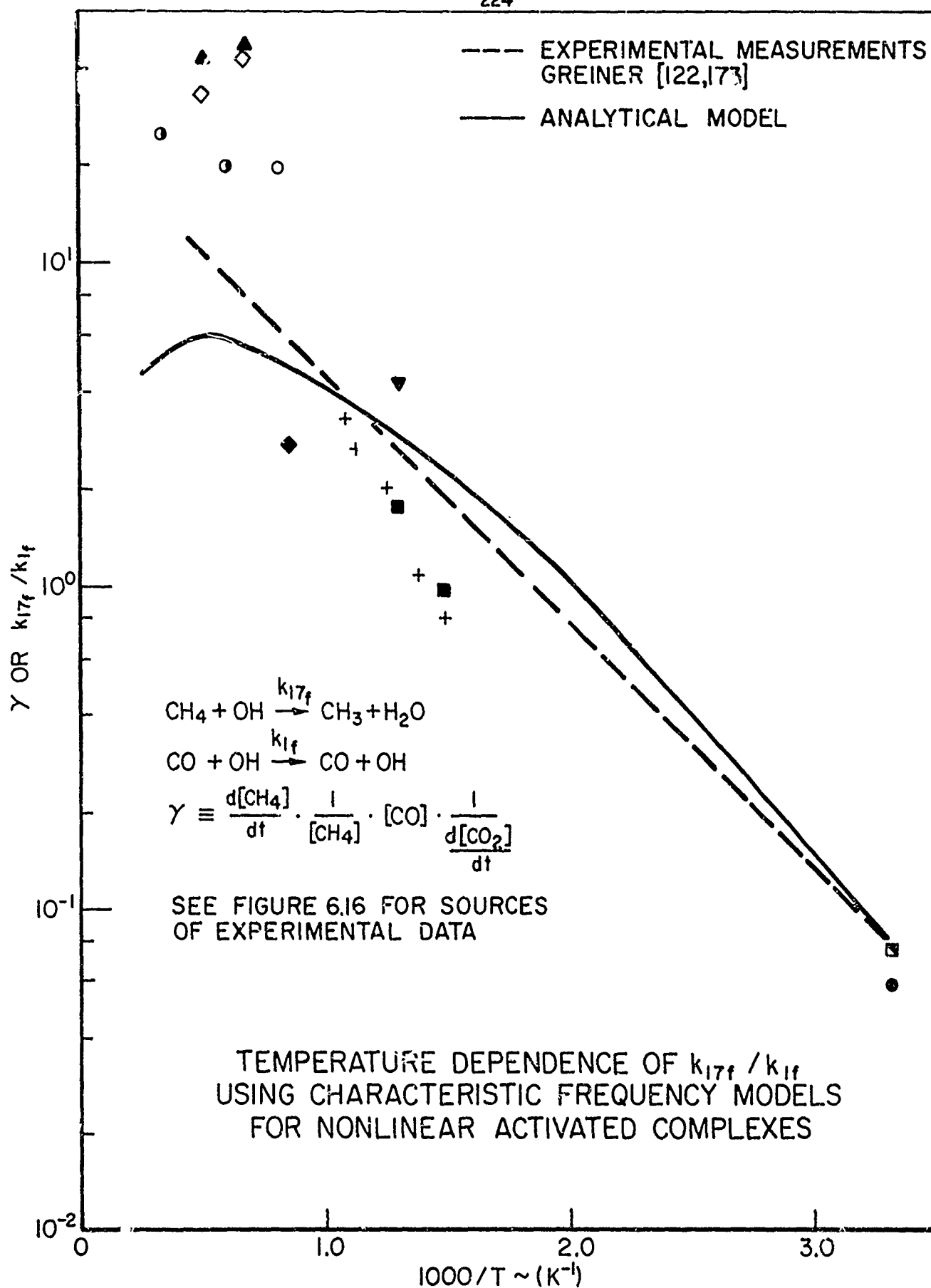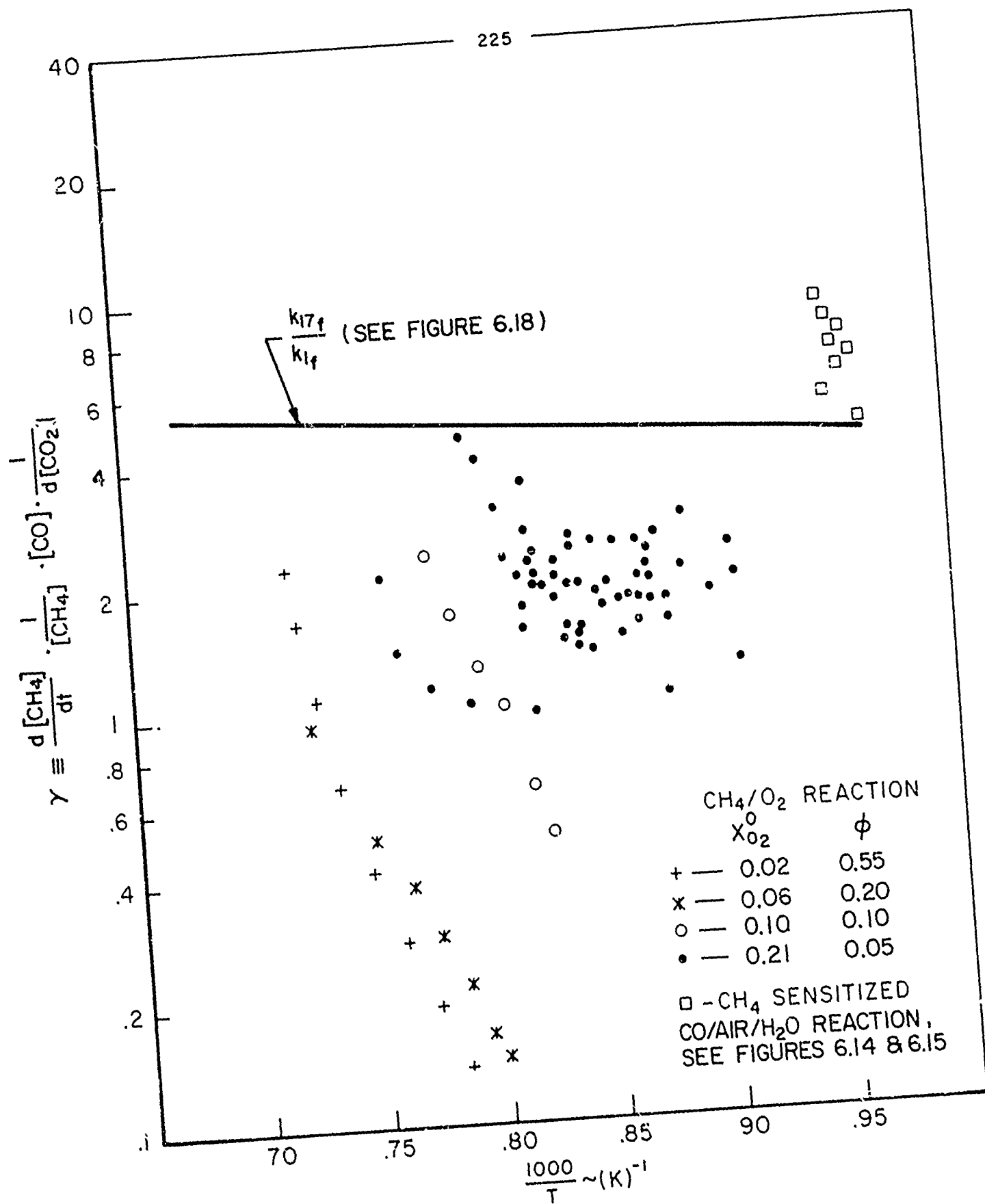
JP.13 12.427° 72

METHANE-OXYGEN REACTION STUDY,
DEPENDENCE OF γ ON EXPERIMENTAL REACTION PARAMETERS

FIGURE 6.19

COMPARISON OF RATE CONSTANTS FOR
CH_4-RADICAL REACTIONS
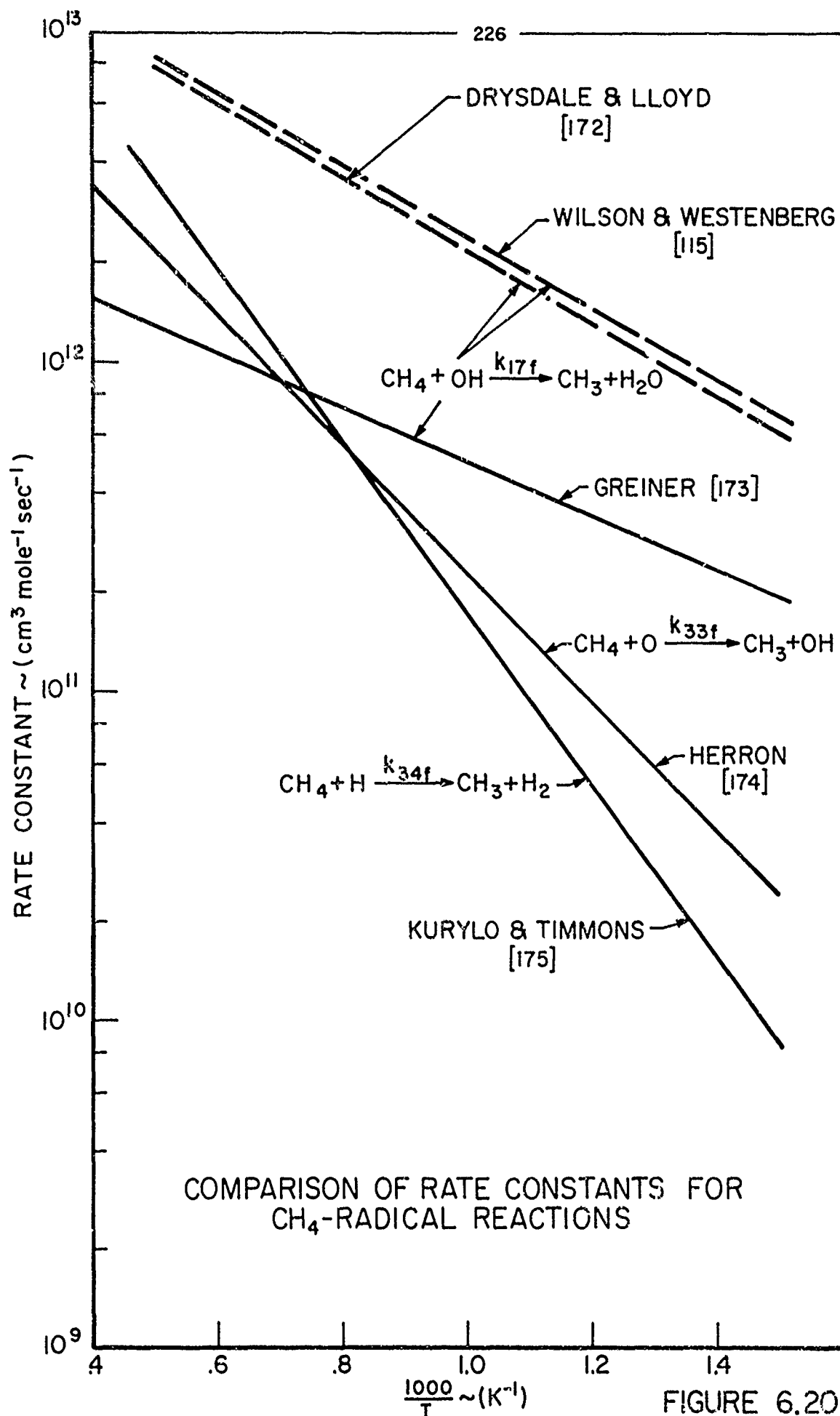
FIGURE 6.20

If the measurements of k_{17f} by Greiner [173] are tentatively accepted as correct, there is convincing evidence that reaction (33f) should not have been neglected in oxygen-rich flame studies. Fristrom [166] suggested [OH] and [O] to be of the same order in the reaction zone of the low pressure, fuel-lean, methane-oxygen flame he studied. Therefore, at 1000-1400K, reactions (33f) and (17f) would have competed on an equal basis for methane, and the disappearance rate which he ascribed entirely to reaction (17f) would be too large. In the study of Dixon-Lewis and Williams [3] at atmospheric pressure, the ratio of [O]/[OH] was estimated by the balanced reaction

$$O + H_2O \rightleftharpoons OH + OH \tag{13}$$
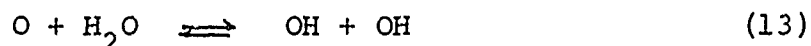
to be approximately 1/7. However, at the observed flame temperature of 1600K, $k_{33f} \approx 2 k_{17f}$, and thus again reactions (17f) and (33f) must have competed for methane. Wilson, et. al. [167] give no estimate for [O]/[OH], but they assumed without further justification that reaction (17f) was the only reaction that consumed methane in oxygen-rich flames.

Finally, it should be recalled that the flame studies of Fenimore and Jones [1] was one of the first works to conclude reaction (33f) to be unimportant in oxygen-rich methane flames. At the point of the maximum disappearance rate of methane (1600K), it was concluded that

$$\frac{[O]}{[OH]} \approx 2 \quad , \quad \frac{[H]}{[OH]} \approx 0.1$$

Thus, while it is clear that reaction (34f) is unimportant, reaction (33f) must be responsible for more than half of the observed rate of consumption of methane. Furthermore, in fuel-rich, methane-oxygen flames, Fenimore and Jones [1] determined

$$\frac{[O]}{[OH]} \approx 5 \quad , \quad \frac{[H]}{[OH]} \approx 5$$

at the point of the maximum rate of disappearance of methane (1200-1400K). Therefore, while (17f) may be neglected, reactions (33f) and (34f) are of equal importance in fuel-rich flames. Thus, reaction (33f) must be considered important in all flame studies of methane and oxygen. In light of this conclusion, there is no doubt that the evaluations of k_{17f} by Drysdale and Lloyd [172], Wilson and Westenberg [115] and Dixon-Lewis and Williams [3] are incorrect. Each evaluation considered reaction (17f) to be the primary disappearance mechanism for methane in oxygen-rich flames. This assumption is clearly invalid, and it explains to a large degree the disagreement in the values of k_{17f} predicted by Wilson and Westenberg [115], Dixon-Lewis and Williams [3] and Greiner [173] at high temperatures. Furthermore, the hypothesis that reaction (17f) and (33f) are of equal importance to the destruction of methane in oxygen-rich reactions qualitatively explains some of the experimental observations in the present flow reactor studies.

It will be remembered that the overall disappearance rate of methane was found to be relatively independent of water concentration (Section 6.2). With the aid of evaluated rate constants pertinent to describing the interdependence

of [O], [OH], and [H] on other species (Figure 6.21), this fact is now understandable. It is clear that water will adjust the concentrations of [O], [OH], and [H] through reactions (11f) and (13f). Since the assumption that $[H] \ll [O]$ in oxygen rich reactions of methane was shown to be true (see Page 227) by Fenimore and Jones [1], reaction (13f) will prevail. However, in Chapter 5, it was shown that reaction (13f) may be considered balanced[*] in high temperature reactions. Thus,

$$\frac{[O]}{[OH]} \approx \frac{k_{13r}}{k_{13f}} \quad \frac{1}{[H_2O]} \quad ,$$

and [OH] will be increased primarily at the expense of oxygen atoms. The destruction of an oxygen atom by reaction (13f) leads to two hydroxyl radicals which may attack methane by reaction (17f). However, an oxygen atom attacking methane directly by reaction (33f) creates a single hydroxyl radical which can attack a second molecule of methane by reaction (17f). Thus, the same number of molecules of methane are attacked whether an oxygen atom proceeds to react with water or directly with methane, and the disappearance rate of methane is independent of the concentration of water.

However, explanation of the magnitude and variation of γ with experimental parameters (Figure 6.19) requires additional consideration of a reverse reaction to reform methane. That is, if only reactions (17f), (33f) and (1f) were of primary importance in the methane oxidation experiments,

---

[*]See Page 152.

COMPARISON OF RATE CONSTANTS FOR SOME H_2-O_2 REACTIONS
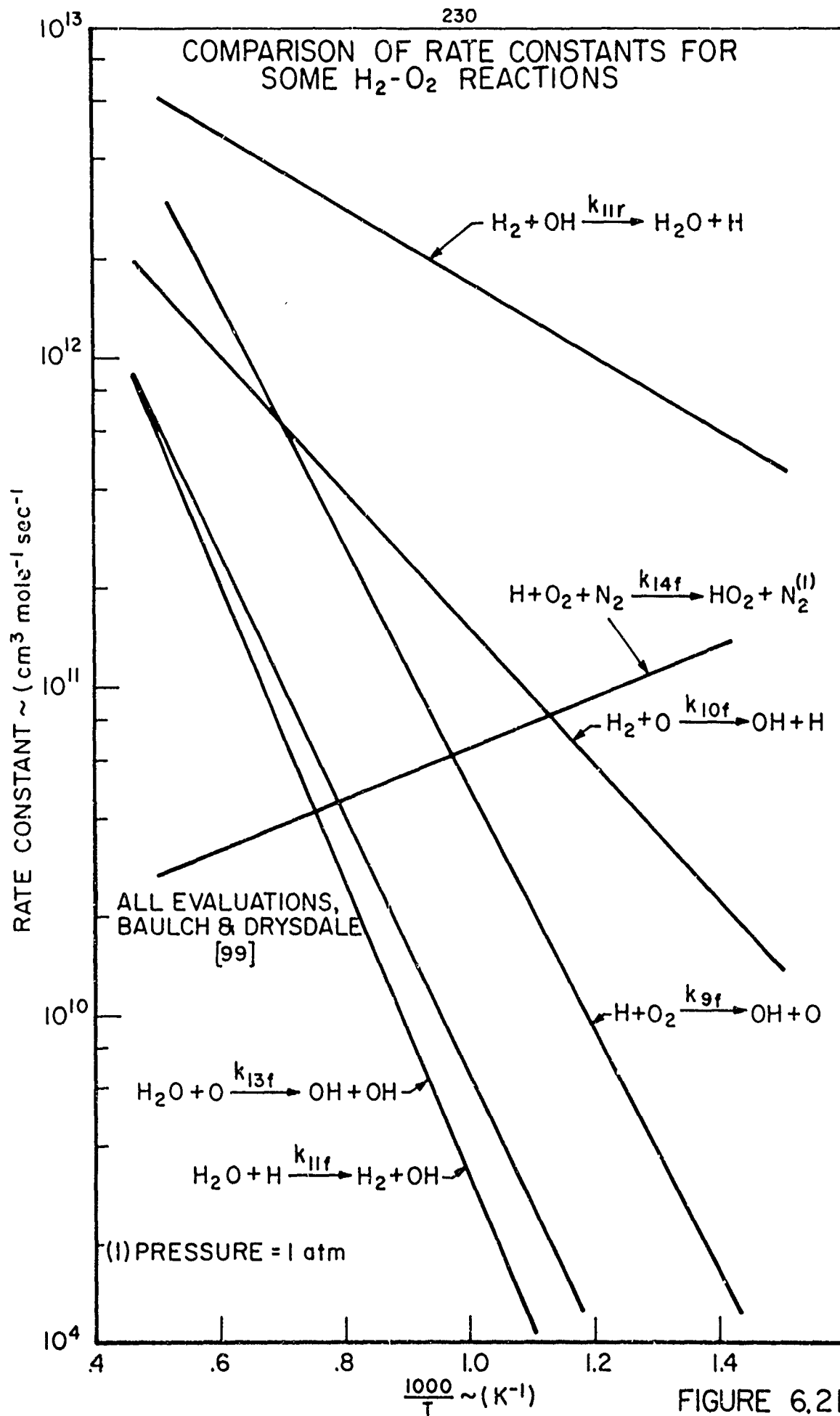
FIGURE 6.21

$$\frac{d[CH_4]}{dt} \cdot \frac{[CO]}{[CH_4]} \cdot \frac{1}{\frac{d[CO_2]}{dt}} \equiv \gamma^{\ell} = \frac{k_{17f}}{k_{1f}} + \frac{k_{33f}}{k_{1f}} \frac{[O]}{[OH]} \gg \frac{k_{17f}}{k_{1f}} \qquad 6.11$$

However, it is clear that at high temperatures and low initial concentrations of oxygen, the experimental measurements of γ^{ℓ} (Figure 6.19) were at least an order of magnitude smaller than k_{17f}/k_{1f} measured by Greiner [122,173]. It will be remembered that reaction (14f) is one of the primary sources of $[HO_2]$, and at 1200K this reaction is not competitive with reaction (10f). Thus, reaction (4f) and an associated increase in rate of formation of CO_2 cannot be responsible for the low value of γ^{ℓ}. Furthermore, a reverse reaction which lowers the net disappearance rate of methane is also supported by the observed fractional methane reaction order in the overall rate of expression of Equation 6.

Reaction (17r) must be considered unlikely because of the large activation energy it must possess, and reaction (33r) is not likely because of the very low concentrations of the reactants, $[CH_3]$ and $[OH]$. In light of the observed concentrations of $[H_2]$ and $[CH_3]$, Baldwin, et. al. [162] have suggested that reaction (34r) may be important. If the contribution of reaction (34r) is added to Equation 6.11,

$$\gamma^{\ell} = \frac{k_{17f}}{k_{1f}} + \frac{k_{33f}}{k_{1f}} \frac{[O]}{[OH]} - \frac{k_{34r}}{k_{1f}} \frac{[CH_3]}{[CH_4]} \frac{[H_2]}{[OH]} \qquad 6.12$$

Walker [168] has evaluated k_{34r} as

$$k_{34r} = 3.3 \times 10^{12} e^{\frac{-12,200}{RT}} \quad cm^3 \ mole^{-1} \ sec^{-1} .$$

Thus around 1200K, k_{34r}/k_{1f} is the order of 5×10^{-1}. The concentration of methyl radicals may be estimated from (39)

$$CH_3 + CH_3 \longrightarrow C_2H_6 \qquad (39)$$

and the experimental measured rate of appearance of ethane.[*] Baldwin [163] has estimated k_{39f}, as

$$k_{39f} = 5.5 \times 10^{18} \ T^{-2} \ cm^3 mole^{-1} \ sec^{-1},$$

and thus, in the experiments near 1200K, $[CH_3]/[CH_4]$ was about 10^{-2}. Furthermore, $[H_2]/[OH]$ was estimated to be no less than 10^2, and therefore the last term in Equation 6.12 is of the right order of magnitude to explain the observed discrepancy between $\mathscr{Y}$ and k_{17f}/k_{1f}.

It should be emphasized that additional considera-tion of reaction (34r) is not relevant to earlier arguments concerning lack of dependence of the rate on water concentra-tion. That reaction (33f) must also be important to the mecha-nism is indicated by the fact that $\mathscr{Y}$ exceeded k_{17f}/k_{1f} in the methane-sensitized carbon-monoxide studies reported in Figures 6.14 and 6.15.

Indeed, Equation 6.12 would appear to qualitatively explain all of the experimental observations summarized in Figure 6.19. While the necessary variations in $[O]/[OH]$, $[CH_3]/[CH_4]$, and $[H_2]/[OH]$ appear reasonable, only quantitative measurements of these ratios would permit one to emphatically state that reactions in addition to those considered in Equation 6.19 do not contribute substantially to the observed

---

[*]This will give a lower limit to the concentration of methyl radicals, since the experimental measurement is the net rate of appearance of ethane.

rates of disappearance of methane and appearance of carbon dioxide in the high temperature, oxygen rich, methane oxidation.

In summary, the present experimental work has shown the function, $\mathcal{Y}$,

$$\mathcal{Y} \equiv \frac{d[CH_4]}{dt} \frac{[CO]}{[CH_4]} \frac{1}{\dfrac{d[CO_2]}{dt}} \neq \frac{k_{17f}}{k_{1f}}$$

to depend on several experimental parameters, including temperature, and it was concluded that consideration of contributions of reaction (4f) to the appearance rate of carbon dioxide could not explain these dependences. In the light of recent absolute measurements of k_{17f}, k_{33f} and k_{34f}, it was shown that reaction (17f) is not the primary disappearance mechanism of methane in oxygen-rich methane flames, and therefore evaluations of k_{17f} which depend upon this assumption (Wilson and Westenberg [115], Dixon-Lewis and Williams [3], Drysdale and Lloyd [172]) are incorrect. Thus, their disagreement with the measurements of k_{17f} by Greiner [173] are to a large extent resolved.

Furthermore, it was shown that the reactions (17f), (33f), (34r) and (1f) qualitatively explain the present experimental measurements of the function, $\mathcal{Y}$, and the overall disappearance rate of methane, and thus Equation 6.3 implicitly includes complex dependences of several radical concentrations on other experimental parameters.

CHAPTER 7 - SUMMARY

The long range objective of this work was to develop experimental techniques for the study of chemical kinetics of hydrocarbon oxidations at high temperature. While the turbulent flow reactor has been demonstrated to be a very useful tool in the study of high temperature reactions, cursory oxidation experiments with hydrocarbons showed that the previously developed experimental technique (the thermal analysis method) generally provides insufficient information to characterize hydrocarbon oxidation kinetics. Supplementary spatial chemical information was required, and chemical sampling and analysis methods for procuring this information were developed.

Gas chromatography was chosen as the primary analysis tool, and thus design of suitable sample storage and transfer facilities was necessary. While continuous, on-line analysis procedures may have been more advantageous in the simple kinetic studies undertaken in this work, these methods would not be adequate to meet the long range objective of studying higher hydrocarbon oxidations. Sample storage and transfer systems were constructed, and a gas chromatographic analysis system was developed with this long range objective in mind. Using cryogenic temperature programming, a separation technique was developed to perform analysis for all of the reactants and intermediary and final products (except H_2O) which might occur in oxidation of the paraffin hydrocarbon series through propane.

Application of the experimental instrumentation and techniques was successfully demonstrated through kinetic studies of the oxidations of carbon monoxide and methane in the turbulent flow reactor.

The carbon-monoxide-oxygen reaction in the presence of water was studied at atmospheric pressure over the range 1030-1230K, the equivalence ratio .04-.3, and over water concentration of 0.1%-3.0%. These experiments provided results for comparison with studies of other investigators, as well as a unique opportunity to evaluate the relative precision of the thermal technique and absolute chemical measurements in the same apparatus. A method to correlate experimental overall chemical rates was developed and demonstrated by its application to the chemical analysis measurements. The overall disappearance rate of carbon monoxide was experimentally shown to be described by

$$-\frac{d[CO]}{dt} = 10^{14.6 \pm .25} \exp\left\{\frac{-40,000 \pm 1250}{RT}\right\} [CO]^{1.0} [H_2O]^{0.5} [O_2]^{0.25}$$

$$\text{mole cm}^{-3} \text{ sec}^{-1} \qquad (7.1)$$

and it was demonstrated that this expression represented both chemical and thermal measurements equally well. Thus, it was concluded that when the assumptions described in Appendix A are met by the studied chemical reaction, the thermal technique offers a simple and precise method of determining overall rate parameters.

The correlation results (Equation 7.1) were compared with other available data on the overall rate of disappearance

of carbon monoxide in hydrocarbon flames and in the $CO(H_2O)/O_2$ reaction. It was found that Equation 7.1 represented results of other investigations of the $CO(H_2O)/O_2$ reaction within a factor of five over the entire temperature range, 970 - 1800K (see Figure 5.7), and the same could not be said for extrapolation of experimental results of these other investigations to experimental conditions outside their respective ranges of study. Furthermore, it was re-emphasized that there is an essential difference in overall measurements of carbon dioxide production in hydrocarbon flames and in the $CO(H_2O)/O_2$ reaction. Assuming that the reaction

$$CO + OH \longrightarrow CO_2 + H \qquad (1)$$
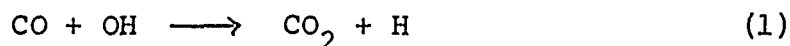
is the primary mechanism through which carbon monoxide disappears and carbon dioxide is formed, it was concluded that available hydroxyl radical concentrations in the $CO(H_2O)/O_2$ reactions exceed those in hydrocarbon flame afterburning zones. Furthermore, on the above premise, it was shown that [OH] exceeds $[OH]_{eq}$ by a factor of 10 - 100 in all studies of the carbon monoxide oxidation.

Alleged discrepancy in high and low temperature measurements of k_{1f} and other evidence which supports that the reaction

$$CO + HO_2 \longrightarrow CO_2 + OH \qquad (4)$$
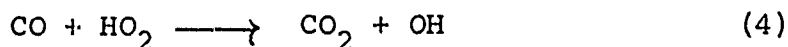
may compete with reaction (1) were reviewed and investigated. It was shown that upon present estimates of k_{4f}/k_{1f}, the ratio $[HO_2]/[OH]$ would have to be unexpectedly high for

reaction (4) to be important. Furthermore, it was shown
that all of the measurements of k_{1f} could be simply explained
by absolute reaction rate theory. While the true activation
energy of reaction (1) was concluded to be near zero, the
temperature dependence of k_{1f} was shown to be significant
at high temperatures because of pre-exponential effects.

Thus, on re-interpretation of available evidence,
reaction (4) is not likely to be important to the formation
of carbon dioxide. However, the hydro-peroxy radical may be
relevant to the high temperature carbon monoxide oxidation in
an indirect fashion. The reactions

$$H + O_2 \longrightarrow OH + O \qquad (9)$$

$$H + O_2 + M \longrightarrow HO_2 + M \qquad (14)$$
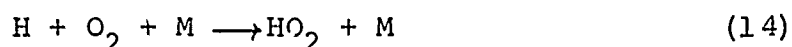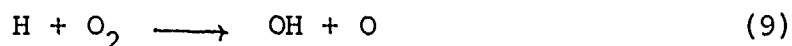
are of equal importance at atmospheric pressure near 1000K,
and thus reaction (14) and other reactions of $[HO_2]$ may be
important to chain branching in the mechanism.

The reaction of methane and oxygen was studied at
atmospheric pressure over the temperature range 1100-1400K
and the equivalence ratio range .05-0.5. The presence of two
well defined reaction stages (induction phase and post-induction
phase) was confirmed, and the disappearance rate of methane
was shown to exhibit contrasting kinetic properties in the two
stages.

While no quantitative study of the induction reaction
was attempted, the methane reaction rate was qualitatively
found to be inhibited by the presence of methane and accelerated

by concentrations of oxygen and carbon monoxide.

The post-induction phase reaction was quantitatively studied, and the overall methane disappearance rate was found to be best described by

$$-\frac{d[CH_4]}{dt} = 10^{13.2\pm0.20} \exp\left\{\frac{-8400\pm1200}{RT}\right\} [CH_4]^{0.7}[O_2]^{0.8}$$

$$\text{mole cm}^{-3} \text{ sec}^{-1} \qquad 7.2$$

The methane oxidation rate was shown to be independent of surface to volume ratio of the reactor and of water concentration.

The carbon dioxide production rate in the post-induction phase reaction was interpreted as the rate of oxidation of carbon monoxide, and it was found that this rate was expressed by

$$\frac{d[CO_2]}{dt} = 10^{14.75\pm0.40} \exp\left\{\frac{-43000\pm2200}{RT}\right\} [CO]^{1.0}[H_2O]^{0.5}[O_2]^{0.25}$$

$$\text{mole cm}^3 \text{ sec}^{-1} \qquad 7.3$$

This correlation represents rates of carbon dioxide formation 3.5 times slower than those occurring in the independent study of the moist carbon monoxide oxidation, and this slower rate was attributed to a lower available concentration of hydroxyl radicals in the methane oxidation. Other experiments showed that the lower hydroxyl radical concentration was due to competing reactions of methane (or its intermediary oxidation products) for hydroxyl radicals.

Relation of experimental observations to a proposed elementary reaction mechanism were discussed. It was shown that the function, $\mathcal{Y}$,

$$\mathcal{Y} \equiv \frac{d[CH_4]}{dt} \, \frac{1}{[CH_4]} \, [CO] \, \frac{1}{\frac{d[CO_2]}{dt}}$$

was dependent on experimental parameters other than temperature, and thus does not represent the measurement of the ratio k_{17f}/k_{1f}. It was concluded that dependence of $\mathcal{Y}$ on the equivalence ratio and oxygen concentration could not be explained by contributions of reaction (4); thus, other alleged evidence supporting this reaction was refuted.

Reactions in addition to (17f) which could contribute to the methane disappearance rate were reviewed, and it was conclusively shown that in light of the recent experimental measurements of Greiner [173], the reaction

$$CH_4 + O \longrightarrow CH_3 + OH \tag{33}$$

cannot be neglected in lean-methane oxygen flames. Thus, the evaluations of k_{17f} which have attributed all of the methane disappearance rate in these flames to (17f) are incorrect. Furthermore, the measurements of Fenimore and Jones [1] were shown to suggest that reaction (33f) is as important as

$$CH_4 + H \longrightarrow CH_3 + H_2 \tag{34}$$

in rich methane-oxygen flames.

While the present experimental measurements support that reaction (33f) cannot be neglected in lean methane oxygen

studies near 1200K, it was shown that reaction (34r) is also important in determining the _net_ disappearance rate of methane. Furthermore, it was shown that if reactions (17f), (33f) and (34r) all contribute to the overall oxidation rate, the rate is relatively independent of water concentration, as was experimentally observed.

Reactions of the methyl radicals produced in the oxidation of methane were concluded to be a relatively difficult process. Detection of intermediary concentrations of ethane and ethylene suggested high concentrations of methyl radicals to be present, and in light of the low concentrations of formaldehyde, it was concluded that a significant portion of methyl radicals may be oxidized through formation of ethane.

Hydrogen peroxide was also detected as a low concentration intermediary, and this suggested that hydroperoxy radicals may also be present. However, it should be re-emphasized that there was no evidence supporting the importance of reaction (4).

In conclusion, the utility of spatial chemical sampling and gas chromatographic analysis techniques in the study of hydrocarbon oxidations in a turbulent flow reactor has been clearly demonstrated, and it has been shown that these techniques can provide quantitative and qualitative information helpful to kinetic modeling and engineering design. While the present experimental results are not directly applicable to

the quasi-global modeling techniques proposed for higher
hydrocarbon oxidations [177,178], they provide the substan-
tial base necessary for higher hydrocarbon studies which
will be of more direct importance.

References

1. Fenimore, C. P. and Jones, G. W., "Rate of Reaction of Methane with H Atoms and OH Radicals in Flames", _J. Chem. Phys._, _65_, 2200 (1961).

2. Westenberg, A. A. and Fristrom, R. M., "Methane Oxygen Flame Structure IV., Chemical Kinetic Considerations", _J. Phys. Chem._, _65_, 591 (1961).

3. Dixon-Lewis, G. and Williams, A., "Some Observations on the Combustion of Methane in Pre-mixed Flames", _Eleventh Symposium (International) on Combustion_, The Combustion Institute, Pittsburgh, 951 (1967).

4. Porter, R. P., Clark, A. H., Kaskan, W. E. and Browne, W. E., "A Study of Hydrocarbon Flames", _Eleventh Symposium (International) on Combustion_, The Combustion Institute, Pittsburgh, 907 (1967).

5. Browne, W. G., Porter, R. P., Verlin, J. D. and Clark, A. H., "A Study of Acetylene-Oxygen Flames", _Twelfth Symposium (International) on Combustion_, The Combustion Institute, Pittsburgh, 1035 (1969).

6. Levy, A. and Weinberg, F. J., "Optical Flame Structure Studies: Examination of Reaction Rate Laws in Lean Ethylene-Air Flames, _Combustion & Flame_, _3_, 229 (1959).

7. Eckert, E. R. G. and Drake, R. M., Jr., _Heat and Mass Transfer_, McGraw-Hill, New York (1959).

8. Batten, J. J., "A Possible Error in the Measurement of Rate Constants of Gaseous Reactions by Flow Techniques", _Aust. J. Appl. Sci._, _12_, 11 (1960).

9. Glassman, I. and Eberstein, I. J., "Reaction Kinetics in Turbulent Flows", ARS 17th Annual Meeting and Space Flight Exposition, Paper No. 2672-62 (1962).

10. Glassman, I. and Eberstein, I. J., "Turbulence Effects in Chemical Reaction Kinetic Measurements", _AIAA Journal_, _1_, 1424 (1963).

11. Crocco, L., Glassman, I. and Smith, I. E., "A Flow Reactor for High Temperature Reaction Kinetics", _Jet Propulsion_, 1266 (1957).

12. Weber, R. J., Dugan, J. F. and Lindens, R. W., "Methane-Fueled Propulsion Systems", AIAA Second Propulsion Joint Specialist Conference, Paper No. 66-685 (1966).

13. Whitlow, J. B., Eisenberg, J. D. and Shovelin, M. D., "Liquid Methane as a Fuel for the Supersonic Transport", Cryogenic Technology, 3, 243 (1967).

14. Crocco, L., Glassman, I. and Smith, I. E., "Kinetics and Mechanism of Ethylene Oxide Decomposition at High Temperatures", J. Chem. Phys., 31, 506 (1959).

15. Eberstein, I. J., "The Gas Phase Decomposition of Hydrazine Propellants", Ph.D. Thesis, Dept. of Aerospace and Mechanical Engineering, Princeton University, (1964).

16. Sawyer, R. F., "The Homogeneous Gas Phase Kinetics of Reactions in the Hydrazine-Nitrogen Tetroxide Propellant System", Ph.D. Thesis, Dept. of Aerospace and Mechanical Engineering, Princeton University, (1965).

17. Freidman, R. and Burke, "Measurement of Temperature Distribution in a Low Pressure Flat Flame", J. Chem. Phys., 22, 824 (1954).

18. Fristrom, R. M. and Westenberg, A. A., "Flame Zone Studies IV., Microstructure and Natural Transport in a Laminar Propane-Air Flame Front", Combustion & Flame, 1, 217 (1957).

19. Fristrom, R. M., Avery, W. H. and Grunfelder, C., "Microstructure of C_2 Hydrocarbon-Oxygen Flames", Seventh Symposium (International) on Combustion, Butterworth and Co., Ltd., London, 304 (1958).

20. Fristrom, R. M., Grunfelder, C. and Favin, S., "Methane-Oxygen Flame Structure: I. Characteristic Profiles in a Low Pressure Laminar Lean Premixed Methane-Oxygen Flame", J. Phys. Chem., 64, 1386 (1960).

21. Burgoyne, J. H. and Hirsch, H., "Combustion of Methane at High Temperatures", Proceedings of the Royal Society, A227, 73 (1954).

22. Pratt, N. H., "Rates of Combustion in Flowing Streams of Gases", Imperial College of Science and Technology, Ph.D. Thesis, Dept. of Chemical Engineering and Applied Chemistry, London, (1962).

23. Kozlov, G. I., "On High Temperature Oxidation of Methane", Seventh Symposium (International) on Combustion, Butterworth & Co., Ltd., London, 142.

24. Ettre, L. S., Open Tubular Columns, Plenum Press, New York (1965).

25. Barnard, G. P., _Modern Mass Spectrometry_, Institute of Physics, London (1954).

26. Swigart, R. J., "A Study of the Kinetics of the Hydrogen-Oxygen Reaction in a New Flow Reactor", Dept. of Aeronautical Engineering Report No. 432, Princeton University, (1958).

27. Eberstein, I. and Glassman, I., "The Gas Phase Decomposition of Hydrazine and Its Methyl Derivatives", _Tenth Symposium (International) on Combustion_, The Combustion Institute, Pittsburgh, 365 (1965).

28. Sawyer, R. F. and Glassman, I., "Gas-Phase Reactions of Hydrazine with Nitrogen Dioxide, Nitric Oxide and Oxygen", _Eleventh Symposium (International) on Combustion_, The Combustion Institute, Pittsburgh, 861 (1967).

29. Sawyer, R. F. and Glassman, I., "The Reactions of Hydrogen with Nitrogen Dioxide, Oxygen and Mixtures of Oxygen and Nitric Oxide", _Twelfth Symposium (International) on Combustion_, The Combustion Institute, Pittsburgh, 469 (1969).

30. Fristrom, R. M. and Westenberg, A. A., _Flame Structure_, McGraw-Hill, (1965).

31. Kaskan, W. E., "The Dependence of Flame Temperature on Flame Mass Velocity", _Sixth Symposium (International) on Combustion_, Reinhold, New York, 134 (1957).

32. Varma, A. K., Harrje, D. T. and Sirignano, W. A., "The Effect of External Periodic Disturbances on Axisymmetric Wake Diffusion Flames", 7th JANAF Combustion Meeting, _CPIA Publication 204_, 1, (1971).

33. Cookson, R. A., "Non-Catalytic Coatings for Thermocouples", Letters to the Editor, _Combustion & Flame_, 8, 168 (1964).

34. Burns, G. W. and Gallagher, J. S., "Reference Tables for the Pt-30 Percent Rh Versus Pt-6 Percent Rh Thermocouple _J. Res. Natl. Bur. Std. 70C_, 89 (1966).

35. Fristrom, R. M., Prescott, R. and Grunfelder, C., "Flame Zone Studies III. Techniques for the Determination of Composition Profiles of Flame Fronts", _Combustion & Flame_, 1, 102 (1957).

36. Fristrom, R. M., "Experimental Determination of Local-Concentrations in Flames", _Experimental Methods in Combustion Research_, Pergamon Press, New York, Sec. 1.4, (1961).

37. Freidman, R. and Cyphers, J., "Flame Structure Studies III. Gas Sampling in a Low Pressure Propane Air Flame", J. Chem. Phys., 23, 1875 (1955).

38. Tiné, G., Gas Sampling and Chemical Analysis in Combustion Processes, Pergamon Press (1961).

39. Beal, J. L. and Grey, J. T., "Sampling and Analysis of Combustion Gases", Journal of American Rocket Society, 23, 174 (1953).

40. Halpern, M. and Ruegg, A., "Sampling in Burners", J. Res. Natl. Bur. Std., 60, 29 (1958).

41. Rosen, P., "Potential Fow of a Fluid into a Sampling Probe", John Hopkins University., Appl. Phys. Lab. Report CF-2248, Silver Spring, Md., (1954).

42. Papa, L. J., "Gas Chromatography-Measuring Exhaust Hydrocarbons Down to Parts Per Billion", S.A.E. Preprint 670494, Chicago, Ill. (1967).

43. Dimitriades, B., Ellis, C. F. and Seizinger, D. E., "Gas Chromatographic Analysis of Vehicular Exhaust Emissions", Advances in Chromatography, 5, 229 (1968).

44. Jeffery, P. G. and Kipping, P. J., Gas Analysis by Gas Chromatography, Pergamon Press, New York (1964).

45. James, A. T. and Martin, A. J. P., Biochem. J., 50, 679 (1952).

46. Knox, J. H., Gas Chromatography, Methuen and Co., Ltd., London, (1962).

47. Purnell, H., Gas Chromatography, John Wiley & Sons, Inc., New York (1962).

48. Dal Nogare, S., Gas Liquid Chromatography, Interscience Publishers, New York (1962).

49. Littlewood, A. B., Gas Chromatography, Academic Press, New York (1962).

50. Kaiser, R., Gas Phase Chromatography, Vols. 1-3, Butterworths, London (1963).

51. McNair, H. M. and Bonelli, E. J., Basic Gas Chromatography, Varian Aerograph (1969).

52. Ambrose, D. and Ambrose, B. A., Gas Chromatography, Newnes, Ltd., London (1961).

53. Keulmans, A. I. M., Gas Chromatography, Reinhold Publishing Corporation, New York (1959).

54. Habgood, H. W. and Harris, W. E., Temperature Programming, John Wiley & Sons, Inc. (1966).

55. Operating and Service Manual 7620A Series Gas Chromatograph System, I-IV, Hewlett Packard Service Manual, 19099-90100, 19106-90100, 19105-90100, 07619-90100, (1969).

56. Leibranc, R. J., "Atlas of Gas Analyses by Gas Chromatography", Hewlett Packard Application Lab Report 1006, June, 1966.

57. Forsey, R. R., "A Dual Column Gas Chromatographic Method for Analysis of Light Gases", J. Gas Chromatography, 6, 555 (1968).

58. Baum, E. H., "Evaluation of Microporous Polyethylene as a Low Temperature Chromatographic Support", J. Gas Chromatography, 1, 13 (1963).

59. Hollis, O. L., Advances in Gas Chromatography 1965, A. Zlatkis and T. S. Ettre, eds. Preston Technical Abstracts Co., Evanston, 56, (1966).

60. Dave, S. B., "A Comparison of the Chromatographic Properties of Porous Polymers, J. Gas Chromatography, 7, 389 (1969).

61. Madison, J. J., "Analysis of Fixed and Condensable Gases by Two-Stage Gas Chromatography", Anal. Chem., 30, 1859 (1958).

62. Personal Communication

63. Green, L., "G. C. Trace Gas Analysis Using a Hot Wire Thermal Conductivity Detector", Facts and Methods (Hewlett Packard), Vol. 8, No. 6., 1 (1967).

64. Messner, A. E., Rosie, D. M., Argabright, R. A., et.al., "Correlation of Thermal Conductivity Cell Response with Molecular Weight and Structure", Anal. Chem., 31, 230 (1959).

65. Dietz, W. A., "Response Factors for Gas Chromatographic Analyses", Gas Chromatography, 5, 68 (1967).

66. Sternberg, J. C., Gallaway, W. S. and Jones, D. T. C., "Gas Chromatography", *Third (International) Symposium, Instrument Society of America*, Academic Press (1962).

67. Operating and Service Manuals for Model 3370A Integrator, Hewlett Packard Service Manual 03370-90000, 03370-90001 (1968).

68. Goland, D. and Peterson, G., "Straight Talk About the Performance of Electronic Digital Integrators on Fused Peaks, Hewlett Packard Application Note ANC-16-70 (1970).

69. Perkins, F. S. and Kipping, B. F., *Organic Chemistry*, T. Y. Crowell Co., New York (1941).

70. Wall, L., "Condensed Phase Combustion Chemistry", Paper presented National Academy of Sciences, Committee on Fire Research, Oct., 1971.

71. Sperling, H. P. and Toby, S., "The Thermal and Photo-Decomposition of Gaseous Formaldehyde", 161st ACS National Meeting Paper No. 145 (Physical Chemistry) (1971).

72. Scott, F. I., Jr. and Rutherford, R. E., "Continuous Ultra-Purity Helium", *American Laboratory*, May, 1970.

73. Freidman, R. and Cyphers, J. A., "On the Burning Rate of Carbon Monoxide", *J. Chem. Phys.*, 25, 448 (1956).

74. Lewis, B. and VonElbe, G., *Combustion, Flames and Explosions of Gases*, Academic Press, Inc., New York (1951).

75. Gordon, A. S., "The Explosive Reaction of Carbon Monoxide and Oxygen at the Second Explosion Limit in Quartz Vessels", *J. Chem. Phys.*, 20, 340 (1952).

76. Gordon, A. S. and Knipe, R. H., "The Explosive Reaction of Carbon Monoxide and Oxygen at the Second Limit in Quartz Vessels", *J. Phys. Chem.*, 59, 1160 (1955).

77. Hoare, D. E. and Walsh, A. D., "The Oxidation and Burning of Carbon Monoxide", *Trans. Faraday Soc.*, 50, 37 (1954).

78. Dickens, P. G., Dove, J. E. and Linnett, J. W., "Explosion Limits of the Dry Carbon-Monoxide and Oxygen Reaction", *Trans Faraday Soc.*, 60, 539 (1964).

79. Brokaw, R. S., "Ignition Kinetics of the Carbon Monoxide-Oxygen Reaction", *Eleventh Symposium (International) on Combustion*, The Combustion Institute, Pittsburgh, 1063, (1967).

80. Sobelev, G. K., "High Temperature Oxidation and Burning of Carbon Monoxide", Seventh Symposium (International) on Combustion, Butterworth and Co., Ltd., London, 386 (1959).

81. Fenimore, C. P. and Jones, G. W., "The Water Catalyzed Oxidation of Carbon Monoxide by Oxygen at High Temperatures", J. Phys. Chem., 61, 651 (1957).

82. Nemeth, A. and Sawyer, R. F., "CO Afterburning in Methane and Methane/Hydrogen Flames, WSCI Paper No. 68-17 (1968).

83. Hottel, H. C., Williams, A., Nerheim, N. M. and Schneider, G. R., "Kinetic Studies in Stirred Reactors: Combustion of Carbon Monoxide and Propane", Tenth Symposium (International) on Combustion, The Combustion Institute, Pittsburgh, 111 (1965).

84. Williams, G. C., Hottel, H. C. and Morgan, A. C., "The Combustion of Methane in a Jet Mixed Reactor", Twelfth Symposium (International) on Combustion, The Combustion Institute, Pittsburgh, 913 (1969).

85. Lavrov, N. V., Karbirnichii-Kuznetsov, V. B., "Experimental Study of Overall Kinetics of CO Combustion", Nank Uzb SSR, 25, 9 (1968).

86. Badami, G. N. and Egerton, A., "The Determination of Burning Velocities of Flow Flames", Proc. Royal Soc., A228, 297 (1955).

87. McDonald, G. E., "Effect of Water on Carbon Monoxide Oxygen Flame Velocity", NACA Research Memorandum E53L08 (1954).

88. Price, T. W. and Potter, J. H., "Factors Affecting Flame Velocity in Stoichiometric Carbon Monoxide Mixtures", Fourth Symposium (International) on Combustion, Williams and Wilkins, Baltimore, 363 (1953).

89. Barskii, G. A. and Zeldovich, Y. B., "Burning Kinetics of Carbon Monoxide", Jhur Fiz. Khim., 25, 523 (1957).

90. Chukhanov, Z. F., "Burning of Carbon", Zh Tekh. Fiz. (USSR), 8, 147 & 621 (1938).

91. Semenov, N. N., "Theory of Normal Flame Propagation", NACA Technical Memorandum 1026, Sept. (1942).

92. Freidman R. and Nugent, R. G., "Flame Structure-IV., Premixed Carbon-Monoxide Combustion", Seventh Symposium (International) on Combustion, Butterworth and Co., Ltd., London, 311 (1959).

93. Kydd, P. H. and Foss, W. I., "Combustion of Fuel Lean Mixtures in Adiabatic Well-Stirred Reactors", Tenth Symposium (International) on Combustion, The Combustion Institute, Pittsburgh, 101 (1965).

94. Avramenko and Lorenzo, R. V., Zh fiz Khim, 24, 207 (1950), (in Russian).

95. Singh, T. and Sawyer, R. F., "CO Reactions in the After-flame Region of Ethylene/Oxygen and Ethane/Oxygen Flames", Thirteenth Symposium (International) on Combustion, The Combustion Institute, Pittsburgh, 403 (1971).

96. Wilson, W. E., "Activation Energies for Hydroxyl Radical Abstraction Reactions", J. Chem. Phys., 53, 1300 (1970).

97. Baldwin, R. R., Jackson, D., Walker, R. W. and Webster, S. J., "The Use of the Hydrogen-Oxygen Reaction in Evaluating Velocity Constants", Tenth Symposium (International) on Combustion, The Combustion Institute, Pittsburgh, 423 (1965).

98. Baldwin, R. R., Walker, R. W. and Webster, S. J., "The Carbon Monoxide-Sensitized Decomposition of Hydrogen-Peroxide", Combustion & Flame, 15, 167 (1970).

99. Baulch, D. L., Drysdale, D. D. and Lloyd, A. C., "Critical Evaluation of Rate Data for Homogeneous Gas Phase Reactions of Interest in High Temperature Systems", School of Chemistry, The University, Leeds 2., Vol. 1-4 (1967-1970).

100. Kaskan, W. E., "The Concentration of Hydroxyl and of Oxygen Atoms in Gases from Lean Hydrogen-Air Flames", Combustion & Flame, 2, 286 (1958).

101. Kaufman, F., "Aeronamic Reaction Involving Hydrogen - A Review of Recent Laboratory Studies", Ann. Geophys., 20, 106 (1964).

102. Foner, S. N. and Hudson, R. L., "Mass Spectrometry of Inorganic Free Radicals", Advanced Chem. Series, 36, 34 (1962).

103. Schofield, K., "An Evaluation of Kinetic Rate Data for Reactions of Neutrals of Atmospheric Interest", Planet Space Sci., 15, 643 (1967).

104. Meyer, E., Olschewski, H. A., Troe, F. and Wagner, N. G., "Investigation of N_2H_4 and H_2O_2 Decomposition in Low and High Pressure Shock Waves", Twelfth Symposium (International) on Combustion, The Combustion Institute, Pittsburgh, 345 (1969).

105. Stull, D. K. (ed), <u>JANAF Thermochemical Tables</u>, Dow Chemical Co., Michigan (1965).

106. Bulewicz, E. M., James, C. G. and Sugden, T. M., "Photometric Investigations of Alkali Metals in Hydrogen Flame Gases. II. The Study of Excess Concentrations of Hydrogen Atoms in Burnt Gas Mixtures", <u>Proc. Roy. Soc.</u>, <u>A235</u>, 89 (1956).

107. Sugden, T. M., "Equilibrium in Flame Gases and General Kinetic Considerations", <u>Trans. Faraday Soc.</u>, <u>52</u>, 1465 (1956).

108. Schott, G. L., "Kinetic Studies of Hydroxyl Radicals in Shock Waves. III. The OH Concentration Maximum in the Hydrogen-Oxygen Reaction", <u>J. Chem. Phys.</u>, <u>32</u>, 710 (1960).

109. Hamilton, C. W. and Schott, G. L., "Post Induction Kinetics in Shock-Initiated H_2-O_2 Reaction", <u>Eleventh Symposium (International) on Combustion</u>, The Combustion Institute, Pittsburgh, 635 (1967).

110. Kaskan, W. C., "Excess Radical Concentrations and the Disappearance of Carbon Monoxide in Flame Gases from Some Lean Flames", <u>Combustion & Flame</u>, <u>3</u>, 49 (1959).

111. Browne, W. G., White, D. R. and Smookler, G. R., "A Study on the Chemical Kinetics of Shock Heated $H_2/CO/O_2$ Mixtures", <u>Twelfth Symposium (International) on Combustion</u>, The Combustion Institute, Pittsburgh, 557 (1969).

112. Westenberg, A. A. and Fristrom, R. M., "H and O Atom Profiles Measured by ESR in C_2 Hydrocarbon-O_2 Flames", <u>Tenth Symposium (International) on Combustion</u>, The Combustion Institute, Pittsburgh, 473 (1965).

113. Fenimore, C. P. and Jones, G. W., "The Reaction of Hydrogen Atoms with Carbon Dioxide", <u>J. Phys. Chem.</u>, <u>62</u>, 1578 (1958).

114. Dixon-Lewis, G., Wilson, W. E. and Westenberg, A. A., "Studies of Hydroxyl Radical Kinetics by Quantitative ESR", <u>J. Chem. Phys.</u>, <u>44</u>, 2877 (1966).

115(a). Wilson, W. E. and Westenberg, A. A., "Study of the Reaction of Hydroxyl Radical with Methane by Quantitative E.S.R.", <u>Eleventh Symposium (International) on Combustion</u>, The Combustion Institute, Pittsburgh, 1143, (1967).

115(B). Westenberg, A. and Wilson, W. E., "Study of the Reaction of Hydroxyl Radical with Methane by Quantitative E.S.R.", <u>J. Chem. Phys.</u>, <u>45</u>, 338 (1966).

116. Greiner, N. R., "Hydroxyl Radical Kinetics by Kinetic Spectroscopy V. Reactions with H_2 and CO at 300K", *J. Chem. Phys.*, 46, 2795 (1967).

117. Wilson, W. E. and O'Donovan, J. T., "Mass Spectrometric Study of Reactor Rate of OH with Itself and with CO", *J. Chem. Phys.*, 47, 5455 (1967).

118. Kaufman, F. and DelGreco, F. P., "Fast Reactions of OH Radicals", *Ninth Symposium (International) on Combustion*, The Combustion Institute, 659 (1963).

119. Wilson, W. E., "A Critical Review of the Gas Phase Reaction Kinetics of the Hydroxyl Radical", Paper presented at WSCI Spring Meeting, (1967).

120. Brabbs, T. A., Belles, F. E., and Brokaw, R. S., "Shock Tube Measurements of Specific Reaction Rates in the Branched-Chain H_2-CO-O_2 System", *Thirteenth Symposium (International) on Combustion*, The Combustion Institute, 129 (1971).

121. Jost, W., Schecker, H. G. and Wagner, H. G., "Messungen der Geschwindigkeis der Einftellung def Wassergas Gleichgewichtes", *Z. fur Phys. Chem., Neue Folge*, 45, 47 (1965), (in German).

122. Greiner, N. R., "Hydroxyl Radical Kinetics by Kinetic Spectroscopy V. Reactions with H_2 and CO in the Range 300-500K", *J. Chem. Phys.*, 51, 11, 5049 (1969).

123. Heath, G. A. and Pearson, G. S., "Perchloric Acid Flames: Part III. Chemical Structure of Methane Flames", *Eleventh Symposium (International) on Combustion*, The Combustion Institute, Pittsburgh, 967 (1965).

124. Baldwin, R. R. and Doran (Unpublished), Baldwin, R. R. and Cowe, D. W., "The Inhibition of the Hydrogen + Oxygen Reaction by Formaldehyde", *Trans Faraday Soc.*, 58, 1768 (1962).

125. Dixon-Lewis, G., Sutton, M. M. and Williams, A., "Reactions Contributing to the Establishment of the Water Gas Equilibrium when Carbon Dioxide is added to a Hydrogen-Oxygen Flame", *Trans Faraday Soc.*, 61, 255 (1965).

126. Baldwin, R. R., Walker, R. W. and Webster, S. J., "The Carbon Monoxide-Sensitized Decomposition of Hydrogen-Peroxide", *Combustion & Flame*, 15, 167 (1970).

127. Ung, A. Y. and Back, R. S., "The Photolysis of Water Vapor and Reactions of Hydroxyl Radicals", *Canadian J. Chem.*, 42, 753 (1964).

128(a). Wong, E. L., Potter, A. E. and Belles, F. E., "Reaction Rates of Carbon Monoxide with Hydroxyl Radicals and Oxygen Atoms", NASA TN D-4162 (1967).

128(b). Wong, E. L. and Belles, F. E., "Activation Energies for Reactions of Hydroxyl Radicals with Hydrogen and Carbon Monoxide", NASA TN D-5707 (1970).

129. Balakhnin, V. P., Gershenzon, Yu. M., Kondratiev, V. R., and Nalbandyan, A. B., "A Quantitative Study of the Mechanism of Hydrogen Combustion Close to the Lower Explosion Limit", Dok-Acad. Nauk. SSSR Doklady. Physical Chemistry, 170, 659 (1966).

130. Laidler, K. F., Chemical Kinetics, McGraw-Hill, New York (1965).

131. Benson, S. W., Thermochemical Kinetics, John Wiley and Sons, Inc., (1968).

132. Herzberg, G., Molecular Spectra and Molecular Structure III. Electronic Spectra and Polyatomic Molecules", D. Van Nostrand Co., Inc., 614 (1967).

133. Bennewitz, K. and Rossner, W. Z., "Uber die Molwarme bon Organchen Dampfen", Z Physik Chem., 39B, 126 (1938), (in German).

134. Meghrebilian, R. V., "Approximate Calculations of Specific Heats for Polyatomic Gases", Journal Amer. Rocket Soc., 21, 127 (1951).

135. Herzberg, G., Molecular Spectra and Molecular Structure I. Spectra of Diatomic Molecules, D. Van Nostrand Co., Inc. (1950).

136. Bone, W. A. and Gardiner, J. B., "Comparative Studies of the Slow Combustion of Methane, Methyl Alcohol, Formaldehyde, and Formic Acid", Proc. Royal Soc., A 154, 297 (1936).

137. Vandeleele, H., Corbeels, R., and van Tigglen, A., "Activation Energy and Reaction Order in Methane-Oxygen Flames", Combustion & Flame, 4, 253 (1960).

138. Skinner, G. B. and Ruerhwein, R. A, "Shock Tube Studies of the Pyrolysis and Oxidation of Methane", J. Phys. Chem., 63, 1736 (1959).

139. Asaba, T., Yoreda, K., Kakihara, N. and Hikita, T., "A Shock Tube Study of Ignition of Methane-Oxygen Mixtures, Ninth Symposium (International) on Combustion, Academic Press, London, 193 (1963).

140. Miyama, H. and Takeyama, T., "Mechanism of Methane Oxidation in Shock Waves", J. Chem. Phys., 40, 2049 (1964).

141. Glass, C. P., Kistiakowsky, G. B., Michel, J. V. and Niki, "The Oxidation Reactions of Acetylene and Methane", Tenth Symposium (International) on Combustion, The Combustion Institute, Pittsburgh, 513 (1965).

142. Seery, D. J. and Bowman, C. T., "An Experimental and Analytical Study of Methane Oxidation Behind Shock Waves", Combustion & Flame, 14, 37 (1970).

143. Higgin, R. M. R. and Williams, A., "A Shock Tube Investigation of the Ignition of Lean Methane, and in Butane Mixtures with Oxygen", Twelfth Symposium (International) on Combustion, The Combustion Institute, 579 (1969).

144. Loyd, P., "Combustion in the Gas Turbine", Proc. Sixth International Congress for Applied Mech., Paris, (1946).

145. Mullins, B. P., "Studies on the Spontaneous Ignition of Fuels Injected into a Hot Air Stream IV. Ignition Delay Measurement on Some Gaseous Fuels at Atmospheric and Reduced Static Pressures", Fuel, 32, 211 and 343 (1953).

146. Nemeth, A. and Sawyer, R. F., "The Overall Kinetics of High-Temperature Methane Oxidation in a Flow Reactor", J. Phys. Chem., 73, 2421 (1969).

147. Brokaw, R. S., "Thermal Ignition with Particular Reference to High Temperature", Selected Combustion Problems II, Butterworths, London, 115 (1956).

148. Bowman, C. T., "An Experimental and Analytical Investigation of the High Temperature Oxidation Mechanisms of Hydrocarbon Fuels", Combustion Science and Technology, 2, 161 (1970).

149. Bricker, C. E. and Johnson, H. R., "Spectrophotometric Method for Determining Formaldehyde", Industrial and Engineering Chemistry, (Analytical Edition), 17, 400 (1945).

150. Egerton, A. C., Everett, A. J., Minkoff, G. J., Rudrakanchana, S., and Salooja, K. C., "The Analysis of Combustion Products I. Some Improvements in the Methods of Analysis of Peroxides", Analytica Chimica Acta, 10, 422 (1954).

151. Egerton, A. C., Minkoff, G. J., Salooja, K. C., "The Slow Oxidation of Methane - The Role of the Surface on the Course of the Oxidation of Methane", <u>Combustion & Flame</u>, <u>1</u>, 25 (1957).

152. Hoare, D. E. and Walsh, A. D., "The Oxidation of Methane Part I. Kinetic Laws at ca. 500°C", <u>Fifth Symposium (International) on Combustion</u>, Reinhold Publishing Corp., New York, 467 (1955).

153. Hoare, D. E. and Walsh, "The Oxidation of Methane Part II. Behavior at Temperatures from 500°C to 750°C", <u>Fifth Symposium (International) on Combustion</u>, Reinhold Publishing Corp., New York, 474 (1955).

154. Conze, A. T., Gaillaird-Cuisin, F., and James, H., "Interactions of Reaction Chains in the High Temperature Combustion of Methane", <u>Bull. Soc. Chim. Fr.</u>, <u>9</u>, 3469 (1967).

155. Meriaux, B., Lucquin, M., "Mild Oxidation of Methane in a Dynamic System I. Temperature Effects", <u>Bull. Soc. Chim. Fr.</u> <u>9</u>, 3581 (1968).

156. Shtern, V. Ya., <u>The Gas Phase Oxidation of Hydrocarbons</u>, The Macmillan Company, New York (1964).

157. Franklin, J. L., "Mechanisms and Kinetics of Hydrocarbon Combustion", <u>Annual Review of Physical Chemistry</u>, Annual Reviews, Inc., <u>18</u>, 261 (1967).

158. Semenov, N. N., <u>Some Problems in Chemical Kinetics and Reactivity</u>, Princeton University Press, Princeton, (1959).

159. Enikolopyan, N. S., "Kinetics and Mechanism of Methane Oxidation", <u>Seventh Symposium (International) on Combustion</u>, Butterworth and Co., London, 157 (1959).

160. Minkoff, G. J. and Tipper, C. F. H., <u>Chemistry of Combustion Reactions</u>, Butterworths, London (1962).

161. Chintz, W., "A Theoretical Analysis of Non-Equilibrium Methane/Air Combustion, <u>Pyrodynamics</u>, <u>3</u>, 197 (1965).

162. Baldwin, R. R., Hopkins, D. E., Norris, A. C., and Walker, "The Addition of Methane to Slowly Reacting Hydrogen-Oxygen Mixtures: Reactions of Methyl Radicals", <u>Combustion & Flame</u>, <u>15</u>, 23 (1970).

163. Baldwin, R. R., Matchan, M. F., and Walker, R. W., "The High-Temperature Oxidation of Acetaldehyde", <u>Combustion & Flame</u>, <u>15</u>, 109 (1970).

16ł.   Hoare, D. E., Low Temperature Oxidation, (ed. W. Jost),
        Gordon and Breach, New York, 125 (1965).

165.   Wong, E. L. and Potter, A. E., "Reaction Rates of
        Hydrogen, Ammonia, and Methane with Mixtures of Atomic
        and Molecular Oxygen", J. Chem. Phys., 39, 2211 (1963).

166.   Fristrom, R. M., "Radical Concentrations and Reactions
        in a Methane-Oxygen Flame", Ninth Symposium (International)
        on Combustion, Academic Press, Inc., New York, 560 (1963).

167.   Wilson, W. E., Jr., O'Donovan, J. T. and Fristrom, R. M.,
        "Flame Inhibition by Halogen Compounds", Twelfth Symposium
        (International) on Combustion, The Combustion Institute,
        929 (1969).

168.   Baldwin, R. R., Norris, A. C. and Walker, R. W.,
        "Reactions of Methane in Slowly Reacting Hydrogen-Oxygen
        Mixtures", Eleventh Symposium (International) on Combus-
        tion, ʾhe Combustion Institute, Pittsburgh, 889 (1967).

169.   Hoare, D. E., "Reactions of Hydroxyl Radicals", Nature,
        194, 283 (1962).

170.   Blundell, R. V., Cook, W. G. A., Hoare, D. E. and Milne,
        G. S., "Rates of Radical Reactions in Methane Oxidation,
        Tenth Symposium (International) on Combustion, The Com-
        bustion Institute, 445 (1965).

171.   Greiner, N. R., Hydroxyl Radical Kinetics by Kinetic
        Spectroscopy I. Reactions with H_2, CO and CH_4 at 300K,
        J. Chem. Phys., 46, 2795 (1967).

172.   Drysdale, D. D. and Lloyd, A. C., "Gas Phase Reactions
        of the Hydroxyl Radical", Oxidation and Combustion Reviews,
        Elsevier Publishing Co., Amsterdam, 4, 157 (1970).

173.   Greiner, N. R., Hydroxyl Radical Kinetics by Kinetic
        Spectroscopy VI. Reactions with Alkanes in the Range
        300-500K, J. Chem. Phys., 53, 3, 1070 (1970).

174.   Herron, J. T., "Evaluation of Rate Data for the Reaction
        of Atomic Oxygen O^3P with Methane and Ethane", Int. J.
        Chem. Kinet, 1, 527 (1969).

175.   Kurylo, M. F. and Timmons, R. B., "ESR Studies of Reac-
        tion of H Atoms with CH_4", J. Chem. Phys., 50, 5076 (1969).

176.   Walker, R. W., "Activation Energies for the Reversible
        Reaction between Hydrogen Atoms and Methane to Give
        Hydrogen and Methyl Radicals", J. Chem. Soc. A, 2391
        (1968).

177.   Edelman, R. B. and Fortune, O. F., "A Quasi-Global Chemical Kinetic Model for the Finite Rate Combustion of Hydrocarbon Fuels with Application to Turbulent Burning and Mixing in Hypersonic Engines and Nozzles", AIAA 7th Aerospace Sciences Meeting, New York, No. 69-86 (1969).

178.   Hammond, P. C. and Mellor, A. M., "Analytical Calculations for the Performance and Pollutant Emissions of Gas Turbine Combustion", AIAA/SAE 7th Propulsion Joint Specialist Conference, AIAA Paper No. 71-711 (1971).

APPENDICES

List of Figures

APPENDIX A

Thermal Analysis Technique

This appendix will present a simple development of the thermal analysis equations for reactions occurring in the turbulent flow reactor.

Consider a one-dimensional flow of a reacting ideal gas mixture through a cylinderical tube of cross-sectional area $\underline{A}$. Let the wall of the tube be adiabatic, (i.e., it prevents energy exchange with the surrounding environment), and let the physical properties, Cp, D and T be constant and the same for all species in the reacting flow. The equations of conservation (in differential form) for energy and any of the reacting species, A, can be derived using the differential volume of Figure A-1.

		Convective Term	Diffusive Term	Source/Sink
A-1	energy	$\dot{m}\,\overline{C_p}\,\dfrac{dT}{dx}$	$-\lambda\,A\dfrac{d^2T}{dx^2}$	$-\dfrac{dQ}{dt}\cdot\underline{A} = 0$
A-2	species	$\dot{m}\,\dfrac{d(a_j/\rho)}{dx}$	$-AD\rho\dfrac{d^2(a_j/\rho)}{dx^2}$	$-\dfrac{da_j}{dt}\cdot\underline{A} = 0$

$\dfrac{dQ}{dt}$ and $\dfrac{da}{dt}j$ represent the time gradient of energy release and species Aj per unit volume due to chemical reaction. If the gradients of energy and species are sufficiently small for the diffusive terms to be neglected, Eqns. A-1 and A-2 can be

$\dot{m}$ = CONSTANT

$x = x_0$
$T = T_0$
$\frac{a}{\rho} = (\frac{a}{\rho})_0$

$x = x$
$T = T$
$\frac{a}{\rho} = \frac{a}{\rho}$

$x = x_f$
$T = T_f$
$(\frac{a}{\rho}) = 0$

$\dot{m} C_p T \longrightarrow \qquad \dot{m} C_p (T + \frac{dT}{dx}\Delta x)$

$\underline{A}\lambda\frac{dT}{dx} \longleftarrow \qquad \underline{A}\lambda\frac{d}{dx}(T + \frac{dT}{dx}\Delta x)$

$(\frac{dQ}{dt})$

$\dot{m}(\frac{a_j}{\rho}) \longrightarrow \qquad \dot{m}(\frac{a_j}{\rho} + \frac{d(a_j/\rho)}{dx}\Delta x)$

$(\frac{da}{dt})$

$\underline{A}D\rho\frac{d(a_j/\rho)}{dx} \longleftarrow \qquad \underline{A}D\rho\frac{d}{dx}(\frac{a_j}{\rho} + \frac{d(a_j/\rho)}{dx}\Delta x)$

Δx
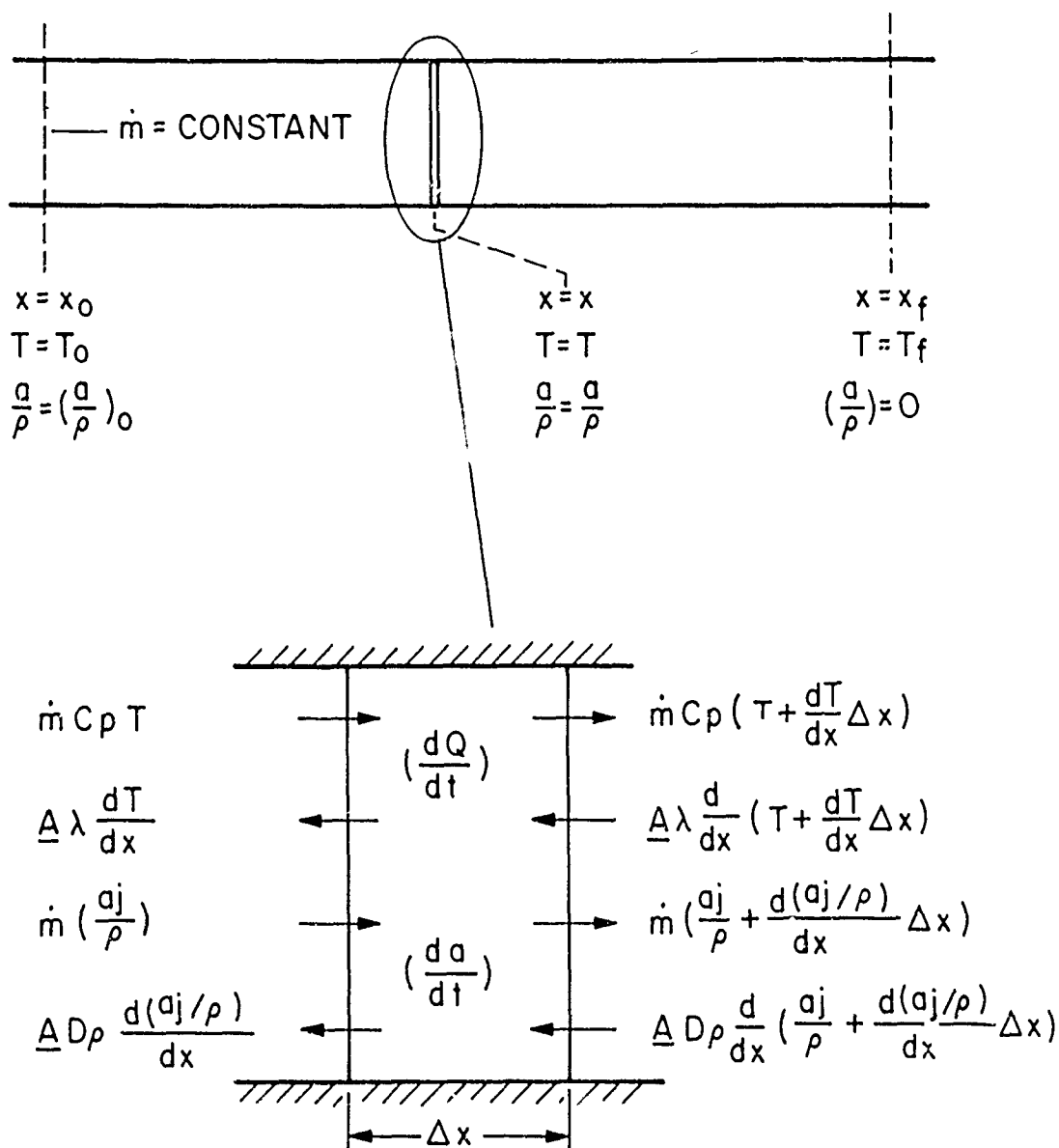
UNITS

MASS FLOW RATE	$\dot{m}$	gm sec^{-1}
CROSSECTIONAL AREA	$\underline{A}$	cm^2
MASS DENSITY SPECIES	A_j a_j	gm cm^{-3}
TOTAL MASS DENSITY	ρ	gm cm^{-3}
TEMPERATURE	T	°K
THERMAL CONDUCTIVITY	λ	cm sec^{-1}
SPECIFIC HEAT	$\bar{C}_p$	k cal gm^{-1} °K^{-1}
DIFFUSION COEFFICIENT	D	cm^2 sec^{-1}

DERIVATION OF CONSERVATION EQUATIONS

FIGURE A-1

combined in differential form to give

$$\frac{dQ}{dt} \cdot \frac{1}{\frac{da_j}{dt}} \, d\left(\frac{a_j}{\rho}\right) = C_p \, dT$$

A-3

Equantion A-3 may be integrated over the boundary conditions
of Fig. A-1.

$$\int_{\left(\frac{a}{\rho}\right)_0}^{\left(a/\rho\right)} \frac{dQ}{dt} \frac{1}{\left(\frac{da_j}{dt}\right)} \, d\left(\frac{a_j}{\rho}\right) = C_p \, (T - T_0)$$

A-4

Although $\frac{dQ}{dt}$ and $\frac{da_j}{dt}$ can be easily envisioned as
functions of $\left(\frac{a_j}{\rho}\right)$, such functions will be dependent upon
the kinetic mechanism of the reaction which is liberating heat
and creating (or destroying) the a_j and are, in general,
unknown.

However, if we assume that for the region $X_0 \leq X \leq X_f$
the occurring chemical reaction adheres to a fixed stoichio-
metric relation,

$$A_1 + \alpha A_2 \longrightarrow \sum_{i=3}^{N} \alpha_i P_i$$

A-5
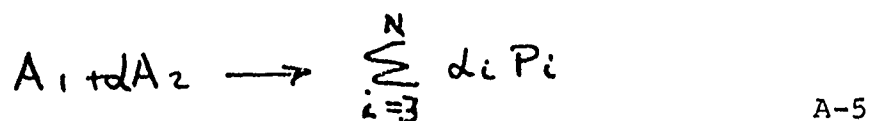
where A_1, A_2 are reactants, and P_i are fixed products
$(\alpha_i, i = 0, 1, 2 \ldots$ are constants), the energy release per
unit time will be related to the rate of disappearance of A_1
or A_2 by a constant, the heat of reaction per mole <u>disappearance</u>
of A_1 or A_2 by a constant, the heat of reaction per mole

<u>disappearance</u> of A_1 or A_2 (Q_j). Then Eqn. A-4 can be integrated, and expressing densities in (moles/cm^3) and in (kcal/mole$^\circ$K), one obtains

$$\left[\frac{[A_j]_0}{[\rho]_0} - \frac{[A_j]}{[\rho]} \right] Q_j = C_p (T - T_0) \qquad \text{A-6}$$

Further, if we choose $[A_1]$ to represent the reactant (A or B) not in excess (of the stoichiometric value), and assume that at $T = T_f$, $[A_1]$ has disappeared, then

$$[A_1] = [A_1]_0 \cdot \frac{[\rho]}{[\rho]_0} \left(\frac{T_f - T}{T_f - T_0} \right) \qquad \text{A-7}$$

For a perfect gas and a constant pressure flow,

$$\frac{[\rho]}{[\rho]_0} = \frac{T_0}{T} \qquad \text{A-8}$$

substitution of A8 and differentiation of A-7 with respect to time to give,

$$\frac{d[A_1]}{dt} = -[A_1]_0 \frac{T_0 T_f}{T^2 (T_f - T_0)} \frac{dT}{dt}$$

Since $\frac{d}{dt}$ in a steady, one dimensional flow is

$$\frac{d}{dt} = \frac{\partial}{\partial t}^{0} + V \frac{d}{dx} \qquad ,$$

$$\frac{d[A_1]}{dt} = -[A_1]_0 \frac{T_0 T_f}{T^2 (T_f - T_0)} \frac{dT}{dx} \cdot V \qquad \text{A-9}$$

Thus using Eqns. A-5, A-7 and A-9, the concentrations and rate of appearance and disappearance of all P_i and A_i as functions of χ can be developed. These concentrations and rates are employable in the usual manner in the expressions for empirical overall rate correlations:

$$\frac{1}{[A_1]^{m_1}} \frac{d[A_1]}{dt} = R_{ov} [A_2]^{m_2} \prod_{i=3}^{N} [P_i]^{n_i}$$

$$R_{ov} = 10^A e^{-E/RT}$$

A-10

where kov, n_i, i = 0, 1....n must be experimentally determined.

Summarizing the assumptions necessary to develop Equations A-7, A-9 and apply A-10 are:

A - I) one dimensional, steady flow

A - II) adiabatic tube wall

A-III) ideal gas (i.e., $P = \rho RT$ and Cp = constant)

A - IV) constant pressure

A - V) longitudinal diffusion effects of energy or species are negligible in comparison to convection effects

A - VI) energy release and reactant disappearance are proportional (Eqn. A-5).

APPENDIX B

Summary of Chemical Analysis Data Reduction Methods

        Because of the quantity of data and character of the necessary calculations, computer reduction techniques were mandatory. A computer program was written in Fortran IV for an IBM 360/91 computing system to calculate temperature, chemical concentration and concentration-time gradient profiles as functions of distance from the fuel injection point through the turbulent flow reactor.

        Inputs to the program include:

(i)   flow parameters and orifice calibrations for calculating carrier and reactant flow rates

(ii) positions at which the reaction was sampled for chemical composition and temperature

(iii) gas chromatograph analysis system set-up conditions and calibration information reaction

(iv) temperature and gas chromatograph analysis results (peak areas and retention times) for each sampled position in the flow reactor

Output of the data reduction program included listing of:

(i)   flow and orifice parameter input and calculated initial concentration of reactants

(ii) the position, temperature and carrier velocity at each sampled location in the flow reactor.

(iii) the mole percent of each specie and its gradient (with time) at each sampled location in the flow reactor.

The program also produces punched card output of
the position, temperature, concentration (mole cm^{-3}) and
concentration time gradient (mole cm^{-3} sec^{-1}) at each sampled
location in the flow reactor. This punched output was used
in other simple linear least square computer programs to ob-
tain the overall rate correlation expressions and other re-
sults.

B1   Calculation Procedures

While a source listing of the program is considered
too lengthy for reproduction here, it is worthwhile to describe
some of the more important features of the calculational tech-
niques that are employed.

B1.1   Flow Rate Calculations

Flow rate calculations for the carrier gas and
oxygen require input of the supply pressure, supply tempera-
ture, molecular weight of the gas and calibration information
for the employed critical orifices. Calculation of fuel flow
rate requires input of the fuel supply pressure, supply tem-
perature, pressure drop across the non-critical orifice, fuel
molecular weight and calibration information for the employed
orifice.

From these data, mass and molar flow rates and
initial mole fractions of each reactant specie are calculated.
The flow through the reactor is assumed to be one dimensional,
and the flow velocity at each longitudinal position is calcu-
lated using the assumptions:

(i)   constant pressure reaction zone (1 atmosphere)

(ii)   no Rayleigh or Fanno effects (Mach No 1)

(iii)   ideal gas

(iv)   fluid properties are those of the inert carrier
gas

B1.2   Reduction of Gas Chromatograph Chemical Analysis Data

The identity and mole percent of every diluted chemical constituent of an analyzed sample are calculated by comparison with calibration input data. Chemical identification is obtained by matching the retention time (or assigned peak number) of an unknown specie to that of a known calibration compound. Concentration is calculated from responses of the GC instrument to known concentrations of the identified compound. The computer program is capable of identifying and evaluating up to fourteen chemical constituents in a particular sample, and a listing of these data, together with input temperature and distance values, are produced.

B1.3   Calculation of Reaction Parameter Profiles

The gradient of specie concentrations with time at each sampled position are obtained by applying the equation

$$\frac{d}{dt} [A] = \frac{d[A]}{dx} v \qquad\qquad B-1$$

This required that carrier flow velocity, v, and gradient of specie concentration with distance be obtained at each sampled position. While the flow velocity can be obtained directly from the incremental measurements of the reaction temperature (see Section B1.1), the incremental data for the specie concentrations versus distance must be approxi-

mated by analytical functions to obtain derivatives with
distance.

The original incremental data are smoothed using
a five point second order smoothing routine (IBM Scientific
Subroutine Number DSE35), and the smoothed data are used to
calculate oxygen and water concentration profiles using the
initial concentrations of reactants and conservation equations
for hydrogen and oxygen atoms. The adjusted incremental data
are also listed for comparison with the original input data.

A second-order fitting function (IBM Scientific
Subroutine Number DDGT3) is applied to the smoothed incre-
mental data to obtain the concentration-distance gradients
necessary for application of Equation B-1.

B2   Sample Output

Computer output of three separate experiments are
reproduced here, and they correspond to the results presented
in Figures 5.1, 6.1 and 6.2, respectively.

CHEMICAL KINETICS FLOW REACTOR DATA SHEET   APRIL 15, 1971 *

CARBON MONOXIDE/AIR/WATER RUN
FREDERICK L DRYER.

RUN NUMBER   1

PROBE BASE   (MV)   2.650
OXIDIZER INJECTION PORT   1

		CARRIER	DILUENT	FUEL	OXIDIZER
CHEMICAL		AIR	N2	CO	O2
MOLECULAR WEIGHT		28.89	28.01	28.01	32.00
INPUT					
PRESSURE	(PSIG)	292.0	0.0	4.4	0.0
TEMPERATURE	(DEGC)	-10.	18.	20.	20.
MANOMETER	(INHG)		0.00	3.80	
CORRECTED					
PRESSURE	(ATMA)	20.88	1.00	1.30	1.00
TEMPERATURE	(DEGK)	263.	291.	293.	293.
MANOMETER	(INHG)		0.00	3.80	
CALCULATED					
FLOW RATE	(GM/SEC)	31.1368	0.0000	0.3229	0.0000
FLOW RATE	(MOLE/SEC)	1.07777	0.00000	0.01152	0.00000
MOLE FRACTION		0.98942	0.00000	0.01058	0.20580

EQUIVALENCE RATIO   0.026

---

* Experimental results dated April 15, 1971, appear in the text as
  Figure 5.1

CHROMATOGRAPH ANALYSIS DATA SHEET   APRIL 15, 1971

CHROMATOGRAPH CALIBRATION DATA

TABLE NUMBER   14   CO   3.00   MINUTES

0.00	0.0000
27.56	0.0300
55.11	0.0360
82.67	0.0400
110.22	0.0440
137.78	0.0460
165.33	0.0500
1377.78	0.1430
2755.56	0.2480
4133.33	0.3540
4767.11	0.4010

TABLE NUMBER   15   CH4   1.00   MINUTES

0.00	0.0000
120000.00	1.0100

TABLE NUMBER   16   CO2   2.00   MINUTES

0.00	0.0000
33490.00	1.9900

TABLE NUMBER   17   C2H4   4.00   MINUTES

0.00	0.0000
229700.00	0.9900

TABLE NUMBER   18   C2H6   5.00   MINUTES

0.00	0.0000
228700.00	0.0990

CHROMATOGRAPH ANALYSIS DATA SHEET   APRIL 15, 1971

COLUMN CONDITIONS

	FLOW RATE (CC/MIN)	TYPE	CARRIER GAS
A	30.0	80/100 MESH, 6FT B, 6FT O, 1/8 S.S.	HELIUM
B	30.0	80/100 MESH, 12FT B, 1/8 S.S.	HELIUM

DETECTOR CONDITIONS

THERMAL CONDUCTIVITY

BRIDGE CURRENT	270.	MA
OVEN TEMP	130.	DEGC
AUXILIARY TEMP	125.	DEGC

FLAME IONIZATION

HYDROGEN	11.	PSI
OXYGEN	21.	PSI
AUXILIARY	40.	CC/MIN
TEMPERATURE	250.	DEGC

TEMPERATURE PROGRAM(S)

START DEGC	PINJ MIN	RT1 D/M	IV1 MIN	TEMP1 DEGC	RT2 D/M	LV2 MIN	TEMP2 DEGC	RT3 D/M	LV3 MIN	TEMP3 DEGC	PCV DEGC	COMMENTS
-95.	0.	4.	0.	-62.	30.	2.	40.	8.	0.	65.	160.	GENERAL PG
140.	0.	0.	0.	0.	0.	0.	0.	0.	0.	0.	0.	H2O & CH2O

MISCELLANEOUS

SAMPLE VOL	0.5	CC	INJ PORT TEMP	160.0	DEGC
SAMPLE TEMP	110.0	DEGC	SPLIT RATIO	2.0	TC/FID
SAMPLE PRESS	38.0	CM HG			

INTEGRATOR PARAMETERS

PROG	INPT	NOISE	UP	DOWN	RRST	PSUM	FNT	PHR
1	TC	3.00	0.10	0.03	0.00	0.00	NO	1000.00
2	TC	3.00	0.10	0.03	0.10	0.00	NO	0.10
3	TC	1.00	0.03	0.01	0.00	0.00	NO	0.10
4	FID	4.00	0.10	0.03	0.10	0.00	NO	0.10

COMMENTS

GAS CHROMATOGRAPH/FLOW REACTOR DATA SHEET   APRIL 15, 1971

CARBON MONOXIDE/AIR/WATER RUN
FREDERICK L DRYER.

			CHEMICAL DATA, MOLAR PERCENT SPECIES			
	CHEMICAL SPECIE		CO	CH4	CO2	C2H4
AV RETENTION TIME (MIN)			3.00	1.00	2.00	4.00
POSITION (CM)	TEMP (DEGK)	VELOCITY (CM/SEC)				
114.73	1119.	1233.	0.000E-01	0.000E-01	1.373E 00	0.000E-01
110.15	1119.	1233.	1.633E-02	0.000E-01	1.339E 00	0.000E-01
105.52	1119.	1233.	3.227E-02	0.000E-01	1.328E 00	0.000E-01
100.84	1119.	1233.	3.773E-02	0.000E-01	1.295E 00	0.000E-01
96.16	1119.	1233.	5.113E-02	0.000E-01	1.298E 00	0.000E-01
91.47	1119.	1233.	5.473E-02	0.000E-01	1.281E 00	0.000E-01
86.76	1119.	1233.	6.785E-02	0.000E-01	1.276E 00	0.000E-01
82.07	1117.	1231.	8.649E-02	0.000E-01	1.255E 00	0.000E-01
77.35	1114.	1228.	1.167E-01	0.000E-01	1.221E 00	0.000E-01
72.58	1109.	1222.	1.604E-01	0.000E-01	1.160E 00	0.000E-01
67.82	1104.	1217.	2.251E-01	0.000E-01	0.000E-01	0.000E-01
63.05	1095.	1207.	3.169E-01	0.000E-01	1.012E 00	0.000E-01
58.09	1087.	1197.	4.284E-01	0.000E-01	9.103E-01	0.000E-01
53.54	1078.	1188.	5.241E-01	0.000E-01	7.974E-01	0.000E-01
48.74	1069.	1178.	6.714E-01	0.000E-01	6.744E-01	0.000E-01
43.93	1059.	1167.	7.935E-01	0.000E-01	5.480E-01	0.000E-01
39.14	1048.	1155.	9.381E-01	0.000E-01	4.189E-01	0.000E-01
34.30	1039.	1145.	1.057E 00	0.000E-01	2.950E-01	0.000E-01
29.46	1031.	1136.	1.211E 00	0.000E-01	1.900E-01	0.000E-01
24.63	1028.	1133.	1.234E 00	0.000E-01	1.346E-01	0.000E-01

GAS CHROMATOGRAPH/FLOW REACTOR DATA SHEET   APRIL 15, 1971

CARBON MONOXIDE/AIR/WATER RUN
FREDERICK L DRYER.

			CHEMICAL DATA, MOLAR PERCENT SPECIES			
	CHEMICAL SPECIE		C2H6	H2O	O2	CTOT
AV RETENTION TIME (MIN)			5.00			
POSITION (CM)	TEMP (DEGK)	VELOCITY (CM/SEC)				
114.73	1119.	1233.	0.000E-01	0.000E-01	0.000E-01	1.373E 00
110.15	1119.	1233.	0.000E-01	0.000E-01	0.000E-01	1.356E 00
105.52	1119.	1233.	0.000E-01	0.000E-01	0.000E-01	1.360E 00
100.84	1119.	1233.	0.000E-01	0.000E-01	0.000E-01	1.333E 00
96.16	1119.	1233.	0.000E-01	0.000E-01	0.000E-01	1.349E 00
91.47	1119.	1233.	0.000E-01	0.000E-01	0.000E-01	1.335E 00
86.76	1119.	1233.	0.000E-01	0.000E-01	0.000E-01	1.344E 00
82.07	1117.	1231.	0.000E-01	0.000E-01	0.000E-01	1.341E 00
77.35	1114.	1228.	0.000E-01	0.000E-01	0.000E-01	1.338E 00
72.58	1109.	1222.	0.000E-01	0.000E-01	0.000E-01	1.320E 00
67.82	1104.	1217.	0.000E-01	0.000E-01	0.000E-01	2.251E-01
63.05	1095.	1207.	0.000E-01	0.000E-01	0.000E-01	1.329E 00
58.09	1087.	1197.	0.000E-01	0.000E-01	0.000E-01	1.339E 00
53.54	1078.	1188.	0.000E-01	0.000E-01	0.000E-01	1.322E 00
48.74	1069.	1178.	0.000E-01	0.000E-01	0.000E-01	1.346E 00
43.93	1059.	1167.	0.000E-01	0.000E-01	0.000E-01	1.341E 00
39.14	1049.	1155.	0.000E-01	0.000E-01	0.000E-01	1.357E 00
34.30	1039.	1145.	0.000E-01	0.000E-01	0.000E-01	1.352E 00
29.46	1031.	1136.	0.000E-01	0.000E-01	0.000E-01	1.401E 00
24.63	1029.	1133.	0.000E-01	0.000E-01	0.000E-01	1.369E 00

GAS CHROMATOGRAPH/FLOW REACTOR DATA SHEET   APRIL 15, 1971

CARBON MONOXIDE/AIR/WATER RUN
FREDERICK L DRYER.

5PT 2ND ORDER SMOOTHING PERFORMED 4 TIMES
MOLAR PERCENT SPECIES

		CHEMICAL SPECIE	CO	CH4	CO2	C2H4
	AV RETENTION	TIME (MIN)	3.00	1.00	2.00	4.00
POSITION (CM)	TEMP (DEGK)	VELOCITY (CM/SEC)				
114.73	1119.	1233.	3.533E-03	0.000E-01	1.372E 00	0.000E-01
110.15	1119.	1233.	1.785E-02	0.000E-01	1.344E 00	0.000E-01
105.52	1119.	1233.	2.999E-02	0.000E-01	1.321E 00	0.000E-01
100.84	1119.	1233.	3.985E-02	0.000E-01	1.304E 00	0.000E-01
96.16	1120.	1233.	4.798E-02	0.000E-01	1.293E 00	0.000E-01
91.47	1120.	1233.	5.611E-02	0.000E-01	1.285E 00	0.000E-01
86.76	1119.	1233.	6.769E-02	0.000E-01	1.275E 00	0.000E-01
82.07	1117.	1231.	8.614E-02	0.000E-01	1.254E 00	0.000E-01
77.35	1114.	1228.	1.158E-01	0.000E-01	1.217E 00	0.000E-01
72.58	1110.	1223.	1.619E-01	0.000E-01	1.163E 00	0.000E-01
67.82	1104.	1216.	2.292E-01	0.000E-01	1.093E 00	0.000E-01
63.05	1096.	1207.	3.165E-01	0.000E-01	1.009E 00	0.000E-01
58.09	1087.	1198.	4.203E-01	0.000E-01	9.101E-01	0.000E-01
53.54	1078.	1188.	5.363E-01	0.000E-01	7.975E-01	0.000E-01
48.74	1069.	1178.	6.628E-01	0.000E-01	6.749E-01	0.000E-01
43.93	1059.	1166.	7.971E-01	0.000E-01	5.464E-01	0.000E-01
39.14	1048.	1155.	9.396E-01	0.000E-01	4.158E-01	0.000E-01
34.30	1039.	1144.	1.081E 00	0.000E-01	2.923E-01	0.000E-01
29.46	1031.	1136.	1.195E 00	0.000E-01	1.919E-01	0.000E-01
24.63	1028.	1133.	1.238E 00	0.000E-01	1.342E-01	0.000E-01

GAS CHROMATOGRAPH/FLOW REACTOR DATA SHEET   APRIL 15, 1971

CARBON MONOXIDE/AIR/WATER RUN
FREDERICK I DRYER.

5PT 2ND ORDER SMOOTHING PERFORMED 4 TIMES
MOLAR PERCENT SPECIES

		CHEMICAL SPECIE	C2H6	H20	02	CTOT
	AV RETENTION TIME (MIN)		5.00			
POSITION (CM)	TEMP (DEGK)	VELOCITY (CM/SEC)				
114.73	1119.	1233.	0.000E-01	2.480E 00	1.989E 01	1.376E 00
110.15	1119.	1233.	0.000E-01	2.480E 00	1.991E 01	1.362E 00
105.52	1119.	1233.	0.000E-01	2.480E 00	1.992E 01	1.351E 00
100.84	1119.	1233.	0.000E-01	2.480E 00	1.993E 01	1.344E 00
96.16	1120.	1233.	0.000E-01	2.480E 00	1.993E 01	1.341E 00
91.47	1120.	1233.	0.000E-01	2.480E 00	1.994E 01	1.341E 00
86.76	1119.	1233.	0.000E-01	2.480E 00	1.994E 01	1.342E 00
82.07	1117.	1231.	0.000E-01	2.480E 00	1.995E 01	1.340E 00
77.35	1114.	1228.	0.000E-01	2.480E 00	1.997E 01	1.333E 00
72.58	1110.	1223.	0.000E-01	2.480E 00	2.000E 01	1.325E 00
67.82	1104.	1216.	0.000E-01	2.480E 00	2.003E 01	1.322E 00
63.05	1096.	1207.	0.000E-01	2.480E 00	2.008E 01	1.326E 00
58.09	1087.	1198.	0.000E-01	2.480E 00	2.012E 01	1.330E 00
53.54	1078.	1188.	0.000E-01	2.480E 00	2.018E 01	1.334E 00
48.74	1069.	1178.	0.000E-01	2.480E 00	2.024E 01	1.338E 00
43.93	1059.	1166.	0.000E-01	2.480E 00	2.031E 01	1.343E 00
39.14	1048.	1155.	0.000E-01	2.480E 00	2.037E 01	1.355E 00
34.30	1039.	1144.	0.000E-01	2.480E 00	2.043E 01	1.374E 00
29.46	1031.	1136.	0.000E-01	2.480E 00	2.048E 01	1.386E 00
24.63	1028.	1133.	0.000E-01	2.480E 00	2.051E 01	1.372E 00

GAS CHROMATOGRAPH/FLOW REACTOR DATA SHEET   APRIL 15, 1971

CARBON MONOXIDE/AIR/WATER RUN
FREDERICK L DRYER.

SMOOTHED FIRST TIME DERIVATIVE OF CHEMICAL DATA
DIMENSIONS ARE (MOLAR PERCENT/SEC)

POSITION (CM)	1000/T 1/(DEGK)	VELOCITY (CM/SEC)	CO 3.00	CH4 1.00	CO2 2.00	C2H4 4.00
114.73	0.8934	1233.	-4.167E 00	0.000E-01	8.281E 00	0.000E-01
110.15	0.8933	1233.	-3.546E 00	0.000E-01	6.833E 00	0.000E-01
105.52	0.8934	1233.	-2.918E 00	0.000E-01	5.316E 00	0.000E-01
100.84	0.8933	1233.	-2.371E 00	0.000E-01	3.726E 00	0.000E-01
96.16	0.8932	1233.	-2.140E 00	0.000E-01	2.512E 00	0.000E-01
91.47	0.8932	1233.	-2.584E 00	0.000E-01	2.381E 00	0.000E-01
86.76	0.8937	1233.	-3.942E 00	0.000E-01	4.055E 00	0.000E-01
82.07	0.8951	1231.	-6.288E 00	0.000E-01	7.501E 00	0.000E-01
77.35	0.8975	1228.	-9.784E 00	0.000E-01	1.176E 01	0.000E-01
72.58	0.9011	1223.	-1.455E 01	0.000E-01	1.590E 01	0.000E-01
67.82	0.9062	1216.	-1.971E 01	0.000E-01	1.961E 01	0.000E-01
63.05	0.9126	1207.	-2.365E 01	0.000E-01	2.267E 01	0.000E-01
58.09	0.9198	1198.	-2.792E 01	0.000E-01	2.691E 01	0.000E-01
53.54	0.9275	1188.	-3.078E 01	0.000E-01	2.985E 01	0.000E-01
48.74	0.9357	1178.	-3.195E 01	0.000E-01	3.077E 01	0.000E-01
43.93	0.9446	1166.	-3.364E 01	0.000E-01	3.148E 01	0.000E-01
39.14	0.9541	1155.	-3.410E 01	0.000E-01	3.048E 01	0.000E-01
34.30	0.9629	1144.	-3.014E 01	0.000E-01	2.647E 01	0.000E-01
29.46	0.9696	1136.	-1.840E 01	0.000E-01	1.857E 01	0.000E-01
24.63	0.9724	1133.	-2.081E 00	0.000E-01	8.545E 00	0.000E-01

GAS CHROMATOGRAPH/FLOW REACTOR DATA SHEET   APRIL 15, 1971

CARBON MONOXIDE/AIR/WATER RUN
FREDERICK L DRYER.

SMOOTHED FIRST TIME DERIVATIVE OF CHEMICAL DATA
DIMENSIONS ARE (MOLAR PERCENT/SEC)

POSITION (CM)	1000/T 1/(DEGK)	VELOCITY (CM/SEC)	C2H6	H2O	O2	CTOT
AV RETENTION TIME (MIN)			5.00			
114.73	0.8934	1233.	0.000E-01	0.000E-01	-4.140E 00	0.000E-01
110.15	0.8933	1233.	0.000E-01	0.000E-01	-3.416E 00	0.000E-01
105.52	0.8934	1233.	0.000E-01	0.000E-01	-2.658E 00	0.000E-01
100.84	0.8933	1233.	0.000E-01	0.000E-01	-1.863E 00	0.000E-01
96.16	0.8932	1233.	0.000E-01	0.000E-01	-1.256E 00	0.000E-01
91.47	0.8932	1233.	0.000E-01	0.000E-01	-1.191E 00	0.000E-01
86.76	0.8937	1233	0.000E-01	0.000E-01	-2.027E 00	0.000E-01
82.07	0.8951	1231.	0.000E-01	0.000E-01	-3.750E 00	0.000E-01
77.35	0.8975	1228.	0.000E-01	0.000E-01	-5.879E 00	0.000E-01
72.58	0.9011	1223.	0.000E-01	0.000E-01	-7.950E 00	0.000E-01
67.82	0.9062	1216.	0.000E-01	0.000E-01	-9.806E 00	0.000E-01
63.05	0.9126	1207.	0.000E-01	0.000E-01	-1.134E 01	0.000E-01
58.09	0.9198	1198.	0.000E-01	0.000E-01	-1.346E 01	0.000E-01
53.54	0.9275	1188.	0.000E-01	0.000E-01	-1.493E 01	0.000E-01
48.74	0.9357	1178.	0.000E-01	0.000E-01	-1.538E 01	0.000E-01
43.93	0.9446	1166.	0.000E-01	0.000E-01	-1.574E 01	0.000E-01
39.14	0.9541	1155.	0.000E-01	0.000E-01	-1.524E 01	0.000E-01
34.30	0.9629	1144.	0.000E-01	0.000E-01	-1.324E 01	0.000E-01
29.46	0.9696	1136.	0.000E-01	0.000E-01	-9.283E 00	0.000E-01
24.63	0.9724	1133.	0.000E-01	0.000E-01	-4.272E 00	0.000E-01

CHEMICAL KINETICS FLOW REACTOR DATA SHEET   JANUARY 15, 1971*

METHANE/OXYGEN/AIR REACTION STUDY
FREDERICK L DRYER

RUN NUMBER   1

PROBE BASE   (EV)   .   3.800
OXIDIZER INJECTION PORT   1

		CARRIER	DILUENT	FUEL	OXIDIZER
CHEMICAL		AIR	N2	CH4	O2
MOLECULAR WEIGHT		28.89	28.01	16.01	32.00
INPUT					
PRESSURE	(PSIG)	151.0	0.0	1.0	17.5
TEMPERATURE	(DEGC)	-4.	36.	34.	36.
MANOMETER	(INHG)		0.00	1.10	
CORRECTED					
PRESSURE	(ATMA)	11.28	1.00	1.07	2.19
TEMPERATURE	(DEGK)	269.	309.	307.	309.
MANOMETER	(INHG)		0.00	1.10	
CALCULATED					
FLOW RATE	(GM/SEC)	16.6499	0.0000	0.0584	0.8166
FLOW RATE	(MOLE/SEC)	0.57632	0.00000	0.00355	0.02552
MOLE FRACTION		0.95183	0.00000	0.00603	0.24013

EQUIVALENCE RATIO   0.050

---

*Experimental results dated January 15, 1971, appear in the text as
Figure 6.1

CHROMATOGRAPH ANALYSIS DATA SHEET   JANUARY 15, 1971

CHROMATOGRAPH CALIBRATION DATA

TABLE NUMBER 14   CO   3.00   MINUTES

0.00	0.0000
26.42	0.0300
52.83	0.0360
79.25	0.0400
105.67	0.0440
132.08	0.0460
158.50	0.0500
1320.82	0.1430
2641.65	0.2480
3962.47	0.3540
4570.05	0.4010

TABLE NUMBER 15   CH4   1.00   MINUTES

0.00	0.0000
236300.00	2.0200

TABLE NUMBER 16   CO2   2.00   MINUTES

0.00	0.0000
108600.00	6.6400

TABLE NUMBER 17   C2H4   4.00   MINUTES

0.00	0.0000
446300.00	1.9900

TABLE NUMBER 18   C2H6   5.00   MINUTES

0.00	0.0000
443800.00	1.9900

CHROMATOGRAPH ANALYSIS DATA SHEET   JANUARY 15, 1971

COLUMN CONDITIONS

	FLOW RATE (CC/MIN)	TYPE	CARRIER GAS
A	30.0	80/100 MESH, 6FT R, 6FT Q, 1/8 S.S.	HELIUM
B	30.0	80/100 MESH, 12FT R, 1/8 S.S.	HELIUM

DETECTOR CONDITIONS

THERMAL CONDUCTIVITY

BRIDGE CURRENT	270.	MA
OVENTEMP	130.	DEGC
AUXILIARY TEMP	125.	DEGC

FLAME IONIZATION

HYDROGEN	11.	PSI
OXYGEN	21.	PSI
AUXILIARY	40.	CC/MIN
TEMPERATURE	250.	DEGC

TEMPERATURE PROGRAM(S)

START DEGC	PINJ MIN	RT1 D/M	LV1 MIN	TEMP1 DEGC	RT2 D/M	LV2 MIN	TEMP2 DEGC	RT3 D/M	LV3 MIN	TEMP3 DEGC	RCV DEGC	COMMENTS
-95.	0.	4.	0.	-62.	36.	2.	40.	8.	0.	65.	160.	GENERAL PG
140.	0.	0.	0.	0.	0.	0.	0.	0.	0.	0.	0.	H2O & CH2O

MISCELLANEOUS

SAMPLE VOL	0.5	CC	INJ PORT TEMP	160.0	DEGC
SAMPLE TEMP	110.0	DEGC	SPLIT RATIO	2.0	TC/FID
SAMPLE PRESS	38.0	CM HG			

INTEGRATOR PARAMETERS

PROG	INPT	NOISE	UP	DOWN	BRST	PSUM	PNT	RHR
1	TC	3.00	0.10	0.03	0.00	0.00	NO	1000.00
2	TC	3.00	0.10	0.03	0.10	0.00	NO	0.10
3	TC	1.00	0.03	0.01	0.00	0.00	NO	0.10
4	FID	4.00	0.10	0.03	0.10	0.00	NO	0.10

COMMENTS

GAS CHROMATOGRAPH/FLOW REACTOR DATA SHEET   JANUARY 15, 1971

METHANE/OXYGEN/AIR REACTION STUDY
FREDERICK L DRYER

			CHEMICAL DATA, MOLAR PERCENT SPECIES			
	CHEMICAL SPECIE		CO	CH4	CO2	C2H4
AV RETENTION TIME (MIN)			3.00	1.00	2.00	4.00
POSITION (CM)	TEMP (DEGK)	VELOCITY (CM/SEC)				
114.59	1196.	732.	0.000E-01	0.000E-01	5.382E-01	0.000E-01
110.70	1196.	732.	3.996E-02	0.000E-01	5.323E-01	0.000E-01
106.60	1196.	732.	5.300E-02	0.000E-01	5.258E-01	0.000E-01
102.43	1193.	731.	8.997E-02	1.923E-03	4.703E-01	0.000E-01
98.28	1186.	726.	1.494E-01	6.856E-03	4.108E-01	0.000E-01
94.12	1175.	720.	2.384E-01	2.714E-02	2.864E-01	1.177E-03
89.94	1163.	712.	2.902E-01	7.406E-02	1.701E-01	3.193E-03
85.78	1149.	703.	3.029E-01	9.856E-02	1.352E-01	4.432E-03
81.61	1138.	697.	2.765E-01	1.586E-01	8.535E-02	6.590E-03
77.42	1129.	691.	2.204E-01	2.288E-01	6.536E-02	7.874E-03
73.26	1119.	686.	1.595E-01	2.946E-01	7.074E-02	7.072E-03
69.07	1113.	682.	1.266E-01	3.403E-01	4.567E-02	6.461E-03
64.85	1109.	679.	1.005E-01	3.787E-01	4.200E-02	5.364E-03
60.66	1106.	677.	7.604E-02	4.015E-01	4.506E-02	4.151E-03
56.42	1102.	675.	5.660E-02	4.306E-01	4.017E-02	2.733E-03
52.23	1101.	674.	3.769E-02	4.627E-01	3.785E-02	1.436E-03
47.99	1099.	673.	3.150E-02	4.737E-01	3.711E-02	8.784E-04
43.77	1098.	672.	0.000E-01	4.913E-01	3.662E-02	4.503E-04
39.51	1097.	672.	0.000E-01	4.969E-01	3.724E-02	0.000E-01
35.26	1097.	672.	0.000E-01	5.079E-01	3.760E-02	0.000E-01

GAS CHROMATOGRAPH/FLOW REACTOR DATA SHEET   JANUARY 15, 1971

METHANE/OXYGEN/AIR REACTION STUDY
FREDERICK L DRYER

			CHEMICAL DATA, MOLAR PERCENT SPECIES			
		CHEMICAL SPECIE	C2H6	H2O	O2	CTOT
	AV RETENTION TIME (MIN)		5.00	7.00	0.00	0.00
POSITION (CM)	TEMP (DEGK)	VELOCITY (CM/SEC)				
114.59	1196.	732.	0.000E-01	0.000E-01	0.000E-01	5.382E-01
110.70	1196.	732.	0.000E-01	0.000E-01	0.000E-01	5.723E-01
106.60	1196.	732.	0.000E-01	0.000E-01	0.000E-01	5.788E-01
102.43	1193.	731.	0.000E-01	0.000E-01	0.000E-01	5.622E-01
98.28	1186.	726.	0.000E-01	0.000E-01	0.000E-01	5.670E-01
94.12	1175.	720.	3.139E-04	0.000E-01	0.000E-01	5.550E-01
89.94	1163.	712.	1.238E-03	0.000E-01	0.000E-01	5.432E-01
85.78	1149.	703.	1.726E-03	0.000E-01	0.000E-01	5.490E-01
81.61	1138.	697.	3.439E-03	0.000E-01	0.000E-01	5.405E-01
77.42	1129.	691.	5.139E-03	0.000E-01	0.000E-01	5.406E-01
73.26	1119.	686.	5.946E-03	0.000E-01	0.000E-01	5.508E-01
69.07	1113.	682.	6.722E-03	0.000E-01	0.000E-01	5.390E-01
64.85	1109.	679.	6.654E-03	0.000E-01	0.000E-01	5.453E-01
60.66	1106.	677.	5.870E-03	0.000E-01	0.000E-01	5.427E-01
56.42	1102.	675.	4.982E-03	0.000E-01	0.000E-01	5.428E-01
52.23	1101.	674.	4.475E-03	0.000E-01	0.000E-01	5.501E-01
47.99	1099.	673.	3.363E-03	0.000E-01	0.000E-01	5.508E-01
43.77	1098.	672.	2.403E-03	0.000E-01	0.000E-01	5.336E-01
39.51	1097.	672.	1.601E-03	0.000E-01	0.000E-01	5.374E-01
35.26	1097.	672.	8.564E-04	0.000E-01	0.000E-01	5.473E-01

GAS CHROMATOGRAPH/FLOW REACTOR DATA SHEET   JANUARY 15, 1971

METHANE/OXYGEN/AIR REACTION STUDY
FREDERICK L DRYER

5PT 2ND ORDER SMOOTHING PERFORMED 4 TIMES
MOLAR PERCENT SPECIES

		CHEMICAL SPECIE	CO	CH4	CO2	C2H4
	AV RETENTION	TIME (MIN)	3.00	1.00	2.00	4.00
POSITION (CM)	TEMP (DEGK)	VELOCITY (CM/SEC)				
114.59	1196.	732.	4.830E-02	0.000E-01	5.372E-01	0.000E-01
110.70	1196.	732.	3.951E-02	9.387E-04	5.366E-01	0.000E-01
106.60	1195.	732.	5.368E-02	0.000E-01	5.194E-01	0.000E-01
102.43	1192.	730.	9.431E-02	8.186E-04	4.733E-01	0.000E-01
98.28	1185.	726.	1.589E-01	1.021E-02	3.923E-01	3.993E-04
94.12	1175.	720.	2.309E-01	3.126E-02	2.893E-01	1.379E-03
89.94	1162.	712.	2.841E-01	6.348E-02	1.928E-01	2.938E-03
85.78	1150.	704.	2.986E-01	1.066E-01	1.251E-01	4.801E-03
81.61	1138.	697.	2.726E-01	1.624E-01	8.807E-02	6.460E-03
77.42	1128.	691.	2.220E-01	2.270E-01	6.988E-02	7.368E-03
73.26	1120.	686.	1.687E-01	2.897E-01	5.907E-02	7.304E-03
69.07	1114.	682.	1.270E-01	3.399E-01	5.064E-02	6.513E-03
64.85	1109.	679.	9.793E-02	3.766E-01	4.468E-02	5.365E-03
60.66	1105.	677.	7.593E-02	4.058E-01	4.167E-02	4.062E-03
56.42	1102.	675.	5.707E-02	4.329E-01	4.016E-02	2.745E-03
52.23	1100.	674.	3.958E-02	4.573E-01	3.852E-02	1.628E-03
47.99	1099.	673.	2.289E-02	4.762E-01	3.711E-02	8.319E-04
43.77	1098.	673.	8.461E-03	4.891E-01	3.672E-02	3.051E-04
39.51	1097.	672.	0.000E-01	4.984E-01	3.717E-02	0.000E-01
35.26	1097.	672.	1.410E-03	5.076E-01	3.762E-02	0.000E-01

GAS CHROMATOGRAPH/FLOW REACTOR DATA SHEET   JANUARY 15, 1971

METHANE/OXYGEN/AIR REACTION STUDY
FREDERICK L DRYER

5PT 2ND ORDER SMOOTHING PERFORMED 4 TIMES
MOLAR PERCENT SPECIES

	CHEMICAL SPECIE		C_2H_6	H_2O	O_2	CTOT
	AV RETENTION TIME (MIN)		5.00	7.00	0.00	0.00
POSITION (CM)	TEMP (DEGK)	VELOCITY (CM/SEC)				
114.59	1196.	732.	0.000E-01	1.096E 00	2.294E 01	5.855E-01
110.70	1196.	732.	0.000E-01	1.077E 00	2.296E 01	5.770E-01
106.60	1195.	732.	0.000E-01	1.070E 00	2.297E 01	5.731E-01
102.43	1192.	730.	0.000E-01	1.060E 00	2.300E 01	5.684E-01
98.28	1185.	726.	0.000E-01	1.028E 00	2.306E 01	5.621E-01
94.12	1175.	720.	3.519E-04	9.682E-01	2.316E ··	5.549E-01
89.94	1162.	712.	1.028E-03	8.855E-01	2..	5.483E-01
85.78	1150.	704.	2.071E-03	7.839E-01	2.338E 01	5.441E-01
81.61	1138.	697.	3.453E-03	6.624E-01	2.349E 01	5.428E-01
77.42	1128.	691.	4.910E-03	5.281E-01	2.361E 01	5.434E-01
73.26	1120.	686.	6.056E-03	4.010E-01	2.371E 01	5.442E-01
69.07	1114.	682.	6.611E-03	2.997E-01	2.379E 01	5.438E-01
64.85	1109.	679.	6.521E-03	2.272E-01	2.384E 01	5.429E-01
60.66	1105.	677.	5.955E-03	1.741E-01	2.388E 01	5.435E-01
56.42	1102.	675.	5.161E-03	1.299E-01	2.392E 01	5.460E-01
52.23	1100.	674.	4.299E-03	8.852E-02	2.395E 01	5.473E-01
47.99	1099.	673.	3.388E-03	4.981E-02	2.398E 01	5.447E-01
43.77	1098.	673.	2.451E-03	1.819E-02	2.400E 01	5.398E-01
39.51	1097.	672.	1.569E-03	6.636E-04	2.401E 01	5.387E-01
35.26	1097.	672.	8.643E-04	3.673E-03	2.401E 01	5.483E-01

GAS CHROMATOGRAPH/FLOW REACTOR DATA SHEET   JANUARY 15, 1971

METHANE/OXYGEN/AIR REACTION STUDY
FREDERICK L DRYER

SMOOTHED FIRST TIME DERIVATIVE OF CHEMICAL DATA
DIMENSIONS ARE (MOLAR PERCENT/SEC)

CHEMICAL SPECIE			CO	CH4	CO2	C2H4
AV RETENTION TIME (MIN)			3.00	1.00	2.00	4.00
POSITION (CM)	1000/T 1/(DEGK)	VELOCITY (CM/SEC)				
114.59	0.8364	732.	3.691E 00	-3.444E-01	-1.324E 00	0.000E-01
110.70	0.8362	732.	-3.834E-01	-9.052E-03	1.549E 00	0.000E-01
106.60	0.8366	732.	-4.812E 00	1.327E-02	5.560E 00	0.000E-01
102.43	0.8387	730.	-9.242E 00	-8.994E-01	1.117E 01	-3.521E-02
98.28	0.8436	726.	-1.193E 01	-2.657E 00	1.607E 01	-1.204E-01
94.12	0.8511	720.	-1.081E 01	-4.591E 00	1.721E 01	-2.188E-01
89.94	0.8603	712.	-5.766E 00	-6.436E 00	1.400E 01	-2.921E-01
85.78	0.8698	704.	9.637E-01	-8.357E 00	8.862E 00	-2.978E-01
81.61	0.8786	697.	6.381E 00	-1.003E 01	4.613E 00	-2.143E-01
77.42	0.8864	691.	8.595E 00	-1.054E 01	2.395E 00	-6.925E-02
73.26	0.8929	686.	7.805E 00	-9.279E 00	1.581E 00	6.973E-02
69.07	0.8980	682.	5.747E 00	-7.050E 00	1.168E 00	1.570E-01
64.85	0.9018	679.	4.122E 00	-5.322E 00	7.227E-01	1.980E-01
60.66	0.9047	677.	3.284E 00	-4.528E 00	3.639E-01	2.104E-01
56.42	0.9071	675.	2.911E 00	-4.123E 00	2.523E-01	1.948E-01
52.23	0.9087	674.	2.734E 00	-3.470E 00	2.445E-01	1.533E-01
47.99	0.9099	673.	2.475E 00	-2.524E 00	1.430E-01	1.051E-01
43.77	0.9107	673.	1.820E 00	-1.758E 00	-4.242E-03	6.614E-02
39.51	0.9113	672.	5.550E-01	-1.460E 00	-7.081E-02	2.404E-02
35.26	0.9118	672.	-1.000E 00	-1.452E 00	-7.095E-02	-2.403E-02

GAS CHROMATOGRAPH/FLOW REACTOR DATA SHEET   JANUARY 15, 1971

METHANE/OXYGEN/AIR REACTION STUDY
FREDERICK L DRYER

SMOOTHED FIRST TIME DERIVATIVE OF CHEMICAL DATA
DIMENSIONS ARE (MOLAR PERCENT/SEC)

			CHEMICAL SPECIE C_2H_6	H_2O	O_2	CTOT
	AV RETENTION TIME (MIN)		5.00	7.00	0.00	0.00
POSITION (CM)	1000/T 1/(DEGK)	VELOCITY (CM/SEC)				
114.59	0.8364	732.	0.000E-01	4.572E 00	-2.807E 00	0.000E-01
110.70	0.8362	732.	0.000E-01	2.399E 00	-2.557E 00	0.000E-01
106.60	0.8366	732.	0.000E-01	1.512E 00	-3.910E 00	0.000E-01
102.43	0.8387	730.	0.000E-01	3.696E 00	-8.401E 00	0.000E-01
98.28	0.8436	726.	-3.067E-02	7.999E 00	-1.410E 01	0.000E-01
94.12	0.8511	720.	-8.854E-02	1.229E 01	-1.795E 01	0.000E-01
89.94	0.8603	712.	-1.469E-01	1.575E 01	-1.899E 01	0.000E-01
85.78	0.8698	704.	-2.049E-01	1.885E 01	-1.877E 01	0.000E-01
81.61	0.8786	697.	-2.367E-01	2.132E 01	-1.846E 01	0.000E-01
77.42	0.8864	691.	-2.152E-01	2.163E 01	-1.751E 01	0.000E-01
73.26	0.8929	686.	-1.400E-01	1.877E 01	-1.487E 01	0.000E-01
69.07	0.8980	682.	-3.810E-02	1.411E 01	-1.109E 01	0.000E-01
64.85	0.9018	679.	5.324E-02	1.014E 01	-7.852E 00	0.000E-01
60.66	0.9047	677.	1.090E-01	7.826E 00	-5.919E 00	0.000E-01
56.42	0.9071	675.	1.327E-01	6.848E 00	-5.132E 00	0.000E-01
52.23	0.9087	674.	1.417E-01	6.405E 00	-4.814E 00	0.000E-01
47.99	0.9099	673.	1.471E-01	5.593E 00	-4.177E 00	0.000E-01
43.77	0.9107	673.	1.443E-01	3.908E 00	-2.860E 00	0.000E-01
39.51	0.9113	672.	1.252E-01	1.143E 00	-7.780E-01	0.000E-01
35.26	0.9118	672.	9.768E-02	-2.093E 00	1.618E 00	0.000E-01

CHEMICAL KINETICS FLOW REACTOR DATA SHEET   NOVEMBER 17, 1970 *

METHANE/AIR RUN
FREDERICK L DRYER

RUN NUMBER   1

PROBE BASE   (MV)   3.670
OXIDIZER INJECTION PORT   1

		CARRIER	DILUENT	FUEL	OXIDIZER
CHEMICAL		AIR	N2	CH4	O2
MOLECULAR WEIGHT		28.89	28.01	16.01	32.00
INPUT					
PRESSURE	(PSIG)	301.0	15.0	11.2	0.0
TEMPERATURE	(DEGC)	3.	21.	21.	20.
MANOMETER	(INHG)		3.30	7.10	
CORRECTED					
PRESSURE	(ATMA)	21.49	2.02	1.76	1.00
TEMPERATURE	(DEGK)	276.	294.	294.	293.
MANOMETER	(INHG)		3.30	7.10	
CALCULATED					
FLOW RATE	(GM/SEC)	31.3387	0.7600	0.1766	0.0000
FLOW RATE	(MOLE/SEC)	1.08476	0.02713	0.01103	0.00000
MOLE FRACTION		0.96602	0.02416	0.00982	0.20093

EQUIVALENCE RATIO   0.098

---

* Experimental results dated November 17, 1970, appear in the text as
Figure 6.2

CHROMATOGRAPH ANALYSIS DATA SHEET   NOVEMBER 17,1970

CHROMATOGRAPH CALIBRATION DATA

TABLE NUMBER 14   CO   3.00   MINUTES

                                0.00   0.0000
                               12.81   0.0300
                               25.62   0.0360
                               38.43   0.0400
                               51.24   0.0440
                               64.05   0.0460
                               76.86   0.0500
                              640.53   0.1430
                             1281.07   0.2480
                             1921.60   0.3540
                             2216.25   0.4010

TABLE NUMBER 15   CH4   1.00   MINUTES

                                0.00   0.0000
                            23100.00   0.2020

TABLE NUMBER 16   CO2   2.00   MINUTES

                                0.00   0.0000
                             5320.00   0.6640

TABLE NUMBER 17   C2H4   4.00   MINUTES

                                0.00   0.0000
                            44300.00   0.2020

TABLE NUMBER 18   C2H6   5.00   MINUTES

                                0.00   0.0000
                            43900.00   0.2020

CHROMATOGRAPH ANALYSIS DATA SHEET   NOVEMBER 17, 1970

COLUMN CONDITIONS

	FLOW RATE (CC/MIN)	TYPE	CARRIER GAS
A	60.0	80/100 MESH, 6FT R, 6FT O, 1/8 S.S.	HELIUM
B	60.0	80/100 MESH, 12FT R, 1/8 S.S.	HELIUM

DETECTOR CONDITIONS

THERMAL CONDUCTIVITY

BRIDGE CURRENT	270.	MA
OVENTEMP	130.	DEGC
AUXILIARY TEMP	125.	DEGC

FLAME IONIZATION

HYDROGEN	11.	PSI
OXYGEN	21.	PSI
AUXILIARY	40.	CC/MIN
TEMPERATURE	250.	DEGC

TEMPERATURE PROGRAM(S)

START DEGC	PINJ MIN	RT1 D/M	LV1 MIN	TEMP1 DEGC	RT2 D/M	LV2 MIN	TEMP2 DEGC	RT3 D/M	LV3 MIN	TEMP3 DEGC	RCV DEGC	COMMENTS
-95.	0.	4.	0.	-70.	30.	2.**********		0.*****		130.		GENERAL PG
105.	0.	0.	0.	0.	0.	0.	0.	0.	0.	0.	0.	H2O & CH2O

MISCELLANEOUS

SAMPLE VOL	0.5	CC	INJ PORT TEMP	160.0	DEGC
SAMPLE TEMP	110.0	DEGC	SPLIT RATIO	2.0	TC/FID
SAMPLE PRESS	38.0	CM HG			

INTEGRATOR PARAMETERS

PROG	IVPT	NOISE	UP	DOWN	BRST	PSUM	PNT	RTR
1	TC	3.00	0.10	0.03	0.00	0.00	NO	1000.00
2	TC	3.00	0.10	0.03	0.10	0.00	NO	0.10
3	TC	1.00	0.03	0.01	0.00	0.00	NO	0.10
4	FID	4.00	0.10	0.03	0.10	0.00	NO	0.10

COMMENTS

GAS CHROMATOGRAPH/FLOW REACTOR DATA SHEET   NOVEMBER 17, 1970

METHANE/AIR RUN
FREDERICK L DRYER

			CHEMICAL DATA, MOLAR PERCENT SPECIES			
	CHEMICAL SPECIE		CO	CH4	CO2	C2H4
AV RETENTION TIME (MIN)			3.00	1.00	2.00	4.00
POSITION (CM)	TEMP (DEGK)	VELOCITY (CM/SEC)				
110.43	1319.	1498.	0.000E-01	0.000E-01	8.718E-01	0.000E-01
106.01	1325.	1505.	0.000E-01	0.000E-01	8.687E-01	0.000E-01
101.60	1325.	1505.	1.405E-02	0.000E-01	8.641E-01	0.000E-01
97.19	1325.	1505.	3.009E-02	2.037E-03	8.565E-01	0.000E-01
92.74	1321.	1500.	7.032E-02	1.016E-02	8.268E-01	0.000E-01
88.30	1311.	1490.	1.337E-01	3.584E-02	7.284E-01	1.482E-03
83.88	1290.	1465.	2.152E-01	1.146E-01	5.669E-01	3.648E-03
79.46	1258.	1428.	2.485E-01	1.840E-01	4.470E-01	6.967E-03
74.99	1240.	1408.	2.329E-01	3.289E-01	2.887E-01	9.471E-03
70.54	1199.	1362.	1.918E-01	4.930E-01	1.629E-01	9.972E-03
66.12	1178.	1338.	1.310E-01	6.016E-01	1.128E-01	8.185E-03
61.68	1161.	1318.	8.335E-02	6.836E-01	8.462E-02	6.083E-03
57.18	1146.	1301.	0.000E-01	0.000E-01	0.000E-01	0.000E-01
52.75	1150.	1306.	4.392E-02	7.589E-01	7.838E-02	2.645E-03
48.23	1147.	1303.	4.268E-02	7.785E-01	8.013E-02	1.860E-03
43.72	1145.	1300.	0.000E-01	8.071E-01	8.050E-02	8.572E-04
39.23	1143.	1298.	0.000E-01	8.182E-01	8.038E-02	3.465E-04

GAS CHROMATOGRAPH/FLOW REACTOR DATA SHEET   NOVEMBER 17,1970

METHANE/AIR RUN
FREDERICK L DRYER

			CHEMICAL DATA, MOLAR PERCENT SPECIES			
		CHEMICAL SPECIE	C2H6	H2O	O2	CTOT
	AV RETENTION TIME (MIN)		5.00	0.00	0.00	0.00
POSITION	TEMP	VELOCITY				
(CM)	(DEGK)	(CM/SEC)				
110.43	1319.	1498.	0.000E-01	0.000E-01	0.000E-01	8.718E-01
106.01	1325.	1505.	0.000E-01	0.000E-01	0.000E-01	8.687E-01
101.60	1325.	1505.	0.000E-01	0.000E-01	0.000E-01	8.781E-01
97.19	1325.	1505.	0.000E-01	0.000E-01	0.000E-01	8.886E-01
92.74	1321.	1500.	0.000E-01	0.000E-01	0.000E-01	9.072E-01
88.30	1311.	1490.	7.316E-04	0.000E-01	0.000E-01	9.023E-01
83.88	1290.	1465.	3.023E-03	0.000E-01	0.000E-01	9.100E-01
79.46	1258.	1428.	5.223E-03	0.000E-01	0.000E-01	9.038E-01
74.99	1240.	1408.	8.890E-03	0.000E-01	0.000E-01	8.872E-01
70.54	1199.	1362.	1.142E-02	0.000E-01	0.000E-01	8.904E-01
66.12	1178.	1338.	1.155E-02	0.000E-01	0.000E-01	8.850E-01
61.68	1161.	1318.	1.075E-02	0.000E-01	0.000E-01	8.852E-01
57.18	1146.	1301.	0.000E-01	0.000E-01	0.000E-01	0.000E-01
52.75	1150.	1306.	7.128E-03	0.000E-01	0.000E-01	9.007E-01
48.23	1147.	1303.	5.793E-03	0.000E-01	0.000E-01	9.166E-01
43.72	1145.	1300.	3.723E-03	0.000E-01	0.000E-01	8.968E-01
39.23	1143.	1298.	2.581E-03	0.000E-01	0.000E-01	9.045E-01

GAS CHROMATOGRAPH/FLOW REACTOR DATA SHEET   NOVEMBER 17,1970

METHANE/AIR RUN
FREDERICK L DRYER

			5PT 2ND ORDER SMOOTHING PERFORMED 4 TIMES			
			MOLAR PERCENT SPECIES			
		CHEMICAL SPECIE	CO	CH4	CO2	C2H4
	AV RETENTION TIME (MIN)		3.00	1.00	2.00	4.00
POSITION (CM)	TEMP (DEGK)	VELOCITY (CM/SEC)				
110.43	1319.	1498.	1.092E-03	0.000E-01	8.726E-01	0.000E-01
106.01	1324.	1504.	1.673E-02	1.203E-03	8.657E-01	0.000E-01
101.60	1326.	1506.	2.060E-02	0.000E-01	8.685E-01	0.000E-01
97.19	1326.	1506.	3.526E-02	0.000E-01	8.581E-01	0.000E-01
92.74	1321.	1500.	7.658E-02	1.108E-02	8.119E-01	4.089E-04
88.30	1309.	1487.	1.410E-01	4.249E-02	7.180E-01	1.704E-03
83.88	1289.	1464.	2.048E-01	1.039E-01	5.842E-01	4.045E-03
79.46	1262.	1434.	2.396E-01	2.028E-01	4.335E-01	6.885E-03
74.99	1233.	1401.	2.319E-01	3.350E-01	2.909E-01	9.046E-03
70.54	1204.	1367.	1.900E-01	4.771E-01	1.795E-01	9.537E-03
66.12	1178.	1338.	1.352E-01	5.984E-01	1.114E-01	8.327E-03
61.68	1160.	1317.	8.861E-02	6.816E-01	8.231E-02	6.258E-03
57.18	1150.	1306.	5.980E-02	7.311E-01	7.552E-02	4.256E-03
52.75	1147.	1303.	4.282E-02	7.614E-01	7.674E-02	2.751E-03
48.23	1146.	1302.	2.689E-02	7.842E-01	7.932E-02	1.711E-03
43.72	1146.	1301.	1.052E-02	8.034E-01	8.104E-02	9.570E-04
39.23	1142.	1298.	0.000E-01	8.192E-01	8.024E-02	3.216E-04

GAS CHROMATOGRAPH/FLOW REACTOR DATA SHEET   NOVEMBER 17,1970

METHANE/AIR RUN
FREDERICK L DRYER

5PT 2ND ORDER SMOOTHING PERFORMED 4 TIMES
MOLAR PERCENT SPECIES

			CHEMICAL SPECIE	C2H6	H2O	O2	CTOT
		AV RETENTION TIME (MIN)		5.00	0.00	0.00	0.00
POSITION (CM)	TEMP (DEGK)	VELOCITY (CM/SEC)					
110.43	1319.	1498.		0.000E-01	1.587E 00	1.851E 01	8.736E-01
106.01	1324.	1504.		0.000E-01	1.605E 00	1.850E 01	8.837E-01
101.60	1326.	1506.		0.000E-01	1.616E 00	1.849E 01	8.891E-01
97.19	1326.	1506.		0.000E-01	1.626E 00	1.848E 01	8.934E-01
92.74	1321.	1500.		0.000E-01	1.618E 00	1.851E 01	9.004E-01
88.30	1309.	1487.		9.460E-04	1.562E 00	1.860E 01	9.067E-01
83.88	1289.	1464.		2.906E-03	1.428E 00	1.877E 01	9.068E-01
79.46	1262.	1434.		5.715E-03	1.205E 00	1.902E 01	9.010E-01
74.99	1233.	1401.		8.713E-03	9.121E-01	1.931E 01	8.934E-01
70.54	1204.	1367.		1.089E-02	6.084E-01	1.959E 01	8.874E-01
66.12	1178.	1338.		1.153E-02	3.610E-01	1.981E 01	8.847E-01
61.68	1160.	1317.		1.073E-02	2.046E-01	1.994E 01	8.865E-01
57.18	1150.	1306.		9.131E-03	1.278E-01	2.000E 01	8.932E-01
52.75	1147.	1303.		7.304E-03	9.142E-02	2.003E 01	9.011E-01
48.23	1146.	1302.		5.526E-03	6.089E-02	2.005E 01	9.049E-01
43.72	1146.	1301.		3.901E-03	2.845E-02	2.007E 01	9.046E-01
39.23	1142.	1298.		2.537E-03	2.882E-03	2.009E 01	9.051E-01

GAS CHROMATOGRAPH/FLOW REACTOR DATA SHEET   NOVEMBER 17,1970

METHANE/AIR RUN
FREDERICK L DRYER

SMOOTHED FIRST TIME DERIVATIVE OF CHEMICAL DATA
DIMENSIONS ARE (MOLAR PERCENT/SEC)

	CHEMICAL SPECIE		CO	CH4	CO2	C2H4
	AV RETENTION TIME (MIN)		3.00	1.00	2.00	4.00
POSITION (CM)	1000/T 1/(DEGK)	VELOCITY (CM/SEC)				
110.43	0.7581	1498.	-7.295E 00	-8.166E-01	3.937E 00	0.000E-01
106.01	0.7552	1504.	-3.319E 00	9.292E-04	6.852E-01	0.000E-01
101.60	0.7539	1506.	-3.165E 00	2.055E-01	1.300E 00	0.000E-01
97.19	0.7543	1506.	-9.473E 00	-1.865E 00	9.569E 00	-6.887E-02
92.74	0.7571	1500.	-1.785E 01	-7.178E 00	2.367E 01	-2.879E-01
88.30	0.7640	1487.	-2.151E 01	-1.560E 01	3.823E 01	-6.109E-01
83.88	0.7760	1464.	-1.633E 01	-2.654E 01	4.710E 01	-9.580E-01
79.46	0.7921	1434.	-4.463E 00	-3.721E 01	4.732E 01	-8.078E-01
74.99	0.8109	1401.	7.809E 00	-4.309E 01	3.987E 01	-4.152E-01
70.54	0.8307	1367.	1.493E 01	-4.058E 01	2.762E 01	1.126E-01
66.12	0.8488	1338.	1.532E 01	-3.091E 01	1.470E 01	4.945E-01
61.68	0.8623	1317.	1.114E 01	-1.962E 01	5.338E 00	5.999E-01
57.18	0.8695	1306.	6.671E 00	-1.163E 01	7.967E-01	5.119E-01
52.75	0.8719	1303.	4.794E 00	-7.753E 00	-5.501E-01	3.719E-01
48.23	0.8723	1302.	4.657E 00	-6.047E 00	-6.203E-01	2.586E-01
43.72	0.8729	1301.	3.884E 00	-5.056E 00	-1.315E-01	2.008E-01
39.23	0.8754	1298.	2.207E 00	-4.101E 00	5.913E-01	1.670E-01

GAS CHROMATOGRAPH/FLOW REACTOR DATA SHEET   NOVEMBER 17, 1970

METHANE/AIR RUN
FREDERICK L DRYER

SMOOTHED FIRST TIME DERIVATIVE OF CHEMICAL DATA
DIMENSIONS ARE (MOLAR PERCENT/SEC)

			C2H6	H20	02	CTOT
	CHEMICAL SPECIE		5.00	0.00	0.00	0.00
	AV RETENTION TIME (MIN)					
POSITION (CM)	1000/T 1/(DEGK)	VELOCITY (CM/SEC)				
110.43	0.7581	1498.	0.000E-01	-7.157E 00	3.289E 00	0.000E-01
106.01	0.7552	1504.	0.000E-01	-5.054E 00	3.501E 00	0.000E-01
101.60	0.7539	1506.	0.000E-01	-3.670E 00	2.118E 00	0.000E-01
97.19	0.7543	1506.	0.000E-01	-2.505E-01	-4.708E 00	0.000E-01
92.74	0.7571	1500.	-1.600E-01	1.088E 01	-2.019E 01	0.000E-01
88.30	0.7640	1487.	-4.884E-01	3.178E 01	-4.337E 01	0.000E-01
83.88	0.7760	1464.	-7.896E-01	5.904E 01	-6.846E 01	0.000E-01
79.46	0.7921	1434.	-9.363E-01	8.317E 01	-8.668E 01	0.000E-01
74.99	0.8109	1401.	-8.117E-01	9.371E 01	-9.062E 01	0.000E-01
70.54	0.8307	1367.	-4.332E-01	8.489E 01	-7.753E 01	0.000E-01
66.12	0.8498	1338.	2.221E-02	6.104E 01	-5.288E 01	0.000E-01
61.68	0.8623	1317.	3.525E-01	3.452E 01	-2.817E 01	0.000E-01
57.18	0.8695	1306.	5.022E-01	1.646E 01	-1.236E 01	0.000E-01
52.75	0.8719	1303.	5.249E-01	9.756E 00	-6.725E 00	0.000E-01
48.23	0.8723	1302.	4.907E-01	9.081E 00	-6.249E 00	0.000E-01
43.72	0.8729	1301.	4.319E-01	8.382E 00	-6.002E 00	0.000E-01
39.23	0.8754	1298.	3.576E-01	6.418E 00	-4.904E 00	0.000E-01

B3   Estimation of Experimental Error

Sawyer [16] has adequately discussed the errors associated with developing overall rate constants using the thermal analysis techniques, and therefore these uncertainties will not be discussed further.

It was shown in Chapters 3 and 4 that the relative precision of the experimental parameters used in the chemical analysis method (specie concentration, position measurements, carrier velocity, reaction temperature) were all better than 2%. The uncertainty associated with developing the gradients of concentrations with distance through the reactor is difficult to estimate in that a closed form of the data smoothing and differentiation process is not available. The uncertainty in tnese processes surely degenerates near the extremities of the incremental data, since the smoothing process does not operate well unless data is available on both sides of the incremental point being adjusted. However, a conservative estimate of the relative uncertainty in the concentration gradient at interior points is about 5%. The relative uncertainty of an overall rate constant will depend on the reaction orders arising in the expression. Since the overall order of most expressions is less that two, the relative uncertainty in the overall rate constant is less than 15%.

APPENDIX C

Summary of Elementary Reaction Rate Data

Appendix C presents a summary of the elementary kinetic reactions enumerated and/or discussed in the text. The reactions are numbered consecutively in order of their introduction.

In the text, the forward direction of the reaction was interpreted as the reaction proceeding left to right. The direction(s) of arrows in the reaction equations or the number of the reaction followed by "f" (forward) or "r" (reverse) signified the reaction direction(s) under discussion.

The elementary specific rate constant for a reaction was denoted as k_{if} or k_{ir} and referred to the "forward" or "reverse" specific rate constant for reaction "i". Similar notation was employed to denote the apparent activation energy (E_{if} or E_{ir}) and the pre-exponential factor (C_{if} or C_{ir}).

Available data for C_{if} and E_{if} are tabulated in Table C-1, along with the elementary reactions. Where reverse specific rate constants were necessary, they were calculated from these data and equilibrium considerations.

Some of the references have considered the values of C_{if} and E_{if} to apply over temperature ranges as large as 2000K. In light of absolute reaction rate theory, the limitations of this statement are once again emphasized.

TABULATION OF ELEMENTARY REACTION DATA

No.	Elementary Reaction	C_{if}	E_{if}	Ref.
1	$CO + OH \rightarrow CO_2 + H$	*	*	-
2	$CO + O + M \rightarrow CO_2 + M$		.	111
3	$CO + O_2 \rightarrow CO_2 + O$	2.5×10^{12}	48,000	79
4	$CO + HO_2 \rightarrow CO_2 + OH$	5.8×10^{13}	24,000	98
5	$HO_2 + H_2 \rightarrow H_2O_2 + H$	9.6×10^{12}	24,000	99
6	$HO_2 + HO_2 \rightarrow H_2O_2 + O_2$	1×10^{21} at 773K		98
7	$H_2O_2 + M \rightarrow 2OH + M$	1.17×10^{17}	45,500 †	99
8	$HO_2 + OH \rightarrow H_2O + O_2$	$\approx 1 \times 10^{12}$ at 300K		102
9	$H + O_2 \rightarrow O + OH$	2.24×10^{14}	16,800	99
10	$H_2 + O \rightarrow H + OH$	1.74×10^{13}	9,450	99
11	$H + H_2O \rightarrow H_2 + OH$	8.41×10^{13}	20,100	99
12	$H + OH + M \rightarrow H_2O + M$	1.17×10^{17} at 2040K		99
13	$O + H_2O \rightarrow OH + OH$	5.75×10^{13}	18,000	99
14	$H + O_2 + N_2 \rightarrow HO_2 + N_2$	3.18×10^{15}	-1000	99
15	$HO_2 + H_2 \rightarrow H_2O_2 + H$	9.6×10^{12}	24,000	99
16	$HO_2 \xrightarrow{\text{wall?}}$ STABLE PRODUCTS	-	-	-
17	$CH_4 + OH \rightarrow CH_3 + H_2O$	3.32×10^{12}	3,772	173
18	$CH_4 + O_2 \rightarrow CH_3 + HO_2$	$\approx 10^{14}$	55,000	30
19	$CH_3 + O_2 + M \rightarrow CH_3O_2^* + M$	-	-	-
20	$CH_3O_2^* \rightarrow H_2CO + OH$	-	-	-
21	$CH_3O_2^* + CH_4 \rightarrow CH_3 + CH_3OOH$	-	-	-
22	$CH_3OOH \rightarrow CH_3O + OH$	-	-	-
23	$CH_3O + CH_4 \rightarrow CH_3OH + CH_3$	-	-	-

* see text
† considered as 1st order reaction

TABLE C-1

No.	Elementary Reaction	C_{if}	E_{if}	Ref.
24	$R + CH_3O \rightarrow CH_2O + RH$	-	-	-
25	$O_2 + CH_2O \rightarrow HCO + HO_2$	-	-	-
26	$HCO + O_2 \rightarrow HO_2 + CO$	-	-	-
27	$HCO + OH \rightarrow CO + H_2O$	$10^{12}-10^{14}$	-	148
28	$CH_4 + O_2 \rightarrow CH_3 + H_2O_2$	-	-	-
29	$CH_2O + HO_2 \rightarrow HCO + H_2O_2$	-	-	-
30	$HO_2, HCO \rightarrow wall$	-	-	-
31	$CH_2O + OH \rightarrow HCO + H_2O$	$10^{13}-10^{15}$	-	142
32	$CH_4 + M \rightarrow CH_3 + H + M$	1×10^{18}	88,000	148
33	$CH_4 + O \rightarrow CH_3 + OH$	2.1×10^{13}	9,040	174
34	$CH_4 + H \rightarrow CH_3 + H_2$	6.9×10^{13}	11,800	175
35	$CH_3 + O_2 \rightarrow HCO + H_2O$	$10^{10}-10^{12}$	-	142
36	$HCO + M \rightarrow H + CO + M$	$2 \times 10^{12} T^{\frac{1}{2}}$	14,400	148
37	$CH_3 + O \rightarrow HCO + H_2$	$10^{11}-10^{14}$	-	148
38	$CH_3 + O_2 + M \rightarrow CH_3O_2 + M$	-	-	-
39	$CH_3 + CH_3 \rightarrow C_2H_6$	$5.5 \times 10^{18} T^{-2}$	0	163
40	$C_2H_6 + H \rightarrow C_2H_5 + H_2$	-	-	-
41	$C_2H_6 + OH \rightarrow C_2H_5 + H_2O$	7.7×10^{13}	7,200	172
42	$C_2H_6 + O \rightarrow C_2H_5 + OH$	2.5×10^{13}	6,360	174

TABLE C-1 (Cont'd.)